

BULLETIN OF MAGNETIC RESONANCE

*The Quarterly Review Journal of the
International Society of Magnetic Resonance*

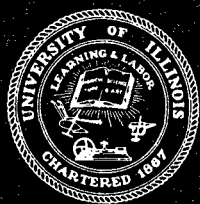
VOLUME 7

APRIL, 1985

NUMBER 1

CONTENTS

MESSAGE FROM THE PRESIDENT OF ISMAR.....	3
REVIEWS	
STOCHASTIC NMR SPECTROSCOPY, B. Blümich	5
ANALYSIS OF CHAIN MICROSTRUCTURE BY ^1H AND ^{13}C NMR SPECTROSCOPY, Yu. E. Shapiro	27
ISMAR MEMBERSHIP LIST AND ADDRESSES, 1984	59
ANNOUNCEMENTS	71
NEW BOOKS	72
INSTRUCTIONS FOR AUTHORS	73
FORTHCOMING PAPERS	75



University of Illinois at Chicago

BULLETIN OF MAGNETIC RESONANCE

*The Quarterly Review Journal of the
International Society of Magnetic Resonance*

Editor:

DAVID G. GORENSTEIN
*Department of Chemistry
University of Illinois at Chicago
Post Office Box 4348
Chicago, Illinois, U.S.A.*

Editorial Board:

E.R. ANDREW
*University of Florida
Gainesville, Florida, U.S.A.*

ROBERT BLINC
*E. Kardelj University of Ljubljana
Ljubljana, Yugoslavia*

H. CHIHARA
*Osaka University
Toyonaka, Japan*

GARETH R. EATON
*University of Denver
Denver, Colorado, U.S.A.*

DANIEL FIAT
*University of Illinois at Chicago
Chicago, Illinois, U.S.A.*

SHIZUO FUJIWARA
*University of Tokyo
Bunkyo-Ku, Tokyo, Japan*

DAVID GRANT
*University of Utah
Salt Lake City, Utah, U.S.A.*

JOHN MARKLEY
*Purdue University
West Lafayette, Indiana, U.S.A.*

MICHAEL PINTAR
*University of Waterloo
Waterloo, Ontario, Canada*

CHARLES P. POOLE, JR.
*University of South Carolina
Columbia, South Carolina, U.S.A.*

JAKOB SMIDT
*Technische Hogeschool Delft
Delft, The Netherlands*

BRIAN SYKES
*University of Alberta
Edmonton, Alberta, Canada*

The *Bulletin of Magnetic Resonance* is a quarterly review journal sponsored by the International Society of Magnetic Resonance. Reviews cover all parts of the broad field of magnetic resonance, viz., the theory and practice of nuclear magnetic resonance, electron paramagnetic resonance, and nuclear quadrupole resonance spectroscopy including applications in physics, chemistry, biology, and medicine. The *BULLETIN* also acts as a house journal for the International Society of Magnetic Resonance.

CODEN: BUMRDT

ISSN: 0163-559X

Bulletin of Magnetic Resonance, The Quarterly Journal of the International Society of Magnetic Resonance. Copyright © 1985 by the International Society of Magnetic Resonance. Rates: Libraries and non-members of ISMAR, \$60.00, members of ISMAR, \$18.00. All subscriptions are for a volume year. All rights reserved. No part of this journal may be reproduced in any form for any purpose or by any means, abstracted, or entered into any data base, electronic or otherwise, without specific permission in writing from the publisher.

Council of the International Society of Magnetic Resonance

E.R. ANDREW, President

C.P. SLICHTER, Vice President

D. FIAT, Secretary-General and Founding Chairman

C.P. POOLE, Jr., Treasurer

E.R. ANDREW
Gainesville

G.J. BENE
Geneve

R. BLINC
Ljubljana

M. BLOOM
Vancouver

W.S. BREY, JR.
Gainesville

V. BYSTROV
Moscow

F. CONTI
Rome

R.R. ERNST
Zurich

D. FIAT
Chicago

S. FORSEN
Lund

S. FUJIWARA
Urawa

M. GOLDMAN
Gif sur Yvette

H.S. GUTOWSKY
Urbana

R.K. HARRIS
Durham

K.H. HAUSSE
Heidelberg

J. HENNEL
Krakow

O. JARDETSKY
Stanford

J. JEENER
Brussels

V.J. KOWALEWSKI
Buenos Aires

P.C. LAUTERBUR
Stony Brook

E. LIPPMAN
Tallin

A. LOSCHE
Leipzig

P.T. NARASIMHAN
Kanpur

D. NORBERG
St. Louis

H. PFEIFER
Leipzig

W. von PHILIPSBORN
Zurich

A. PINES
Berkeley

L.W. REEVES
Waterloo

R. RICHARDS
Oxford

J. D. ROBERTS
Altadena

J. SMIDT
Delft

J. STANKOWSKY
Poznan

I. URSU
Bucharest

N.V. VUGMAN
Rio de Janeiro

H.C. WOLF
Stuttgart

The aims of the International Society of Magnetic Resonance are to advance and diffuse knowledge of magnetic resonance and its applications in physics, chemistry, biology, and medicine, and to encourage and develop international contacts between scientists.

The Society sponsors international meetings and schools in magnetic resonance and its applications and publishes the quarterly review journal, *The Bulletin of Magnetic Resonance*, the house journal of ISMAR.

The annual fee for ISMAR membership is \$20 plus \$18 for a member subscription to the *Bulletin of Magnetic Resonance*.

Send subscription to:

International Society of Magnetic Resonance
Professor Charles P. Poole, Jr.
Treasurer
Department of Physics & Astronomy
University of South Carolina
Columbia, South Carolina 29208 U.S.A.

MESSAGE FROM THE PRESIDENT OF ISMAR

As I approach the half-way mark in my term of three years as President of ISMAR, I am very happy to accept the Editor's invitation to write a message to members of the Society and to subscribers and readers of the *Bulletin*.

First of all I want to let you know that the date and location of the next ISMAR Conference has been fixed by the Council. It will be held at the Hotel Gloria, Rio de Janeiro, 29 June - 5 July 1986, and will be organized by Dr. Ney Vernon Vugman from whom further information may be obtained. His address is Dr. N.V. Vugman, Instituto de Fisica, Universidade Federal de Rio de Janeiro, Cidade Universitaria, Bloco A - CCMN, Rio de Janeiro 21945, Brazil. We hope you will plan to be there and help to make this a really successful international magnetic resonance meeting.

Now let me turn to some domestic matters. At the last ISMAR meeting in Chicago in August 1983, a new ISMAR Constitution was presented to the Council and to a Business Meeting of the Society, who both approved it with minor amendments. It was then circulated to the whole membership for ballot by mail, and was overwhelmingly approved. At the same time a list of candidates for the various offices and for the Council was circulated for election by mail ballot. The following officers were elected: President: E. R. Andrew, Vice-President: C. P. Slichter, Secretary-General: D. Fiat, Treasurer: C.P. Poole. A full list of Council members elected appears at the front of the *Bulletin*. Those elected assumed office in January 1984. In recognition of his special contributions to the establishment of the Society, Professor Daniel Fiat was accorded in the Constitution the personal office of Founding Chairman.

The Secretary-General maintains the records of the Society and any questions concerning membership and general information should be addressed to him (Professor D. Fiat, E-207 MSA, University of Illinois Medical Center, P.O. Box 6998, Chicago, Illinois 60680, U.S.A.).

The Treasurer looks after the finances of the

Society and deals with dues and *Bulletin* subscriptions. The Society has opened a bank account in Columbia, South Carolina, where the Treasurer lives. A certified public accountant in Columbia has been appointed to carry out an annual audit of the Society's accounts. Any questions concerning dues and *Bulletin* subscriptions should be addressed to the Treasurer (Professor C.P. Poole, Department of Physics, University of South Carolina, Columbia, S.C. 29208 U.S.A.).

Between the triennial meetings of the Society the Council carries out its business by correspondence. I write to Council members four times a year and I am most grateful for their advice.

The Society's journal, *Bulletin of Magnetic Resonance*, is prospering under the energetic editorship of Professor David Gorenstein. He is shortly moving to a new appointment in the Department of Chemistry at Purdue University and will continue to edit the *Bulletin* from there.

As we look to the future, the next ISMAR triennial meeting after Rio de Janeiro will be held in 1989. It will be recalled that previous international magnetic resonance meetings have been held in Tokyo (1965), Sao Paulo (1968), Melbourne (1969), Israel (1971), Bombay (1974), Banff (1977), Delft (1980) (jointly with the Groupement Ampere), Chicago (1983). Any members who have suggestions for 1989 or about any other aspect of the Society's activities, should write to me at the address below.

Finally I send my cordial greetings to all members of ISMAR and my best wishes for your life and work.

Raymond Andrew
President, ISMAR
Department of Physics
University of Florida
Gainesville, Florida 32611
U.S.A.

NINTH WATERLOO NMR SUMMER INSTITUTE

ADVANCES IN NUCLEAR MAGNETIC RESONANCE JUNE 10-17, 1985

Lectures will be held on nuclear spin thermodynamics, r.f. pulse technology, two dimensional NMR, double resonances, multiquantum NMR, quadrupole NMR, spin polarization spectroscopy, and on applications in biophysics, chemical physics and solid state physics. On Saturday, June 15 there will be a NMR Imaging Symposium.

Invited Speakers

P. Allen (*Edmonton*), R. Andrew (*Gainesville, Fl.*), R. Armstrong (*Toronto*), P. Beckmann (*Bryn Mawr Penn.*), R. Blinc (*Ljubljana, Yugoslavia*), M. Bloom (*UBC, Vancouver*), E. Burnell (*UBC, Vancouver*), S. Clough (*Nottingham, England*), F. Conti (*Rome, Italy*), W. Doane (*Kent, Ohio*), R. Dong (*Brandon, Ma.*), D. Edmonds (*Oxford*), D. Gorenstein (*Chicago*), R. Griffin (*MIT*), E. Hahn (*Berkeley*), J. Jeener (*Bruxelles, Belgium*), K. Jeffrey (*Guelph*), R. Kaiser (*UNB, Fredericton*), P. Lauterbur (*Stony Brook, N.Y.*), I. Lowe (*Pittsburgh, Penn.*), A. Pines (*Berkeley*), P. Mansfield (*Nottingham, England*), M. Mehring (*Stuttgart, FRG*), K. Packer (*Norwich, England*), H. Peemoeller (*UNB, Fredericton*), M. Pintar (*Waterloo*), C. Poole (*S. Carolina*), L. Reeves (*Waterloo*), B. Sanctuary (*McGill*), I.C.P. Smith (*NRC, Ottawa*) and J. Stankowski (*Poznan, Poland*). Some speakers have not confirmed their participation.

For the instructions during the first and second week only 4th year quantum mechanics will be assumed. For the advances in NMR (third week) it is expected that graduate students and younger researchers with a basic familiarity with the field will benefit most. The number of participants will be limited to 90. A single room with breakfast daily will cost \$24 Can. per day. For the first two weeks students add a \$20 Can. fee, non-students \$60. For the advances in NMR (third week) students add a \$40 Can. fee, non-students \$120. If registering after May 23 please add \$30 Can. to cover late registration expenses. Applications and inquiries about the full programme, registration, board and lodging should be forwarded to:

Summer School in Basic NMR

May 27-June 7, 1985

An introductory course on NMR will cover basic theory, magnetic dipolar broadening in rigid lattices, spin-lattice relaxation, experimental methods and spectrometer design. This course will be taught by D. Nicoll and M. Pintar during the first week. Following will be a week of introductory review lectures on NMR concepts (density matrix, spin temperature, quadrupole interaction) and applications (membranes, phase transitions, liquid crystals, biological activity, NMR of mammalian tissues, NMR imaging, topical NMR, instrumentation fine tuning and others). The reviews will be given by R. Armstrong (*Toronto*), G. Chidichimo (*U Calabria, Italy*), J. Davis (*Guelph*), R. Kind (*Zurich, Switzerland*), E. Fukushima (*Los Alamos*), K. Jeffrey (*Guelph*), R. Lenkinski (*Guelph*), F. Prato (*U of Western Ontario*), W. Sobol (*Silesian U, Poland*), R. Thompson (*U of Western Ontario*).

Le matériel couvert pendant les deux premières semaines nécessite l'équivalent du cours de mécanique quantique de 4^e année. Il est prévu que la section concernant les progrès en RMN (3^e semaine) profitera surtout aux étudiants gradués et aux nouveaux venus possédant une connaissance de base du domaine. Le nombre de participants sera limité à 90. Une chambre simple avec petit déjeuner sera disponible au coût de 24\$ Cdn. par jour. Pour les deux premières semaines, prévoir un coût supplémentaire de 20\$ Cdn. pour étudiants, et 60\$ pour autres. Pour la 3^e semaine, ajouter 40\$ Cdn. de frais pour étudiants, et 120\$ pour autres. Pour les inscriptions en retard (après le 23 mai), ajouter 30\$ Cdn. pour couvrir les frais d'administration supplémentaires. Faire parvenir applications et toutes questions à:

Cathy Walmsley, Admin. Director
NMR Summer Institute
Department of Physics
University of Waterloo, Waterloo
Ontario, Canada N2L 3G1
Tel. 519-885-1211, Ext. 6238

STOCHASTIC NMR SPECTROSCOPY

Bernhard Blümich

*MPI für Polymerforschung
Postfach 3148
6500 Mainz
Federal Republic of Germany*

	Page
I. Introduction	5
II. General Perspectives	6
A. History of Stochastic NMR	6
B. Related Research	9
III. Perturbative Descriptions of Nonlinear Systems	10
A. Volterra Series	10
B. Wiener Series	10
C. Cross-Correlation	11
D. Symmetry	12
E. Time-Dependent Perturbation Theory	12
F. Frequency Domain Analysis	13
IV. Theory of Stochastic NMR	14
A. Interpretation of Kernels	14
B. Simulated Spectra	16
V. Practice of Stochastic NMR	19
A. The Experiment	19
B. Data Evaluation	19
VI. Developments in Stochastic Resonance	21
A. Time Resolved CIDNP Spectroscopy	21
B. NMR Imaging	22
C. Stochastic ENDOR	22
D. Outlook	22
References	23

I. INTRODUCTION

Among the different forms of spectroscopy, nuclear magnetic resonance (NMR) shows an intimate connection between theory and experiment. NMR therefore enjoys great popularity in the development of new methods. Following the rapid development in electronic and computer technology, NMR techniques evolved from single-channel to multi-channel and multi-dimensional modes. The original continuous wave (CW) method (1-3) was extended to two dimensions

with the introduction of double resonance (4-6). The CW techniques were replaced by corresponding multi-channel methods because of signal-to-noise improvements resulting from broadband excitation. The routine NMR methods are now *one-dimensional* (1D) (7,8) and *two-dimensional* (2D) (9-13) *Fourier transform* (FT) spectroscopy. The excitation energy is focused into a few pulses per experiment and the spectrum is computed from the experimental data by 1D or 2D Fourier transformation.

A conceptually more difficult method is

stochastic NMR (14,15). It employs a random excitation, which continuously supplies excitation energy and leads to significantly reduced input power. Again, the excitation spectrum is characterized by a broad frequency range, but the frequency components do not exhibit a well defined phase relationship. Sensitivity and resolution can be optimized separately in stochastic NMR.

An abstract representation of a stochastic NMR experiment is given in Figure 1. A nonlinear system is investigated which responds to an input signal $x(t)$ with an output signal $y(t)$. In

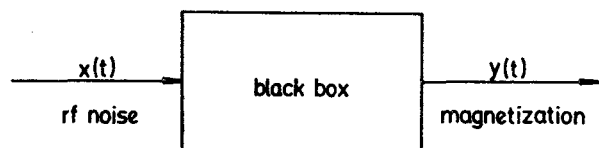


Figure 1. System analytical abstraction of stochastic NMR. The magnetic spin system is excited with radiofrequency noise $x(t)$ and responds with transverse magnetization $y(t)$.

the experiment, records of both signals are acquired. The NMR spectrum is derived from the experimental data by extensive numerical data manipulation involving correlation of excitation and response records. Multi-dimensional cross-correlation leads to multi-dimensional spectra, which display information similar to 2D FT spectra (16-19).

Section II reviews the historical development of stochastic NMR spectroscopy and relates the technique to methods in other fields of science. Section III summarizes the relevant background on nonlinear system analysis. The theory of stochastic resonance is interpreted in Section IV in terms of pulse sequences for multi-dimensional FT spectroscopy and illustrated by theoretical spectra. The practical aspects of stochastic NMR are covered in Section V. Some future trends are indicated in Section VI.

II. GENERAL PERSPECTIVE

A. History of Stochastic NMR

The idea of stochastic NMR can be traced to a paper by Primas (20) in 1961 on quantum mechanical systems with a stochastic

Hamiltonian operator in extension to Kubo's theory of fluctuation and dissipation (21-23). The standard approach to relaxation requires that the response of a driven quantum mechanical systems is iteratively expanded into a perturbation series (24). The different order terms of this series are defined by the powers of the perturbing Hamiltonian. In the field of nonlinear system analysis such a series expansion is called a *Volterra series* (25). It serves to define the nonlinear *impulse response* or *after effect functions*. The Fourier transforms of the after effect functions are called *transfer functions*, *generalized admittances*, *susceptibilities*, or *multi-dimensional spectra*.

For the description of nonlinear systems, a Volterra expansion is of limited value only, since it often diverges. However, for a white noise perturbation with a Gaussian probability distribution, Wiener has shown that the system response can be expanded into a simple convergent series with orthogonal functionals (26). The different order terms of the *Wiener series* are not defined by the power of the perturbation, but its leading terms agree with the Volterra series. Consequently the terms of both expansions have a number of properties in common. The Wiener series has found widespread use in science, because 1) according to Wiener, white noise is the most general test signal for the analysis of nonlinear systems, and 2) the nonlinear after effect functions are accessible via multi-dimensional cross-correlation of input and output records (27).

Primas has established a basis for the noise analysis of nonlinear systems in quantum mechanics by expanding the response of a quantum mechanical nonlinear system into a Wiener series. The first application of his theory to nuclear magnetic resonance systems followed in 1963 by Ernst and Primas (28) with a paper on NMR with stochastic high frequency fields. It is based on Ernst's thesis (29) and investigates double resonance with a strong stochastic perturbation. A comparative evaluation of the stochastic double resonance method led to the introduction of broad band noise decoupling in 1966 (30).

The first pure stochastic NMR data, however, did not appear until 1970, when Ernst and Kaiser independently reported their experiments in two succeeding papers in the *Journal of Magnetic Resonance* (14, 15). Ernst used shift register generated binary phase modulation of the radiofrequency (rf) input, while Kaiser modulated the magnetic field with Gaussian probability. In either case the systems were driven li-

nearly such that nonlinear response terms could be neglected.

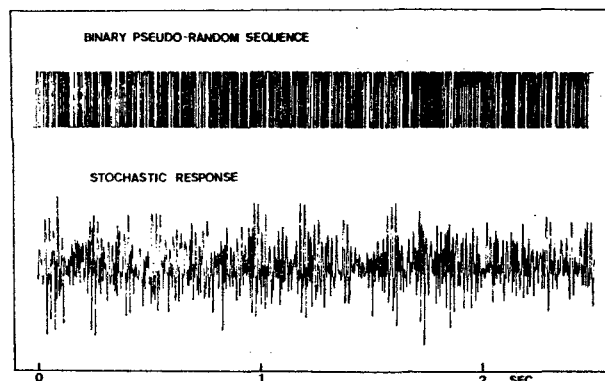


Figure 2. Binary excitation pulse sequence (top) and corresponding stochastic response (bottom) of the ^1F resonance of 40 vol. % 2,4-difluorotoluene at a frequency of 56.4 MHz. Cited with permission from ref. (14).

Figure 2 illustrates the input and output signals of Ernst's experiment (14). The excitation record (top) is a binary set of flip angles and the response record (bottom) is the resulting transverse magnetization. One-dimensional spectra were obtained on a digital computer from complex multiplication of excitation and response spectra. This data evaluation scheme is equivalent to one-dimensional cross-correlation of excitation and response records and subsequent Fourier transformation. The two papers showed, that in comparison with pulsed FT NMR, stochastic resonance

- 1) has the same sensitivity;
- 2) allows an independent optimization of sensitivity and resolution in contrast to pulsed FT NMR (31);
- 3) reduces the problems in the receiving electronics associated with the large dynamic range of impulsive signals;
- 4) reduces the peak excitation power such that wider dynamic ranges may be covered;
- 5) admits coherent averaging of the system response in connection with cyclic excitation;
- 6) will exhibit different saturation features. In particular, the nonlinear response will involve double resonance effects;
- 7) investigates the spin system in dynamic equilibrium with the excitation and not the

unperturbed thermodynamic equilibrium state.

An interesting application of stochastic resonance to solvent line suppression was demonstrated by Tomlinson and Hill in 1973 (32). A continuous string of radiofrequency pulses is synthesized by inverse Fourier transformation such that the excitation spectrum fits a predetermined pattern with zero intensity at the locations of solvent lines. In the same paper different rf modulation schemes are evaluated. Two basic approaches to modulate the flip angles in a string of successive pulses are feasible (Figure

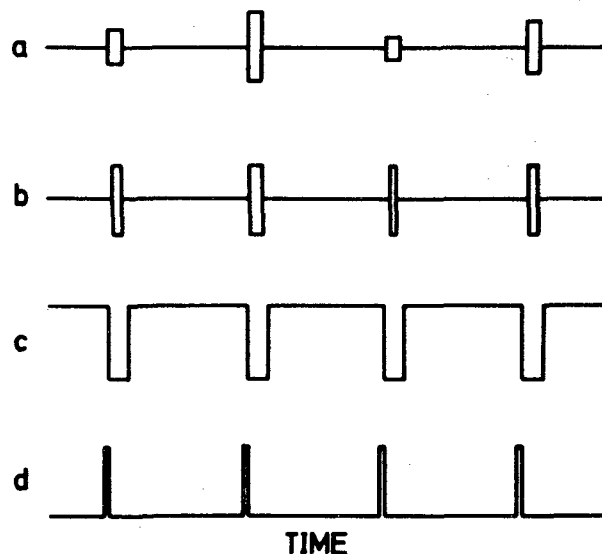


Figure 3. Timing diagram of the excitation sequence. The spin system is excited by a continuous string of equally spaced pulses with either amplitude modulation (a) or pulse width modulation (b). The receiver (c) is turned off for a constant time period centered about each pulse. The signal from the receiver is sampled (d) by an analog-to-digital converter just before the receiver is blanked for each pulse. Cited with permission from ref. (32).

- 3). Either the amplitude at constant width or the width at constant amplitude can be varied. A negative flip angle is realized by a 180° rf phase shift. In the first case a double balanced mixer is employed, but the conditions for linear operation are rather critical. Pulse width modulation requires a slightly more complex timing sequence in order to center the pulses at equidistant time intervals, but it is insensitive to mixer and

amplifier nonlinearities. Thus, a nonlinear rf amplifier can be used, which produces less noise while the pulses are off. To avoid rf leakage problems the receiver is blanked (33) for constant time intervals, which are centered at the pulse midpoints. The magnetization is sampled just before the receiver is blanked for each pulse.

Fourier synthesized excitation has also been used for the observation of broad line transients by multiple frequency modulation of a single pulse (34). This method combines the observation of a free induction decay of pulsed FT NMR with low power broad band excitation similar to stochastic NMR.

With application to solvent line suppression, the method of *correlation NMR spectroscopy* was introduced by Dadok in 1974 (35-37). The spins are excited by a fast linear sweep, which gives rise to spectral distortions of the linear response. The undistorted spectrum is restored by cross-correlation of excitation and response. The excitation power spectrum covers a well defined region and aliasing of response signals is avoided. As in stochastic NMR, excitation power requirements are low and spectra are computed by cross-correlation.

The execution of a cross-correlation on a digital computer is a rather time consuming process. However, for certain pseudo random input signals the linear cross-correlation can be replaced by a fast transformation of the response. This idea has been realized in *Hadamard NMR spectroscopy*. The method was suggested by Ziessow (38) and introduced independently by Ziessow (39) and Kaiser (40). The excitation is based on *maximum length binary sequences* or *m-sequences*, which are generated in m-stage shift registers (38, 39, 41). The output of a shift register is a sequence of $2^m - 1$ bits (0,1) with a perfectly white power spectrum. The values of the bits are used to shift the phase of the rf excitation by +90 and -90 degrees, respectively. Cross-correlation of the linear response with such sequences is equivalent to multiplication of the response with a Hadamard matrix. For the multiplication a fast algorithm exists (42), which, on account of the binary nature of the m-sequences, is even faster than the fast Fourier transformation.

The work reviewed so far has dealt with linearly driven systems only, where the output is proportional to the input. Ernst has pointed out already in 1969 that the nonlinear response of nuclear spin systems should yield information similar to that obtained in multiple resonance experiments (43). However, efforts to formulate a theory of stochastic resonance, which correctly

describes the linear as well as the nonlinear stochastic response encountered considerable difficulty. Already the linear solution of the stochastic Bloch equations produced unphysical results (14). At this point a serious discrepancy between the theory of stochastic differential equations (44, 45) and physical reality was encountered. While the Itô formalism of stochastic integrals is mathematically more satisfactory, the Stratonovich interpretation gives the correct results. This has been demonstrated by Bartholdi, Wokaun and Ernst in 1976 with a solution of the stochastic Bloch equations in the rotating frame (46, 47). In particular, the saturation behavior of the linear response is predicted in agreement with experimental data and an evaluation of the line intensities for multispin systems is given. In his thesis (46), Bartholdi also evaluates the third-order nonlinear response of the Bloch equations in the rotating frame.

The nonlinear response of nuclear spin systems was investigated in a more empirical manner by Blümich and Ziessow (18, 48). Starting with an analysis of the characteristic saturation lineshapes in Hadamard NMR spectroscopy, a heuristic solution of the Bloch equations for arbitrary excitation was found in terms of a closed expression for a Volterra series. After the advent of 2D FT spectroscopy (9, 10) it was evident that the nonlinear stochastic response should reveal information similar to 2D NMR. Especially, the indirect spin coupling should be detectable. Different experimental schemes were tried (18) until the coupling information was indeed found in terms of cross-peaks in a 2D spectrum, which itself is a particular 2D cross-section through a 3D spectrum (49, 50). This cross-section not only revealed cross-peaks for indirect coupling (18, 49, 51, 52) but also for chemical exchange (18, 49-51). The excitation in these experiments was binary white noise, realized by a string of radiofrequency pulses with binary random phase modulation (52). A theory for the interpretation of the data was developed in the general language of time-dependent perturbation theory (18, 19, 51). It led to a definition of multi-dimensional spectra different from multiple pulse FT NMR and was able to explain the origin of the connectivity cross-peaks as well as the general lineshapes (19, 53). The characteristic saturation behavior (16-18, 51), however, could not be derived from it.

The general theory of stochastic NMR spectroscopy was developed by Kaiser and Knight (54, 55) in 1982. It gives the exact solutions of the density matrix equation of motion for cross-correlations of arbitrary order with Gaussian

white noise input. The theory insinuates to interpret the generation of multi-dimensional stochastic NMR spectra in terms of multiple pulse sequences similar to those encountered in multi-dimensional FT NMR. It explains how J-coupling, multiple quantum transitions, chemical exchange, cross-relaxation and relaxation times enter stochastic NMR spectra (19, 53, 56). This information is acquired summarily in a single stochastic experiment, because in contrast to pulsed excitation, which can be tailored to focus its energy on the measurement of specific effects, white noise is the most general form of excitation and thus is nonselective.

Recently, stochastic NMR has been tested on a modern commercial high resolution spectrometer (57, 58). It was demonstrated that for strong samples the multi-dimensional information can be derived from data acquired in less time and stored in less memory volume than necessary for the data of just one 2D experiment with comparable resolution. The present state of stochastic NMR will be reviewed in logical context in Sections IV and V.

B. Related Research

Apart from practical applications, stochastic NMR is an excellent example for testing the theories of stochastic differential equations (46, 47) and for studying the stochastic analysis of nonlinear systems. Stochastic processes and stochastic nonlinear systems are of great interest in current research in physics, chemistry and biology (59-62) and no attempt shall be made to cover this vast field of research. Rather a variety of fields is listed where stochastic nonlinear system analysis is applied, such that the method of stochastic NMR can be related to other research activities.

Two general classes are distinguished: the system response may be modulated either by an externally applied random force or by equilibrium fluctuations in the system itself. In order to gain insight into the properties of the system, the response is cross-correlated with the input in the first class, while in the second class the auto-correlation of the response is formed.

1. Systems Investigated by Cross-correlation

The mathematical term *cross-correlation* can be translated into popular English with the word *comparison*. The cross-correlation function of two signals shows characteristic peaks, whenever the signals are similar or alike. A comprehensive introduction to correlation methods in

chemical data measurement is given by Horlick and Hieftje (63).

Cross-correlation has been utilized originally for the detection of communication type signals and signal filtering (64-66). In system analysis the method was applied rather early for the characterization of nuclear reactors (67, 68) and electronic circuits (69). In analytical chemistry new techniques evolved such as stochastic chromatography (70), stochastic faradaic admittance measurements (71, 72), time-resolved fluorimetry (73-76), and stochastic photolysis (77). In biology, noise excitation is extensively used for the study of neural networks (78, 79). Also, the Hadamard transformation is applied in infrared spectroscopy (80-82).

Often, an advantage of stochastic over pulsed excitation is that the system is not driven far from equilibrium. This advantage, however, does not apply to NMR, since the nonlinear response to a single pulse of arbitrary flip angle is proportional to the linear response stimulated by a vanishingly small pulse (48). Therefore the flip angle can be optimized for maximum amplitude of the linear response in NMR. A further advantage of stochastic excitation is the time multiplexing of the input. Deviations from ideality of the input are averaged out, as long as the mean of the excitation is zero.

Typically most of the system analytical techniques evaluate only the linear response, not because the systems are all linear, but because the linear response theory is best understood and the experimental effort is relatively small. In the study of electronic and neural networks often the second-order response and rarely the third-order response are evaluated as well. Stochastic NMR is believed to be the first method which seriously exploits the third-order response.

A method for the characterization of the nonlinear response in rainfall-runoff processes has been proposed in hydrology (83) with a least-squares fitting procedure formulated instead of the cross-correlation method. The general theory of stochastic nonlinear system analysis is covered in recent books by Marmarelis and Marmarelis (79), Schetzen (84), and Rugh (85). Schetzen's book includes a historical bibliography.

2. Systems Investigated by Auto-correlation

The auto-correlation of a signal measures the coherence within the signal. For instance, if the signal modulation arises from fluctuating molecules, the auto-correlation function reveals information about the molecular motion (86, 87).

Given the size of molecules, light is often used in correlation spectroscopy (88-92). Other correlation techniques extract chemical kinetic information from fluorescence (93) and conductivity attenuation (94-96) measurements. The latter methods depend upon spontaneous fluctuations in local component concentrations. The development of auto-correlation methods shows great promise for the study of kinetic phenomena at equilibrium (63, 77).

III. PERTURBATIVE DESCRIPTIONS OF NONLINEAR SYSTEMS

A nonlinear system (Figure 1) transforms the input signal $x(t)$ into the output signal $y(t)$ in a nonlinear fashion. Since the details of the transformation are unknown, the system response is expanded into a series of the input. The most popular expansions in nonlinear system analysis are the Volterra (25) and the Wiener (26) series. A similar expansion is known in quantum mechanics by the name of *time-dependent perturbation theory* (19, 51).

A. Volterra Series

The Volterra functional series (25, 97) has been recognized by Wiener to be suitable for the description of the input/output relation of nonlinear systems (26). The output may be expanded into a power series of the input:

$$\begin{aligned} y(t) &= \sum_{n=0}^{\infty} y_n(t), \\ y_0(t) &= k_0, \\ y_1(t) &= \int_{-\infty}^{\infty} k_1(\tau) x(t-\tau) d\tau, \\ y_2(t) &= \int_{-\infty}^{\infty} \int_{-\infty}^{\infty} \bar{k}_2(\tau_1, \tau_2) x(t-\tau_1) x(t-\tau_2) d\tau_2 d\tau_1, \\ y_3(t) &= \int_{-\infty}^{\infty} \int_{-\infty}^{\infty} \int_{-\infty}^{\infty} \bar{k}_3(\tau_1, \tau_2, \tau_3) \times \\ &\quad x(t-\tau_1) x(t-\tau_2) x(t-\tau_3) d\tau_3 d\tau_2 d\tau_1. \end{aligned} \quad (1)$$

Each expansion term is a function of the input function. A function of a function is called a *functional*. The time dependence of the functionals depends on the input as well as on the particular system. The system part reflects the memory of the system. For instance, the free oscillation of a pendulum in response to an impulsive input demonstrates that while the response has not completely relaxed, the system still memorizes the input. The memory time is given by the damping constant of the free response. Most systems encountered in real life have finite

memory and the impulse response dies away with time.

For linear systems, the higher order responses y_i , $i > 1$ are zero and the impulse response is given by k_1 . In NMR k_1 is the free induction decay (FID). The functions \bar{k}_i are called kernels in mathematics. The bar marks their invariance against permutation of time arguments. The number of arguments is specified by the index and is equal to the order of the excitation product in the functional. Since physical systems do not anticipate an input, all kernels vanish if a time argument assumes a negative value.

The input/output relationship (eqn. 1) has been formulated for time-invariant systems. For time-dependent systems, the kernels also depend on the time t . Complete knowledge of all kernels entirely characterizes the system. In different disciplines the kernels are called by different names and often their Fourier transforms are primarily referred to. The kernels are also denoted as *after effect functions* or *response functions* of different order. Their Fourier transforms are known as *nonlinear transfer functions*, *generalized admittances*, or *susceptibilities*, or as *multi-dimensional spectra*. The denomination of the kernel Fourier transforms as spectra is rather old in theory of nonlinear systems (98, 99). Recently, their relationship to the multi-dimensional spectra encountered in FT NMR spectroscopy has been elaborated (19). Remembering that k_1 is the FID, it is obvious to NMR spectroscopists to call its Fourier transform a spectrum.

The Volterra series is an expansion in terms of nonlinear convolutions. Though the concept is formally appealing, the series is often found to converge slowly or not at all. For simulation and analysis of the system response an expansion with good convergence properties is needed. Such an expansion was derived by Wiener from the Volterra series by orthogonalization of functionals with respect to Gaussian white noise input (26). Wiener has focused his attention on Gaussian white noise, because 1) noise is the most general test signal for nonlinear systems, and 2) the orthogonal expansion assumes its simplest form for a Gaussian input distribution. The Wiener series can be shown to converge in the least squares sense.

B. Wiener Series

The Wiener Series is an expansion of the system response to zero mean Gaussian white noise input into a set of orthogonal functionals. An orthogonal expansion is advantageous

whenever the system response is to be approximated in the least-squares sense by a varying number of functionals or if the kernels are to be computed by multi-dimensional cross-correlation. The Wiener series is derived from the Volterra series by Schmidt orthogonalization of higher order functionals with respect to the lower order ones. Consequently the lower order Wiener kernels involve parts of the higher order Volterra kernels (79) and therefore depend on the input power. Denoting the Wiener kernels by \hat{h}_i and the second moment or power level of the Gaussian white noise input by μ_2 , the first terms of the Wiener series are given by (26, 27):

$$\begin{aligned} y(t) &= \sum_{n=0}^{\infty} \hat{y}_n(t), \\ \hat{y}_0(t) &= h_0, \\ \hat{y}_1(t) &= \int_{-\infty}^{\infty} \hat{h}_1(\tau) x(t-\tau) d\tau, \\ \hat{y}_2(t) &= \iint_{-\infty}^{\infty} \hat{h}_2(\tau_1, \tau_2) x(t-\tau_1) x(t-\tau_2) d\tau_2 d\tau_1 - \\ &\quad \mu_2 \int_{-\infty}^{\infty} \hat{h}_2(\tau_2, \tau_2) d\tau_2, \\ \hat{y}_3(t) &= \iiint_{-\infty}^{\infty} \hat{h}_3(\tau_1, \tau_2, \tau_3) x(t-\tau_1) x(t-\tau_2) x(t-\tau_3) d\tau_3 d\tau_2 d\tau_1 - \\ &\quad 3\mu_2 \iint_{-\infty}^{\infty} \hat{h}_3(\tau_1, \tau_2, \tau_2) x(t-\tau_1) d\tau_1 d\tau_2. \end{aligned} \quad (2)$$

The coefficients of the terms in the Wiener functionals are the coefficients in Hermite polynomials (27). For zero mean white noise with arbitrary distribution function the orthogonal functionals up to third order are given in (18) and (51). The power dependence of the Wiener kernels is manifested in stochastic NMR spectroscopy by saturation broadening (16-18, 49, 51). For vanishing input power only the leading term of each functional remains, and the Wiener series approaches the Volterra limit.

C. Cross-correlation

The goal in system analysis is the determination of the kernels from input and output records. Wiener originally proposed to expand the kernels into a set of orthogonal functionals and to determine the coefficients in a least-squares fitting procedure (18, 26, 83). However, Lee and Schetzen (27) showed in 1965 that the Wiener kernels are most easily retrieved by multi-dimensional cross-correlation of input and

output records. Cross-correlation has become a fundamental tool in the noise analysis of nonlinear systems.

Unless two or more time arguments are equal, the n 'th order kernel is proportional to the n 'th order cross-correlation

$$\int_{-\infty}^{\infty} y(t) x(t-\sigma_1) \cdots x(t-\sigma_n) dt = n! \mu_2^n h_n(\sigma_1, \dots, \sigma_n). \quad (3)$$

The values of the cross-correlation for equal time arguments depend on the particular distribution function of the white noise input (18, 51, 79).

A multi-dimensional cross-correlation operation can be visualized in terms of a multiple

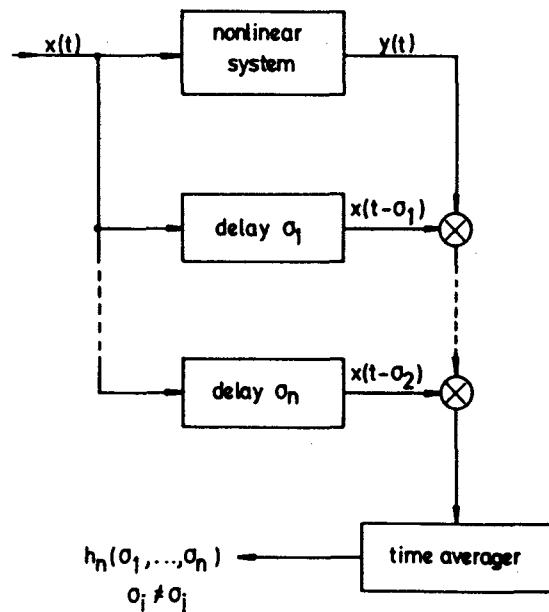


Figure 4. Analog representation of a multi-dimensional cross-correlation.

delay averager (Figure 4). The input signal $x(t)$ is applied not only to the nonlinear system under investigation, but also to a number of independent time delay devices. The delayed input signals are multiplied with the system response and the product is integrated over time.

An example for a 1D delay averager is the Michelson interferometer (88, 100), which forms the basis of Fourier infrared spectroscopy. The white input light is split into two beams. One beam passes through the sample and the other is

delayed by changing its path length with a movable mirror. Multiplication and integration of the two modified beams is achieved in a slow intensity detector. The detector measures the square of the sum or the two signals, which involves the cross-product of interest. The integration time is the detector response time, which is longer than a period of the infrared signal by several orders of magnitude. The time resolution of the interferometer is given by the resolution of the delay σ . Thus an analogue cross-correlator can achieve high time resolution with slow devices. For slow processes, such as NMR, input and output records are sampled and the cross-correlation is performed numerically on a digital computer.

D. Symmetry

In theory of nonlinear systems, kernels are defined symmetric with respect to permutation of time arguments. If an asymmetric kernel is encountered, it can be symmetrized without affecting the values of the functional simply by averaging all kernels which arise from permutation of arguments (26)

$$\bar{h}_n = h_{\text{sym}}(\tau_1, \dots, \tau_n) = \frac{1}{n!} \sum_{\text{perm.}} h_{\text{asym}}(\tau_1, \dots, \tau_n). \quad (4)$$

In mathematics, symmetric kernels are preferred because there is only one symmetric kernel for a given functional, but several asymmetric ones are possible. On the other hand, the expansion used in conventional time-dependent perturbation theory immediately leads to a Volterra series with asymmetric kernels (19). The n 'th order functional is given by

$$y_n(t) = \int_{-\infty}^{\infty} \int_{-\infty}^{\infty} \dots \int_{-\infty}^{\infty} h_n(\tau_1, \tau_2, \dots, \tau_n) \times x(t-\tau_1) x(t-\tau_2) \dots x(t-\tau_n) d\tau_n \dots d\tau_2 d\tau_1. \quad (5)$$

Its kernel vanishes outside the interval

$$0 \leq \tau_n \leq \dots \leq \tau_2 \leq \tau_1. \quad (6)$$

Kernels with the definition range of eqn. 6 are sometimes called *triangular kernels* (85). Such kernels obey the principle of causality in the sense that the time arguments of the excitation product in eqn. 5 render the excitation values distinguishable. By symmetrization the time variables are permuted and identical definition ranges are introduced. This artificially destroys the time ordered sequence of stimuli. Stochastic

NMR is a good example of how spectral information can be disguised by kernel symmetrization. Nonetheless, symmetric kernels are useful because their Fourier transforms can be computed rather quickly at selected spectral regions. To distinguish symmetric from triangular kernels, symmetric ones are marked by a bar.

The different triangular kernels obtained by permutation of arguments in eqn. 4 occupy different volume elements in multi-dimensional time space. The sum of all volume elements fills the entire time space. Symmetric as well as triangular kernels can be derived from input and output records by multi-dimensional cross-correlation. For symmetric kernels the definition ranges for the different delays are equal, while for the computation of triangular kernels the delays must be time ordered according to eqn. 6. A particularity arises at the boundaries of the triangular volume elements. If two or more time arguments are equal, the corresponding excitation values are indistinguishable and the triangular kernel value is given by the value of the symmetric kernel divided by the number of permutations of indistinguishable time arguments (19, 85).

E. Time Dependent Perturbation Theory

Iterative approximation of the solution of the density matrix equation of motion leads to a Volterra type expansion of a quantum mechanical observable (19, 51). In spectroscopy the observable is usually related to a sample polarization in response to an electric or magnetic field. The integration limits in the nonlinear perturbation functionals are time ordered as in eqns. 5 and 6. The resulting kernels are given in terms of multiple products of decaying exponentials which oscillate with the energy level differences of the unperturbed sample. The susceptibilities are the Fourier transforms of these triangular kernels. They are multiple products of Lorentzian lines, for example

$$H_{ba}^{(1)}(\omega_1) = \frac{-i\sigma[I_{x,\rho_0}]_{ba}}{[r_{ba} - i(\omega_1 - \omega_{ba})]}, \quad (7a)$$

$$H_{ba}^{(2)}(\omega_1, \omega_2) = \frac{-\sigma^2 \sum_c I_{bc}^* [I_{x,\rho_0}]_{ca}}{[r_{ca} - i(\omega_1 - \omega_{ca})][r_{ba} - i(\omega_1 + \omega_2 - \omega_{ba})]}, \quad (7b)$$

$$H_{ba}^{(3)}(\omega_1, \omega_2, \omega_3) = \frac{i\sigma^3 \sum_{cd} I_{bc}^* I_{cd}^* [I_x, \rho_0]_{da}}{[r_{da} - i(\omega_1 - \omega_{da})][r_{ca} - i(\omega_1 + \omega_2 - \omega_{ca})]} \times \frac{1}{[r_{ba} - i(\omega_1 + \omega_2 + \omega_3 - \omega_{ba})]} \quad (7c)$$

In these equations, σ measures the excitation amplitude, I_x is the x-component of the dipole moment operator, ρ_0 is the equilibrium density matrix, r is a phenomenological relaxation rate and a,b,c,d number succeeding energy levels. In the second- and third-order susceptibilities (eqns. 7b and 7c), ω_{ba} and ω_{ca} resonate at sum and difference frequencies of the input frequencies ω_1 , ω_2 and ω_3 . At resonance, the input frequencies are single quantum transitions. Consequently the higher order susceptibilities describe multiple quantum transitions. They are responsible for a wide range of frequency mixing phenomena encountered in nonlinear optics (101-105).

In contradistinction to NMR the optical wavelengths are small compared to typical sample dimensions and the optical polarization is not directly observed. The occurrence of sum and difference frequencies in the optical response is the result of scattering of induced sample polarizations. In NMR the wavelengths are large compared to the sample dimensions and the nuclear polarization is monitored directly. Sum and difference frequencies in the response can be observed with appreciable intensity only if they arise at a Larmor frequency.

F. Frequency Domain Analysis

Numerical computation of cross-correlations is extremely time consuming and becomes largely impossible if kernels higher than second order are to be evaluated. In spectroscopy, however, the Fourier transforms, not the kernels, are of primary concern. These can be obtained directly in the frequency domain by slicing the experimental excitation and response records into sample records $x_i(t)$ and $y_i(t)$ and Fourier transforming each record. The resulting sample spectra $X_i(\nu)$ and $Y_i(\nu)$ are multiplied and averaged. From Fourier transformation of eqn. 3 one obtains for first, second and third order (66, 106, 107)

$$H_1(\nu) = \frac{\langle Y(\nu) X^*(\nu) \rangle}{\langle |X(\nu)|^2 \rangle}, \quad (8a)$$

$$\bar{H}_2(\nu_1, \nu_2) = \frac{\langle Y_2(\nu_1 + \nu_2) X^*(\nu_1) X^*(\nu_2) \rangle}{2! \langle |X(\nu_1)|^2 |X(\nu_2)|^2 \rangle}, \quad (8b)$$

$$Y_2(\nu) = Y(\nu) - H_0,$$

$$\bar{H}_3(\nu_1, \nu_2, \nu_3) = \frac{\langle Y_3(\nu_1 + \nu_2 + \nu_3) X^*(\nu_1) X^*(\nu_2) X^*(\nu_3) \rangle}{3! \langle |X(\nu_1)|^2 |X(\nu_2)|^2 |X(\nu_3)|^2 \rangle} \quad (8c)$$

$$Y_3(\nu) = Y(\nu) - H_1(\nu) X(\nu),$$

where $2\pi\nu = \omega$. The second moment has been replaced by its frequency dependent estimate $\mu_2 = |X(\nu)|^2$. These formulas are valid only for zero mean Gaussian signals (18,51).

The frequency domain technique yields access to selected regions of a multi-dimensional spectrum without having to compute the complete multi-dimensional kernel. Since the spectral regions of interest in NMR can be predicted from the one-dimensional spectrum (eqn. 8a), tremendous savings in computation times result. The formulas for spectra of more than three dimensions can be extrapolated from the given ones, but no applications seem to have been published. This is attributed to increasing computational complexity as well as to decreasing signal strengths. For the computation of higher order spectra the lower order responses must be subtracted from the system response. Since in practice the amount of experimental data is finite, the different order spectra cannot be separated completely and the stronger signals of the lower order spectra cross-talk into the higher order spectra.

The frequency domain formulas yield the symmetrized spectra \bar{H}_n . By Fourier transformation of eqn. 4 they are recognized as the average of all asymmetric spectra which result from permutation of arguments (19)

$$\bar{H}_n(\nu_1, \dots, \nu_n) = (1/n!) \sum_{\text{perm.}} H_n(\nu_1, \dots, \nu_n). \quad (9)$$

In order to relate the signals within a selected region of a symmetric spectrum to the different asymmetric spectra, it has been proposed to transform the part of interest of \bar{H}_n into the time domain, select a triangular kernel element and

back-transform it into the frequency domain (56).

IV. THEORY OF STOCHASTIC NMR

The general theory of stochastic NMR with Gaussian white noise excitation was formulated by Kaiser and Knight (54, 55). By converting the Bloch equations into an integral equation, the previous method of solution (46, 47) was simplified and generalized. The theory yields cross-correlations of the magnetization with arbitrary powers of the excitation. These are neither restricted to equal relaxation times nor to a rotating coordinate frame.

The Bloch kernels exhibit different longitudinal and transverse saturation rates as well as a phase shift of the y-component of the response and a frequency shift of the resonance frequency from the Larmor frequency. Within the validity range of the Bloch equations, however, phase and frequency shifts are insignificantly small and the resulting multi-dimensional spectra exhibit the same lineshapes (eqn. 7) as derived by time-dependent perturbation theory (19, 53).

A response to odd order products in the excitation arises only in transverse magnetization, while a response to even order products results in longitudinal magnetization. This general feature is a consequence of the rotational symmetry of the problem: the transverse magnetization is proportional to the sine of the excitation flip angle and the longitudinal magnetization is proportional to the cosine. Either function expands into only odd or even powers of the excitation. Thus the first nonlinear response in stochastic NMR arises in third order.

The theory of stochastic NMR is based on Gaussian white noise input with unit spectral density. The input amplitude is traditionally denoted by σ (not to be confused with the delays in Figure 4). Because of the normalization of the input, σ has the physical dimension of Hz^2 . It is approximately related to the root mean square (rms) flip angle α_{rms} of a random sequence of pulses by

$$\alpha_{\text{rms}} \approx \sigma \sqrt{\Delta t}; \quad (10)$$

where Δt is the pulse spacing.

The variance of the transverse magnetization is a function of the excitation amplitude σ and of the relaxation times (46, 47). There exists an optimum excitation value σ_{opt} for which the transverse response is maximal. The maximum peak height in the first-order Bloch spectrum is reached for a value of σ just below σ_{opt} , that in

the third-order spectrum for a value just above σ_{opt} (51, 53). Since the maxima are rather broad, peak heights for 1D and 3D spectra as well as sensitivity are optimized simultaneously in the response maximum.

The validity of solution of the stochastic Bloch equations is confirmed by a numerical simulation of a 2D cross-section through the symmetric third-order spectrum (53). Different 1D cross-sections through the asymmetric third-order spectrum can be employed for the determination of longitudinal and transverse relaxation rates independent of magnetic field inhomogeneity. Other 1D cross-sections exhibit peaks at the line positions of the conventional 1D spectra but with saturation dependent linewidths, which, compared to the widths in single pulse response spectra, can be narrower by a factor of down to 0.66 in the response maximum (53).

The stochastic density matrix equation of motion was solved by the same method developed for the Bloch equations (55). The intricate path of solution will not be repeated, but the results of the multi-dimensional cross-correlations are rather simple. They admit a pictorial interpretation in terms of a pseudo-pulse experiment, which is exemplified below with the third-order response.

A. Interpretation of Kernels

The n 'th order triangular Wiener kernel of the density matrix equation of motion is (55)

$$h_n(\tau_1, \dots, \tau_n) = \frac{(\sigma/2)^n}{n!} \langle e^{\mathbf{C}\tau_1} \mathbf{B} e^{\mathbf{C}\tau_2} \dots \mathbf{B} e^{\mathbf{C}\tau_n} \rangle \quad (11)$$

The result is general, but the notation will be explained with respect to NMR. The operator \mathbf{C} is the effective Liouvillean

$$\mathbf{C} = -i\mathbf{H}_0^D - \mathbf{F} - \frac{1}{2}(\sigma \mathbf{F}_x^D)^2 + \Xi. \quad (12)$$

\mathbf{H}_0^D is the commutator with the Hamiltonian of the unperturbed system. The imaginary term defines the energy levels and accounts for cross-peaks in nonlinear spectra, which are based for instance on the indirect coupling interaction. The real terms determine the lineshape of the linear spectrum and may also give rise to cross-peaks in higher order spectra. \mathbf{F} is the relaxation matrix and Ξ accounts for chemical exchange. The term quadratic in the excitation amplitude σ

causes saturation broadening. It distinguishes the effective Liouvillean from the Liouvillean of the free precession.

A simulation has proven that the relaxation matrix produces cross-peaks in the third-order spectrum for cross-relaxing spins. Similarly cross-peaks arising from intramolecular chemical exchange have been simulated (56) as well as measured (49-52). However, no peaks have been observed yet, which originate in the saturation term. The term should be expected to cause multiple quantum peaks from the absorption of several identical photons in the same way as multiple quantum signals are observed for critical excitation levels in the CW NMR of strongly coupled systems (108-110).

The matrix \mathbf{B} is the linear term of the pulse rotation operator $\exp\{i\alpha\mathbf{F}_x^D\}$. If F_x is the x-component of the total angular momentum operator, then \mathbf{B} denotes the imaginary commutator with F_x , for instance

$$\mathbf{B}|\bar{\rho}\rangle = i\mathbf{F}_x^D|\bar{\rho}\rangle = i[F_x, \bar{\rho}]. \quad (13)$$

Consequently \mathbf{B} performs an infinitesimal rotation and may be interpreted as a pseudo-pulse. The right hand side of eqn. 11 can then be read as the time evolution of an equilibrium density matrix $\bar{\rho}$ under a multiple pseudo-pulse excitation with variable pulse separations $\tau_{n-1}-\tau_n$. The time evolution of the density matrix between the pulses follows the effective Liouvillean \mathbf{C} . The fact that the pulses do not affect a finite rotation is a consequence of the statistical independence of the input.

The equilibrium density matrix $\bar{\rho}$ denotes the spin statistics in equilibrium with excitation and relaxation

$$|\bar{\rho}\rangle = -\mathbf{C}^{-1}\mathbf{F}|\rho_0\rangle. \quad (14)$$

In most cases the dynamic equilibrium density matrix $\bar{\rho}$ is distinguished from the thermodynamic equilibrium density matrix ρ_0 only by reduced population differences. Under rare circumstances, when two coupled resonances overlap such that a zero quantum transition frequency becomes comparable to or smaller than some characteristic relaxation rate, zero quantum elements will be excited (56).

The interpretation of eqn. 11 by a multiple pulse experiment is illustrated in Figure 5 for a three-dimensional kernel. Since the kernel acts as a memory function, which relates different events of the past to the present, the times τ_i count from the moment of observation into the past. In triple pulse spectroscopy, the time

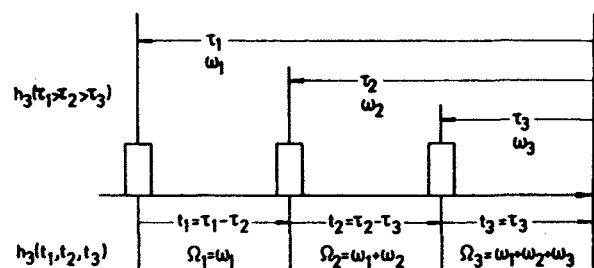


Figure 5. Time and frequency conventions in 3D stochastic NMR and triple pulse FT NMR. In FT NMR the pulses represent finite rotations of the density matrix while in stochastic NMR they represent infinitesimal rotations.

variables t_i denote the separation of events. A kernel written in the latter notation is called a *regular kernel* (85). In accordance with the different time conventions a kernel may be Fourier transformed either with respect to the τ_i yielding frequencies $\omega_i = 2\pi\nu_i$ or with respect to the t_i yielding frequencies Ω_i . In either case the result is a multidimensional spectrum. The peaks, however, are found at different coordinates (56). The interrelationship of frequencies is given in Figure 5. In the ω -coordinate frame of multidimensional spectra all peaks occur at the cross-coordinates of single quantum transitions.

Fourier transformation of the triangular third-order kernel yields the third-order susceptibility

$$H_3(\omega_1, \omega_2, \omega_3) = -(\sigma^3/8)\langle F_x | [+i(\omega_1 + \omega_2 + \omega_3)]^{-1} \mathbf{B} \times [\mathbf{C} + i(\omega_1 + \omega_2)]^{-1} \mathbf{B} [\mathbf{C} + i\omega_1]^{-1} \mathbf{B} |\bar{\rho}\rangle. \quad (15)$$

It can be written as a sum of various resonances if effective relaxation rates r are introduced to account for spin relaxation, saturation, and exchange in eqn. 12. Then the kernel, eqn. 7c, results, which has been derived by time dependent perturbation theory.

For the denominator to be at resonance, the individual frequencies ω_i , $i = 1, 2, 3$, must correspond to single quantum transitions, since only single quantum transitions are connected by infinitesimal rotations \mathbf{B} . The sum frequency

$\omega_1 + \omega_2 + \omega_3$ must also be a single quantum transition in order to match F_- . This can be explained with eqn. 8c: the kernel is computed from the response at the sum frequency. Since the response is measured at the Larmor frequency, the sum frequency must be a Larmor frequency just like the individual frequencies. Therefore one frequency in the sum must be negative. Positive frequencies signify absorption and negative frequencies signify emission of rf photons.

Reading eqn. 15 from right to left, the first **B** converts population differences to single quantum transitions. The second **B** establishes a connection to neighboring transitions with the sum coherence being a double quantum transition for progressive connectivity, a zero quantum transition for regressive connectivity or a population difference if the transition of the first **B** is reversed. The third **B** converts the population differences, zero and double quantum coherences to triple and single quantum coherences. Since only the latter are measured, the experimental third-order susceptibility carries connectivity information in terms of population effects, zero and double quantum transitions. Population effects are either coherent differential longitudinal magnetization exchange due to indirect coupling, or incoherent net longitudinal magnetization exchange caused by chemical exchange or cross-relaxation.

In the third-order spectrum, the connectivity information which involves two resonances (Larmor frequencies) arises from two quanta being absorbed at two transitions which share an energy level, and one quantum being emitted at either one of the transitions. Thus all connectivity peaks for two resonances are found on *sub-diagonal 2D cross-sections* through the third-order susceptibility, because such cross-sections are characterized by two positive frequencies and one negative frequency equal in magnitude to one of the positive frequencies. There is a total of 6 such 2D cross-sections in 3D frequency space, amounting to three pairs which separate the connectivity types according to population effects, zero quantum coherences and double quantum coherences.

B. Simulated Spectra

Because experimental data are evaluated in the frequency domain (cf. eqns. 8), the resulting spectra are symmetric. The six sub-diagonal 2D cross-sections through a symmetric 3D spectrum are equivalent. Each is the average of the 6 sub-diagonal 2D cross-sections through the

asymmetric 3D spectrum (cf. eqn. 9). Figure 6

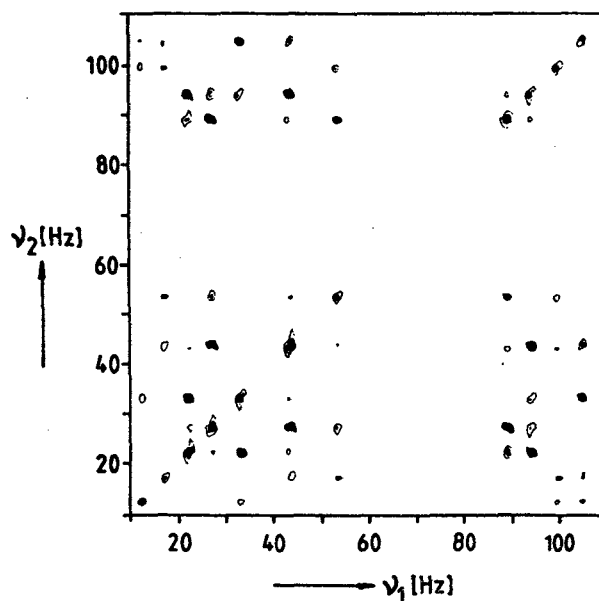


Figure 6. Simulated real part of the sub-diagonal 2D cross-section $\bar{H}_3(\nu_1, \nu_2, -\nu_2)$ through the symmetric 3D spectrum of 2,3-dibromopropionic acid. Negative signals are filled in black between the outer two contours.

shows the real part of the simulated cross-section $\bar{H}_3(\nu_1, \nu_2, -\nu_2)$ through the symmetric 3D spectrum of a three spin system. The simulation was based on eqns. 15 and 9. It is in excellent agreement with the experimental 90 MHz proton spectrum of 2,3-dibromopropionic acid in CDCl_3 (51). The 1D spectrum appears along the diagonal. Positive and negative cross-peaks on the corners of squares reveal the resonance connectivities. Negative peaks are filled in black. They indicate progressive connectivity. Positive cross-peaks indicate regressive connectivity. The arrangement of peaks is similar to the one in correlated 2D spectra measured with a $90^\circ - t_1 - 45^\circ - t_2$ pulse sequence (10, 111). Cross-peaks between resonances which are not direct neighbors in the energy level diagram do not occur.

The share of signals in Figure 6 which arises from population transfer is shown in Figure 7. It is the sum of two cross-sections, through the asymmetric 3D spectrum. The particular sub-diagonal 2D cross-sections are identified from the

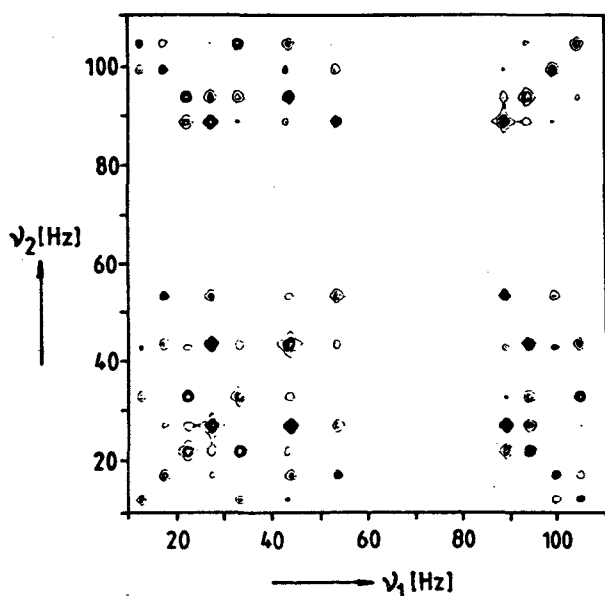


Figure 7. The sum spectrum $H_3(\nu_2, -\nu_2, \nu_1) + H_3(-\nu_2, \nu_2, \nu_1)$ has the depicted pure absorption mode real part. The cross-peaks arise from coherent longitudinal magnetization exchange.

condition that $\omega_1 + \omega_2 = 0$ must be fulfilled in eqns. 7c or 15. They are $H_3(\nu_2, -\nu_2, \nu_1)$ and $H_3(-\nu_2, \nu_2, \nu_1)$. The peak positions in Figure 7 agree with those in Figure 6, but the lineshapes are now pure Lorentzian. Some peaks, which do not belong to a cross-multiplet originate in the overlapping tails of resonances. Other than in Figure 6, the average intensity of a cross-multiplet is now zero, unless the spins are also coupled by chemical exchange or cross-relaxation. Chemical exchange causes strong positive cross-peaks. For cross-relaxation the cross-peaks are positive for long correlation times and negative for short correlation times (56) in agreement with 2D FT spectroscopy (112).

The 2D FT experiment for the detection of longitudinal magnetization exchange employs three pulses (113, 114). The pulse separation t_2 between the second and the third pulse is a fixed mixing time. The 2D Fourier transformation is applied with respect to the separation t_1 of the first and the second pulse and the detection period t_3 after the third pulse. The stochastic 3D spectrum also includes a Fourier transformation over the mixing time, so that peak intensities

there reflect the integral over all mixing times.

A further difference between 2D and stochastic NMR results from the difference between real pulses and pseudo pulses: in 2D FT exchange spectra coherent longitudinal magnetization exchange does not contribute to cross-peaks, but multiple quantum coherences do (112-115). In stochastic NMR the situation is inverted. Multiple quantum contributions are not found in the cross-sections in question, but cross-peaks from coherent magnetization exchange superpose exchange peaks. One way to discard the coherent exchange peaks is to replace each peak by the average of the cross-multiplet.

Sub-diagonal 2D cross-sections with zero or double quantum peaks are identified in the third-order susceptibility eqns. 7c or 15 by ω_1 and ω_2 having opposite signs or the same sign, respectively. Figure 8 shows the magnitude mode of the zero quantum cross-section $H_3(-\nu_2, \nu_1, \nu_2)$ and of the double quantum cross-section $H_3(\nu_2, \nu_1, -\nu_2)$. The zero quantum cross-peaks are found at the positions of the peaks indicating regressive connectivity in Figure 6 and the double quantum cross-peaks at the positions indicating progressive connectivity. The line-shapes of the peaks in the different cross-sections are discussed in (53, 56). The peak amplitudes do not add consistently so that apart from strong coupling effects, positive and negative cross-peaks in the cross-section (Figure 6) through the symmetrical spectrum show different intensity.

Spectra with zero or double quantum peaks at the cross-coordinates of single quantum transitions are rather easy to interpret. In 2D FT spectra, however, multiple quantum peaks are traditionally displayed at their actual multiple quantum frequencies. This is a convention based on the generating pulse sequence (cf. Figure 5), which requires a fixed preparation time t_1 . A 2D Fourier transformation is performed with respect to t_2 and t_3 (10). Stochastic zero and double quantum spectra can be transformed into this coordinate frame with the introduction of difference and sum frequencies (Figure 9). Mareci and Freeman have pointed out that inspection of the tilts of the cross-peak multiplets yields the relative signs of the coupling constants (116).

It is interesting to note that the double quantum signals can be isolated from the symmetric 3D spectrum if the input consists of two independent noise sources in quadrature (56). Unfortunately the peak amplitudes in the two double quantum sub-diagonal 2D cross-sections have opposite sign, so that apart from lineshape effects, the sum of the 2D double quantum

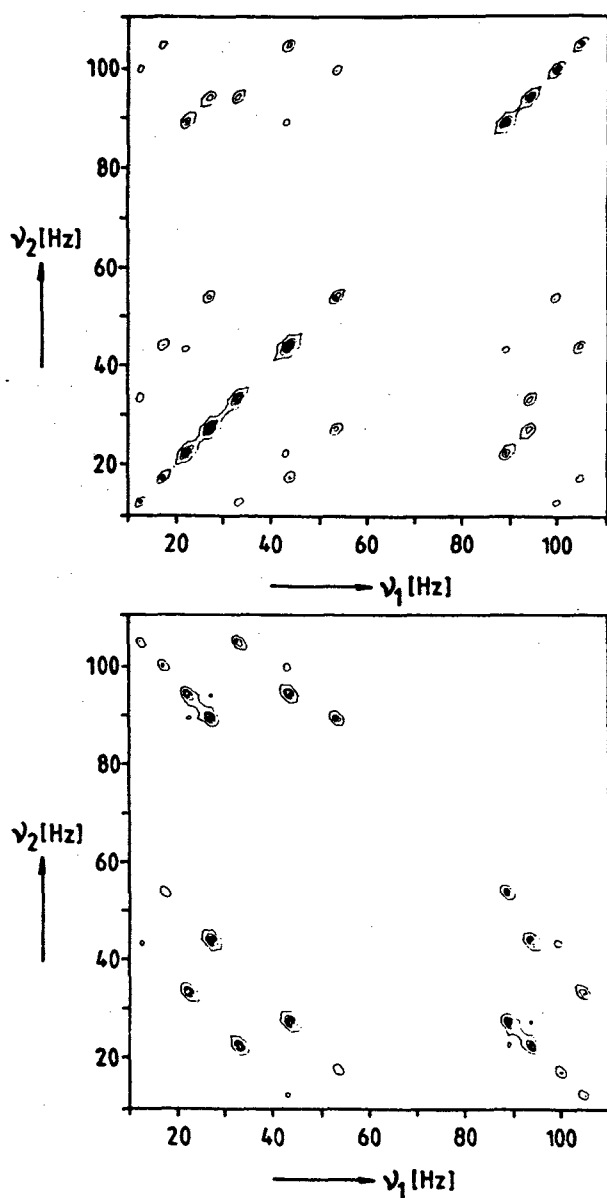


Figure 8. Zero quantum cross-section $|H_3(-\nu_2, \nu_1, \nu_2)|$ (top) and double quantum cross-section $|H_3(\nu_2, \nu_1, -\nu_2)|$ (bottom). The peaks occur at the cross-coordinates of single quantum transitions.

spectra vanishes.

The third-order susceptibility of coupled spin systems also exhibits cross-peaks, which do not lie on a sub-diagonal 2D cross-section. One such

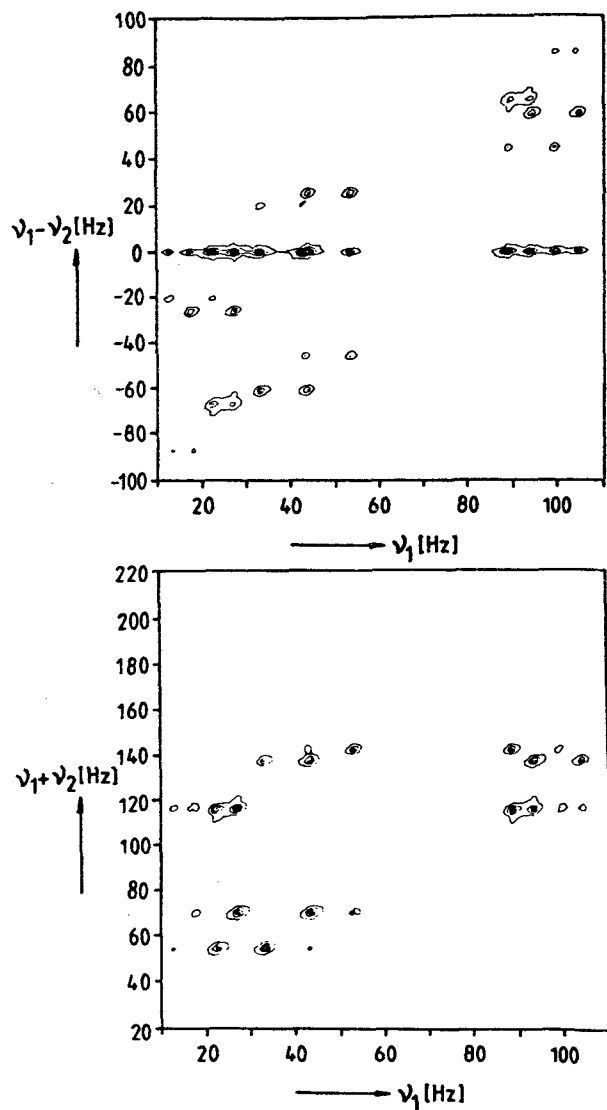


Figure 9. Introduction of a difference and a sum frequency axis transforms the peaks in Figure 8 into zero quantum frequencies (top) and double quantum frequencies (bottom).

cross-peak identifies three different resonances, which belong to a ring of four in the energy level diagram (51).

Stochastic excitation can also be employed in heteronuclear experiments. Both nuclear species

A and X shall be excited by the same input. If the response of species A is evaluated, then the 3D spectrum exhibits the cross-peaks of A with A and of A with those of nuclei of X, which are coupled to A (51). Heteronuclear stochastic NMR with two independent noise inputs has not been investigated yet.

V. PRACTICE OF STOCHASTIC NMR

The practical aspects of stochastic NMR are treated in (52). A commercial spectrometer has recently been converted to enable stochastic NMR in liquids (58). A detailed account of this work is available in a report (57). It includes complete circuit diagrams and program listings of the spectrometer modifications.

A. The Experiment

Most stochastic NMR experiments have been performed with a randomly modulated string of rf pulses as input. The basic timing diagram is given in Figure 3. Binary excitation is most easily realized with random shifts of the rf phase through $+90$ and -90 degrees. This introduces a random sequence of pulses with flip angles $+\alpha$ and $-\alpha$. In general, binary excitation is not feasible for the investigation of the nonlinear response, since kernel regions with two or more equal time arguments are underdetermined (117). It has been shown, however, that in the special case of NMR, the sub-diagonal 2D cross-section through the third-order spectrum can still be retrieved without error (18, 51). For the unambiguous determination of the complete third-order spectrum, noise input with four or more levels is required. It is readily generated by pulse width modulation (cf. Figure 3) (57).

The random sequence of numbers used for modulation is generated either by hardware or by software. Since a copy of the input is required for data processing, either the generating algorithm should be known, a copy should be resident on a data carrier, or the input values must be acquired simultaneously with the response. In the last case three analog-to-digital converter channels are needed to enable quadrature phase detection of the response. Shift register generation of binary excitation for investigation of the nonlinear response is unsuitable because of unfavorable higher order auto-correlation functions of m-sequences (118). In experiments with binary excitation the phase values were therefore often derived from the signs of sampled Gaussian white noise (18, 49-52).

In stochastic 100 MHz proton NMR a typical

flip angle is 3 degrees. Apart from the spectral width, the rms flip angle or the excitation amplitude is the only parameter to adjust in a stochastic experiment. It is tuned for maximum oscillations in the transverse magnetization either by feedback from the response or on the basis of estimated relaxation times and experience. After acquisition of 10^6 to 10^7 input and output values the experiment is terminated or repeated with the same excitation for coherent averaging of the response. The actual stochastic experiment is as simple as a CW experiment. The amount of information gained, however, is considerably more. Stochastic NMR acquires a large amount of information with a small amount of spectrometer time and experimental difficulty.

The stochastic raw data can be stored at low digital resolution (52, 57, 58), because the signal-to-noise ratio of the final spectra is determined to a large degree by systematic noise as a result of the finite amount of raw data. The discretization noise of the raw data is considerably reduced by the formation of averages (cf. eqns. 8) when calculating the spectra.

B. Data Evaluation

The simplicity of the stochastic NMR experiment is contrasted by more sophisticated data treatment. Once, however, the appropriate software has been designed, the experimenter will only have to ask for the conventional first-order spectrum, and after inspection possibly request higher spectral resolution or additional information on indirect coupling, chemical exchange, cross-relaxation, or relaxation times of selected multiplets. The answers to all these questions can, at least in principle, be obtained from a single set of experimental raw data.

The information is derived from the evaluation of multi-dimensional spectra (19, 53, 56), in particular the 1D and 3D spectrum. Ordinarily they are computed in the frequency domain according to eqns. 8a and 8c: the experimental record of data is sliced into sample records of equal length. All sample records are Fourier transformed. The resulting sample spectra are multiplied and averaged. Depending on the length of the sample records, spectra with different frequency resolution are obtained. The four 1D spectra in Figure 10 (57) have been computed with different resolution from the same 31800 input and output data pairs. Careful inspection shows that the noise level does not depend on the spectral resolution. It is primarily a function of the total number of data.

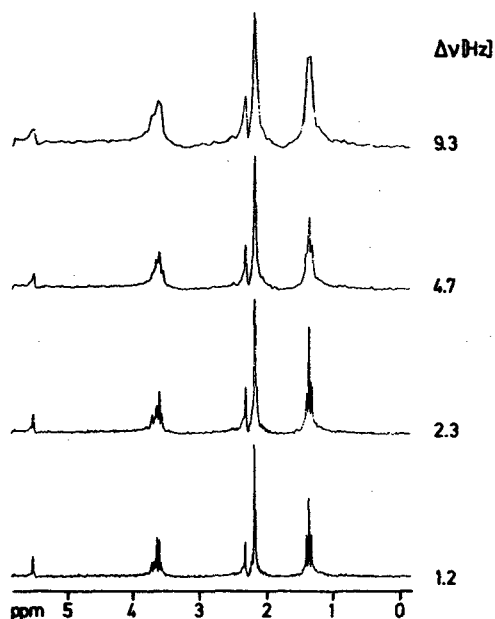


Figure 10. 1D magnitude spectra of acetylacetone and ethanol in acetone- d_6 . All spectra have been computed from the same 31800 data pairs but the length of the sample records varied from 256 to 512, 1024 and 2048 data, resulting in different spectral resolution $\Delta\nu$. The magnetization was scaled to less than 6 bits digital resolution.

The coupling information is gathered from the sub-diagonal 2D cross-section through the 3D spectrum. It is calculated for a series of frequency windows which are selected for the lines of interest in the 1D spectrum. Figure 11 gives an example. The data were measured with four-level excitation on a modified Varian XL200 spectrometer (57, 58) and evaluated on an IBM 3032 computer. The spectra have been computed from 10^6 data pairs which have been stored in 1 megabyte on disk. Each byte reserved 6 bits for the magnetization and 2 bits for the excitation. The data acquisition time was 25 minutes. The 1D spectrum was computed in 3 minutes; each of the 128×128 point 2D spectra was computed in 7 minutes. The 2D spectra have been phase adjusted in direction ν_1 with phase angles determined from the linear spectrum. They were then smoothed with a digital filter and symmetrized with respect to the diagonal (119) in order to reduce systematic noise and cross-talk from the

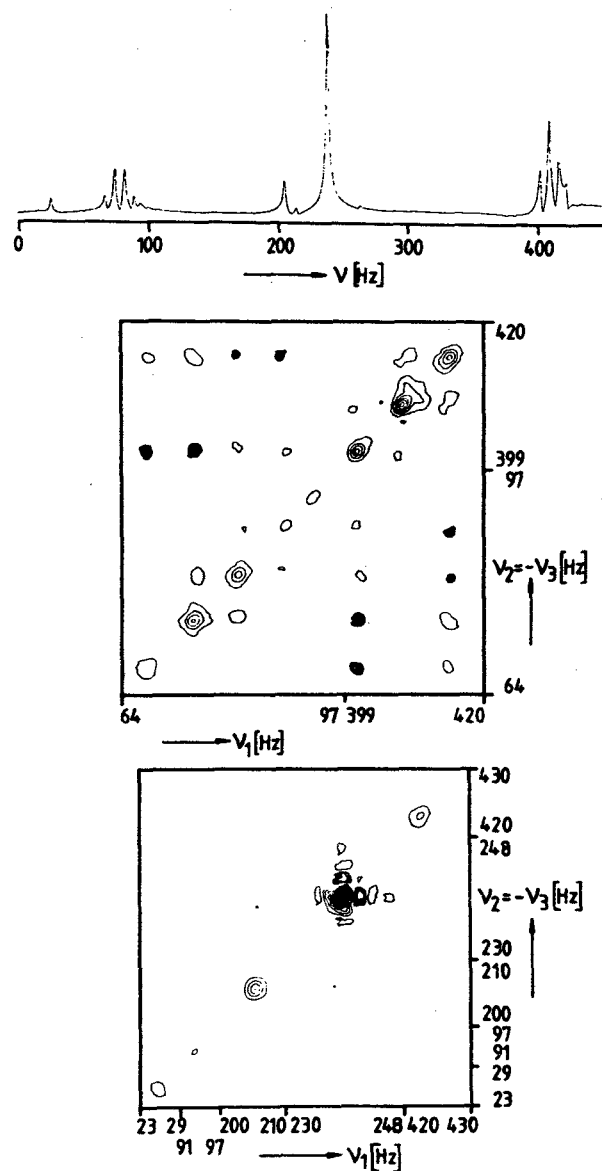


Figure 11. Spectra of acetylacetone and ethanol in methanol- d_4 which have been computed from 10^6 excitation and response data pairs. Top: first-order 1D magnitude spectrum. The water resonance has been folded to 420 Hz. Middle and bottom: sub-diagonal 2D cross-sections through the symmetric 3D spectrum for the ethanol and acetylacetone multiplets. Negative peaks are marked in black. The top and middle spectra are cited with permission from ref. (58).

1D spectrum. It should be noted that a 2D FT

experiment with comparable spectral resolution would require 60 minutes acquisition time and four times as much data storage volume. This difference is a consequence of the higher digital resolution and of the rigid pulse timing schemes in 2D FT NMR. These pulse schemes demand acquisition of a minimum number of data regardless of the signal intensity.

The different steps in the evaluation of the nonlinear response are summarized as follows:

- 1) Determination of the frequency windows of interest from the first-order spectrum.
- 2) Computation of the sub-diagonal 2D cross-section through the symmetric third-order spectrum at the coordinates of interest. High frequency resolution is necessary, so that application of a noise filter does not lead to intolerable line broadening.
- 3) Phase correction in direction ν_1 with phase values determined from the 1D spectrum.
- 4) Filtering of systematic noise.
- 5) Symmetrization of the cross-section with respect to the diagonal, possibly followed by additional filtering.
- 6) Two-color contour plot of the 2D cross-section for the discrimination of positive and negative peaks.

Indirectly coupled signals are identified by rectangular groups of cross-peaks with symmetrically alternating signs of the peak amplitudes. Chemical exchange and cross-relaxation lead to either positive or negative cross-peaks only. In the presence of indirect coupling the peak amplitudes of all effects are superimposed. To separate coupling from exchange or cross-relaxation peaks, the symmetric 3D spectrum must be decomposed into its asymmetric constituents by inverse Fourier transformation (56). Then the magnetization transfer cross-sections $H_3(\nu_2, -\nu_2, \nu_1)$ and $H_3(-\nu_2, \nu_2, \nu_1)$ must be isolated and the average formed of a cross-peak multiplet in the sum of these two spectra. The result is different from zero if chemical exchange or cross-relaxation are present.

The decomposition of a symmetric 3D spectrum still needs to be confirmed with experimental data. The same applies to the existence of cross-relaxation peaks and the determination of relaxation times. The latter can be derived from a least-squares fit of selected theoretical 1D cross-sections through a 3D resonance to experimental cross-sections, provided the excitation amplitude σ is known (53). It remains to be seen how accurate the method proves to be. Furthermore, it still needs to be investigated how far conformational information can be derived from stochastic cross-relaxation peaks, because they

correspond to an integral of mixing times in 2D FT NMR. A stochastic 2D cross-relaxation spectrum for a fixed mixing time can be derived from the raw data only by explicit cross-correlation in the time domain.

Stochastic zero and double quantum spectra are not believed to yield new information other than multiple quantum relaxation times. They essentially separate the regressive and progressive cross-peaks into different spectra. The same connectivity information is available from the phase of the cross-peaks in the symmetric 3D spectrum.

The simplicity of the experiment together with an appropriate software support for data evaluation designate stochastic NMR as a suitable candidate for highly automated nuclear magnetic resonance. The fundamental difference to other NMR methods is that stochastic NMR measures information nonselectively, while with tailored excitation schemes information is measured selectively. Stochastic excitation may be regarded as the sum of all tailored excitation sequences. Consequently spectrometer time is saved in stochastic NMR at the expense of computer time.

VI. DEVELOPMENTS IN STOCHASTIC RESONANCE

A. Time Resolved CIDNP Spectroscopy

In a chemically induced dynamic nuclear polarization (CIDNP) experiment two input signals are transformed into one output signal in a nonlinear fashion. Input 1 stimulates a chemical reaction. It is usually light, which is modulated in amplitude. Input 2 is a rf signal, which is modulated in amplitude, phase or frequency. The chemical stimulus creates a nuclear non-equilibrium state, which is interrogated by the rf input.

A particularly simple situation is created in a double pulse experiment. The first pulse is the chemical stimulus and the second is a rf pulse, which probes the progress of the stimulated reaction (120). This scheme has become the basis for fast submicrosecond time resolved flash photolysis (121). The time resolution of the double pulse experiment is limited by the length of the interrogating rf pulse, which itself is bound by the input power.

Random modulation of both input signals preserves the broadband character but drastically reduces the power requirements. In a theoretical study (122) it has been shown that the double pulse information can be obtained from

the second-order triangular cross-kernel in an experiment with two independent random binary inputs: amplitude modulated light and phase modulated rf. In multiple input nonlinear system analysis (69, 79) the cross-kernels relate to different inputs, while the auto-kernels relate to only one of the inputs.

The second-order cross-kernel for the CIDNP experiment is favorably retrieved by analog on-line cross-correlation for fast processes. In this way rapid sampling rates are avoided. The kernel transforms into a stack of pure CIDNP spectra. Each individual spectrum reflects a momentary state of the stimulated chemical reaction, so that the complete stack of spectra reveals the evolution of the reaction. It can be expected that this concept will also find application for the investigation of other time-dependent processes, such as dielectric and mechanic relaxation of liquid crystals or polymers.

B. NMR Imaging

The NMR imaging experiment (123) aims at the measurement of the spin density distribution as a function of space coordinates. For enhancement of image contrast in living tissues, the retrieved spin density should be weighted with a function of transverse and longitudinal relaxation times T_1 and T_2 . To achieve spacial resolution it is necessary to apply time-dependent magnetic field gradients across the sample. Thus there are four variables in an imaging experiment:

- 1) the shape of the radiofrequency input signals and
- 2-4) the modulation of x, y, and z gradients.

Consequently the imaging system is either a *four input time-invariant* system or a *one input time-dependent* system where the time dependence is imposed by the field gradients.

Stochastic excitation in NMR imaging has three advantages over conventional methods with sparsely pulsed rf input:

- 1) The excitation power is reduced by several orders of magnitude.
- 2) Since no deterministic pulse cycle exists, every additionally acquired data point increases the quality of the entire image.
- 3) For slowly moving objects, reconstruction of the image can be restricted to those data, during the acquisition of which the object was in approximately the same state.

When treating the imaging system as a linear time dependent system the spin density distribution can be retrieved under certain conditions by cross-correlation of the transverse magnetization with the product of the rf

excitation and functions of the field gradients. A particular three-dimensional imaging scheme with stochastic rf input and random field gradient modulation has recently been proposed (18, 124). T_2 contrast is varied in the image by selection of different time delays in the cross-correlation and T_1 contrast is achieved by proper selection of the rf excitation level during the experiment.

C. Stochastic ENDOR

In electron nuclear double resonance (ENDOR) spectroscopy (125), the electron spin resonance (ESR) is observed as a function of the NMR frequency. Due to the presence of radicals, the nuclear resonances may cover spectral widths of the order of MHz. Long nuclear relaxation times often impede rapid repetition of experiments. It has been shown (126, 127) that instead of a linear sweep, pulsed excitation at pseudo randomly selected nuclear frequencies circumvents the relaxation time problem and leads to increased measurement efficiency.

The ESR response is acquired as a function of the excitation frequency and accumulated for reoccurring frequencies. The frequency coordinates are selected in a way to insure that the average excitation history is the same for all frequencies. If the excitation amplitude is kept constant, then the response is proportional to the NMR spectrum plus a frequency independent term which involves the nuclear relaxation times.

D. Outlook

The primary accomplishments of stochastic NMR so far are, that development of the technique has significantly contributed to the understanding of stochastic differential equations and the perturbative noise analysis of nonlinear systems. These results are a consequence of the close connection between theory and experiment. The experience gained is expected to fertilize methodical research in other areas of science. In the past, for instance, the progress in nonlinear optics has benefitted significantly from methodical developments in NMR (128-133). The similarity of NMR and nonlinear optics is put into evidence, for instance, by the formal agreement of the nonlinear susceptibilities. The interpretation of the generation of multi-dimensional kernels in terms of multiple pseudopulse sequences has helped to develop new methods in time resolved spectroscopy and NMR imaging.

Stochastic excitation is distinguished from

continuous wave and sparsely pulsed excitation by low input power in connection with large bandwidth. This important property cannot be exploited in high resolution NMR in liquids, because here, excitation power is not a restricting factor. The situation is different in fast time resolved spectroscopy, imaging and wideline NMR in solids. The required large spectral bandwidths, however, need fast modulation rates and receiver deadtime is expected to demand careful attention.

The unique attributes of stochastic NMR are 1) that no minimum time for a data acquisition cycle exists, so that, at the expense of signal-to-noise ratio, strong samples can be investigated faster with stochastic NMR than with pulsed FT NMR. 2) Stochastic excitation extensively tests the sample and measures a maximum amount of information in a single experiment. This feature will be of particular interest for the investigation of short-lived samples and samples with little *a priori* information. 3) An experiment with stochastic excitation is particularly simple to perform and the data processing is rather complex.

The last feature is likely to stimulate application and development of new data processing schemes. In particular, the various methods of time series analysis (134) known in geophysics have not been exploited yet. With regard to the slicing of the experimental raw data into sample records for the computation of the spectrum, it can be expected that spectral estimation (135) of the sample records by means of the *maximum entropy method* (MEM) (136) instead of an ordinary Fourier transformation will lead to increased resolution with shorter records. MEM extrapolates the length of a given record such that its entropy is maximized (137). Application of such techniques should balance some of the signal loss induced by grouping functionally related response data points into independently used sample records.

Other stochastic stimuli such as multi-level constant amplitude random phase signals deserve investigation with regard to excitation and saturation properties. The results will be of interest to the understanding of strongly driven atomic transitions in LASER noise fields (138).

So far stochastic NMR has only been applied to the measurement of ^{19}F (14) and protons. Single phase detection has been used throughout. Applications to ^{13}C , heteronuclear systems and solids have not been reported yet. Further practical experience is needed to determine how far stochastic NMR will turn out to be a competitor to presently established NMR methods.

Acknowledgments

The author's contributions to the development of stochastic NMR spectroscopy have benefitted from stimulating cooperation with Professors D. Ziessow and R. Kaiser. Support by the DAAD (Deutscher Akademischer Austauschdienst) with a NATO overseas fellowship and by the DFG (Deutsche Forschungsgemeinschaft) with travel grants and a research stipend is gratefully acknowledged.

REFERENCES

- ¹E. M. Purcell, H. C. Torrey, and R. V. Pound, *Phys. Rev.* **69**, 37 (1946).
- ²F. Bloch, W. W. Hansen, and M. Packard, *Phys. Rev.* **69**, 127 (1946).
- ³F. Bloch, *Phys. Rev.* **70**, 460 (1946).
- ⁴W. A. Anderson and R. Freeman, *J. Chem. Phys.* **37**, 85 (1962).
- ⁵R. Freeman and W. A. Anderson, *J. Chem. Phys.* **37**, 2053 (1962).
- ⁶R. Kaiser, *J. Chem. Phys.* **39**, 2435 (1963).
- ⁷I. J. Lowe and R. E. Norberg, *Phys. Rev.* **107**, 46 (1957).
- ⁸R. R. Ernst and W. A. Anderson, *Rev. Sci. Instrum.* **37**, 93 (1966).
- ⁹J. Jeener, *Ampère International Summer School II, Basko Polje, Yugoslavia*, 1971, unpublished.
- ¹⁰W. P. Aue, E. Bartholdi, and R. R. Ernst, *J. Chem. Phys.* **64**, 2229 (1976).
- ¹¹R. Freeman and G. A. Morris, *Bull. Magn. Reson.* **1**, 5 (1979).
- ¹²R. Freeman, *Proc. Roy. Soc. Lond., Ser. A* **373**, 149 (1980).
- ¹³R. Benn and H. Günther, *Angew. Chem.* **22**, 350 (1983).
- ¹⁴R. R. Ernst, *J. Magn. Reson.* **3**, 10 (1970).
- ¹⁵R. Kaiser, *J. Magn. Reson.* **3**, 28 (1970).
- ¹⁶E. Bartholdi, *Theorie der stochastischen Kernresonanz: Das Modell der stochastischen Differentialgleichung*, Dissertation 5638, ETH Zürich, 1975.
- ¹⁷E. Bartholdi, A. Wokaun, and R. R. Ernst, *Chem. Phys.* **18**, 57 (1976).
- ¹⁸B. Blümich, *Nichtlineare Rauschanalyse in der magnetischen Kernresonanzspektroskopie*, Dissertation, TU Berlin, D83, 1981.
- ¹⁹B. Blümich and D. Ziessow, *Mol. Phys.* **48**, 955 (1983).
- ²⁰H. Primas, *Helv. Phys. Acta* **34**, 36 (1961).
- ²¹R. Kubo and K. Tomita, *J. Phys. Soc. Jap.* **9**, 888 (1954).
- ²²R. Kubo, *J. Phys. Soc. Jap.* **9**, 935 (1954).
- ²³W. Bernard and H. B. Callen, *Rev. Mod. Phys.* **31**, 1017 (1959).

- ²⁴A. Abragam, *The Principles of Nuclear Magnetism*, Oxford Univ. Press, Oxford, 1961.
- ²⁵V. Volterra, *Theory of Functionals*, Dover, New York, 1959.
- ²⁶N. Wiener, *Nonlinear Problems in Random Theory*, Wiley, New York, 1958.
- ²⁷Y. W. Lee and M. Schetzen, *Int. J. Control* **2**, 237 (1965).
- ²⁸R. R. Ernst and H. Primas, *Helv. Phys. Acta* **36**, 583 (1963).
- ²⁹R. R. Ernst, *Kernresonanz-Spektroskopie mit stochastischen Hochfrequenzfeldern*, Dissertation Nr. 3300, ETH Zürich, 1962.
- ³⁰R. R. Ernst, *J. Chem. Phys.* **45**, 3845 (1966).
- ³¹R. R. Ernst, *Adv. Magn. Reson.* **2**, 1 (1966).
- ³²B. L. Tomlinson and H. D. W. Hill, *J. Chem. Phys.* **59**, 1775 (1973).
- ³³D. Ziessow and S. R. Lipsky, *J. Phys.* **E5**, 437 (1972).
- ³⁴D. E. Wemmer, E. K. Wolf, and M. Meh-ring, *J. Magn. Reson.* **42**, 460 (1981).
- ³⁵J. Dadok and R. F. Sprecher, *J. Magn. Reson.* **13**, 243 (1974).
- ³⁶R. K. Gupta, J. A. Ferretti, and E. D. Becker, *J. Magn. Reson.* **13**, 275 (1974).
- ³⁷J. A. Ferretti and R. R. Ernst, *J. Chem. Phys.* **65**, 4283 (1976).
- ³⁸D. Ziessow, *On-line Rechner in der Chemie*, de Gruyter, Berlin, 1973.
- ³⁹D. Ziessow and B. Blümich, *Ber. Bunsenges. Phys. Chem.* **78**, 1168 (1974).
- ⁴⁰R. Kaiser, *J. Magn. Reson.* **15**, 44 (1974).
- ⁴¹G. A. Korn, *Random Process, Stimulation and Measurement*, McGraw-Hill, New York, 1966, p. 83-.
- ⁴²W. K. Pratt, J. Kane, and H. C. Andrews, *Proc. IEEE* **57**, 58 (1969).
- ⁴³R. R. Ernst, *Herbstschule über Hochfrequenzspektroskopie*, Leipsig, 1969, p. 31-.
- ⁴⁴L. Arnold, *Stochastische Differentialgleichungen*, Oldenburg, München, 1973.
- ⁴⁵I. I. Gichman and A. W. Skorochod, *Stochastische Differentialgleichungen*, Akademie-Verlag, Berlin, 1971.
- ⁴⁶E. Bartholdi, *Theorie der stochastischen Kernresonanz. Das Modell der stochastischen Differentialgleichung*, Dissertation Nr. 5638, ETH Zürich, 1975.
- ⁴⁷E. Bartholdi, A. Wokaun, and R. R. Ernst, *Chem. Phys.* **18**, 57 (1976).
- ⁴⁸B. Blümich and D. Ziessow, *J. Magn. Reson.* **46**, 385 (1982).
- ⁴⁹B. Blümich and D. Ziessow, *Ber. Bunsenges. Phys. Chem.* **84**, 1090 (1980).
- ⁵⁰B. Blümich and D. Ziessow, *Bull. Magn. Reson.* **2**, 299 (1981).
- ⁵¹B. Blümich and D. Ziessow, *J. Chem. Phys.* **78**, 1059 (1983).
- ⁵²B. Blümich and D. Ziessow, *J. Magn. Reson.* **52**, 42 (1983).
- ⁵³B. Blümich, *Mol. Phys.* **48**, 969 (1983).
- ⁵⁴W. R. Knight and R. Kaiser, *J. Magn. Reson.* **48**, 293 (1982).
- ⁵⁵R. Kaiser and W. R. Knight, *J. Magn. Reson.* **50**, 467 (1982).
- ⁵⁶B. Blümich and R. Kaiser, *J. Magn. Reson.* **54**, 486 (1983).
- ⁵⁷B. Blümich, *Stochastic NMR on the XL200*, Report, Physics Department, University of New Brunswick at Fredericton, 1983. Available from the author upon request.
- ⁵⁸B. Blümich and R. Kaiser, *J. Magn. Reson.* **58**, 149 (1984).
- ⁵⁹N. G. van Kampen, *Stochastic Processes in Physics and Chemistry*, North-Holland, Amsterdam, 1981.
- ⁶⁰L. Arnold and R. Lefever, Eds., *Stochastic Nonlinear Systems in Physics, Chemistry, and Biology*, Springer, Berlin, 1981.
- ⁶¹C. De Witt-Morette and K. D. Elworthy, Eds., *New Stochastic Methods in Physics*, North-Holland, Amsterdam, 1981.
- ⁶²G. S. Agarwal and S. Dattagupta, Eds., *Stochastic Processes, Formalism and Applications*, Springer, Berlin, 1983.
- ⁶³G. Horlick and G. M. Hieftje, *Cont. Top. Anal. Clin. Chem.* **3**, 153 (1978).
- ⁶⁴Y. W. Lee, *Statistical Theory of Communication*, Wiley, New York, 1960.
- ⁶⁵F. H. Lange, *Correlation Techniques*, Van Nostrand, Princeton, 1967.
- ⁶⁶J. S. Bendat and A. G. Piersol, *Random Data: Analysis and Measurement Procedures*, Wiley-Interscience, New York, 1971.
- ⁶⁷R. E. Uhrig, *Neutron Noise Waves and Pulse Propagation*, Proc. Sym. Univ. Florida, 1967.
- ⁶⁸W. Bastl, *Regelungsmechanik* **14**, 56 (1966).
- ⁶⁹J. J. Bussgang, L. Ehrman, and J. W. Graham, *Proc. IEEE*, **62**, 1088 (1974).
- ⁷⁰R. Annino and L. E. Bullock, *Anal. Chem.* **45**, 1221 (1973).
- ⁷¹S. C. Creason and D. E. Smith, *J. Electroanal. Chem.* **36**, App. 1 (1972).
- ⁷²S. C. Creason, J. W. Hayes, and D. E. Smith, *Electroanal. Chem. Interfac. Chem.* **47**, 9 (1973).
- ⁷³G. M. Hieftje and E. E. Vogelstein in *Modern Fluorescence Spectroscopy*, E. L. Wehry, Ed., Chapt. 2, Plenum, New York, 1981.
- ⁷⁴G. M. Hieftje and G. R. Haugen, *Anal. Chem.* **53**, 755A (1981).
- ⁷⁵J. M. Ramsey, G. M. Hieftje, and G. R.

- Haugen, *Applied Optics* **18**, 1913 (1979).
- ⁷⁶C. C. Dorsey, M. J. Pelletier, and J. M. Harris, *Rev. Sci. Instrum.* **50**, 333 (1979).
- ⁷⁷G. R. Haugen, G. M. Hieftje, L. L. Steinmetz, and R. E. Russo, *Appl. Spectrosc.* **36**, 203 (1982).
- ⁷⁸G. Hung and L. Stark, *Math. Biosc.* **37**, 135 (1977).
- ⁷⁹P. Z. Marmarelis and V. Z. Marmarelis, *Analysis of Physiological Systems: the White Noise Approach*, Plenum, New York, 1978.
- ⁸⁰J. A. Decker Jr. and M. O. Harwitt, *Appl. Optics* **8**, 2552 (1969).
- ⁸¹E. D. Nelson and R. Fredman, *J. Opt. Soc. Am.* **60**, 1664 (1970).
- ⁸²M. Harwit and N. J. A. Sloane, *Hadamard Transform Optics*, Academic Press, New York, 1979.
- ⁸³J. Amorochio and A. Brandstetter, *Water Resources Res.* **7**, 1087 (1971).
- ⁸⁴M. Schetzen, *The Volterra and Wiener Theories of Nonlinear Systems*, Wiley, New York, 1980.
- ⁸⁵W. J. Rugh, *Nonlinear Systems Theory: The Volterra/Wiener Approach*, Johns Hopkins University Press, Baltimore, 1981.
- ⁸⁶R. G. Gordon, *Adv. Magn. Reson.* **3**, 1 (1968).
- ⁸⁷B. J. Berne and G. D. Harp, *On the Calculation of Time Correlation Functions*, *Adv. Chem. Phys.*, XVII, Wiley, New York, 1970.
- ⁸⁸E. Wolf, *Jap. J. Appl. Phys.* **4**, 1 (1965).
- ⁸⁹B. J. Berne and R. Pecora, *Dynamic Light Scattering*, Wiley, New York, 1978.
- ⁹⁰H. Z. Cummins and E. R. Pike, Eds., *Photon Correlation and Light Beating Spectroscopy*, Plenum, New York, 1974.
- ⁹¹R. E. Pike and E. Jakeman, *Adv. Quant. Electr.* **2**, 1 (1974).
- ⁹²W. Buchard and G. D. Patterson, *Light Scattering from Polymers*, *Adv. Polym. Science* **48**, Springer, Berlin, 1983.
- ⁹³E. L. Elson and D. Magde, *Biopolymers* **13**, 1 (1974).
- ⁹⁴G. Feher and M. Weissman, *Proc. Nat. Acad. Sci. USA* **70**, 870 (1973).
- ⁹⁵Y.-D. Chen, *Adv. Chem. Phys.* **37**, 67 (1978).
- ⁹⁶Y.-D. Chen, *J. Chem. Phys.* **59**, 8510 (1973).
- ⁹⁷V. Volterra, *Rend. R. Accademia dei Lincei*, 2 Sem., 1887, pp. 97-105, 141-146, and 153-158.
- ⁹⁸D. R. Brillinger, *Ann. Math. Stat.* **36**, 1351 (1965).
- ⁹⁹D. R. Brillinger, *J. Sound. Vib.* **12**, 301 (1970).
- ¹⁰⁰A. A. Michelson, *Light Waves and their Uses*, The Univ. of Chicago Press, Chicago, 1903.
- ¹⁰¹N. Bloembergen, *Nonlinear Optics*, Benjamin, New York, 1965.
- ¹⁰²P. D. Maker and R. W. Terhune, *Phys. Rev.* **137**, A801 (1965).
- ¹⁰²M. D. Levenson, *Introduction to Nonlinear Laser Spectroscopy*, Academic Press, New York, 1982.
- ¹⁰⁴N. Bloembergen, *Rev. Mod. Phys.* **54**, 685 (1982).
- ¹⁰⁵R. M. Hochstrasser and H. P. Trommsdorf, *Acc. Chem. Res.* **16**, 376 (1983).
- ¹⁰⁶A. S. French and E. G. Butz, *Int. J. Control*, **17**, 529 (1973).
- ¹⁰⁷A. S. French, *Biol. Cybern.* **24**, 111 (1976).
- ¹⁰⁸S. Yatsiv, *Phys. Rev.* **113**, 1522 (1958).
- ¹⁰⁹W. A. Anderson and R. Freeman, *J. Chem. Phys.* **39**, 1518 (1963).
- ¹¹⁰P. L. Corio, *Structure of High-Resolution NMR Spectra*, Academic Press, New York, 1966.
- ¹¹¹A. Bax and R. Freeman, *J. Magn. Reson.* **44**, 542 (1981).
- ¹¹²S. Macura, Y. Huang, D. Suter, and R. R. Ernst, *J. Magn. Reson.* **43**, 259 (1981).
- ¹¹³J. Jeener, B. H. Meier, P. Bachmann, and R. R. Ernst, *J. Chem. Phys.* **71**, 4546 (1979).
- ¹¹⁴S. Macura and R. R. Ernst, *Mol. Phys.* **41**, 95 (1980).
- ¹¹⁵S. Macura, K. Wüthrich, and R. R. Ernst, *J. Magn. Reson.* **47**, 351 (1982).
- ¹¹⁶T. H. Mareci and R. Freeman, *J. Magn. Reson.* **51**, 531 (1983).
- ¹¹⁷S. Yasui, *IEEE Trans. Aut. Contr.* **AC-24**, 230 (1979).
- ¹¹⁸H. A. Baker and T. Pradisthayon, *Proc. IEE*, **117**, 1857 (1970).
- ¹¹⁹R. Bauman, G. Wider, R. R. Ernst, and K. Wüthrich, *J. Magn. Reson.* **44**, 402 (1981).
- ¹²⁰S. Schaublin, A. Wokaun, and R. R. Ernst, *J. Magn. Reson.* **27**, 273 (1977).
- ¹²¹R. J. Miller and G. L. Closs, *Rev. Sci. Instrum.* **52**, 1876 (1981).
- ¹²²B. Blümich, *Mol. Phys.* **51**, 1283 (1984).
- ¹²³P. Mansfield and P. G. Morris, *NMR Imaging in Biomedicine*, *Adv. Magn. Reson.*, Suppl. 2, Academic Press, New York, 1982.
- ¹²⁴B. Blümich, *J. Magn. Reson.* **60**, 37 (1984).
- ¹²⁵L. Kevan and L. D. Kispert, *Electron Spin Double Resonance Spectroscopy*, Wiley, New York, 1976.
- ¹²⁶T. Lange and H. Ziegler, *Verh. DPG* **1**, 136 (1984).
- ¹²⁷J. R. Niklas, J.-M. Spaeth, and H. Ziegler,

Verh. DPG **1**, 137 (1984).

¹²⁸R. P. Feynman, F. L. Vernon, R. W. Hellwarth, *J. Appl. Phys.* **28**, 49 (1957).

¹²⁹N. A. Kurnit, I. D. Abella, and S. R. Hartman, *Phys. Rev. Lett.* **13**, 567 (1964).

¹³⁰R. G. Brewer in *Nonlinear Spectroscopy*, N. Bloembergen, Ed., E. Fermi Course **64**, 87, North-Holland, Amsterdam, 1977.

¹³¹M. M. Salour and C. Cohen-Tannoudji, *Phys. Rev. Lett.* **38**, 757 (1977).

¹³²S. C. Rand, A. Wokaun, R. G. DeVoe, and R. G. Brewer, *Phys. Rev. Lett.* **43**, 1868 (1979).

¹³³W. S. Warren and A. H. Zewail, *J. Chem.*

Phys. **78**, 2279, 2298, 3583 (1983).

¹³⁴E. R. Kasanewich, *Time Sequence Analysis in Geophysics*, 3rd Ed., University of Alberta Press, Edmonton, 1981.

¹³⁵Special issue on *Spectral Estimation*, *Proc. IEEE* **70** (9), 1982.

¹³⁶S. Kaykin, Ed., *Nonlinear Methods of Spectral Analysis*, *Topics in Appl. Phys.* **34**, 2nd Ed., No. 2, Springer, Berlin, 1983.

¹³⁷S. Kavata, K. Minami, and S. Minami, *Appl. Optics* **22**, 3593 (1983).

¹³⁸A. T. Georges and P. Lambropoulos, *Adv. Electron. Electron Phys.* **54**, 191 (1980).

ANALYSIS OF CHAIN MICROSTRUCTURE BY ^1H AND ^{13}C NMR SPECTROSCOPY

Yury E. Shapiro

NMR Laboratory
Yaroslavl Polytechnic Institute
USSR

	Page
I. Introduction	27
A. Microstructure of Macromolecules	27
B. Conformational Statistics and the Mechanism of Chain Growth	28
II. Analysis of Chain Microstructure by ^1H NMR Spectroscopy	30
A. Assignment of NMR Signals in Accordance with the Dyad or Triad Theory	30
B. Expansion of ^1H NMR Spectroscopy Capabilities by Use of Superconducting Magnets. Assignment of Signals by Tetrad and Higher Order Theories	33
C. Polymer Chain Microstructure Influence on Segmental Mobility	37
III. Investigation of Chain Microstructure by ^{13}C NMR Spectroscopy	38
A. Advantage of ^{13}C NMR Compared with ^1H NMR in Microstructure Analysis	38
B. Nuclear Relaxation and the Nuclear Overhauser Effect	38
C. Microstructure Analysis of Macromolecules with the Aid of ^{13}C NMR Spectroscopy	40
IV. New Methods of Microstructure Analysis	49
A. Use of Shift Reagents for Chain Microstructure Analysis	49
B. Magic Angle Spinning and High Resolution NMR Spectroscopy in Solid Polymers	52
V. Conclusions	54
References	54

I. INTRODUCTION

The aim of this review is to cover the contribution of high resolution NMR spectroscopy to the study of polymer microstructure, particularly after the years 1974-5, thus continuing the series of previous reviews (1-6).

The impact of stereospecific catalysts on the polymer world has created new demands for methods of studying the stereochemical configuration of polymer chains. NMR spectroscopy has become a very important method in this field through its ability to discriminate between different structures in a quantitative manner. The study of polymer configuration involves consideration of the polymer chain as sequences of iso-, hetero- and syndiotactic monomer placements,

i.e., as triads. Use of superconducting magnets and ^{13}C NMR allows one to obtain information about the content of tetrads, pentads and higher order sequences.

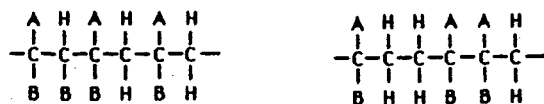
The analysis of triads and tetrads has been found to be very useful in the general interpretation of polymer structural problems. More specific information is forthcoming which may be used in a special way, e.g., in correlations with statistical polymerization theory.

A. Microstructure of Macromolecules

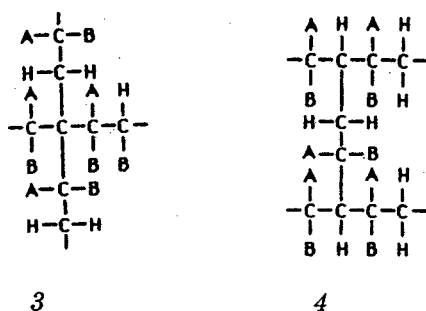
1. Vinyl Polymers

Vinyl monomers $\text{C(A)B}=\text{CH}_2$ (where A and B are H or a substituent) have various

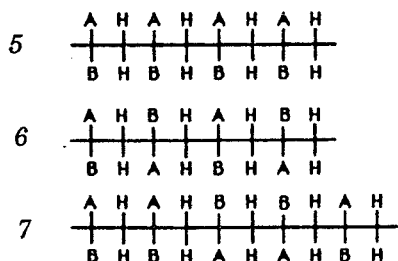
possibilities of joining into polymer chains: configurations "head-to-tail, 1, "head-to-head" and "tail-to-tail", 2;



formation of branching points, 3, and joining, 4, of chains is also possible.



Even stereoregular polymers are not always of very high stereochemical purity, and most polymers are composed of isotactic, 5, syndiotactic, 6, and heterotactic, 7, sequences or may be regarded as copolymers of such units (1).

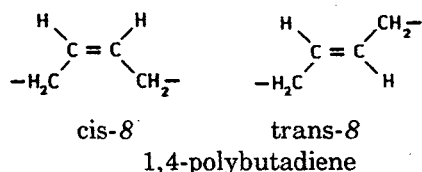


NMR spectroscopy has clarified these structures.

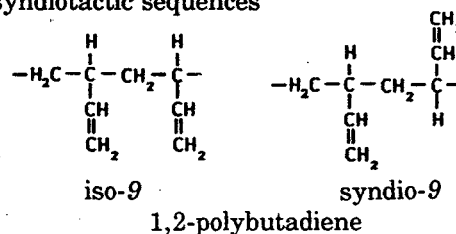
Asymmetric centers in these chains are actually pseudoasymmetrical (2) and such polymers have no optical activity.

2. Diene Polymers

The diene forms 1,4-(cis or trans), 8, and 1,2- configurations, 9, by polymerization.



1,2-structures have been discovered in iso- or syndiotactic sequences



3. Vinyl and Diene Copolymers

The different monomer units A and B form the following sequences in copolymer chains:

Dyads	AA	AB or BA	BB
m	$\bullet \bullet$	$\bullet \circ$	$\circ \circ$
r	$\bullet \bullet$	$\bullet \circ$	$\circ \circ$
Triads	AAA	AAB or BAA	BAB
mm	$\bullet \bullet \bullet$	$\bullet \bullet \circ$	$\circ \bullet \circ$
mr	$\bullet \bullet \bullet$	$\bullet \bullet \circ$	$\circ \bullet \circ$
rr	$\bullet \bullet \bullet$	$\bullet \bullet \circ$	$\circ \bullet \circ$

An additional 10 triads formed by replacement of designations o and • are also possible.

All of these and higher order sequences can be discriminated by NMR (4-6).

B. Conformational Statistics and Mechanism of Chain Growth

1. Homopolymerization

The possibility of determining vinyl polymer chain configuration by high resolution NMR is based on the sensitivity of this method to magnetically nonequivalent nuclei in different sequences. Table 1 presents the designations of dyads and triads.

The quantities m, r, i, h and s as obtained from NMR spectra are usually normalized according to the equations (2) $m + r = 1$ and $i + h + s = 1$.

The values of i, h and s have been coupled with various considerations of polymerization theories. Perhaps the simplest of these, according to Bovey and Tiers (1), is the most generally applicable and involves the parameter P_m , the probability that a polymer chain will add a

Table 1.

Designation	Projection	Bernoullian Probability
Dyad meso, m		P_m
racemic, r		$1 - P_m$
Triad isotactic, i, mm		P_m^2
heterotactic, h, mr		$2 P_m (1 - P_m)$
syndiotactic, s, rr		$(1 - P_m)^2$
Tetrad mmm		P_m^3
mmr		$2 P_m^2 (1 - P_m)$
rmr		$P_m (1 - P_m)^2$
rrm		$P_m^2 (1 - P_m)$
rrm		$2 P_m (1 - P_m)^2$
rrr		$(1 - P_m)^3$
Pentad mmmm (isotactic)		P_m^4
mmmr		$2 P_m^3 (1 - P_m)$
rmmr		$P_m^2 (1 - P_m)^2$
mmrm		$2 P_m^3 (1 - P_m)$
mmrr		$2 P_m^2 (1 - P_m)^2$
rmrm (heterotactic)		$2 P_m^2 (1 - P_m)^2$
rmrr		$2 P_m (1 - P_m)^3$
mrrm		$P_m^2 (1 - P_m)^2$
rrrm		$2 P_m (1 - P_m)^3$
rrrr (syndiotactic)		$(1 - P_m)^4$

monomer unit to give the same configuration as that of the last unit at its growing end. In this case the chain growth process follows Bernoullian statistics (Table 1).

Theoretical graphs of normalized i , h and s against P_m have been constructed and it has been found that methyl methacrylate free-radical polymers give Bernoullian statistical propagation whereas anionic polymers show a different behavior, which may be called non-Bernoullian

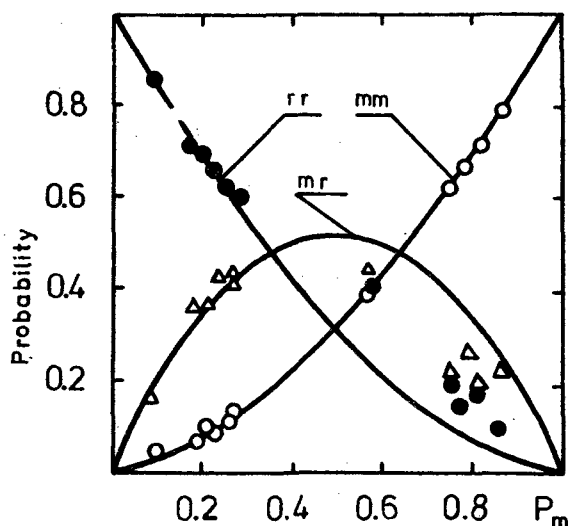


Figure 1. Relationship between i , s , h -triad possibilities and P_m . Points on the left of $P_m = 0.5$ are for methyl methacrylate free-radical polymers; points on the right are for anionic polymers (4).

propagation (Figure 1).

The first-order Markovian sequence is formed by chain growth, with the stereochemistry of chain-growth end effects influencing connecting monomer units. We have now four conditional probabilities $P_{m/m}$, $P_{r/m}$, $P_{m/r}$, $P_{r/r}$ which describe the connection process ($P_{r/m}$ is the probability of monomer unit connection in the m -configuration to the chain end with r -configuration). They are

$$P_{m/r} = (mr)/[2(mm) + (mr)] \quad [\equiv (1 - P_m)] \quad (1)$$

$$P_{r/m} = (mr)/[2(rr) + (mr)] \quad [\equiv P_m] \quad (2)$$

$$P_{m/m} = 1 - P_{m/r} \quad (3)$$

$$P_{r/r} = 1 - P_{r/m} \quad (4)$$

Thus Markovian first-order statistics is controlled by two independent parameters $P_{m/r}$ and $P_{r/m}$ (7).

The average sequence lengths may be calculated from the following equations (1-3, 7):

$$\langle n_m \rangle = [(r)(P_{m/r} + P_{r/m})]^{-1} \quad (5)$$

$$\langle n_r \rangle = [(m)(P_{m/r} + P_{r/m})]^{-1} \quad (6)$$

The Markovian second-order statistics have four independent probabilities. It takes into consideration the influence of the second unit from the chain end (7).

Non-Markovian processes are possible too. One of them is the Coleman-Fox process (8, 9), which explains block configuration by chain growth. According to this model the block configurations come into being by formation of chain end and anti-ion chelate complexes with its subsequent destruction.

2. Copolymerization

Assuming that the statistical copolymerization of monomers A and B is controlled by the Markovian first-order statistics, it holds for the low conversion limit (10):

$$P_{A/B} = (1 + r_A[A]/[B])^{-1};$$

$$P_{B/A} = (1 + r_B[B]/[A])^{-1} \quad (7)$$

r_A and r_B represent copolymerization reactivity ratio parameters and $[A]$ and $[B]$ represent mole fractions of monomers in the initial system.

The way in which the copolymer is synthesized markedly affects the copolymerization reactivity ratios r_A and r_B and the coisotacticity parameter P_m from the Bernoullian model (11). Plate and coworkers (12, 13) use only Markovian first-order statistics and introduce the two parameters of coisotacticity $P_{A/B}$ and $P_{B/A}$.

II. ANALYSIS OF CHAIN MICROSTRUCTURE BY 1H NMR SPECTROSCOPY

A. Assignment of NMR Signals in Accordance with the Dyad or Triad Theory

Two types of assignments may be distinguished: those which follow purely from NMR

spectra and those which are taken from non-NMR evidence. Although the interpretation of some polymer spectra is now relatively easy, in other cases serious complexities remain. Spin-spin decoupling has been used to simplify polymer spectra by eliminating the effect of spin coupling. Double irradiation becomes increasing difficult as the chemical shifts of the two coupled protons come closer together, as for example in polypropylene.

Another method of NMR spectral simplification is to replace particular protons with other atoms that do not give an observable signal. One way of doing this is by deuteration, although substitution by halogen might also be considered. In this way, not only the signal of the substituted group removed from the spectrum, but also the spin-coupling effect of the substituted group is very much reduced. The interpretation of spectra of deuterated materials usually follows more readily than it does for decoupled spectra, and the assignments could be made with greater certainty.

Model compound of polymers have been used extensively in NMR spectroscopy in two main ways. Firstly, to correlate chemical shifts found in polymers with those of well-defined small molecules in order to identify the presence of particular groupings. Secondly, the use of more sophisticated model compounds such as isomers of the 2,4-disubstituted pentane type as models of different configurations in the correlation of splitting patterns observed in polymer spectra. The study of the second type has been extended to the 2,4,6-trisubstituted heptanes, and considerable insight into polymer conformational studies has been gained (14, 15).

1. Homopolymers

One classical example of polymer microstructure investigation is NMR analysis of poly(methyl methacrylate) (PMMA) samples (1-4, 7, 16, 17). Bovey found that in CDCl_3 solution three α -methyl peaks appeared at 0.91, 1.05 and 1.22 ppm. They were due to syndio-, hetero-, and isotactic forms, respectively. Also, the isotactic methylene signal was an AB-quartet ($J = -14.9$ Hz), whereas the syndiotactic one was a singlet (Figure 2). The observation of an AB quartet methylene signal is an absolute determination of the presence of isotactic structures and is independent of any other type of evidence. The stereoregularity of anionic produced polymers has been shown (7, 16) to be dependent on the solvent. For a free-radical-initiated polymer it has been claimed (1) that the

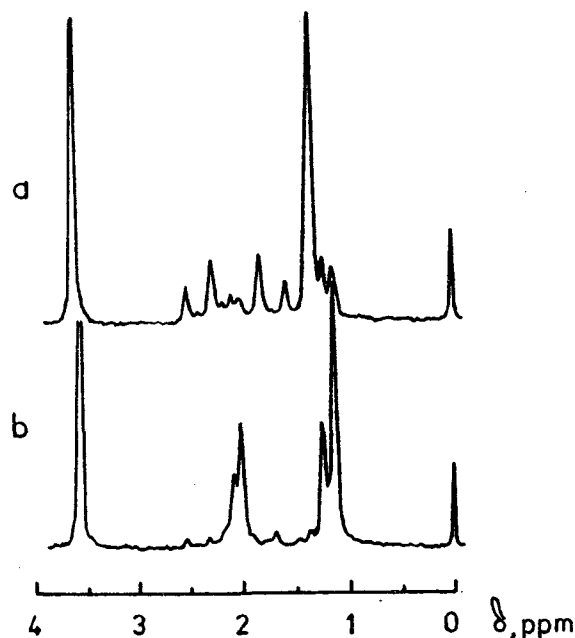


Figure 2. ^1H NMR spectra of PMMA solution in *o*-dichlorobenzene, 160°C ; (a) predominantly isotactic polymer, (b) predominantly syndiotactic polymer (4).

syndiotacticity was not solvent dependent, but its temperature dependence was illustrated (16). It was found that the P_m value for free-radical MMA polymerization was 0.13 at -78°C and 0.36 at 250°C . Highly syndiotactic crystallizable samples of PMMA prepared by Ziegler catalysts were discussed (16).

The new possibilities of conformational analysis of PMMA appear by the study of a model compound and MMA oligomers (17). It was analyzed in relation to the stereospecific conformation, taking into account the structural end group effects and the characteristics of the geminal methylene proton signals.

In polymer stereoisomerism investigations, serious difficulties can be found. The problems arise from the necessity of summary spectra separating subspectra with many components. Therefore the number of polymers for which the microtacticity may be determined from ^1H NMR spectra is now restricted (4). Recently increasing success has been achieved by use of partially deuterated monomers (18).

The use of computer calculations for investigation of polymers is indispensable. First work in

this way has been performed for analysis of poly(vinyl chloride) (PVC) ^1H spectrum (2). The spectrum of PVC methylene protons is the superposition of six mmm, mmr, rmr, mrm, rrm and rrr tetrad subspectra. Each of these subspectra is a complex spin-spin multiplet. Therefore $\alpha,\beta\text{-d}_2$ -PVC was synthesized for the stereoisomerism investigation (19). Figure 3 shows the tetrad assignment in this polymer. The same work was done for methine proton pentade shifts

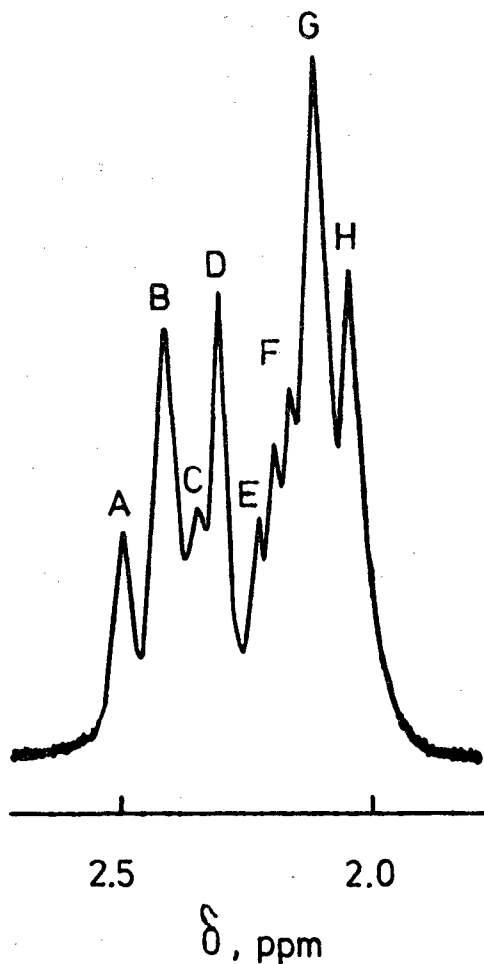


Figure 3. 100 MHz ^1H NMR spectrum of poly(α -cis- β - d_2 -vinyl chloride) in CDCl_3 . A, E - rmr; B - mmr + mmm; C - mmm; D - mmr; F, H - mrr; G - mrm + rrr (19).

of $\beta\beta\text{-d}_2$ -PVC (Figure 4).

Zymonas and Harwood (21) interpreted the ^1H NMR spectra of iso-syndio- and heterotactic

1,2-polybutadienes. The methylene proton resonances can provide information about the meso dyad. The chemical shifts of methylene type vinyl protons in iso and syndio forms differ by 0.14 ppm, indicating that the resonance of such protons can provide information about the relative amounts of i, h, s-triads. Chemical shifts and coupling constants were estimated to obtain an approximate fit of calculated lines to each spectrum with the aid of the iterative program LAOCOON 3.

2. Copolymers

The methyl methacrylate-styrene and methyl methacrylate (MMA)-methacrylic acid (MAA) copolymers are the most investigated systems. Such copolymers have been mentioned in an earlier paper (1), where the effects of styrene blocks cleaving the aromatic signal and the random styrene units dividing the methoxyl resonance were featured, but the α -methyl signal was not resolved well enough for tacticity determination. Radical copolymers have been the subject of further detailed study (4), and the twelve triads involving composition and configuration in relation to a central MMA unit have been divided between the three methoxy resonances. The ^1H NMR spectra of random and alternating copolymers of styrene and methyl, ethyl, butyl and octyl methacrylates were analyzed in (11). The way in which the copolymerization mechanism follows therefrom markedly affect the magnitude of the parameter of coisotacticity P_m : for all comonomer pairs under study, P_m is higher when an organometallic catalyst is used (alternating) than in the case of a radical initiator (statistical). With increasing number of carbon atoms in the n-alkyl alcohol residue, P_m decreases to a limiting value.

The chemical shifts of the methoxyl and α -methyl protons in the alternating MMA-styrene copolymer are calculated by taking into account the contributions of the diamagnetic shielding and the magnetic anisotropy effect of the benzene rings in styrene units (22, 23). Three- and four-bond interaction parameters, which are necessary for the calculation of conformational probabilities of dyad sequences in a copolymer chain may be estimated from the parameters determined for the homopolymers.

Klesper and Gronsky (24) investigated the monomer distribution and microtacticity of the MMA-MAA copolymers. By using model compounds they offered the well-founded assignment of twenty stereoisomeric triads to six components of the α -methyl spectrum.

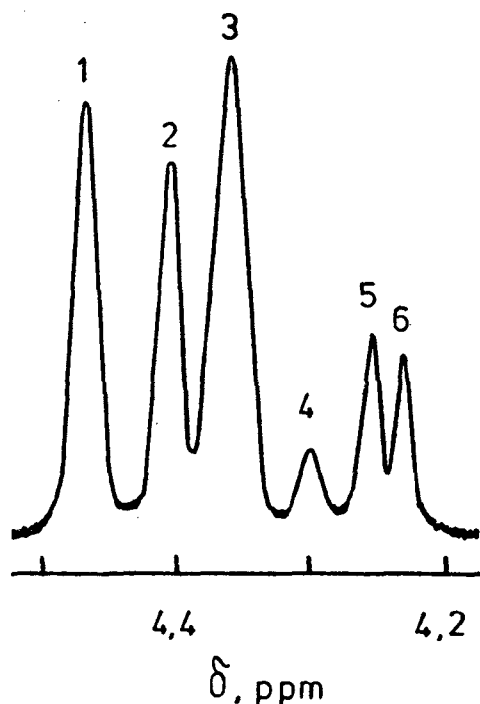


Figure 4. 100 MHz $^1\text{H}\{^2\text{H}\}$ NMR spectrum of poly(β , β - d_2 -vinyl chloride) in C_2HCl_5 1 - rrrr + rrrm + mrrm; 2 - rrrm + mrrm; 3 - rrrmr + rrrmr; 4 - mrrmr; 5 - rrrmr; 6 - rrrmr (20).

The contribution of this investigation to polymer chemistry consists in the fact that these copolymers represent the best model for studying the unit distribution change and tacticity by copolymerization and chemical modification of copolymers. The copolymer list may be extended to the spectrally similar copolymers: phenylmethacrylate-MMA (25), benzilmethacrylate-MAA and diphenyl methyl methacrylate-MAA (26), and at the expense of the systems, which turn into spectrally similar copolymers by analogous polymer reactions (MMA-ethyl, isopropyl, tert-butyl, benzil, α -methyl benzil, diphenyl, 1,1-diphenylethyl, α,α -dimethylbenzil, trityl, 1-naphtyl methacrylates) (27). The reactivities of the monomers have been explained in terms of the polar effect of the ester groups in radical and anionic copolymerizations. Coisotactic parameters have been determined by assuming the terminal model statistics.

Usually only dyad and triad sequences in polymer chains may be identified at frequencies lower than 200 MHz. However in copolymers

with the polar monomer units, sometimes longer sequences may be discovered. For example, the pentads were found in the 100 MHz spectra of the MMA-acrylonitrile copolymer solution in DMSO- d_6 (28). Splitting of the MMA α -methyl signal on MMA pentad components shows the copolymers have block-sequences with the MMA units having more than three components.

B. Expansion of ^1H NMR Spectroscopy Capabilities by Use of Superconducting Magnets. Assignment of Signals by Tetrad and Higher Order Theories

Development of high frequency spectrometers (220-600 MHz) with superconducting magnets has been of principal importance in polymer microstructure investigations. The major contemporary technical difficulty stems from the fact that a high resolution NMR spectrum of a macromolecule is generally a broad, featureless, and uninformative envelop of many overlapping lines of chemically related monomers and chain sequences, even at the highest resolution available (29).

1. Homopolymers

Figure 5 shows ^1H NMR spectra of the same samples of PMMA that are shown in Figure 2

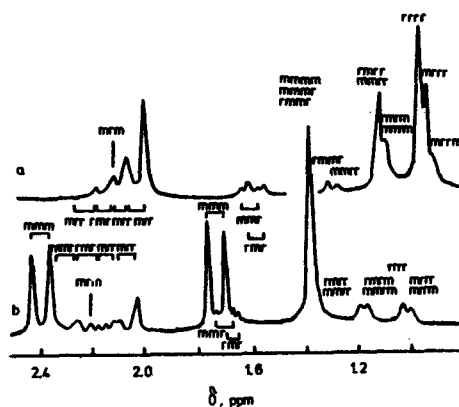


Figure 5. 220 MHz ^1H NMR spectra of PMMA solution in *o*-dichlorobenzene (4); (a) predominantly isotactic polymer, (b) predominantly syndiotactic polymer.

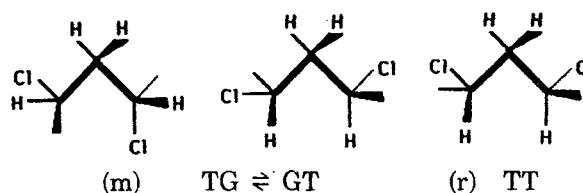
but at 220 MHz. The latent tetrad structure of methylene signals at 60 MHz is obvious at 220 MHz (2, 4). The pentad signals, which lead to the asymmetry of α -methyl signals at 220 MHz,

are distinguished beautifully at 300 MHz (Figure 6) (30). The fine hexad structure of CH_2 -signals is visible as well at this frequency.

Spectroscopy at 220 MHz is effective in the study of the ionic polymerization mechanism (31, 32). The polymers of 1,2-butylene oxide and α -methylstyrene prepared under anionic polymerization have the Markovian first-order chain growth mechanism. The cationic poly(1,2-butylene oxide) and poly(α -methyl styrene) prepared at temperatures above -25°C follow Bernoullian statistics with $P_m = 0.26$. The information was obtained from tetrad/pentad sequences (32). Anionic and cationic poly(p-isopropyl- α -methylstyrene)'s have the opposite chain growth mechanisms (33).

The longest sequences in polyolefins were obtained from 300 MHz spectra of predominantly isotactic polystyrene. Flory (34) calculated the chemical shifts for methine and aromatic protons of the central $>\text{CHAr}$ group in the all-meso nonad m_8 and in the nonads rrm_6 , $mrrm_5$, $m_2r_2m_4$, $m_3r_2m_2$ containing a single racemic triad. The magnetic shielding by phenyl groups that were first and second neighbors along the chain were computed according to their distances and orientations relative to the given proton in each conformation of the chain using the ring current representation of the π electrons or, alternatively, the magnetic anisotropy of the phenyl group and the McConnell equation. The resulting chemical shifts were averaged over all conformations. The calculations for the methine proton are in excellent agreement with the 300 MHz spectrum. Treatment of the chemical shifts for the aromatic protons in ortho and meta positions is indecisive owing to the extraordinary sensitivity of the shielding to torsional angles in the chain backbone.

For the first time the conformation of a polymer chain was determined in Bovey's elegant paper (35) with the aid of model spectral simulation. Figure 7 shows the synthesis of the polyvinyl chloride (PVC) methylene and methine 220 MHz spectra from the tetrad and pentad sub-spectra. The PVC spectra give moreover much structural information, for example, the chemical shifts and spin-spin coupling constants. It was ascertained that the m-dyads had the $\text{TG} \rightleftharpoons \text{GT}$ conformation in atactic PVC chain since their vicinal spin-spin coupling constants were the same as for the model meso-dimer. r-Dyads had the TT conformation. Therefore the majority of loops in PVC chain must occur in the mr link-up of TGTT and GTTT forms and their mirror representations.



Tanaka and Sato (36) studied the distribution of cis- and trans-1,4 units in various kinds of 1,4-polybutadienes (PB) and -polyisoprenes including cis-trans equibinary PB and UV-isomerized PB by use of ^1H NMR spectroscopy at 60, 100, 220, and 300 MHz. Poly(butadiene-2,3- d_2) was used for the peak assignment. The resonance of methylene protons in cis-trans linkage was described as an A_2B_2 system. Figure 8a shows the spectra of poly(butadiene-2,3- d_2) prepared by butyl lithium. The splitting of the signal is identical with that of the methylene proton signal decoupled from the methine proton in PB as shown in Figure 8b. In Figure 8a the central peak due to the cis-trans linkages in the 60 and 100 MHz spectra separates into two parts at 220 MHz and 300 MHz. This indicates the existence of two types of methylene protons in cis-trans and trans-cis linkages. A computer simulation was carried out as shown in Figure 8b and the intensity ratio of the peaks was chosen so as to follow Bernoullian statistics.

The same results were obtained for poly(2,3-dimethyl-1,3-butadiene) (PDMB). The 220 MHz spectra of PDMB prepared by butyl lithium in cyclohexane were compared to those of free-radical PDMB (37). By aid of measurements done on cis- and trans-1,4 PDMB prepared by Ziegler catalysts, it was determined that both polymers were Bernoullian with probabilities of cis placement of 0.24 and 0.40, respectively. It was shown that the anionic sample was largely trans. Anionically prepared PB was predominantly trans too (36) and had as much as 23% cyclic structures (38).

2. Copolymers

NMR spectroscopy at high frequencies (220-600 MHz) allows one to determine the monomer unit distribution as well as the microtacticity of these units in copolymer chains. Investigations of a number of copolymers indicate that the copolymerization kinetics deviates from the simple Mayo-Lewis scheme. In (39) 220 MHz ^1H NMR spectra of some free-radically prepared MMA-chloroprene copolymers have been recorded. The intensities of the α -methyl signals are related to the relative proportions of various MMA centered triads and pentads. Triad

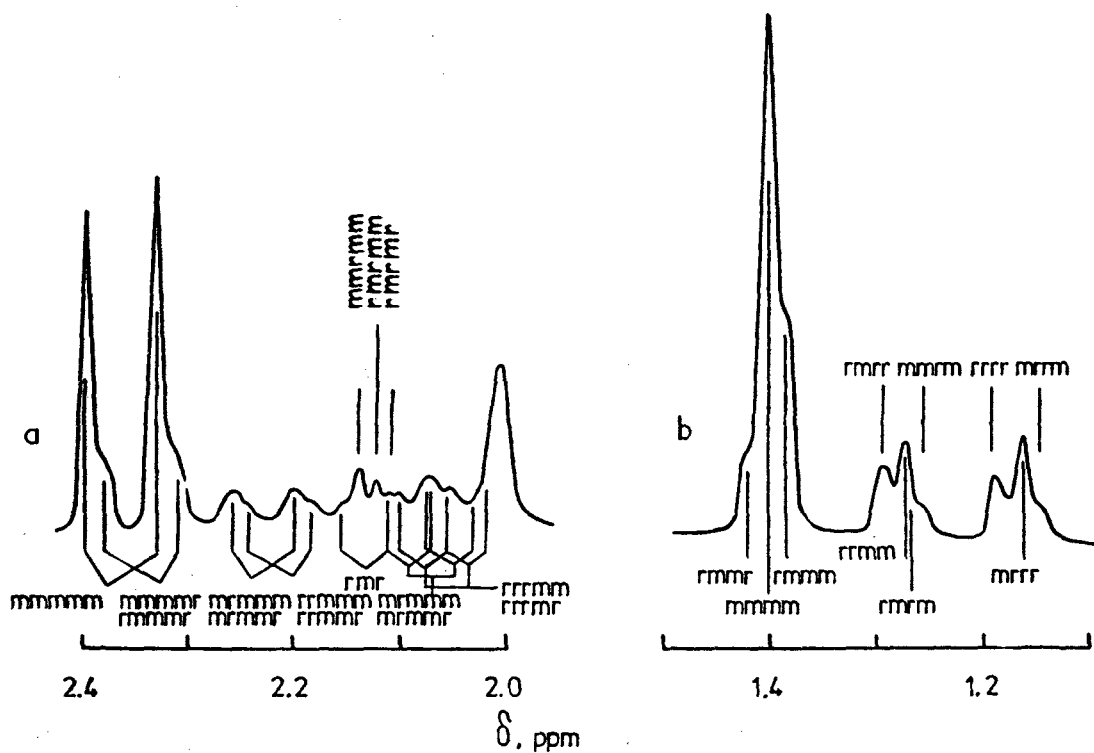


Figure 6. 300 MHz ^1H NMR spectra of erythro-methylene (a) and α -methyl (b) protons of PMMA solution in *o*-dichlorobenzene, 120° C (30).

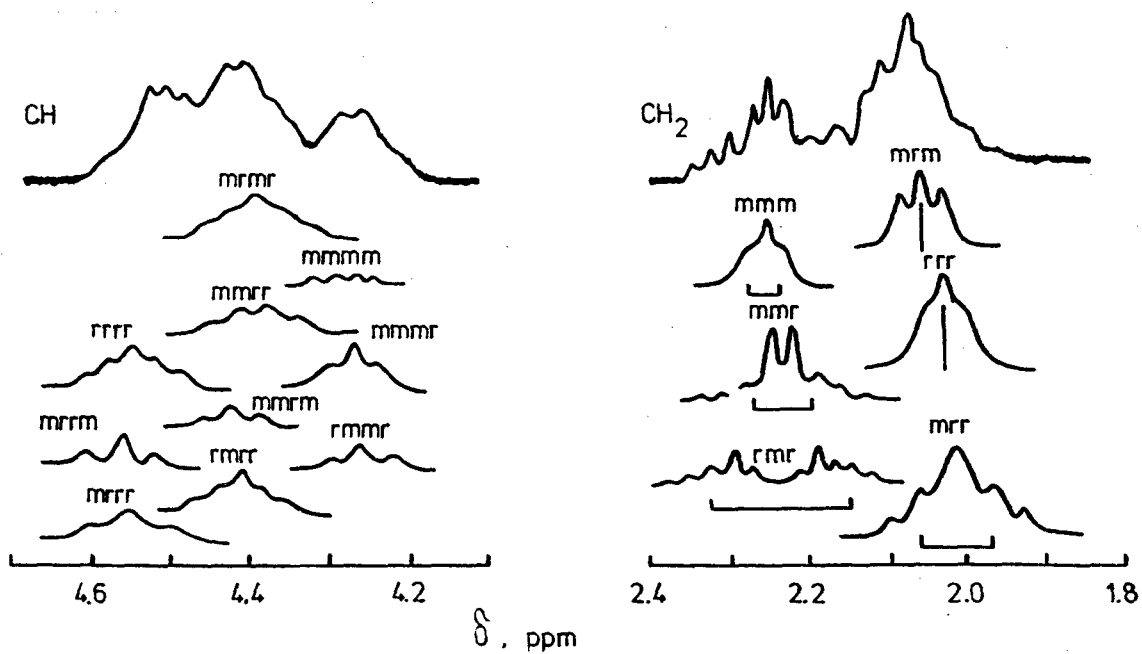


Figure 7. Computer synthesis of the PVC methylene and methine 220 MHz spectra from the tetrad and pentad subspectra (35). The top spectra are experimental (*o*-dichlorobenzene, 140° C).

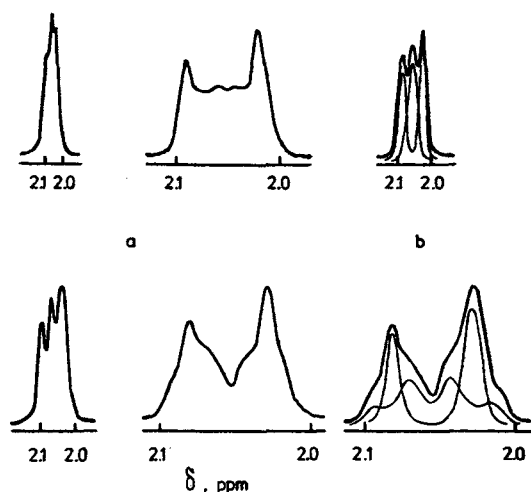


Figure 8. ^1H NMR spectra of poly(butadiene-2,3- d_2) obtained at 60, 100, 220, and 300 MHz (a) and decoupled ^1H NMR spectra of isomerized polybutadiene (b) in the methylene region obtained at 100 and 300 MHz (36).

fractions indicate that the Mayo-Lewis scheme is not strictly applicable to this system and is in good agreement with those calculated from the penultimate reactivity ratios $r_{11} = 0.107$, $r_{21} = 0.057$, and $r_2 = 6.7$ where MMA is monomer 1. However, although a small penultimate group effect is indicated, some deviation from the Mayo-Lewis scheme may be due to the occurrence of anomalous head-to-head and tail-to-tail MMA-chloroprene linkages. A similar analysis has been described for acrylic monomer-2-substituted-1,3-diene and alternating (40, 41) and conventional butadiene- d_4 -acrylonitrile (42) copolymers. Alternating copolymers were prepared under $\text{Et}_3\text{Al}_2\text{Cl}_3/\text{VOCl}_3$ or ZnCl_2 catalysts. The random copolymers are in good agreement with the Markovian first-order statistics. The reactivity ratios are $r_{11} = 0.18$, $r_2 = 0.62$ and $r_{11} = 0.26$, $r_2 = 0.63$ (where MMA is monomer 1) for MMA-butadiene and MMA-isoprene, respectively (40, 41).

Constant composition copolymers of MMA or methacrylonitrile and vinylidene chloride produced by radical copolymerization were studied by ^1H NMR at 60, 250 (43) and 220 MHz (44). The monomer dyad/triad sequences and some of the tetrad/pentad sequences were obtained from spectra (Figure 9). In (43) a new graphical

method of reactivity ratio calculations is proposed, based on the use of specific values of the triad distribution functions and the Coleman-Fox

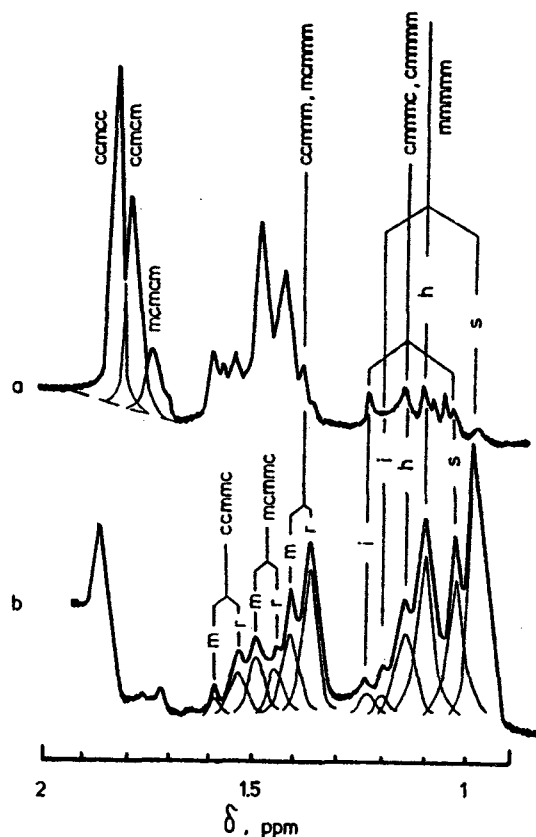


Figure 9. 250 MHz ^1H spectra of the α -methyl proton region of copolymer MMA and vinylidene chloride. [MMA] = 29% (a) and 81% (b). Pentad decomposition is attributed (43).

model. It is possible to detect a penultimate effect for the vinylidene chloride-rich region. In the same region, a change in tacticity of the triads on the MMA sequences, as compared with homopolymers, is observed; it is suggested that the anomaly is caused by the competition of the depropagation reaction. It can be shown that the bulk copolymerization kinetics deviates from the Mayo-Lewis scheme (Figure 10). Small differences were found between the bulk and solution copolymerization (44) since the bulk process was heterogeneous. This could indicate that solvation effects were important.

When assigning sequences in NMR spectra of

vinyl polymers, it is usually assumed that nearest-neighbor monomer units possess a larger influence on the chemical shifts of the central unit than on monomer units further removed. Strasilla and Klesper (26, 45) studied the proton- OCH_3 resonances of MMA-methacrylic acid (MAA) and MMA-diphenylmethyl-methacrylate copolymers. In fact, the differentiation of nearest neighbors appears to vanish in the present case, and within the limits of detection, only the units removed were responsible for resolving the $-\text{OCH}_3$ resonance of the MMA units into triad peaks. The detection of such an effect by intensity measurement is possible only with non-Bernoullian copolymers, particularly with copolymers possessing a strong tendency toward alternation. In copolymers with alternating character, the statistics of sequences composed of nearest neighbors differs much from the statistics of sequences composed of next to nearest neighbors than in the case of copolymers of block-like character, e.g. in styrene-MMA copolymers (45a). An assignment of such "next to nearest neighbor" triads appears possible if it is assumed that the syndiotactic chain is in an all-trans conformation.

C. Polymer Chain Microstructure Influence on Segmental Mobility

The relationship between microstructure and segmental mobility of polymer chain may be better studied with the aid of proton spin-lattice relaxation times than with ^{13}C T_1 measurements. However, this is not correct since proton and carbon-13 T_1 values are the complement of one another and are not always identical. Accounts of nuclear magnetic relaxation and the theories of polymer chain motions can be found in a number of reviews. The last among them is (46).

Spevacek and Schneider (47) showed with the aid of a T_1 ^1H study that PMMA formed stereocomplexes in CCl_6 , CD_3CN , toluene and benzene solution. The smallest syndiotactic sequence length in complexes is 8 (in benzene solution) or 3 (CCl_4 , CD_3CN solution) monomer blocks. The relationship between iso- and syndiosequences in a stereocomplex is 1:1.5. The stereocomplexes between iso- and syndiotactic PMMA have been formed by means of exchange interaction between the ester groups. In dilute solutions of s-PMMA a considerable portion (76%) of polymer segments are intramolecularly associated. The motion of associated segments appears as isotropic with an effective correlation frequency of 10^6 - 10^7 Hz.

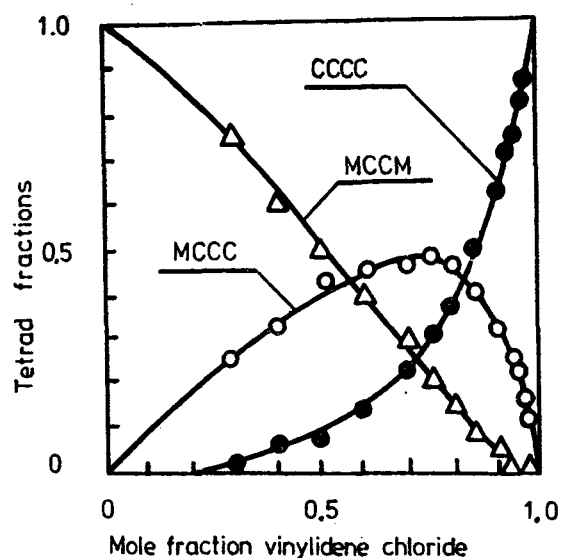


Figure 10. Measured tetrad distributions in bulk prepared MAA-vinylidene chloride copolymers compared with distributions calculated from $r_1 = 0.40$ and $r_2 = 2.5$ (solid lines) (44).

Hatada and coworkers (48) have shown that the tacticities of poly(alkyl methacrylates) can be worked out in detail by using the large difference in spin-lattice relaxation times of protons in α -Me and ester groups to eliminate the ester group resonance overlap with the α -Me signal which normally obscures splittings due to tacticity. Data were given for several C_1 - C_5 -alkyl methacrylate homopolymers. In other work (49) Hatada demonstrated that T_1 values for isotactic sequences were longer than for syndiotactic. Table 2 shows the correlation times for Me and α -Me groups which were calculated from ^1H and ^{13}C T_1 -values for iso- and syndiotactic PMMA.

With the aid of proton spin-lattice relaxation measurements at 100 and 250 MHz, the segmental motion of poly(4-vinyl-pyridinium bromide) in methanol was studied (50). The necessary geometrical parameters were received from the conformational calculation of hexads rmrmm assuming two models with and without Br^- ion near pyridinium. For these two models of the charge distribution, the potential barriers of the rm triad mobility have been calculated. The best agreement between experimental data and temperature curves of T_1 was achieved by $\Delta H_R^\ddagger = 6$ kcal/mol, $(\tau_R)_0 = 10^{-13}$ s for the

Table 2. ^1H and ^{13}C Correlation Times for Iso- and Syndiotactic PMMA ($\tau_c \times 10^{11}$ s) (57).

Group	i		s	
	^1H	^{13}C	^1H	^{13}C
$\alpha\text{-CH}_3$	3.7	3.1	7.7	7.1
CH_3	8.8	8.4	16	22

aliphatic chain and $\Delta H_g^\ddagger = 2$ kcal/mol, $(\tau_g)_0 = 1.4 \times 10^{-11}$ s for pyridinium ion. In the temperature range of 250-350 K the vibrational amplitude of the chain increases from 40° to 85° .

III. INVESTIGATION OF CHAIN MICROSTRUCTURE BY ^{13}C NMR SPECTROSCOPY

A. Advantage of ^{13}C NMR compared with ^1H NMR in Microstructure Analysis

Since the advent of commercial pulsed Fourier transform ^{13}C NMR instrumentation, great advances have been made in the elucidation of polymer microstructure (51, 52). Firstly, the twenty-fold increase in chemical shift range over ^1H NMR allows much better resolution of small structural differences. Secondly, the relaxation times of ^{13}C nuclei in CH_n groups ($n > 0$) are dominated by dipolar interaction with the attached protons. Since the C-H bond length remains constant from one polymer to another, ^{13}C relaxation times are a reliable probe of molecular mobility.

Figure 11a, the proton NMR spectrum for an isoprene-acrylonitrile copolymer, shows characteristic broad peaks and yields little structural information. Figure 11b, the proton decoupled ^{13}C NMR spectrum for the same sample, gives sharp peaks for each type of carbon atom, and is used with the coupled spectrum to assign the peaks (53). The peaks corresponding to CN-carbon atoms are still not singlets in the decoupled spectrum. This is because of the microstructure effect which may be observed for other carbon atoms. Table 3 presents the structure composition of poly(isoprene-acrylonitrile)'s (54).

Matsuzaki's poly(2-vinylpyridine) investigation (55) may be cited as another example of the advantage of ^{13}C NMR. The ^1H NMR spectrum

of the poly(2-vinylpyridine- $\beta,\beta\text{-d}_2$) in D_2SO_4 (Figure 12a) shows three peaks of methine protons, which are assigned to i, s and h triads. Since the absorption peaks of hetero- and syndiotactic triads of methine protons overlap those of methylene protons in nondeuterated polymers, only isotactic triad intensities can be obtained from ^1H NMR spectra of poly(2-vinylpyridine). The ^{13}C signals (Figure 12b) split into a number of peaks. This splitting may be due to pentad tacticity. The results (Table 4) show that poly(2-vinylpyridine) obtained by radical polymerization (with AIBN as initiator) is an atactic polymer with Bernoullian statistics. The pentad tacticities of the isotactic polymer (prepared with PhMgBr as initiator) were then calculated on the basis of a first-order Markovian process.

Finally one must note that ^{13}C NMR spectroscopy allows one to obtain microstructure information inaccessible by other means.

B. Nuclear Relaxation and the Nuclear Overhauser Effect

Noise decoupling in ^{13}C NMR spectroscopy aids assignment by collapsing multiplets to singlets, and in addition selectively enhances the signals through the nuclear Overhauser enhancement (NOE). It has been found that the intensities of carbons of similar hybridization and number of attached protons are directly correlated (46, 51). Carbons of different type are usually correlated by a single empirical NOE factor measured directly from the spectra (49, 56-59). It has been found (46, 53, 56, 59, 60) that the NOE factor for the carbon-13 nucleus in a main chain or near it is the same for a number of polymers in solution. This is proven by the agreement of the ^1H and ^{13}C microstructural data. Recently a number of authors makes use of paramagnetic additions (nitroxil radicals (56), or

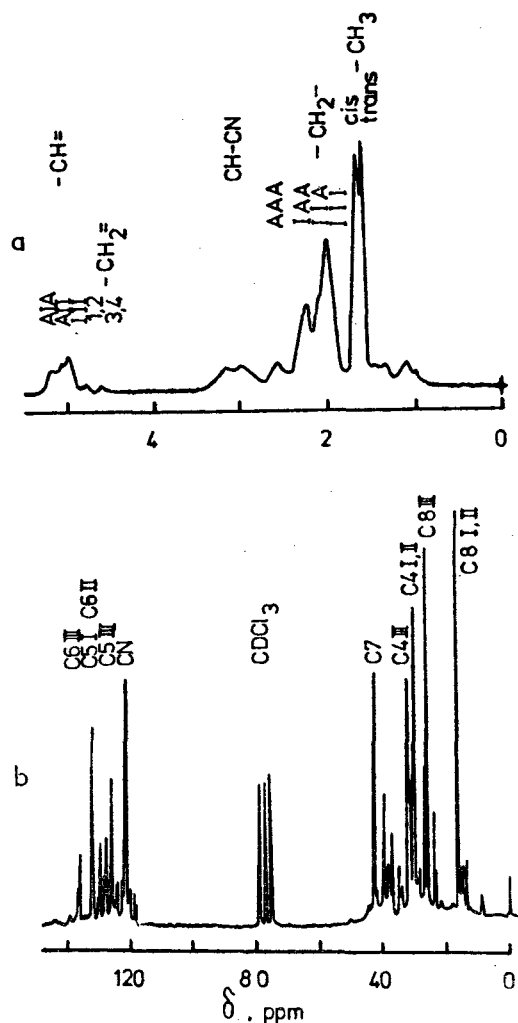


Figure 11. ^1H NMR at 80 MHz and $^{13}\text{C}\{^1\text{H}\}$ at 20 MHz (b) spectra of isoprene-acrylonitrile copolymer (A content is 38 mol %) dissolved in CCl_4 and CDCl_3 (53).

acetylacetonate of Cr (60-62) and of Fe(III) (63) in order to decrease the NOE effect.

The influence of stereochemistry on relaxation has been investigated for a few polymers. Isotactic PMMA is appreciably more mobile than syndiotactic, the T_1 values being in the ratio 1:1.5 (see Table 2). Inoue et al. (64, 65, 66) report a T_1 -iso/ T_1 -syndio ratio of 2 for C_6D_6 solutions at 80°C. For polystyrene and poly(α -methylstyrene) (59, 65, 66) on the other hand, the isotactic form is slightly less mobile.

Table 3. Structure Composition of Poly(isoprene-acrylonitrile)'s (62).

Sequence	[A], mass%	
	18	34
AI*-tail-to-tail	0.458	0.638
AI-head-to-head	0.125	0.190
III (II)	0.417	0.172
IAI	0.854	0.761
IAA	0.101	0.177
AAA	0.045	0.062

* I-isoprene, A-acrylonitrile

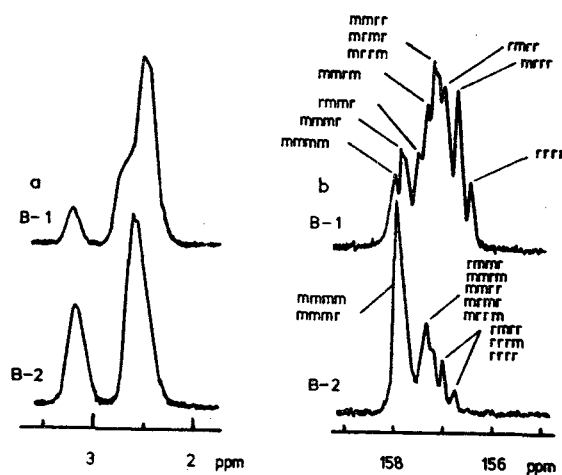


Figure 12. ^1H at 100 MHz (2) and $^{13}\text{C}\{^1\text{H}\}$ at 25.1 MHz (b) NMR spectra of poly(2-vinylpyridine) observed in D_2SO_4 at 60°C. (Samples B-1 and B-2 were prepared with AIBN and PhMgBr as initiator) (55).

Table 4. Pentad Tacticity of Poly(2-vinylpyridine) (63).

Pentad	Composition	
	Observed	Calculated
mmmm	0.04	0.05
mmmr	0.10	0.12
rmmr	0.07	0.06
mrrm	0.16	0.12
mmrr		0.12*
rmm	0.32	0.12*
mrrm		0.06*
rmrr	0.11	0.14
rrrm	0.16	0.14
rrrr	0.04	0.07

* Total mmrr+rmm+mrrm: 0.30

The T_1 activation energies are independent of configuration. Randall (67) and Asakura (67a) have measured the ^{13}C relaxation times of numerous stereochemical sequences in the CH_1 , CH_2 and CH_3 regions of an atactic polypropylene sample. The carbons from isotactic sequences tended to exhibit the longest T_1 values, but the largest differences between iso- and syndiotactic units was 32% for CH carbons (Figure 13). The activation energies for all T_1 values were independent of configuration, as for polystyrene. The origin of the small stereochemical dependence of T_1 in polystyrene and polypropylene is probably connected therefore with slightly different values of the force constants (46).

Gronski et al. have studied the dependence of ^{13}C T_1 values on sequence distribution in styrene-butadiene (68) and 1,4-1,2-butadiene (69, 70) copolymers. In the styrene-butadiene system, the T_1 values for the para-phenyl carbon for two samples with average block lengths of 1 and 6 are 0.56 and 0.33 s respectively in CHCl_3 at 53°C and 60 wt%. The comparable value for polystyrene is 0.11 s. The factor of 3 increase shown by the sample with $\langle n_B \rangle = 6$ is indicative of segmental motions involving the cooperation of perhaps three or four monomer units. Similar effects are observed in the 1,4-1,2 butadiene copolymer. For example, the T_1 value for the CH of a 1,2-butadiene unit is 0.80 s when its neighbors are also 1,2-units, but 1.65 s when its neighbors are cis-1,4-units.

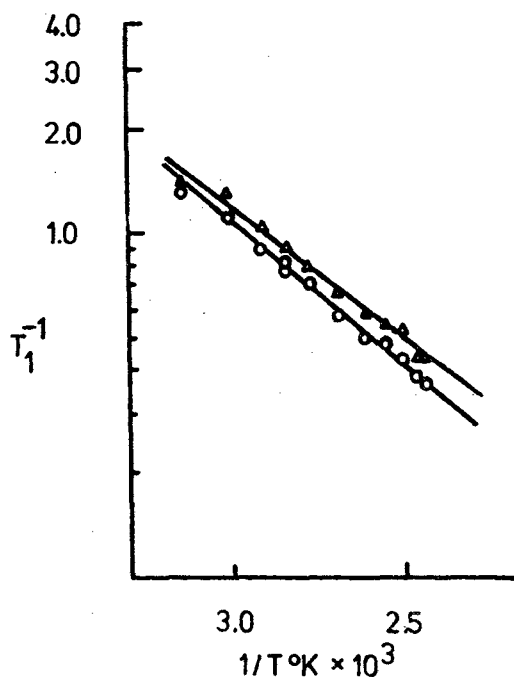


Figure 13. Arrhenius plot of syndiotactic (Δ) and isotactic (o) polypropylene methyl relaxation (67).

It may be pointed out that the carbon relaxation study acquired greater significance than ^1H because of their simpler interpretation and of a possibility of evaluating polymer segmental mobility in solids (71).

C. Microstructure Analysis of Macromolecules with the Aid of ^{13}C NMR Spectroscopy

1. Polyolefins

^{13}C NMR has proven to be an informative technique for measuring stereochemical sequence distributions in vinyl polymers. Chemical shift sensitivities to tetrad, pentad and hexad placements have been reported for ^{13}C NMR spectra of branched polyethylenes, polypropylene (PP), polyvinylchloride (PVC), polyvinylalcohol (PVA), and polystyrene (PS).

Pulsed FT ^{13}C NMR studies clearly demonstrated the presence of ethyl, butyl and longer chain branches in low density polyethylene (72-75). The concentrations of ethyl, n-butyl, and longer chain branches were determined as 3-4,

10-13, and 8-21 per 1000 carbon atoms accordingly. The methyl carbon of the ethyl branch was seen as three resonances. These were associated with isolated butene units (11.2 ppm) and adjacent butene-1 units as m and r dyads (10.8 and 10.4 ppm respectively). The same study was made for PVC (73, 73a) (2-4 branches per 1000 carbons).

Randall (63, 67) made PP ^{13}C resonance assignments with the aid of T_1 's and the model compound study of Zambelli et al. (76) where only nine resonances were observed. Figure 14 shows ^{13}C NMR spectra of PP with the peak assignments.

Tonelli (77) demonstrated that the stereosequence-dependent ^{13}C NMR chemical shifts observed in hydrocarbon polymers can be understood on the basis of the interaction between carbons separated by three bonds.

A chemical inversion in PP chain was considered in papers (78-81). The sequence distributions of inverted propylene units were attributed to Bernoullian (79) or in an opposite view, to first-order Markovian (80) statistics. Isotactic PP was prepared in the presence of organometallic cocatalysts bearing ^{13}C -enriched methyl substituents (81). The enriched methyl carbon is detected, in stereoregular placement, on the end groups and never undergoes transformation to methylene. Therefore it is unlikely that intermediates are involved in the polymerization mechanism. In addition, since neither a chiral carbon nor a spiralized chain participates in the two addition steps, the steric control arises, unequivocally, from the chirality of the catalytic center.

The effects of the tacticity on the ^{13}C NMR spectra of PVC were calculated and observed in (82-84). Keller and coworkers showed in their investigations that ^{13}C NMR spectroscopy allowed immediate determination of CCl_2 groups in chlorinated polyethylene, PP (85), and PVC (86). By combination with proton resonance investigations the quantitative analysis of chlorinated polymers with respect to the constitution, i.e., CH_2 , CHCl , and CCl_2 group content proved possible. The constitution curves obtained deviate slightly from those calculated for the chlorination of CH_2 groups by Bernoullian statistics. The deviations can be sufficiently described by substitution statistics proposed by Frensdorff and Ekiner (87) for parameters $\lambda = 0.6$ for chlorinated polyethylene and 0.9 or 1.6 for PVC, and are discussed with respect to the chlorination model of Kolinski and coworkers (88).

By using the appropriate experimental conditions (in DMSO solution) Wu (89) resolved the methine carbon signal into a triplet of triplets in

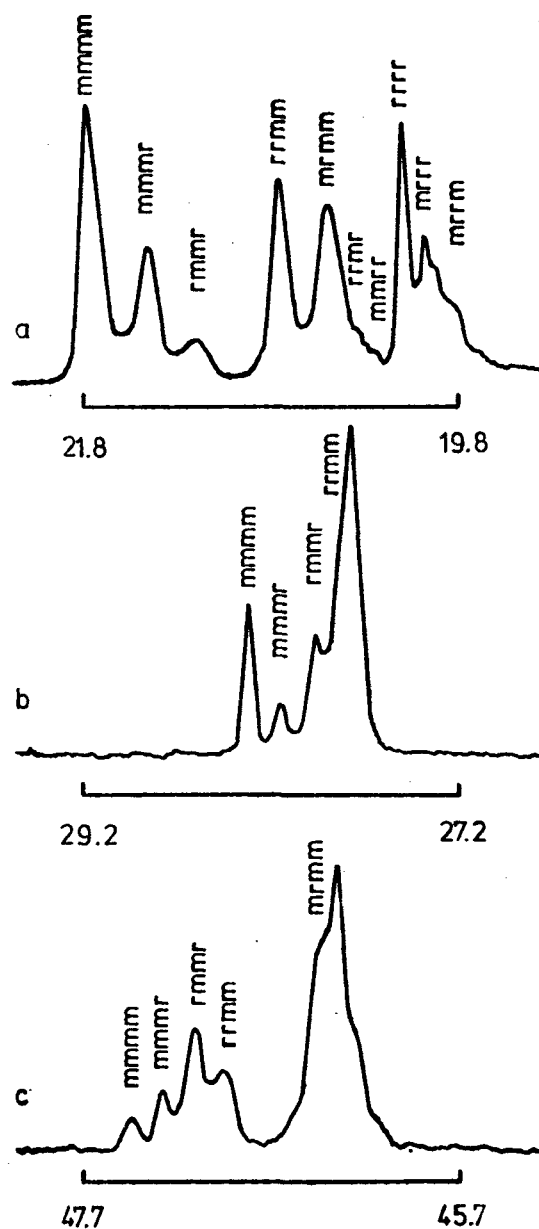


Figure 14. $^{13}\text{C}\{^1\text{H}\}$ NMR spectra of methyl (a), methine (b), and methylene (c) carbons in PP at 120°C (67).

PVA spectra at 67.9 MHz which was readily assignable to pentad tacticity. Quantitative analysis of this spectra proved that stereoregularity of radical-initiated polymerization of vinyl acetate was almost atactic. The stereochemical sequence distribution in the isopoly(vinyl alcohol)

derived from cationic polymerization conforms to first-order Markovian statistics. The conformational aspects of poly(vinyl acetate) have been discussed in (90).

Randall (91) has made an assignment of signals in ^{13}C NMR spectra of amorphous polystyrene (PS) with the aid of model compounds (92) and Paul-Grant calculations of the chemical shifts (71). It has been found that ring currents of neighboring phenyls influenced the methylene

carbon chemical shifts. The stereochemical sequence distribution in PS is in accord with Bernoullian statistics (92a). By using the induced currents approach the increments for the chemical shift of a quaternary carbon due to diamagnetic screening by the neighboring aromatic substituents for atactic (55, 93, 94) and regular conformations (95) of the iso- and syndiofragments of PS, poly-2-vinylpyridine and

Table 5. Assignment of ^{13}C NMR Signals of 1,4-PI (115).

Carbon	Chemical Shift (ppm from TMS)			
	trans-trans	trans-cis	cis-trans	cis-cis
C (1)	39.67	39.91	32.01	32.25
C (2)	134.38	134.55	134.68	134.85
C (4)	26.69	26.55	26.45	26.36

Table 6. Sequence Distributions of 1,4-PI (115).

Sample	Fractions of Dyad Sequence			
	trans-trans	trans-cis	cis-trans	cis-cis
Chicle	66.1	0	0	33.9
Isomerized gutta percha	60.1	12.4	15.3	6.3
	(61.5) *	(16.9) *	(16.9)	(4.7)
Isomerized cis-PI	24.9	25.1	24.6	25.4
	(25.0) *	(25.0)	(25.0)	(25.0)

* The values in parantheses are calculated from Bernoullian statistics.

poly-4-vinylpyridine were calculated. The temperature dependence of chemical shifts of the triads of quarternary carbon of atactic poly-2-vinylpyridine was studied from -20° to 50° C. On the basis of the theoretical and experimental data, a model of an atactic chain was presented for polymers with a different amplitude of torsional oscillations for different structures in the absence of free rotation. Conclusions concerning a conformational set of the irregular chain of macromolecules were made: the isofragments were predominantly from the right-hand and left-hand spirals of the 3_1 type; the syndiofragments contained equal parts of trans-conformation and spiral structures 2_1 (95).

2. Polydienes

Recently several papers were published concerning the sequence distribution study in polybutadiene (36, 52, 96-105) (PB) and polyisoprene (36, 106-109) (PI) by ^{13}C NMR spectroscopy. The ^{13}C peak assignments were made with the aid of model compound spectra (96-98) and of the Grant-Paul additivity coefficient calculations.

Each of the olefinic-carbon signals of the cis-1,4 and trans-1,4 units in PB were reported (36, 99) to split into two peaks which were tentatively assigned to the olefinic carbons of the central monomer unit in the triad sequences of cis-1,4 (C) and trans-1,4 (T) units (Figure 15). The ultrasonic irradiation of the polymer solution caused an enhancement of the resolution in ^{13}C NMR spectra as well as in the decoupled ^1H spectrum (Figure 15c). The observed dyad fractions fitted well to the theoretical curves calculated by assuming Bernoullian statistics (Figure 16). It is in good agreement with those obtained by ^1H NMR and IR measurements. The distribution of cis and trans configurations in 1,4-poly(2,3-dimethyl-1,3-butadiene) follows Bernoullian statistics as well (100).

The ^{13}C NMR spectra of chickie PI and cis-trans isomerized 1,4-PI's were studied in the C_1 , C_2 , and C_4 carbon* signals of the isomerized PI's. The new signals were assigned to the carbon atoms in cis-trans linkages (Table 5). Table 6 shows the fractions of the dyad sequences. It was found that the cis-1,4 and trans-1,4 units were randomly distributed in the isomerized PI's.

Randall has shown (101) that the sequence distribution of 1,2- and 1,4-units in hydrogenated PB's conforms to the first-order Markovian

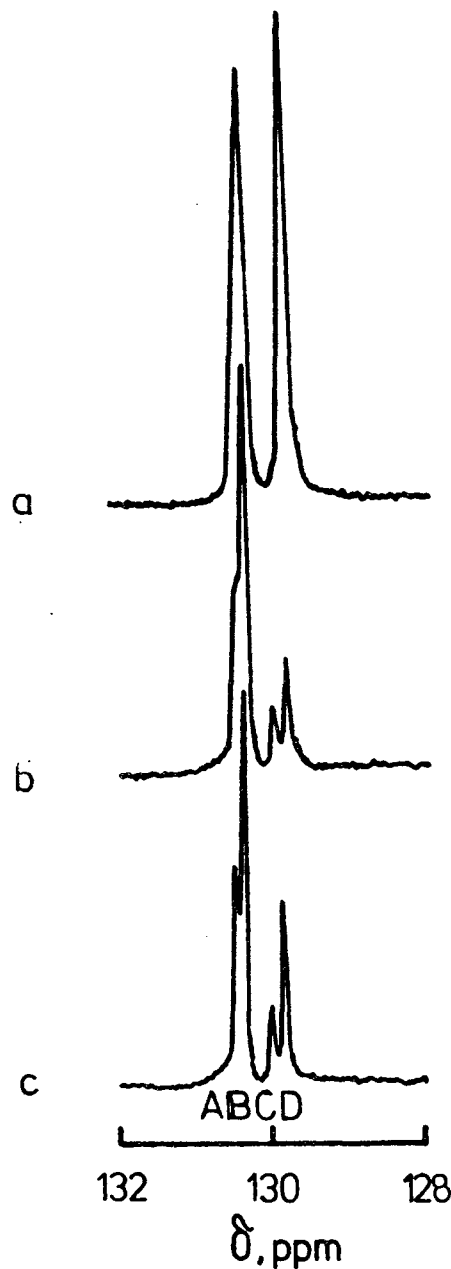


Figure 15. $^{13}\text{C}\{^1\text{H}\}$ NMR spectra of a mixture of cis-1,4 and trans-1,4 PB's (a), isomerized PB (b) and (c) ultrasonic-irradiated product of (b) (36).

* $\text{-(C(1)H}_2\text{-C(2)C(5)H}_3\text{=C(3)H-C(4)H}_2\text{)-}_n$

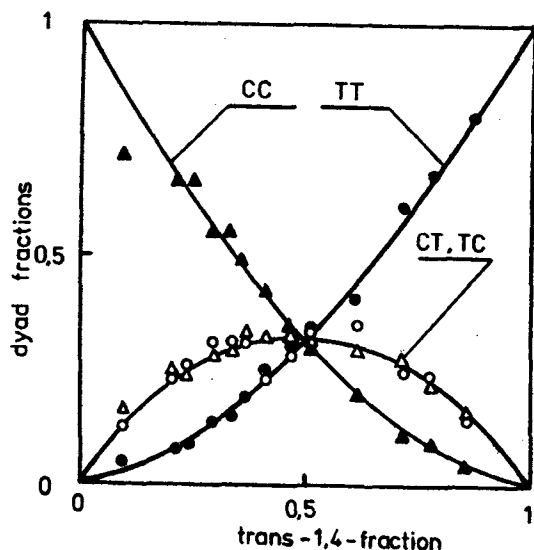


Figure 16. The dyad distributions of cis-1,4 and trans-1,4 units in isomerized PB's (106).

statistics. It may be explained by the steric dependence of a terminal 1,2-unit upon polymerization. Similar results were obtained from ^{13}C NMR spectra of poly(2-phenyl-1,3-butadiene) (102). The consideration of position distributions of 1,2-units in the PB chain makes it possible to assign 64 various triads (103, 103a). The triad assignment of PB aliphatic carbons was made in (104, 105, 105a).

Gronski and coworkers (107) and Beebe (108) published the ^{13}C NMR microstructure results of a binary PI with 3,4-cis-1,4 structural units and of a ternary PI with 3,4 and cis/trans-1,4 units. It has been shown that for all signals, the best agreements between predicted and experimental intensities is found for the Markov model.

Coleman (110) has studied polychloroprene at 67.91 MHz. The dyad and triad microstructure was characterized. The back turning of trans-1,4 and cis-1,4, and isomerized 1,2- and 3,4 units was determined.

^{13}C NMR spectroscopic data obtained for model compounds imitating regular and irregular addition of monomer units in linear PI were compared with the chemical shifts calculated using the empirical regularities found for the branched alkanes and alkenes and a good correlation was established (109). The validity of the

results obtained was confirmed by investigation of the carbon spectra of hydrogenated and deuterated PI's which contain chain fragments with irregular addition of units. Samples of hydrogenated PI's shown in Figure 17 give resonance lines that correspond to the methylene carbons at

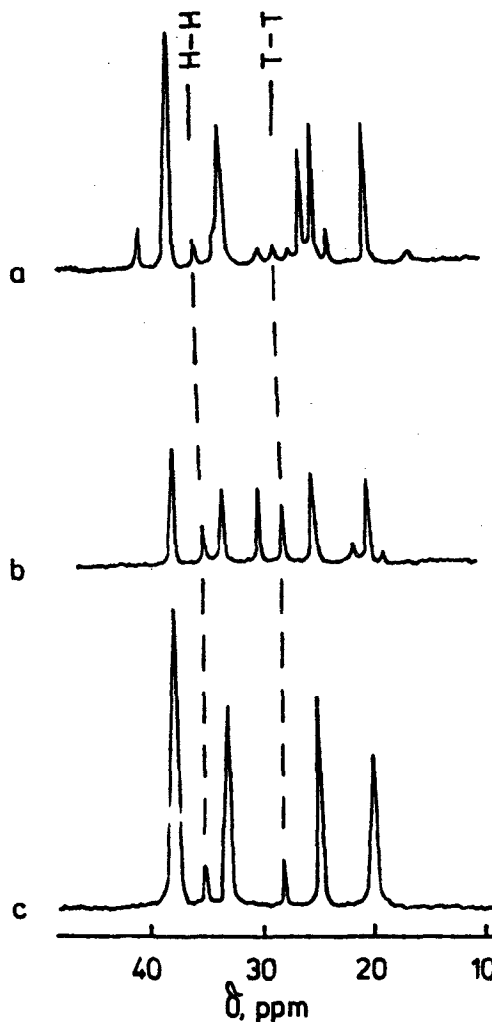


Figure 17. Aliphatic part of the ^{13}C NMR spectra at 67.88 MHz of PI's (109).

34.62 and 27.61 ppm, respectively. For the deuterated PI's, the methylene carbon resonances of trans- and cis-units in head-to-head addition was found at 38.6 and 31.4 ppm, with those in the tail-to-tail addition of both isomers at 28.4-28.8 ppm. The latter findings offer a practical means of characterizing irregularities in PI.

3. Olefinic Copolymers

Ethylene-propylene copolymers (EPC) have been well studied (111-114) with the aid of ^{13}C NMR spectra of model alkanes (112, 113). Carman and Elgert (111, 112) have developed a mathematical model of EPC polymerization which accurately accounts for the intensity of each peak in any spectrum of EPC. This is a terpolymer model in which the propylene is added by either primary or secondary insertion. Thus propylene inversion is determined from the ratio of contiguous to isolated propylene sequences. The stereochemical environment of the isolated ethylene units, and the arrangement of the neighboring propylene units in EPC, prepared in the presence of syndiotactic- and isotactic-specific catalysts were investigated (113, 115) by comparing ^{13}C NMR spectra of selectively ^{13}C -enriched copolymers. The implications of copolymer structure on polymerization mechanisms are considered. In the presence of homogeneous syndiotactic specific catalyst systems, both the regiospecificity and stereospecificity are controlled by the last unit of the growing chain end. Stereoregulation is transmitted through achiral ethylene units, but not in isotactic polymerization. The meaning of these facts is that

the isotactic regulation arises from the asymmetric spatial arrangement of the ligands in the catalytic centers, whereas the syndiotactic regulation arises from the asymmetry of the last unit of the growing chain end; syndiotactic regulation is therefore last whenever the last unit is achiral.

The dyad-tetrad sequence distribution in propylene-butene-1 copolymers was determined in (114-116). The monomer distribution is in good agreement with Bernoullian statistics (115). The analysis of methine triads and tetrads of backbone methylene carbons have been verified using first-order Markovian theory (116). Coisotactic shift contributions also account for the reverse order of the propylene-centered from that predicted by the Grant-Paul equation.

Quite a number of authors (51, 89, 117, 118) investigated ethylene-vinyl acetate copolymers. The intensities of the methine and methylene peaks were related to the triad populations. The plots of triad population variations with monomer ratios are given in Figure 18. The similar triad splitting of the quarternary carbon, CN or CO groups was obtained in ^{13}C spectra of random styrene copolymers with acrylonitrile (119, 120), acrylic acid (121) and MMA (51) and alternating styrene-MMA copolymers (122).

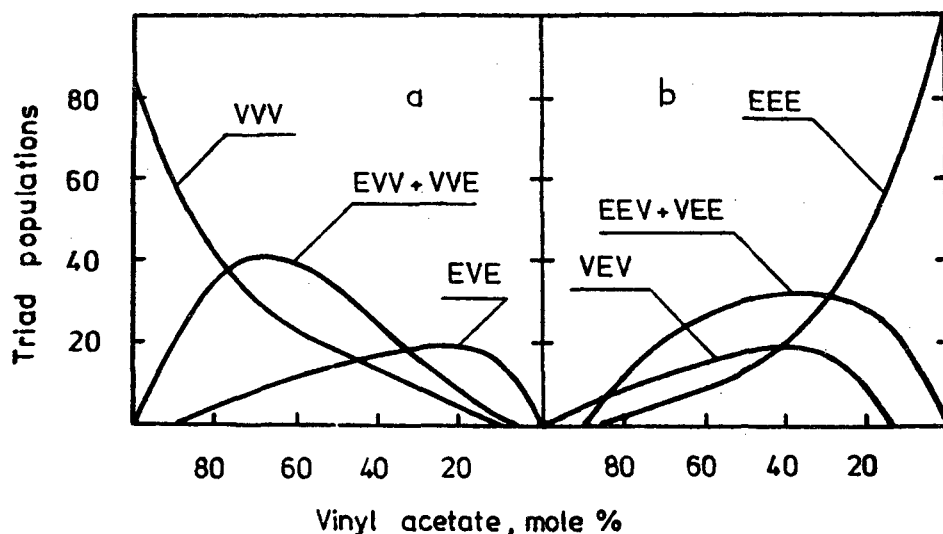


Figure 18. Variation of (a) V-centered and (b) E-centered triad populations in ethylene-vinyl acetate copolymer with copolymer composition (51).

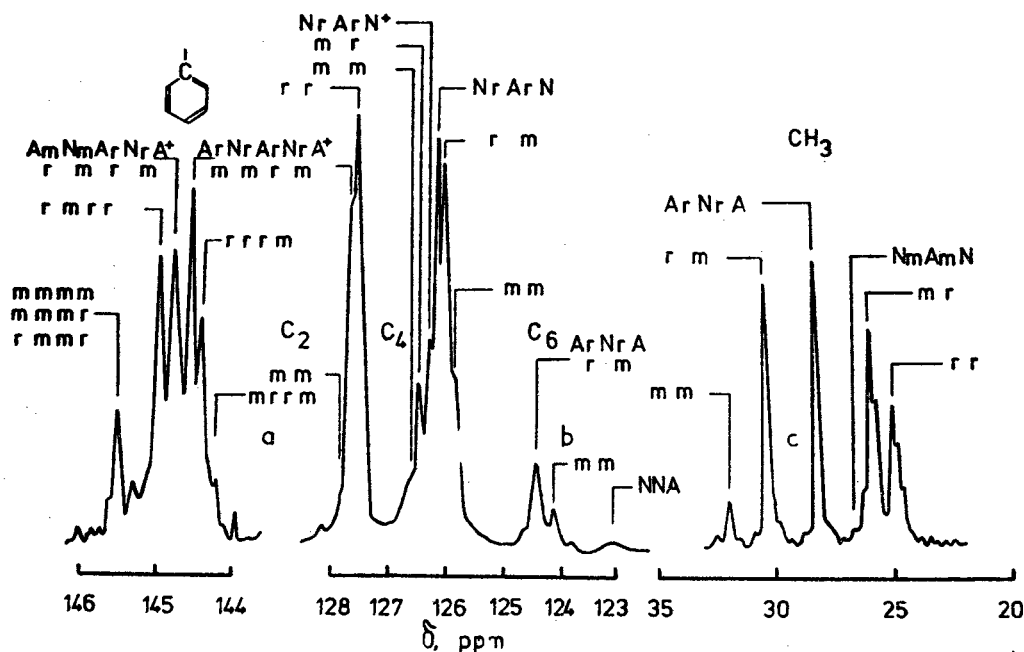


Figure 19. ^{13}C NMR spectrum of an alternating copolymer from α -methylstyrene and methacrylonitrile. Resonance regions: aromatic (a), nitrilic (b) and methyl (c) carbons (123).

Comparison of the ^{13}C NMR spectrum at 67.88 MHz of alternating methacrylonitrile- α -methylstyrene copolymer with those of the syndiotactic homopolymers showed that the copolymer had the random configuration with dominantly syndiotactic enchainment of monomers (123), in contrast to ^1H NMR results. Figure 19 shows the triad and pentad peak assignments. The relative configurational enchainment of α -methylstyrene (A) and methacrylonitrile (N) in erythro-diisotactic structure is m, whereas in threo-diisotactic is r. Slight deviation from exact alternating copolymerization was shown by the presence of NNA triad or its corresponding pentads.

The radical copolymers of MMA with MAA and α -methacrylophenone were studied (124, 125). In this case Bernoullian statistics describes the chain growth too. The steric factors and high polarizability of aromatic keto-groups caused the large values of $P_m = 0.40-0.43$ (125).

4. Diene Copolymers

The first peak assignments for alternating butadiene-propene, -acrylonitrile, isoprene-propene, -acrylonitrile and some polyalkenylenes and polypentadienes has been obtained by Gatti and Carbonaro (126) with the aid of

off-resonance experiments and of calculations by the Grant and Paul scheme.

The ^{13}C NMR spectrum of butadiene-styrene copolymer has 30 peaks at 25-46 ppm and 19 peaks at 114-146 ppm assigned to 152 possible triads of 6 units: cis-1,4; trans-1,4; "head-to-tail" and "head-to-head"-1,2-butadiene (B); "head-to-tail" and "head-to-head" styrene (S) (51, 127-129). In general, one would expect all the styrene in samples to be in BSB triads and would therefore expect a pattern of absorptions (BS and SB) very similar to that of the vinyl units (Bv and vB), also expected to be randomly distributed (51, 127). Styrene average block lengths were found to vary greatly (1.2-5.9 units) while vinyl butadiene units showed no tendency to block together, cis units only a small tendency (1.0-1.7) and trans units a moderate tendency (1.2-3.4). Styrene units display a tendency to block with trans units whereas vinyl and cis units generally prefer to block with trans units (127, 129).

The butadiene-vinylchloride copolymers obtained by radiation copolymerization in channel complexes of urea have randomly distributed units. Vinylchloride forms predominantly syndiotactic sequences (130).

Emulsion processed butadiene-acrylonitrile (51) and isoprene-acrylonitrile (53, 54)

copolymers were investigated. The vinyl and CN peaks were the most sensitive to environment and splitting into triad components. The structure of these copolymers is highly alternating (see Table 3). At 28% acrylonitrile it is essentially block butadiene with short runs (1–3 units) of alternating A and B increasing to 7–8 unit lengths at 40% (51). With increasing conversion the content of block-triads increases. The data prove that the theories of Medvedev and Smith-Ewart apply to emulsion polymerization (54).

We also studied the microstructure of copolymers of α,β -unsaturated ketones (K) with isoprene (I) by ^{13}C NMR spectroscopy (60). Figure 20 shows the spectra of copolymers of isoprene with alkylvinylketones $\text{CH}_2=\text{CH}-\text{COR}$ ($\text{R} =$

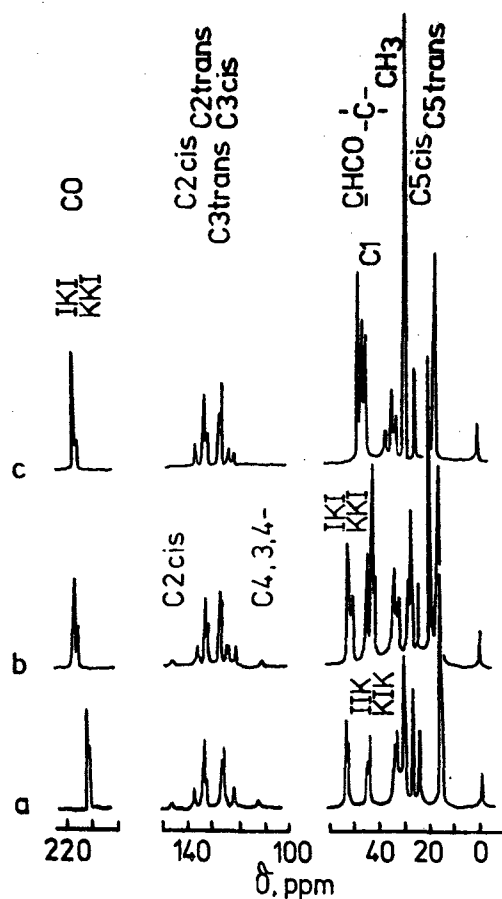


Figure 20. ^{13}C NMR spectra of copolymers isoprene with methyl- (a) isopropyl- (b) and tert-butylvinylketone (c) in CDCl_3 (60).

CH_3 , $\text{CH}(\text{CH}_3)_2$ or $\text{C}(\text{CH}_3)_3$). The splitting of

signals into two components corresponding to KII and KIK, IKI and IKK triads demonstrates the tendency of these copolymers to alternation at radical polymerization. The statistical treatment of the data obtained shows (Table 7) that the character of polymer chain propagation follows first-order Markovian statistics, and the average length of alternated sections depends on the conformation of the alkyl substituent in α,β -unsaturated ketones (S-cis or S-trans). Similar alternation was discovered for radical polymerized butadiene-methacrylate copolymers (131).

Table 7. The Values of Conditional Probabilities, Average Lengths of Block $\langle n_{\text{KK}}(\text{II}) \rangle$ and Alternating Unit $\langle n_{\text{KI}}(\text{IK}) \rangle$, and Isomeric Composition of Isoprene with Alkylvinylketones Copolymers (68).

Parameter	R		
	$-\text{CH}_3$	$-\text{CH}(\text{CH}_3)_2$	$-\text{C}(\text{CH}_3)_3$
[K]	0.480	0.485	0.545
P _{KK} (II)/K _I (IK)	1	1	1
P _{KI} (IK)/K _K (II)	0.103	0.167	0.053
P _{KI} (IK)/K _I (IK)	0.897	0.833	0.947
P _{KK} (II)/K _K (II)	0	0	0
$\langle n_{\text{KK}}(\text{II}) \rangle$	0.82	1.00	1.00
$\langle n_{\text{KI}}(\text{IK}) \rangle$	9.67	5.99	19.0
trans-1,4 I	0.695	0.510	0.673
cis-1,4 I	0.244	0.353	0.327
3,4 I	0.062	0.138	0

Microstructure of chloroprene-2,3-dichlorobutadiene copolymers prepared in free-radical-initiated systems have been studied (132). The assignments were given in dyad form as combinations of tail-to-head, head-to-tail, or cis-chloroprene components. The calculated monomer reactivity ratio product, $r_1 \cdot r_2 > 1$, showed that the copolymers had a slight tendency toward blockiness. The monomer composition influenced microblockiness.

To analyze the effect of monomer composition on a microstructure of copolymers of piperylene with acrylonitrile obtained by the polymerization in DMSO, the ^{13}C NMR at 67.88 MHz was used (61). The peak assignments in ^{13}C spectra (Figure 21) were made with the aid

of chemical shifts calculated by the additive scheme of Lindeman and Adams. The data on a triad composition in copolymer

chain show (Table 8) that the character of chain propagation accord with the first-order Markovian statistics.

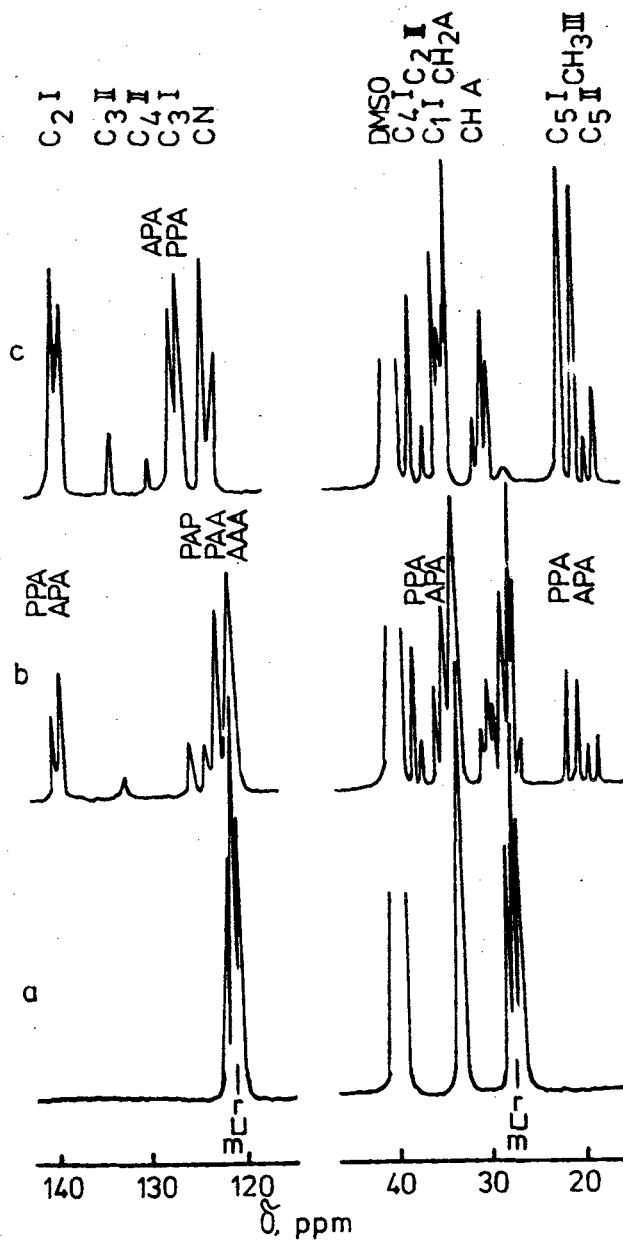
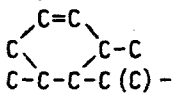


Figure 21. $^{13}\text{C}\{^1\text{H}\}$ NMR spectra of polyacrylonitrile (a) and copolymers piperylene with acrylonitrile, containing 75.6 (b) and 51.5 (c) mol.% acrylonitrile in DMSO-d_6 (61).

Table 8. The Values of Conditional Probabilities, Average Lengths of Block $\langle n_{AA}(PP) \rangle$ and Alternating Unit $\langle n_{AP}(PA) \rangle$, and Isomeric Composition of Piperylene in Copolymers with Acrylonitrile (69).

Parameter	Acrylonitrile Content, mol.%			
	51.5	65.1	75.6	89.5
$P_{AA}(PP) / AP(PA)$	1.00	0.680	0.397	0.104
$P_{AP}(PA) / AA(PP)$	0.261	0.429	0.503	0.552
$P_{AP}(PA) / AP(PA)$	0.739	0.571	0.497	0.448
$P_{AA}(PP) / AA(PP)$	0	0.320	0.603	0.896
$\langle n_{AA}(PP) \rangle$	1.00	1.47	2.52	9.65
$\langle n_{AP}(PA) \rangle$	3.83	2.33	1.99	1.81
trans-1,4 P	0.873	0.876	0.888	0.925
cis-3,4 P	0.105	0.096	0.064	0
	0.022	0.028	0.048	0.075

At more than 67 mol.% content acrylonitrile in the copolymer, the chain is transformed from syndiotactic into isotactic. The increase of acrylonitrile content also increases the possibility of 1,4-trans-addition and decreases the possibility of 3,4-cis and cyclic addition of piperylene. In copolymer with 73.8 mol.% of acrylonitrile obtained by emulsion polymerization, cyclic structures are absent.

The quantity of the above examples is large enough so as to be convinced of the considerable achievements of ^{13}C NMR in microstructure analysis of macromolecules. However, ^{13}C NMR has the same difficulties as that of ^1H NMR: limited precision of sequence analysis through line superposition and complexity of well-founded line assignments.

IV. NEW METHODS OF MICROSTRUCTURE ANALYSIS

A. Use of Shift Reagents for Chain Microstructure Analysis

Recently, paramagnetic salts containing lanthanides such as europium or praseodymium have been effectively used for the investigation of polymer and copolymer microstructure and chain conformation. The first applications of paramagnetic shift reagents to a number of polymers containing a basic lone-pair

functionality in the monomer unit were made for spectral simplification (133-143). It has been reported that the use of $\text{Eu}(\text{dpm})_3$, $\text{Eu}(\text{fod})_3$ and $\text{Pr}(\text{fod})_3$ improved the resolution in 100 and 220 MHz spectra of PMMA, poly(vinyl methyl ether), poly(vinyl acetate), poly(propylene oxide), polysiloxanes (64, 133, 134), polyethers (135, 136), polyoles (137-139), polylactones (140), etc. Guillet et al. (134) found that the order of shifts for the various peaks in o-dichlorobenzene as solvent was $s\text{-C-CH}_3 > i\text{-C-CH}_3 > h\text{-C-CH}_3 > i\text{-OCH}_3 > s\text{-OCH}_3 > h\text{-OCH}_3$ for the triad sequence peaks of the methyl and methoxycarbonyl signals. It had been found that in benzene solution at room temperature, the order of shifts obtained was $i\text{-C-CH}_3 > h\text{-C-CH}_3 > s\text{-C-CH}_3 > i\text{-OCH}_3 > h\text{-OCH}_3 > s\text{-OCH}_3$. The explanation of this is primarily a reflection of the dependence of polymer conformation on tacticity (133-135). Figure 22 shows the ^1H NMR spectrum of a sample of poly(vinyl acetate) in CDCl_3 , and the effect of the addition of small quantities of $\text{Eu}(\text{fod})_3$ and $\text{Pr}(\text{fod})_3$ to the solution. It can be seen that with both reagents the methoxycarbonyl protons are readily separated into the absorptions for iso-, hetero- and syndiotactic triads. The slopes of the lines in the diagram give a clear indication of the degree of shift and it is noted that the $\text{Pr}(\text{fod})_3$ gives larger shifts than $\text{Eu}(\text{fod})_3$ but in the former the broadening is a bit greater.

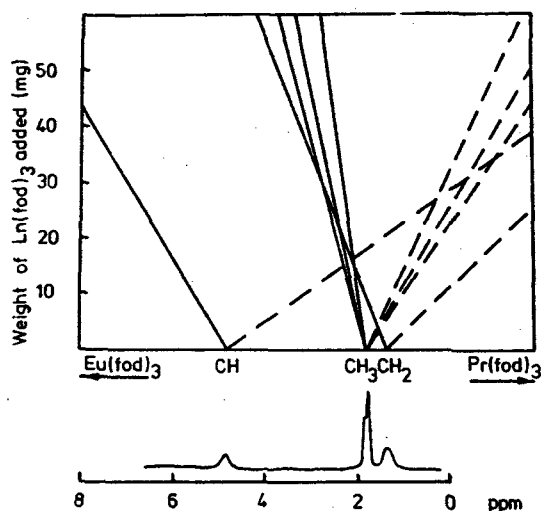


Figure 22. Effect on the ^1H NMR spectrum of poly(vinyl acetate) of adding $\text{Eu}(\text{fod})_3$ and $\text{Pr}(\text{fod})_3$ (133).

Slonim and coworkers (137) have shown that the values of paramagnetic shifts depended on the europium distribution between different coordinating centers of polyethylene glycol and polyformaldehyde chains. To determine the content of ordered trans-gauche-trans (TGT) conformation in polyethylene glycol ^1H NMR spectra were measured. The singlet peak at the lowest field was assigned to the TGT conformation of the COCCOC sequence (138). The stereospecific contact interactions in the NMR spectra of polyol-lanthanide (La^{3+} , Pr^{3+} , Nd^{3+} , Eu^{3+} , Tb^{3+} , Yb^{3+}) complexes were investigated (139). It has been shown that the contact increment in paramagnetic shifts is greatest if the chain is planar zig-zag. In other cases the isotropic proton shift is pseudocontact predominantly.

Inoue and Konno (64) established the possible conformations in solution of iso- and syndiotactic PMMA, by comparing the observed values of pseudocontact shift with the values of the geometrical factor $(1 - 3\cos^2\theta)/r^3$, in the McConnell-Robertson equation, calculated for any glide plane or heliocoidal chain conformations. Figure 23 shows the paramagnetically induced proton shifts $\Delta\delta$ of the three groups, $\alpha\text{-CH}_3$, CH_2 , and OCH_3 of iso- and syndiotactic PMMA in CDCl_3 and C_6D_6 solutions with increasing $\text{Eu}(\text{dpm})_3$

concentration. The values can be related to the relative distance of protons from the coordinating site and they are dependent on solvent for syndiotactic PMMA. In general the flexible polymer chain in solution cannot always take the specially fixed conformation. However, it has been shown that isotactic PMMA has the right-handed (10/1) helix conformation. The trans zig-zag conformation suggested for syndiotactic PMMA is a special case of glide-plane or heliocoidal conformations.

The effect of paramagnetic shift reagents $\text{Eu}(\text{dpm})_3$ and $\text{Pr}(\text{dpm})_3$ on the ^1H NMR spectra of atactic poly-4-vinylpyridine (P-4-VP) was studied in CDCl_3 solution in the temperature range 28–100°C (140). From the analysis of ^1H (360 MHz) and ^{13}C (22.63 MHz) spectra the microtacticity of radical P-4-VP was determined and was well described by Bernoullian statistics with $P_m = 0.52$. It was shown also that ^1H shifts of signals induced by $\text{Eu}(\text{dpm})_3$ were pseudocontact by nature. The values of the geometrical factor were calculated for the fragments of regular conformations of iso- and syndiochains of a macromolecule. Based on a comparative analysis (according to a principle of maximum probability) of the experimental and calculated values of shifts induced by $\text{Eu}(\text{dpm})_3$, the conformational composition of the polymer was determined. It has been shown that the structural contents were $[2,] = 47$ mol.% (TTGG), $[Z_s] = 28$ mol.% (trans-zig-zag) and $[3,] = 25$ mol.% (iso) which were in agreement with the model of P-4-VP microtacticity (55, 95). From the temperature relationship of the ^1H shifts of signals a conclusion was made about the variation of P-4-VP conformational set to the direction of the increase of the syndiotrans-form content.

We suggested an analytical method of investigating microstructure of copolymers with the use of shift reagents. The possibility of practical application of this method has been shown, the analysis of butadiene or isoprene and acrylonitrile, MMA, or alkylvinylketone copolymers being examples (54, 141–143). Figure 24 shows the resulting spectral effect of $\text{Eu}(\text{fod})_3$ addition to the isoprene-acrylonitrile (38 mol % A) copolymer solution. The values of paramagnetic shifts of methyl, methylene, and vinylidene triad signals decrease in AAA, AAI, IAI, and AIA, AII, III succession. Quantitative data were calculated from the content of triads in the copolymers obtained under emulsion copolymerization on sodium alkylsulfonate (ASS) and potassium abietate (AP) micelles, in mass or solution with different monomer content and conversion. It

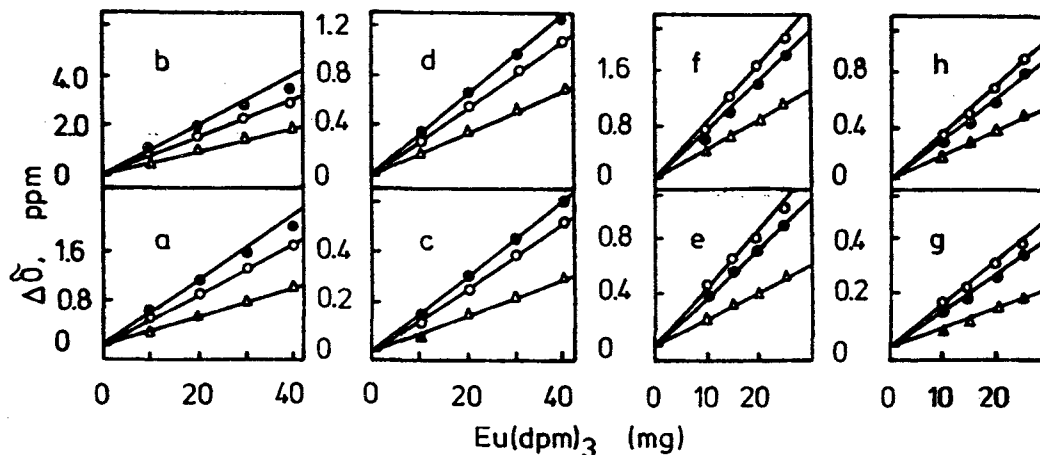


Figure 23. Variation of the paramagnetically induced proton shift with the amount of Eu(dpm)_3 for isotactic (a, b, e, f) and syndiotactic (c, d, g, h) PMMA at 25°C (a-d) and 80°C (e-h) in solutions in CDCl_3 (a, c, e, g) and C_6D_6 (b, d, f, h). Concentration of polymer was 20 mg/0.4 mL. (●): CH_2 ; (○) $-\text{CH}_3$; (Δ): OCH_3 (64).

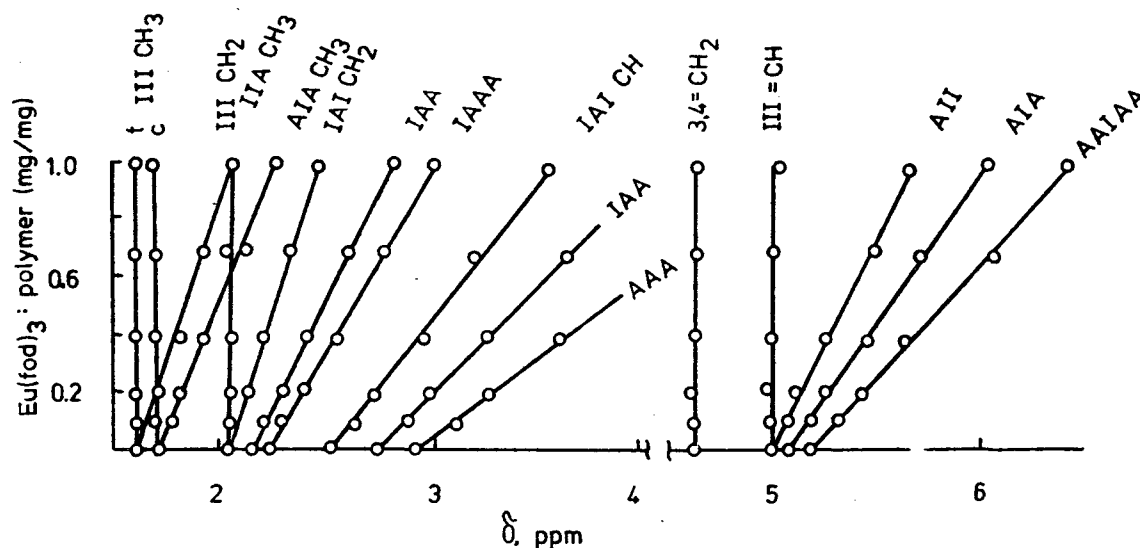


Figure 24. Relationship between induced paramagnetic shift of triad-tetrad signals in the ^1H NMR spectra of isoprene-acrylonitrile copolymers and Eu(fod)_3 : copolymer (w/w) ratio (142).

was found that a blocking level of the copolymers increased with an increase of local concentration and a decrease of polar monomer molecule diffusion velocity in the micelle matrix (54, 143). The stability analysis of aqueous mixed ASS-AP

micelles and micelles of fatty acids (144, 145) with the relaxation probe Mn^{2+} allowed us to make a conclusion about the principal influence of detergent association in the micelle matrix upon microstructure (54, 145). The isoprene with

acrylonitrile or MMA copolymers obtained on matrices of different ASS-AP compositions have a maximum blocking level with a maximum stability at 66.7 mol. % AP. Figure 25 shows the

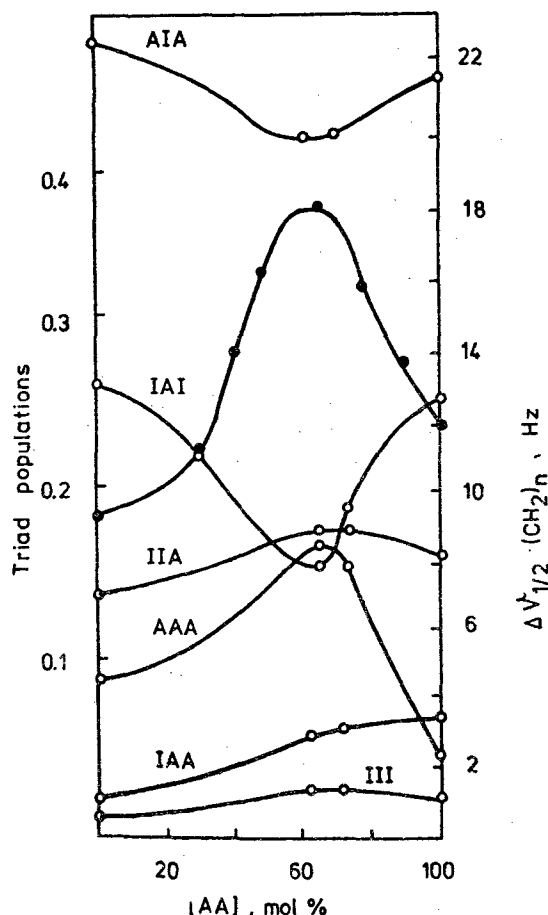


Figure 25. Relationship between triad contents and $\Delta\nu_{1/2}(\text{CH}_2)_n$ in ^1H NMR spectra of ASS-AP micelles and AP contents in them (145).

relationship between the matrix stability criterion ($\Delta\nu_{1/2}$ of the $(\text{CH}_2)_n$ signal in the spectrum of mixed micelles) and triad content. The chain-growth statistics of emulsion copolymers are first- or second-order Markovian (145). The same results were obtained for styrene-MMA copolymers investigated without shift reagents (146).

The ^1H NMR spectra of ethylene- and vinyl chloride-vinyl acetate copolymers with low vinyl acetate (VA) content were measured by use of $\text{Eu}(\text{fod})_3$. The shifted signals of the acetate

methyl and methine protons were tentatively assigned to the triad sequences with a VA unit as a center, and their evaluated concentrations were compared with calculated concentrations by means of the random copolymerization theory (147). Similar investigations were made for chloroprene-MMA copolymer with aid of $\text{Eu}(\text{dpm})_3$ (148).

The investigation of microstructure of the unsaturated polymers and copolymers without polar groups is performed by the use of the composite complex: double bond- AgNO_3 - $\text{Eu}(\text{fod})_3$ (148a).

The examples show that use of shift reagents for microstructure analysis and for the study of the polymerization mechanism of polymers having unresolved monomer unit spectra is particularly effective.

B. Magic Angle Spinning and High Resolution NMR Spectroscopy in Solid Polymers

Two sorts of line-narrowing techniques are employed to obtain high-resolution, natural abundance ^{13}C NMR spectra of solid polymers. Dipolar broadening of the ^{13}C lines by protons is removed by strong resonant decoupling (referred to as dipolar decoupling) by using ^1H decoupling rf fields of about 10 G (149). These decoupling fields are comparable to the proton linewidth. In most cases the resulting ^{13}C NMR spectra are still severely complicated by chemical shift anisotropies, so that, in general, only a few broad lines are observed. A dramatic improvement of the resolution can be achieved by additional mechanical spinning of polymer samples at the so-called "magic angle" with a frequency somewhat greater than the dispersion of chemical shifts (149, 150).

Even with the resolution achieved by a combination of dipolar decoupling and magic angle spinning, a FT experiment on a solid polymer still has a serious limitation. Namely, a delay time of several ^{13}C spin-lattice relaxation times (T_1) must be tolerated before data sampling can be repeated. These repetitions are necessary to provide a suitably strong signal by a time-averaging process. Since some ^{13}C T_1 's for solid polymers are on the order of tens of seconds (149), the time-averaging process becomes tedious. These delays can be avoided, however, by performing a matched spin-lock (or Hartmann-Hahn) cross-polarization (CP) experiment (151). With this technique, polarization of the carbons is achieved by a polarization transfer from nearby protons, spin-locked in their own rf field, via static dipolar interactions in a time $T_{\text{CH}}(\text{SL})$.

This polarization transfer is a spin-spin or T_2 -type process and generally requires no more than 100 μ s (149). Most important, the CP transfer can be repeated and more data accumulated after allowing the protons to repolarize in the static field. For glassy polymers near room temperature this is more efficient than ^{13}C repolarization by spin-lattice processes and generally occurs in less than a half second (152).

Schaefer (149, 153) has discovered that CP and magic angle spinning are compatible. As shown in Figure 26, high resolution in the dipolar-decoupled ^{13}C spectrum of solid PMMA is achieved with quite low spinning frequencies, of the order of 500 Hz. This is true despite the fact that the chemical shift dispersion of the low-field resonance arising from the carbonyl carbon is about 3 KHz (154).

With separate lines resolved for individual carbons, a variety of relaxation experiments can be performed and interpreted in terms of the motions of the polymers in the solid state. It is well known that a ^1H rotating-frame relaxation time ($T_{1\rho}$) is sensitive to motions associated with frequencies in the 10-100 KHz range.

Figure 27 shows the results of ^{13}C $T_{1\rho}$ experiments for solid polycarbonate, both with and without magic angle spinning, at 3 KHz (149). Five lines are well resolved. The lowest field line arises from the overlap of the carboxyl carbon resonance with that of the nonprotonated aromatic carbons. This line has the longest $T_{1\rho}$. The two lines just to higher field arise from the protonated aromatic carbons. These lines have the same relaxation behavior as one another and are characterized by a short $T_{1\rho}$. The two lines at high field are due to the quarternary and methyl carbons. The methyl carbon $T_{1\rho}$ is intermediate between that of the low field combination line, and that of the protonated aromatic-carbon line. This behavior simply reflects the weaker coupling of nonprotonated carbons to more distant protons as determined by the inverse sixth power dependence on the internuclear separation common to all dipolar interactions.

The ^{13}C $T_{1\rho}$ and $T_{\text{CH}}(\text{SL})$ have been measured also for poly(phenylene oxide), polystyrene, polysulfone, poly(ether sulfone), PVC (149, 155), polybutadiene and poly(ethylene oxide) (156).

The ^{13}C $T_{1\rho}$ at 32 KHz is dominated by spin-lattice processes rather than spin-spin processes. This means that the $T_{1\rho}$'s contain information about the motions of the polymers in the 10–50 KHz region, while the T_{CH} 's contain information about the near static interactions. The T_1 's and NOE factors contain information

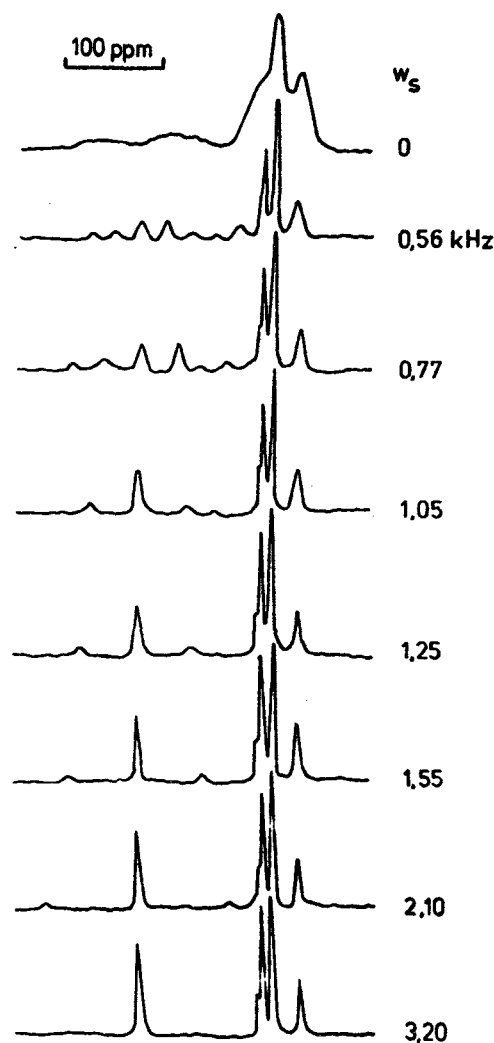


Figure 26. 10 G dipolar-decoupled ^{13}C NMR spectra of PMMA magic angle rotor, as a function of spinning frequency. The CP was performed with spin-temperature alternation to remove artifacts (154).

about the motions in the 5–30 MHz regions. Interpretation of the $T_{1\rho}$'s of these polymers emphasises the dynamic heterogeneity of the glassy state. Details of the relaxation processes establish the short-range nature of certain low frequency side-group motions, while clearly defining the long-range cooperative nature or some of the main-chain motions, the latter not consistent with a local-mode interpretation of motion. For instance, polystyrene the T_{CH} and $T_{1\rho}$ values are 1.2 and 3.5 ms for aromatic rings, 0.5 and 3.6–4.1 ms for main chain carbons (155). These motions involve cooperative

torsional oscillations within conformations rather than another (149, 153). The ratio of T_{CH} to $T_{1\rho}$ for protonated carbons in the main chain of

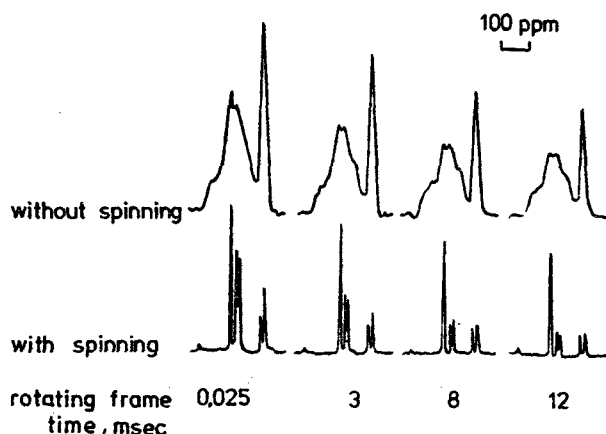


Figure 27. CP ^{13}C NMR spectra of polycarbonate with and without magic angle spinning, as a function of the time the carbon magnetization was held in the rotating frame without CP contact (149).

each polymer is found to have a direct correlation with the toughness or impact strength for all studied polymers (149). This empirical correlation was rationalized in terms of energy dissipation for chains in the amorphous state in which low-frequency cooperative motions were determined by the same inter- and intrachain steric interactions.

Thus one-hundred Hertz resolution has been achieved in the ^{13}C NMR spectra of solid polymers by a combination of dipolar decoupling and magic angle spinning. The high resolution permits individual resonance lines to be assigned to specific carbons and monomer unit sequences in the polymer.

V. CONCLUSIONS

Finishing on this consideration of microstructure analysis of polymer chains with the aid of ^1H and ^{13}C NMR spectroscopy, one must note that this field of polymer physical chemistry set the powerful arsenal of varied investigation methods against extremely intricate problems.

The use of spectrometers with superconducting magnets, shift reagents and magic angle rotation represents the newest directions in

NMR. However, actually all of these methods will not be able to secure the complete resolution of signals in the ^1H and ^{13}C NMR spectra of polymers. Therefore the extraction of spectral information about microtacticity and conformation of the chain with the aid of computers is widely practiced.

We may expect increased understanding of the microstructures of mainly linear polymers and copolymers as experimental techniques improve. In turn this should lead to better understanding and hence control of the chain growth mechanism through variation of the conditions of synthesis. Great possibilities then open up for the design of polymers of specific physical characteristics for industrial application leading to increased cost effectiveness and quality improvement. It is hoped that this review will have shown that this subject offers considerable intellectual challenge together with its potential economic importance.

REFERENCES

- ¹F. A. Bovey and G. V. D. Tiers, *J. Polym. Sci.* **44**, 173 (1960); *Fortschr. Hochpolym.-Forsch.* **3**, 139 (1963); F. A. Bovey, *Pure and Appl. Chem.* **12**, 525 (1966).
- ²F. A. Bovey, *High Resolution NMR of Macromolecules*, Academic Press, New York, 1972.
- ³I. D. Robb, in *Nuclear Magnetic Resonance*, Vol. 5, Academic Press, London, 1976, p. 205.
- ⁴N. A. Plate and L. B. Stroganov, *Vysokomol. Soed. (USSR)* **18**, 955 (1976).
- ⁵F. Heatley, in *Nuclear Magnetic Resonance*, Vol. 9, Academic Press, London, 1980, p. 204.
- ⁶R. K. Harris, K. J. Packer, and B. J. Say, *Makromol. Chem. Suppl.* **4**, 117 (1981).
- ⁷D. Yan, *Makromol. Chem.* **184**, 91 (1983).
- ⁸B. D. Coleman and T. G. Fox, *J. Polym. Sci. Part A*, **1**, 3183 (1963); *J. Chem. Phys.* **38**, 1065 (1963); *J. Am. Chem. Soc.* **85**, 1241 (1963).
- ⁹B. D. Coleman, T. G. Fox, and M. Reinmüller, *J. Polym. Sci. Part B*, **4**, 1029 (1966).
- ¹⁰H. J. Harwood and W. Richey, *J. Polym. Sci. Part B* **3**, 419 (1965).
- ¹¹J. Podešva and D. Doskočilova, *Makromol. Chem.* **178**, 2383 (1977).
- ¹²L. B. Stroganov, N. A. Plate, V. P. Zubov, S. Yu. Fedorova, and Yu. A. Strelenko, *Vysokomol. Soed. (USSR)* **A16**, 2616 (1974).
- ¹³N. A. Plate, L. B. Stroganov, and P. M. Nedoresova, *Vysokomol. Soed. (USSR)* **A14**, 440 (1972).
- ¹⁴A. Provasoli and D. R. Ferro, *Macromol. Chem.* **10**, 874 (1977).

- ¹⁵W. Ritter, M. Möller, and H.-J. Gantov, *Makromol. Chem.* **179**, 823 (1978).
- ¹⁶H. Yuki and K. Hatada, in *Advances in Polymer Science*, Vol. 31, 1979, p. 3.
- ¹⁷Sh. Fujishiga, *Makromol. Chem.* **176**, 225 (1975); *ibid.* **177**, 375 (1976).
- ¹⁸K. J. Ivin and M. Navratil, *J. Polym. Sci. Part A* **1**, 8, 3373 (1970); *ibid.* **9**, 1 (1971).
- ¹⁹T. Yoshino and J. Komiyama, *J. Polym. Sci. Part B* **3**, 311 (1965).
- ²⁰L. Cavalli, G. C. Botsini, G. Carravo, and G. Confalonieri, *J. Polym. Sci. Part A* **1**, 8, 801 (1970).
- ²¹J. Zymonas and J. Harwood, *Am. Chem. Soc., Polym. Prepr.* **12**, 330 (1971); J. Zymonas, E. R. Santee, and H. J. Harwood, *Macromol.* **6**, 129 (1973).
- ²²J. San Roman, E. L. Madruga, and M. A. Del Puerto, *Angew. Makromolek. Chem.* **78**, 129 (1979).
- ²³H. Koinuma, T. Tanabe, and H. Hirai, *Makromol. Chem.* **181**, 383 (1980).
- ²⁴E. K. Klesper, *J. Polym. Sci. Part B*, **6**, 313, 663 (1978); E. K. Klesper and W. Gronsky, *J. Polym. Sci. Part B*, **7**, 727 (1969); E. K. Klesper, A. Johnsen, W. Gronsky, and F. W. Wehrly, *Makromol. Chem.* **176**, 1071 (1975).
- ²⁵H. J. Harwood and T. Susuki, *J. Polym. Sci., Polym. Chem. Ed.* **13**, 526 (1975).
- ²⁶D. Strasilla and E. Klesper, *Makromol. Chem.* **175**, 535 (1974).
- ²⁷H. Yuki, Y. Okamoto, K. Ohta, and K. Hatada, *J. Polym. Sci., Polym. Chem. Ed.* **13**, 1161 (1975); H. Yuki, Y. Okamoto, Y. Shimada, and K. Ohta, *ibid.* **17**, 1215 (1979).
- ²⁸A. K. Kashyap and V. Kalpagam, *J. Indian Chem. Soc.* **54**, 524 (1977).
- ²⁹O. Jardetsky and N. G. Wade-Jardetsky, *Ann. Rev. of Biochem.* **40**, 766 (1971).
- ³⁰T. Suzuki and H. J. Harwood, *Polym. Preprints* **16**, 638 (1975).
- ³¹S. L. Malhotra and L. P. Blanchard, *J. Macromol. Sci. Part A*, **11**, 1809 (1977).
- ³²S. L. Malhotra, *J. Macromol. Sci. Part A*, **11**, 2213 (1977); *ibid. Part A*, **12**, 73 (1978).
- ³³J. Leonard and S. L. Malhotra, *J. Polym. Sci., Polym. Chem. Ed.* **12**, 2391 (1974).
- ³⁴D. Y. Yoon and P. J. Flory, *Macromol.* **10**, 562 (1977).
- ³⁵F. Heatley and F. A. Bovey, *Macromol.* **2**, 241 (1969).
- ³⁶Y. Tanaka, H. Sato, K. Hatada, Y. Terawaki, and H. Okuda, *Makromol. Chem.* **178**, 1823 (1977); *Rubber Chem. and Technol.* **51**, 168 (1978); H. Sato and Y. Tanaka, *J. Polym. Sci., Polym. Chem. Ed.* **17**, 3551 (1979).
- ³⁷D. Blondin, J. Regis, and J. Prud'homme, *Macromol.* **7**, 187 (1974).
- ³⁸G. Quack and L. J. Fetters, *Macromolec.* **11**, 369 (1978).
- ³⁹J. R. Ebdon, *Polymer* **15**, 782 (1974).
- ⁴⁰J. R. Ebdon, *J. Macromol. Sci. Part A*, **8**, 417 (1974).
- ⁴¹T. Suzuki, K. Mitani, J. Takegami, J. Furukawa, E. Kobayashi, and Y. Arai, *Polym. J.* **6**, 496 (1974); *J. Polym. Sci., Polym. Chem. Ed.* **14**, 2553 (1976).
- ⁴²G. A. Lindsay, E. R. Santee, and H. J. Harwood, *Appl. Polym. Symp.* **25**, 41 (1974); *Polym. Prepr. Am. Chem. Soc., Polym. Chem.* **14**, 646 (1973).
- ⁴³T. Chi Chang, Q.-T. Pham, and A. Guyot, *J. Polym. Sci., Polym. Chem. Ed.* **15**, 2173 (1977); Q.-T. Pham, *Trends Anal. Chem.* **2**, 67 (1983).
- ⁴⁴J. R. Suggate, *Makromol. Chem.* **179**, 1219 (1978); *ibid.* **180**, 679 (1979).
- ⁴⁵D. Strasilla and E. Klesper, *J. Polym. Sci., Polym. Lett. Ed.* **15**, 199 (1977).
- ⁴⁶F. J. Dinan and J. J. Uebel, *Am. Chem. Soc., Polym. Prepr.* **24**, 241 (1983).
- ⁴⁷F. Heatley, in *Progr. in NMR Spectroscopy*, Vol. 13, Pergamon Press, Oxford, 1979, p. 47.
- ⁴⁸J. Spevacek and B. Schneider, *Makromol. Chem.* **175**, 2939 (1974); *ibid.* **176**, 729 (1975); *Polymer* **19**, 63 (1978); *Polymer Bulletin* **2**, 227 (1980); *J. Polym. Sci., Polym. Phys. Ed.* **20**, 1623 (1982).
- ⁴⁹K. Hatada, K. Ohta, Y. Okamoto, T. Kitayama, Y. Umemura, and H. Yuki, *J. Polym. Sci., Polym. Lett. Ed.* **14**, 531 (1976); *Makromol. Chem.* **179**, 485 (1978).
- ⁵⁰K. Hatada, H. Ishikawa, T. Kitayama, and H. Yuki, *Makromol. Chem.* **178**, 2753 (1977).
- ⁵¹D. Ghesquire and C. Chachaty, *Macromol.* **11**, 246 (1978).
- ⁵²A. R. Katritzky and D. E. Weiss, *Chem. Brit.* **12**, 45 (1976).
- ⁵³Y. Tanaka and S. Sato, *J. Soc. Rubber Ind. Japan* **50**, 182 (1977).
- ⁵⁴Yu. E. Shapiro, O. K. Shwetsov, and B. F. Ustavshikov, *Vysokomol. Soed. (USSR)* **19B**, 636 (1976).
- ⁵⁵O. K. Švetsov, N. M. Mironova, Yu. E. Šapiro, N. P. Petuchov, V. Yu. Erofeev, A. A. Ersov, N. P. Dozorova, T. D. Sivaeva, and B. F. Ustavšikov, *Faserforsch. u. Textiltech.* **28**, 217 (1977); O. K. Shwetsov, Yu. E. Shapiro, and T. D. Zukova, *Vyokomol. Soed. (USSR)* **25A**, 2541 (1983).
- ⁵⁶K. Matsuzaki, T. Kanai, T. Matsubara, and S. Matsumoto, *J. Polym. Sci., Polym. Chem. Ed.* **14**, 1475 (1976).
- ⁵⁷J. Schaefer and D. F. Natusch, *Macromol.*

- 5, 416 (1972).
- ⁵⁷N. Tsuchihashi, M. Hatano, and J. Sohma, *Makromol. Chem.* **177**, 2739 (1976).
- ⁵⁸J. Sanders and R. A. Komoroski, *Macromol.* **10**, 1214 (1977).
- ⁵⁹W. Gronski and N. Murayama, *Makromol. Chem.* **179**, 1509 (1978); *ibid.* **179**, 1521 (1978).
- ⁶⁰Yu. E. Shapiro, Yu. Yu. Musabekov, V. Yu. Erofeev, and N. M. Mironova, *Vysokomol. Soed. (USSR)* **21B**, 1737 (1979).
- ⁶¹Yu. E. Shapiro, S. I. Shkurenko, O. K. Shvetsov, and A. S. Khachaturov, *Vyskomol. Soed. (USSR)* **21A**, 803 (1979).
- ⁶²A. A. Panasenkov, V. N. Odinkov, Yu. B. Monakov, L. M. Khalilov, and A. S. Besgina, *Vysokomol. Soed. (USSR)* **19B**, 656 (1977).
- ⁶³J. C. Randall, *J. Polym. Sci., Polym. Phys. Ed.* **12**, 703 (1974); *ibid.* **14**, 283 (1976).
- ⁶⁴J. Inoue and T. Konno, *Makromol. Chem.* **179**, 1311 (1978).
- ⁶⁵Y. Inoue and T. Konno, *Polymer J.* **8**, 457 (1976); Y. Inoue and Y. Kawamura, *Polymer* **23**, 1997 (1982).
- ⁶⁶K. Hatada, J. Okamoto, K. Ohta, and H. Yuki, *J. Polym. Sci., Polym. Chem. Ed.* **14**, 51 (1976).
- ⁶⁷J. C. Randall, *J. Polym. Sci., Polym. Phys. Ed.* **14**, 1693 (1976).
- ⁶⁸T. Asakura and Y. Doi, *Macromol.* **13**, 454 (1980); *ibid.* **14**, 72 (1981); *ibid.* **16**, 786 (1983).
- ⁶⁹W. Gronski, N. Murayama, C. Mannewitz, and H.-J. Gantow, *Makromol. Chem.* **176** (Suppl. 1), 485 (1975).
- ⁷⁰W. Gronski, G. Quack, N. Murayama, and K.-T. Elgert, *Makromol. Chem.* **176**, 3605 (1975).
- ⁷¹W. Gronski and N. Murayama, *Makromol. Chem.* **177**, 3017 (1976); *Coll. & Polymer Sci.* **254**, 168 (1976).
- ⁷²G. C. Levy and G. L. Nelson, *Carbon-13 Nuclear Magnetic Resonance for Organic Chemists*, Wiley-Interscience, New York, 1972, p. 197.
- ⁷³A. Nishioka, I. Ando, and J. Matsumoto, *Bunseki Kagaku* **26**, 308 (1977).
- ⁷⁴E. C. Bezdadea, D. Braun, E. C. Buruina, A. Caraculacu, and G. Robila, *Angew. Makromol. Chem.* **37**, 35 (1974).
- ⁷⁵K. B. Abbas, *Pure & Appl. Chem.* **53**, 411 (1981).
- ⁷⁶D. E. Axelson, G. C. Levy, L. Mandelkern, *Macromol.* **12**, 41 (1979).
- ⁷⁷J. C. Randall, *Am. Chem. Soc., Polymer Prepr.* **20**, 235 (1979); J. C. Randall, F. J. Zoepfl, and J. Silverman, *Macromol. Chem. Rapid Commun.* **4**, 149 (1983).
- ⁷⁸A. Zambelli, P. Locatelli, G. Baio, and F. A. Bovey, *Macromol.* **8**, 687 (1975); *ibid.* **12**, 154 (1979).
- ⁷⁹A. E. Tonelli, *Macromol.* **12**, 83, 252, 255 (1979); F. C. Schilling and A. E. Tonelli, *ibid.* **13**, 270 (1980).
- ⁸⁰T. Asakura, I. Ando, A. Nishioka, Y. Doi, and T. Keii, *Makromol. Chem.* **178**, 791 (1977).
- ⁸¹A. Zambelli and G. Gatti, *Macromol.* **11**, 485 (1978); A. Zambelli, P. Locatelli, and E. Rigamonti, *ibid.* **12**, 156 (1979).
- ⁸²Y. Doi, *Macromol.* **12**, 248 (1979); *Macromol. Chem., Rapid Commun.* **3**, 635 (1982).
- ⁸³A. Zambelli, P. Locatelli, M. C. Sacchi, and E. Rigamonti, *Macromol.* **13**, 798 (1980).
- ⁸⁴C. J. Carman, *Macromol.* **6**, 725 (1973).
- ⁸⁵I. Ando, Y. Kato, and A. Nishioka, *Makromol. Chem.* **177**, 2759 (1976).
- ⁸⁶A. E. Tonelli, F. C. Schilling, W. H. Starnes, L. Shepherd, and I. M. Plitz, *Makromol.* **12**, 78 (1979).
- ⁸⁷F. Keller, *Faserforsch. u. Textiltechn.* **28**, 515 (1977); F. Keller and M. Clemans, *Plast. u. Kautsch.* **24**, 88 (1977); F. Keller and H. Schwind, *Faserforsch. u. Textiltechn. tiltechn.* **29**, 135 (1978); F. Keller, *Plast. u. Kautsch.* **2**, 80 (1979); *ibid.* **3**, 136 (1979); P. Pinther, F. Keller, and M. Hartmann, *Acta Polym.* **31**, 299 (1980); *ibid.* **32**, 82 (1981).
- ⁸⁸F. Keller, H. Opitz, B. Hösselbarth, D. Beckert, and W. Reichardt, *Faserforsch. u. Textiltechn.* **26**, 329 (1975); F. Keller and B. Hösselbarth, *ibid.* **27**, 453 (1976); F. Keller, S. Zepnik, and B. Hösselbarth, *ibid.* **28**, 287 (1977); *ibid.* **29**, 152 (1978).
- ⁸⁹H. K. Frensdorff and O. Ekiner, *J. Polym. Sci., Polym. Phys. Ed.* **5**, 791 (1967); *ibid.* **5**, 1157 (1967).
- ⁹⁰M. Kolinsky, D. Doskocilova, and B. Schneider, *J. Polym. Sci., Polym. Chem. Ed.* **9**, 791 (1971).
- ⁹¹T. K. Wu and D. W. Ovenall, *Macromol.* **6**, 582 (1973); T. K. Wu and M. L. Sheer, *Macromol.* **10**, 529 (1977); T. K. Wu, D. W. Ovenall, and G. S. Reddy, *J. Polym. Sci., Polym. Phys. Ed.* **12**, 901 (1974).
- ⁹²P. R. Sundaranajan, *Macromol.* **11**, 256 (1978).
- ⁹³J. C. Randall, *J. Polym. Sci., Polym. Phys. Ed.* **13**, 889 (1975).
- ⁹⁴F. Laupretre, B. Jasse, and L. Monnerie, *C. R. Acad. Sci. Paris* **280C**, 1255 (1975).
- ⁹⁵T. Kawamura, T. Uryu, and K. Matsuki, *Makromol. Chem., Rapid Commun.* **3**, 661 (1982).
- ⁹⁶G. M. Lukovkin, O. P. Komarova, V. P. Fortshilin, and Yu. Kirsh, *Vysokomol. Soed.*

(USSR) 15A, 443 (1973).

⁹⁴M. Brigodiot, H. Cheradame, M. Fontanille, and J. P. Vairont, *Polymer* 17, 254 (1976).

⁹⁵E. D. Vorontsov, G. M. Lukovkin, V. V. Gusev, A. F. Rusak, N. N. Nikolaev, L. V. Golina, and V. P. Evdakov, *Vysokomol. Soed. (USSR)* 21A, 895 (1979).

⁹⁶V. D. Mochel, *J. Polym. Sci. Part A*, 10, 1009 (1972); *Rubber Chem. & Technol.* 45, 1282 (1972).

⁹⁷A. D. H. Clague, J. A. M. Van Brockhoven, and J. W. De Haan, *J. Polym. Sci., Polym. Lett. Ed.* 11, 305 (1973); *Rubber Chem. & Technol.* 47, 1136 (1974).

⁹⁸E. Walckiers and M. Julemont, *Makromol. Chem.* 182, 1541 (1981).

⁹⁹J. Tanaka, Y. Takeuchi, M. Kobayaschi, and M. Tadokoro, *J. Polym. Sci. Part A* 2, 9, 43 (1971); Y. Tanaka, H. Sato, M. Ogawa, K. Hatada, and Y. Terawaki, *J. Polym. Sci., Polym. Lett. Ed.* 12, 369 (1974); Y. Tanaka and H. Sato, *Polymer* 17, 113 (1976).

¹⁰⁰W. Ritter, K. F. Elgert, and H. J. Gantow, *Makromol. Chem.* 178, 557 (1977).

¹⁰¹J. C. Randall, *J. Polym. Sci., Polym. Phys. Ed.* 13, 1975 (1975).

¹⁰²T. Suzuki, Y. Tsuji, Y. Takegami, and H. J. Harwood, *Macromol.* 12, 234 (1979).

¹⁰³F. Conti, M. Delfini, A. L. Segre, D. Pini, and L. Porri, *Polymer* 15, 816 (1974).

^{103a}D. Kumar, M. Rama Rao, and K. V. Rao, *J. Polym. Sci., Polym. Chem. Ed.* 21, 365 (1983).

¹⁰⁴K. F. Elgert, G. Quack, and B. Stützel, *Makromol. Chem.* 175, 1955 (1974); *ibid.* 176, 759 (1975); *Polymer* 15, 5, 612 (1974).

¹⁰⁵P. T. Suman and D. D. Werstler, *J. Polym. Sci., Polym. Chem. Ed.* 13, 1963 (1975).

^{105a}S. Bywater, *Polymer Commun.* 24, 203 (1983).

¹⁰⁶Y. Tanaka, H. Sato, and T. Seimiya, *Polym. J.* 7, 264 (1975); Y. Tanaka, H. Sato, and A. Ono, *Polymer* 18, 580 (1977).

¹⁰⁷W. Gronski, N. Murayama, H. J. Gantow, and T. Miyamoto, *Polymer* 17, 358 (1976).

¹⁰⁸D. H. Beebe, *Polymer* 19, 231 (1978).

¹⁰⁹A. S. Khachaturov, *Vysokomol. Soed. (USSR)* 19B, 515 (1977); A. S. Khachaturov, E. R. Dolinskaya, and E. L. Abramenko, *ibid.* 19B, 518 (1977); A. S. Khachaturov, E. R. Dolinskaya, L. K. Prozenko, E. L. Abramenko, and V. A. Kormer, *Polymer* 18, 871 (1977); E. R. Dolinskaya, A. S. Khachaturov, I. A. Poletayeva, and V. A. Kormer, *Makromol. Chem.* 179, 409 (1978).

¹¹⁰M. M. Coleman, D. L. Tabb, and E. G. Brame, *Rubber Chem. & Technol.* 50, 49 (1977).

¹¹¹C. J. Carman, R. A. Harrington, and C. E. Wilkers, *Macromol.* 10, 536 (1977); *Rubber Chem. & Technol.* 44, 781 (1971); *ibid.* 51, 149 (1978); *J. Polym. Sci.* 43, 237 (1973).

¹¹²K. F. Elgert and W. Ritter, *Makromol. Chem.* 177, 2781 (1976); *ibid.* 178, 2857, 2843 (1977).

¹¹³A. Zambelli, G. Baio, and E. Rigamonti, *Makromol. Chem.* 179, 1249 (1978).

¹¹⁴G. J. Ray, P. E. Johnson, and J. R. Knox, *Macromol.* 10, 773 (1978); G. J. Ray, J. Spanwick, and J. R. Knox, *ibid.* 14, 1323 (1981).

¹¹⁵J. C. Randall, *Macromol.* 11, 592 (1978); J. C. Randall and E. F. Hsieh, *ibid.* 15, 1584 (1982); *ibid.* 15, 353 (1982).

¹¹⁶T. Usami, Y. Mosugi, and T. Takeuchi, *J. Polym. Sci., Polym. Phys. Ed.* 17, 1413 (1979).

¹¹⁷W. Hoffman and F. Keller, *Plaste u. Kautsch.* 21, 359 (1974); F. Keller, *ibid.* 22, 8 (1975).

¹¹⁸I. Badreldin, A. R. Katritzky, A. Smith, and D. E. Weiss, *J. Chem. Soc., Perkin Trans. II*, 1537 (1974).

¹¹⁹K. Arita, T. Ohtomo, and Y. Tsurumi, *J. Polym. Sci., Polym. Lett. Ed.* 19, 211 (1981).

¹²⁰B. Sander, F. Keller, and H. Roth, *Plaste u. Kautsch.* 26, 278 (1975).

¹²¹S. Toppet, M. Slinckx, and G. Smets, *J. Polym. Sci., Polym. Chem. Ed.* 13, 1879 (1975).

¹²²H. Hirai, H. Koinuma, T. Tanabe, and K. Takeuchi, *J. Polym. Sci., Polym. Chem. Ed.* 17, 1339 (1979); H. Koinuma, T. Tanabe, and H. Hirai, *Macromol.* 14, 883 (1981).

¹²³K. F. Elgert and B. Stützel, *Polymer* 16, 758 (1975).

¹²⁴A. Johnson, E. Klesper, and T. Wirthlin, *Makromol. Chem.* 177, 2397 (1976).

¹²⁵R. Rousset and J. C. Galin, *J. Macromol. Sci. Part A*, 11, 347 (1977).

¹²⁶G. Gatti and A. Carbonaro, *Makromol. Chem.* 175, 1627 (1974).

¹²⁷A. R. Katritzky and D. E. Weiss, *J. Chem. Soc., Perkin Trans. II*, 21, 27 (1975); *Rubber Chem. & Technol.* Vol. 48, 1055 (1975).

¹²⁸A. L. Segre, M. Delfini, F. Conti, and A. N. Boicelli, *Polymer* 16, 338 (1975); *ibid.* 18, 310 (1977).

¹²⁹J. C. Randall, *J. Polym. Sci., Polym. Phys. Ed.* 15, 1451 (1977).

¹³⁰C. E. Wilkes, *J. Polym. Sci., Polym. Symp.* # 60, 161 (1977).

¹³¹J. R. Ebdon and S. H. Kandil, *J. Macromol. Sci. A*, 14, 409 (1980).

¹³²E. G. Brame and A. A. Khan, *Rubber Chem. & Technol.* 50, 272 (1977).

¹³³A. R. Katritzky and A. Smith, *Tetrahedron Lett.* 21, 1765 (1971); *Brit. Polym. J.* 4, 199

- (1972).
- ¹³⁴J. E. Guillet, I. K. Reat, and W. F. Reynolds, *Tetrahedron Lett.* **38**, 3493 (1971).
- ¹³⁵S. Amiya, I. Ando, and R. Chujo, *Polym. J.* **4**, 385 (1973); *ibid.* **6**, 194 (1974).
- ¹³⁶R. Chujo, K. Koyama, I. Ando, and J. Inoue, *Polymer J.* **3**, 394 (1972).
- ¹³⁷A. K. Bulay, A. G. Gruznov, Ja. G. Urman, L. M. Romanov, I. Ja. Slonim, *Vysokomol. Soed. (USSR)* **16A**, 2203 (1974).
- ¹³⁸T. Okada, *J. Polym. Sci., Polym. Chem. Ed.* **17**, 155 (1979).
- ¹³⁹S. J. Angyal, D. Greeves, and V. A. Pickels, *J. Chem. Soc., Chem. Commun.*, 589 (1974).
- ¹⁴⁰E. D. Vorontsov, A. F. Rusak, V. V. Gusev, E. E. Filippova, N. N. Nikolaev, and V. P. Evdakov, *Vysokomol. Soed. (USSR)* **21A**, 1415 (1979).
- ¹⁴¹N. P. Dozorova, Yu. E. Shapiro, and N. D. Zakharov, *Izv. VUS'ov Chemistry (USSR)* **20**, 423 (1977).
- ¹⁴²Yu. E. Shapiro, N. P. Dozorova, B. S. Turov, and O. K. Shwetsov, *J. Anal. Chem. (USSR)* **33**, 393 (1978).
- ¹⁴³V. J. Erofeev, N. M. Mironova, Yu. Yu. Musabekov, Yu. E. Shapiro, and B. F. Ustavshikov, *Vysokomol. Soed. (USSR)* **20B**, 63 (1978); *ibid.* **21A**, 1938 (1979).
- ¹⁴⁴Yu. E. Shapiro, O. K. Shwetsov, N. P. Dozorova, and A. A. Ershov, *Coll. J. (USSR)* **38**, 943 (1976).
- ¹⁴⁵Yu. E. Shapiro, O. K. Shwetsov, N. P. Dozorova, and A. A. Ershov, *Vysokomol. Soed. (USSR)* **20B**, 328 (1978); Yu. E. Shapiro, N. P. Dozorova, N. M. Mironova, and T. G. Balyberdina, *ibid.* **23A**, 1374 (1981).
- ¹⁴⁶V. B. Muratshov, A. Kh. Bulay, M. V. Terganova, A. G. Levina, and M. F. Margaritova, *Vysokomol. Soed. (USSR)* **19A**, 2269 (1977).
- ¹⁴⁷T. Okada and T. Ikushige, *Polymer J.* **9**, 121 (1977); T. Okada, K. Hashimoto, and T. Ikushige, *J. Polym. Sci., Polym. Chem. Ed.* **19**, 1821 (1981).
- ¹⁴⁸T. Okada, M. Izuhara, and T. Hashimoto, *Polymer J.* **17**, 1 (1975); *J. Appl. Polym. Sci.* **23**, 2215 (1979).
- ¹⁴⁹Yu. E. Shapiro, N. P. Dozorova, B. S. Turov, and V. A. Efimov, *Vysokomol. Soed. (USSR)* **25A**, 955 (1983).
- ¹⁴⁹J. Shaefer, E. O. Steiskal, and R. Buchdahl, *Macromol.* **8**, 291 (1975); *ibid.* **10**, 384 (1977); *J. Macromol. Sci.-Phys.* **B13**, 665 (1977).
- ¹⁵⁰E. R. Andrew, *Progr. Nucl. Magn. Reson. Spectrosc.* **8**, 1 (1971).
- ¹⁵¹A. Pines, M. G. Gibby, and J. S. Waugh, *J. Chem. Phys.* **159**, 569 (1973).
- ¹⁵²D. W. McCall and D. R. Falcone, *Trans. Faraday Soc.* **66**, 262 (1970).
- ¹⁵³D. Doskocilova and B. H. Schneider, *Adv. Colloid & Interface Sci.* **9**, 63 (1978).
- ¹⁵⁴E. O. Steiskal, J. Schaefer, and R. A. McKay, *J. Magn. Reson.* **25**, 569 (1977); J. Schaefer, R. A. McKay, E. O. Steiskal, and W. T. Dixon, *J. Magn. Reson.* **32**, 123 (1983).
- ¹⁵⁵R. Richter, G. Hempel, and H. Schneider, *Plaste u. Kautsch.* **25**, 625 (1978).
- ¹⁵⁶J. R. Lyster, H. Vanni, C. S. Yannoni, and C. A. Fyfe, *Am. Chem. Soc., Polymer Prepr.* **20**, 255 (1979); J. R. Lyster in *Methods of Experimental Physics*, Vol. 16A, 1980, p. 241.

ISMAR MEMBERS FOR 1984

Amy Abe
The Upjohn Company
Mail Code 7831-259-22
Kalamazoo, MI 49001

Jerome L. Ackerman
Department of Chemistry #172
University of Cincinnati
Cincinnati, OH 45224

Jerzy Adamski
Clinical Radiospectroscopy Lab.
Polna 33
60535 Poznan, Poland

Paul F. Agris
Division of Biological
Science and Dept. of Med.
University of Missouri
Tucker Hall
Columbia, MO 65211

Lars O. Andersson
Varian AG, Steinhauserstrasse
CH-6300 Zug, Switzerland

E. Raymond Andrew
Department of Physics
University of Florida
Gainesville, FL 32611

Tse T. Ang
School of Chemical Sciences
University of Science Malaysia
Penang, Malaysia

Marc Anteunis
Universiteit Gent
Laboratorium v. Org. Scheik
Krujgslaan 271 - S 4
Gent, Belgium

Ian M. Armitage
Yale University
Department of Molecular
Biophysics and Biochemistry
Sterling Hall of Medicine
333 Cedar Street
P.O. Box 3333
New Haven, CT 06510

Robin L. Armstrong
Department of Physics
University of Toronto
Toronto, Ontario
Canada M5S 1A7

Friedrich Baer
Fachbereich Chemie
Philipps Universitaet
Hans Meerwein Str. Lahnberge
Marburg D-3550 West Germany

F. Barbalat
52 av. A. Dubois
1217 Meyrin, Switzerland

Yves Barjhoux
Service RMN
CGR.MEV (Inst.)
BP 34 F78530
Buc, France

Peter F. Barron
Brisbane NMR Centre
Griffith University
Nathan, Queensland
Australia 4111

Mario Barzaghi
CNR Center Study Struct
Reactive
Istituto Di Chimica Fisica
Department Phys. Chem.
Golgi 19
20133 Milano, Italy

Riccardo Basosi
Department of Chemistry
Pian dei Mantellini, 44
University of Siena
53100-Siena - Italy

Wolfgang J. Baumann
The Hormel Institute
University of Minnesota
Austin, MN 55912

Edwin Becker
Building 1, Room 118
National Institutes of Health
Bethesda, MD 20205

Peter Beckmann
Department of Physics
Bryn Mawr College
Bryn Mawr, PA 19010

Georges J. Bene
Universite de Geneve
Institut de Physique Experimentale
32, Bd. D'Yvoy
1211 Geneve, 4, Switzerland

Stefan Berger
Fachbereich Chemie
der Philipps-Universitaet
Hans-Meerwein-Strasse
D-3550 Marburg, West Germany

L.J. Berliner
Chemistry Department
Ohio State University
140 West 18th Avenue
Columbus, OH 43210

William A. Bernhard
Radiation Biology & Biophysics
School of Medicine & Dentistry
The University of Rochester
Rochester, NY 14642

A.P. Bhaduri, Ph.D.
Scientist
Medicinal Chemistry Division
Central Drug Research Institute
Lucknow-226 001
U.P., India

P.D. Bhattacharyya
Hoffman-LaRoche, Inc.
Analytical Research Bldg. 86
Nutley, NJ 07110

Robert Blinc
Institute "J. Stefan"
University of Ljubljana
Ljubljana, Yugoslavia

Bernhard Bluemich
Max Planck Inst. Polymerforsch.
Postfach 3148
Mainz D-6500 West Germany

S. Morry Blumenfeld
General Electric Co.
Medical Systems Operations
P.O. Box 414
Milwaukee, WI 53201

Bruno Boddenberg
Lehrstuhl für Physikalische
Chemie II, University Dortmund
Otto-Hahn-Str. Postfach 500500
4600 Dortmund 50
West Germany

Yvan Boulanger
Institute of Biomedical Engineering
C.P. 6128 SUCC.A
Universite de Montreal,
Montreal, Quebec, H3C 3J7, Canada

Craig H. Bradley
Cryomagnetic Systems, Inc.
5508 Elmwood #410
Indianapolis, IN 46203

Richard Bramley
Australian Natl. University
Res. Sch. of Chemistry
G.O.P. Box 4
Canberra, A.C.T. 2601
Australia

Wallace S. Brey, Jr.
Department of Chemistry
University of Florida
Gainesville, FL 32611

Roselyne Briere
C.E.A. - C.E.N. Grenoble
DRF-G/Chimie Organique Physique
85X
38041 Grenoble-Cedex
France

Richard W. Briggs
Department of Radiology
The Milton S. Hershey
Medical Center
The Pennsylvania State Univ.
Hershey, PA 17033

Charles Eric Brown
Biochemistry, Room 301
Medical College of Wisconsin
8701 Watertown Plank Road
Milwaukee, WI 53226

Robert J.S. Brown
Chevron Oil Field Research Company
P.O. Box 446
La Habra, CA 90631

Martha D. Bruch
University of Delaware
2002 Point Hamlet
Newark, DE 19702

Steven Brumby
Department of Chemistry
National University
of Singapore
Kent Ridge, Singapore 0511

Patrick J. Bryan
University Hospitals of Cleveland
University Circle
2706 Abington Road
Cleveland OH 44106

Harvey A. Buckmaster
Dept. of Physics
The University of Calgary
2500 University Drive N.W.
Calgary, Alberta
Canada, T2N 1N4

D.H. Buttlare
Department of Chemistry
San Francisco State University
1600 Holloway Avenue
San Francisco, CA 94132

Vladimir Bystrov
USSR Academy of Sciences
Snemyakin Inst. of Bioorganic Chemistry
Ul. Vavilova 32
117988 Moscow, B-334 USSR

Horia Caldararu
ICECHIM - Institute of
Physical Chemistry
Spl. Independentei 202
77208 Bucharest, Romania

Paul T. Callaghan
Department of Chemistry
Biochemistry and Biophysics
Massey University
Palmerston North, New Zealand

W. Robert Carper
Department of Chemistry
Wichita State University
Wichita, KS 67208

Herman Y. Carr
Professor of Physics
Department of Physics & Astronomy
Rutgers The State University of
New Jersey
P.O. Box 849
Piscataway, NJ 08854

Britton Chance
Johnson Research Foundation
University of Pennsylvania
D501 Richards Building
37th & Hamilton Walk
Philadelphia, PA 19104

Marcel Chatel
Department of Neurology
and Neuropathology
Centre Hospitalier Universitaire
3500 Rennes France

R. Chatterjee
University of Calgary
Department of Physics
2500 University Drive N.W.
Calgary, Alberta
Canada T2N 1N4

Chen-Loung Chen
Department of Wood
and Paper Sciences
P.O. Box 5488
North Carolina State University
Raleigh, NC 27650

Hideaki Chihara
Chemistry Department
Faculty of Science
Osaka University
Tonoyaka, Osaka 560 Japan

R. Fraser Code
Department of Physics
University of Toronto, Room 304
McLennan Physical Laboratories
Toronto, Canada M5S 1A7

Charles M. Combs
6814 Kembell Drive
Evansville, IN 47710

Filippo Conti
Universita Di Roma
Dipartimento Di Chimica
P.le delle Scienze, 5
00185 Roma, Italy

Thomas F. Conway
CPC International, Inc.
Research Department, Moffett
Technical Center
P.O. Box 345
Argo, IL 60501

Robert J. Cushley
Chemistry Department
Simon Fraser University
Burnaby, B.C. Canada V5A 1S6

Frederick W. Dahlquist
Institute of Molecular Biology
University of Oregon
Eugene, OR 97403

Photis Dais
Chemistry Department
McGill University
3420 University Street
Montreal, PQ
Canada H3A 2A7

Mr. Neal Dando
Univ. of Delaware
Chem. Dept.
Newark, DE 19711

Francoise Darcel
Neurologie
Centre Hospitalier Universitaire
2, Rue H. Le Guillou
Rennes 35033 France

Ronaldo S. de Biasi
Inst. Militar de Engenharia
Pr. Gen. Tiburcio s/n s/8
22290 Rio de Janeiro RJ, Brazil

Engbert De Boer
Department of Physical Chemistry
University of Nijmegen
Nijmegen, The Netherlands

Hadassa Degani
Isotope Department
Weizmann Institute
Rehovot 76100 Israel

Hans G. Dehmelt
1600-43rd Avenue-East
EA-4-2018
Seattle, WA 98102

Fernand Dejehet
Universite De Louvain
Laboratoire de Chimie
Inorganique et Nucleaire
Chemin du Cyclotron 2
B - 1348 Louvain-La-Neuve
Belgium

Edward A. Dennis
Chemistry Department (M-001)
University of California
at San Diego
La Jolla, CA 92093

Joseph Depireux
Institut de Physique
B 4000 Sart-Tilman
Liege, Belgium

Eric G.J. Derouane
Mobile Research & Development Corp.
Central Research Division
P.O. Box 1025
Princeton, NJ 08540

R. Mathur De Vre
Institut d'Hygiene
et d'Epidemiologie
14, Rue Juliette Wytman
1050 Brussels Belgium

P. Diehl
Physikalisches Institut
der Universitat
Klingelbergstrasse 82
CH-4056 Basel
Switzerland

Ernesto Diez
Facultado de Ciencias C-II 1
Universidad Autonoma
Canto Blanco, Madrid 34
Spain

Stanley B. Digerness
Surgery
708 Zeigler Bldg.
University of Alabama
University Station
Birmingham, AL 35294

Joseph W. Doane
Department of Physics
Kent State University
Kent, OH 44242

Dorothy H. Driscoll
561 Judson Street
Philadelphia, PA 19130

Martin J. Durbin
DePaul University
Department of Physics
2219 N. Kenmore
Chicago, IL 60614

Robert W. Dykstra
Technical Center
Union Carbide Corp.
P.O. Box 8361
Bldg. 770-334
So. Charleston, WV 25303

George W. Eastland, Jr.
Department of Chemistry
Saginaw Valley State College
2250 Pierce Road
University Center, MI 48710

Gareth R. Eaton
Department of Chemistry
University of Denver
Denver, CO 80208

William M. Egan
Biophysics Branch
Bureau of Biologics
8800 Rockville Pike
Bethesda, MD 20205

Richard L. Ehman
Department of Diagnostic
Radiology
Mayo Clinic
Rochester, MN 55905

Richard R. Ernst
Laboratoire for Physikalische
Chemie
ETH-Zentrum
8092 Zurich, Switzerland

C. Anderson Evans
235 Birchwood Avenue
Cranford, NJ 07016

Frederick E. Evans
Chief, Spectros. Tech. Br., HFT-154
Dept. of Health & Human Services
National Center for Toxicological Res.
Jefferson, AR 72079

Jeremy Everett
Beecham Pharmaceuticals
Brockham Park Betchworth
Surrey RH3 7AJ
United Kingdom

Sylvia A. Farnum
University of North Dakota
Energy Research Center
Box 8213 University Station
Grand Forks, ND 58202

Daniel Fiat
E-207 CMW-MSA
University of Illinois at Chicago
Health Sciences Center
P.O. Box 6998
Chicago, IL 60680

James J. Fischer
Dept. of Therapeutic Radiology
Yale University
School of Medicine
333 Cedar Street
New Haven, CT 06510

Anthony Foris
E.I. duPont de Nemours and Co.
Chemicals, Dyes and
Pigments Dept.
Jackson Lab.
Wilmington, DE 19898

Sture Forsen
Chemical Center, Box 124
The Lund Institute of Technology
Lund S-22100 Sweden

Denise M. Frechet
Department of Chemistry
Hunter College
695 Park Avenue
New York, NY 10021

Horst Friebolin
Organic Chemistry
Institut d'Universitat
Jm Neuenheimer Feld 270
D-6900 Heidelberg
West Germany

Roux Fromy
Centre d'Etudes Nucleaires
de Saclay
Dept. de Biologie
B.P. No. 2
91190 Gif sur Yvette, France

Mr. Charles G. Fry
Department of Chemistry
Iowa State University
225 Spedding Hall, Ames Lab.
Ames, IA 50011

Fred. Y. Fujiwara
Instituto de Quimica
Universidade Estadual de Campinas
13100 Campinas, S.P.
Brazil

H. Fukui
Department of Industrial Chemistry
Kitami Institute of Technology
165 Koencho, Kitami 090
Hokkaido, Japan

Adrian O. Fulea
Calea Plevne 127
Bucharest, Romania
Cod 77103

Robert Gampe, Jr.
University of Texas Medical School
Department of Biochemistry
and Molecular Biology
P.O. Box 20708
Houston, TX 77225

Jean Gariepy
Department of Medical
Microbiology
Stanford University
School of Medicine
Stanford, CA 94305

Giuseppe Gatti
Bruker Spectrospin Italiana S.r.l
Via G. Pascoli, 70/3
20133 Milan, Italy

Michael Geoffroy
Department of Physical Chemistry
Sciences II
30 Quai Ernest Ansermet
1211 Geneve, Switzerland

Ioannis P. Gerothanassis
Department of Physical Chemistry
University of Ioannina
Ioannina, Greece

Peter Gettins
Vanderbilt University
Department of Biochemistry
School of Medicine
Nashville, TN 37232

Atholl Gibson
Physics Department
Texas A & M University
College Station, TX 77843

Julius Glaser
Royal Institute of Technology
Dept. of Inorganic Chemistry
S-100 44 Stockholm, Sweden

Thomas Glonek
NMR Laboratory
Chicago College of
Osteopathic Medicine
5200 South Ellis Ave.
Chicago, IL 60615

Ira B. Goldberg
Science Center Rockwell Institute
1049 Camino Dos Rios
Thousand Oaks, CA 91360

David Gorenstein
Department of Chemistry
University of Illinois
Chicago Circle
Chicago, IL 60615

Girjesh Govil
Tata Inst. of Fundamental Research
Homi Bhabha Road
Bombay 400 005, India

Mr. David W. Graden
Apt. 32F
Franklin Greens
Somerset, NJ 08873

David M. Grant
Chemistry Department
University of Utah
Salt Lake City, UT 34112

Frederick T. Greenaway
Chemistry Department
Clark University
Worcester, MA 01610

Hubert Greppin
Plant Physiology Lab.
University of Geneva
3 Place de l'Universite
Geneve 4 CH-1211 Switzerland

Hermann J. Gruber
333 Chemistry Department
Purdue University
West LaFayette, IN 47907

John B. Grutzner
Department of Chemistry
Purdue University
West LaFayette, IN 47907

Hans-Hch Gunthard
Eidgenossische
Technische Hochschule
CH-8092 Zurich
Switzerland

Dr. Harald Gunther
University of Siegen
Fachbereich 8 - OC II
Adolf-Reichwein-Strasse 2
5900 Siegen, Germany

Quanzhong Guo
Department of Physics
North Texas State University
P.O. Box 5368
Denton, TX 76203

Herbert S. Gutowsky
Chemistry Department
177 Noyes Laboratory, Box 25
University of Illinois
Urbana, IL 61801

Ms. Myrna Lee Hagedorn
International Flavors &
Fragrances/RD
1515 Hwy 36
Union Beach, NJ 07735

Steven E. Harms
9125 Seagrove
Dallas, TX 75243

Ernst Haslinger
Institut fur organische Chemie
Universitat Wien
Wahringer 38, Wien 9. STRASSE
A-1090 Wien, Austria

Koichi Hatada
Department of Chemistry
Faculty of Engineering Science
Osaka University
Toyonaka, Osaka, 560 Japan

Erhard Haupt
Institut f. Anorganische U.
Angewandte Chemie
Universitat Hamburg
Martin-Luther-King Pl 6
D-2000 Hamburg 13
West Germany

Karl H. Hausser
Max Planck Institute
Jahnstrasse 29
69 Heidelberg 1, West Germany

Richard Angus Hearmon
R & T Department, Room D-111
1c1 PLC Petrochemicals & Plastics
Division
P.O. Box 90
Middlesbrough Cleveland
TS6 8JE, England

Mahmoud A. Hefni
Physics Department
Assiut University
Faculty of Science
Assiut, Egypt

Jacek Hennel
Institute of Nuclear Physics
ul. Radzikowskiego
152 Krakow, Poland

John Higinbotham
Department of Physics
Napier College
Colinton Road
Edinburgh EH10 5DT, Scotland

Daniel A. Hill
Argonne National Laboratory
9700 S. Cass Ave., Bldg. 362
Argonne, IL 60439

Kunio Hikichi
Department of Polymer Science
Faculty of Science
Hokkaido University
Sapporo, 060 Japan

Kimiyoshi Hirakawa
Dept. of Neurosurgery
Kyoto Prefectural Univ. of Med.
Kawaramachi-Hirokoji
Kamigyo-Ku, Kyoto, 602
Japan

August Hochrainer
Chemische Fabrik Uetikon
CH-8707 Uetikon am See
Switzerland

R. V. Hosur
Tata Institute of Fundamental
Research
Chemical Physics Group
Homi Bhabha Road
Bombay 400 005, India

Shuyen L. Huang
113-4 Nimitz Drive
West Lafayette, IN 47906

Tai-Huang Huang
Department of Physics and Astronomy
Bennett Hall
University of Maine at Orono
Orono, ME 04469

Atsushi Hyono
Osaka City University
Medical School
Biophysics Laboratory
Asahi-machi
Abeno-ku, Osaka 545 Japan

Mohd Ilyas
Department of Chemistry
Aligarh Muslim University
Aligarh 202001 India

Roger W. Inch
Experimental Oncology Group
Ontario Cancer Treatment and
Research Foundation
South Street, London
Toronto, Ontario
Canada, N6A 4G5

Roland Inglis
Chirurg, Unfallchirurg
Hof Kaninchenberg
2400 Lubeck, West Germany

Joanne S. Ingwall
NMR Laboratory, Rm. 252
Harvard Medical School
221 Longwood Avenue
Boston, MA 02114

Junichi Isoya
University of Library and
Information Science
1-2 Kasuga, Yatabe-machi,
Tsukuba, Ibaraki-ken,
305 Japan

Lennox E. Iton
Materials Science & Technology Div.
Argonne National Laboratory
9700 South Cass Avenue
Argonne, IL 60439

Masamoto Iwaizumi
Chemical Research Institute
of Non-aqueous Solutions
Tohoku University
Katahira 2, Sendai, Japan 980

Lloyd M. Jackman
152 Davey Laboratory
Department of Chemistry
Pennsylvania State University
University Park, PA 16802

Morton H. Jacobs
Int'l Flavors & Fragrances Inc.
R and D
1515 Highway 36
Union Beach, NJ 07735

Vimal K. Jain
Department of Physics
Maharshi Dayanand University
Rohtak 124 011 India

Thomas L. James
Department of Pharmaceutical
Chemistry 926-S
University of California
San Francisco, CA 94143

Oleg Jardetzky
Stanford Magnetic Resonance Lab.
Stanford University
Stanford, CA 94305

Jean Jeener
CP-232 ULB-Plaine
BD. Du Triomphe
B-1050-Brussels, Belgium

Mr. LeRoy Johnson
General Electric Company
Medical System Group
NMR Instruments
255 Fourier Avenue
Fremont, CA 94539

Michael E. Johnson
Medicinal Chem.
545 Pharm.
University of Illinois
Health Science Center
P.O. Box 6998
Chicago, IL 60680

Graham P. Jones
Department of Plant Physiology
Waite Institute
Glen Osmond
S.A. 5064 Australia

Nagabushanam Kalyanam
Ciba-Geigy Research Center
Post Box 9002
Bombay, 400 063 India

Mohammed Kamil
Research Officer (DSRU)
AMU, Aligarh
Aligarh 202001
India

Keiko Kanamori
Department of Chemistry
University of California
405 Hilgard Ave.
Los Angeles, CA 90024

Asako Kawamori
Faculty of Science
Kwansei Gakuin University
Nishinomiya, 662
Japan

Yoshikane Kawasaki
Department of Applied
Fine Chemistry
Osaka University
Yamadaoka, Suita, Osaka 565
Japan

John F.W. Keana
University of Oregon
Dept. of Chemistry
Eugene, OR 97403

Dr. Zbigniew Kecki
Department of Chemistry
University of Warsaw
ul. Pasteura 1
02-093 Warsaw, Poland

David P. Kelly
Department of Organic
Chemistry
University of Melbourne
Parkville, Victoria, Australia

Umakant Waman Kenkare
Molecular Biology Unit
Tata Institute of Fundamental Res
Homi Bhabha Road, Bombay 400 005
India

Jean C. Kertesz
2329 W. 2nd Street #7
Los Angeles, CA 90057

T.R. Kesavan
Dept. of Physics
Indian Institute of Technology
Madras 6000 36, India

Larry Kevan
Department of Chemistry
University of Houston
Houston, TX 77004

C.L. Khetrpal
Raman Research Institute
Bangalore 560 080 India

Rainer Kimmich
Universitat Ulm
Sektion Kernresonanzspektroskopie
D-7900 Ulm (Donau)
Oberer Eselsberg
Postfach 4066, West Germany

Lowell Kispert
P.O. Box H
Chemistry Department
The University of Alabama
Tuscaloosa, AL 35486

J. Philip Kistler
Neurology, Burnham 802
Massachusetts General Hospital
Boston, MA 02114

Philip Klein
8 Summerhouse Close
Godalming
Surrey GU7 1PZ Great Britain

Ernst G. Klesper
Lehrstuhl für Makromolekulare Chemie
RWTH Aachen
Worringerweg 1, D-5100 Aachen
West Germany

Thomas Knox
Medical College of Wisconsin
Department of Neurosurgery
8700 W. Wisconsin Avenue
Milwaukee, WI 53226

Andrew Kolbert
F. Bitter Nat. Magnet Lab.
Building NW 14-5110
Massachusetts Inst. of Technology
Cambridge, MA 02139

Jan Komusinski
Kirkuk Cement Plant
Kirkuk P.O. Box 152
Iraq

Dr. Robert Kosfeld
FB6-Physikalische Chemie
Universität Duisburg
D-4100 Duisburg
Bismarkstrasse 90
West Germany

Dora G. de Kowalewski
Facultad de Ciencias Exactas y Naturales
Universidad de Buenos Aires
C.P. 1428 Nunez
Buenos Aires, Argentina

Valdemar J. Kowalewski
Facultad de Ciencias Exactas
y Naturales
Universidad de Buenos Aires
C.P. 1428 Nunez
Buenos Aires, Argentina

Ram Kripal
Scientists' Pool
Department of Physics
University of Allahabad
Allahabad 211002, India

Ryszard Krzyminiewski
Institute of Physics
A. Mickiewicz University
Grunwaldzka 6 Poznan
60-780 Poland

Philip W. Kuchel
Dept. of Biochemistry
University of Sydney
Sydney 2006 NSW
Australia

K.A. Kunert
Technical University
Chemical Department
Faculty of Polymer Technology
3 Noakowskiego Street
00-664 Warsaw, Poland

Joseph B. Lambert
Department of Chemistry
Northwestern University
Evanston, IL 60201

Frank R. Landsberger
The Rockefeller University
1230 York Avenue
New York, NY 10021

David G. Lange
Johns Hopkins
Department of
Anesthesiology
600 N. Wolfe Street
Baltimore, MD 21218

Randall B. Lauffer
Research 501
Massachusetts General Hospital
Boston, MA 02114

Gunther Laukien
7501 Bruker-Physik AG
Karlsruhe-Forchheim
Am Silberstreifen, West Germany

Paul Lauterbur
Department of Chemistry
State University of New York
at Stony Brook
Stony Brook, NY 11794

Jurgen Lauterwein
Institut de Chimie Organique
Université de Lausanne
Rue De La Barre 2
CH-1005 Lausanne, Switzerland

Hans Lechert
Institute of Physical Chemistry
University of Hamburg
Laufgraben 24, 2000 Hamburg 13
West Germany

Jens J. Led
Department of Chemical Physics
University of Copenhagen
The H.C. Orsted Institute
Universitetsparken 5, DK-2100
Copenhagen, Denmark

Rudolf Lenk
Department of Physical Chemistry
of the University of Geneva
Rue des Rois 2, CH-1204
Geneva, Switzerland

Irwin C. Lewis
Parma Technical Center
Union Carbide Corporation
12900 Snow Road
Parma, OH 44130

Anson Li
University of Petroleum
and Minerals
Department of Chemistry
P.O. Box 144, UPM Box 651
Dhahran, Saudi Arabia

Mr. Septimus Hsien-Chai Liang
Chemistry Department
Simon Fraser University
Burnaby, B.C. V5A 1S6
Canada V5A 1S6

Arthur C. Lind
Chemical Physics Department
McDonnell Douglas Research
Laboratories, Bldg. 110
P.O. Box 516
St. Louis, MO 63166

Max Linder
Eastman Kodak Company
Research Laboratory Bldg 81
1669 Lake Avenue
Rochester, NY 14650

Bjorn Lindman
Physical Chemistry
Chemical Center
P.O. Box 740
S 22007 Lund, Sweden

Endel Lippmaa
Inst. of Chemical Physics
and Biophysics
Estonian Acad. of Sci.
Lenini Puiestee 10
Tallin 200 001 Estonia, USSR

Lawrence Litt
Department of Anesthesia
University of California SF
Medical Center S436
San Francisco, CA 94143

James L. Littlefield
Nuclear Medicine Section - 115.
St. Louis Veteran's Hospital
915 N. Grand
St. Louis, MO 63135

Ralph Livingston
144 Westlock Circle
Oak Ridge, TN 37830

Miguel Llinas
Department of Chemistry
Carnegie-Mellon University
4400 Fifth Avenue
Pittsburgh, PA 15213

Ronald E. Loomis
Department of Oral Biology
Schools of Medicine and Dentistry
312 Cary Hall
Buffalo, NY 14214

Artur Losche
Sektion Physik
Karl Marx Universität
701 Leipzig, Linnestraesse 5
East Germany

Ernest Lustig
Gesellschaft für Biotechnologische
Forschung mbH
3300 Braunschweig 66, West Germany

Otto Lutz
Physikalisches Institut
Universität Tübingen
D-7400 Tübingen
Morgenstelle, West Germany

George G. McDonald
329 Ripplewood Dr.
Mesquite, TX 75150

Sorin Mager
Dept. of Organic Chemistry
University Babes Bolyai
Arany Janos Str 11
Cluj-Napoca
3400 Cluj, Romania

P.P. Mahendroo
WIC Conner Research Center
Alcon Labs, Inc.
P.O. Box 1959
Fort Worth, TX 76101

Bruno Maraviglia
Professor of Physics
Department of Physics
Piazzale A. Moro 2
00185 Rome, Italy

Thomas H. Mareci
University of Florida
Department of Radiology
Division of Radiation Physics
Box J-385 JHM Health Center
Gainesville, FL 32610

Robert A. Marino
Department of Physics & Astronomy
Hunter College of CUNY
695 Park Avenue
New York, NY 10021

John L. Markley
Department of Chemistry
Purdue University
West Lafayette, IN 47907

Luigi G. Marzilli
Chemistry Department
Emory University
Atlanta, GA 30322

Armando Marzotto
Institute of Inorganic Chemistry
University of Padova
Via Loredan 4
35100 Padova, Italy

Jerzy T. Masiakowski
Institute of Physics
Adama Mickiewicz University
60-780 Poznan
Grunwaldzka 6 Poland

Karol Maskos
Institute of Biochemistry
University of Wrocław
Tamka 2 50-137 Wrocław
Poland

G.N. Mathur
Dept. of Plastics Technology
Harcourt Butler Technological Inst
Kanpur 208 002 India

Marek Matlengiewicz
Institute of Polymer Chemistry
Polish Academy of Sciences
M. Curie-Skłodowskiej 34
PL-41800 Zabrze, Poland

Matao Matsui
Gen. Chemistry Department
Daiichi Col. of Pharm Sciences
22-1 Tamagawa-cho Minami-Ku
Kukuoka 815 Japan

Shigeru Matsui
Central Research Laboratory
Hitachi Limited
Hitachi-Koigakubo 1-280 Kuki
Tokyo 185 Japan

Elizabeth Mei
842 Morningside Drive
Millbrae, CA 94030

Michael H. Melner
Department of Biochemistry
University of Miami
P.O. Box 016960
Miami, FL 33101

Donald M. Miller
Department of Physiol. &
Pharm.
Southern Illinois University
Carbondale, IL 62901

Gerald Ray Miller
Department of Chemistry
University of Maryland
College Park, MD 20742

Luciano Milone
Istituto Di Chimica Generale
Ed Inorganica
Università Di Torino
Facoltà Di Farmacia
Via Pietro Giuria 9
Torino, Italy

Michael J. Minch
Department of Chemistry
University of the Pacific
Pacific Ave.
Stockton, CA 95204

Alan Mintz
Chairman
Department of Radiology
Hyde Park Community Hospital
5800 Stony Island
Chicago, IL 60637

Shigeru Mita
Department of Chemistry
Faculty of Science
Science University of Tokyo
Kagurazaka, Shinjuku-ku
Tokyo 162, Japan

Ichiro Miyagawa
Department of Physics & Astronomy
P.O. Box 1921
University of Alabama
University, AL 35486

Vladimir Mlynarik
Department of Physical Chemistry
Czechoslovak Inst. of Metrology
Geologická 1
825 62 Bratislava, Czechoslovakia

Rosanna Mondelli
Istituto di Biochimica Generale
Università di Milano
Via Celoria 2
20133 Milano, Italy

Walter J. Moore
Department of Chemistry
Indiana University
Bloomington, IN 47405

Joel D. Morrisett
The Methodist Hospital, A 601
Baylor College of Medicine
Houston, TX 77030

James B. Morton
Schering Corporation
60 Orange Street
Bloomfield, NJ 07003

K. Alex Muller
IBM Zurich Research Laboratory
Saumerstrasse 4
8803 Rueschlikon
Switzerland

Joseph Murphy-Boesch
University of California
School of Pharmacy, 926-S
San Francisco, CA 94143

V.S. Murthy
Department of Physics
Indian Institute of Technology
Madras, India 600036

Joachim H. Nagel
Zentralinstitut f.
Biomedizinische Technik
FRG
Universitat Erlangen
Turnstrasse 5, D-852 Erlange
West Germany

H. Nakajima
Department of Physics
Hokkaido University
Sapporo, Japan 060

Daiyu Nakamura
Department of Chemistry
Faculty of Science
Nagoya University
Chikusa, Nagoya 464
Japan

Nobuo Nakamura
Department of Chemistry
Faculty of Science
Osaka University
Toyonaka, Osaka, 560 Japan

P.T. Narasimhan
Department of Chemistry
Indian Institute of Technology -
Kanpur
IIT Post Office
Kanpur, 208016, UP, India

Vytautas Narutis
4711 St. Joseph, Apt. 4E
Lisle, IL 60532

Natuurkundig Laboratorium
Valakenierstraat 65
1018 XE Amsterdam
The Netherlands

Milan Navratil
Research Institute of Macro-
molecular Chemistry
Tkalcova 2
656 49 Brno
Czechoslovakia

Daniel A. Netzel
P.O. Box 3395
University Station
Laramie, WY 82071

Constance T. Noguchi
Laboratory of Chemical Biology
National Institute of Health
Bldg. 10 Room 9N307
Bethesda, MD 20205

Richard E. Norberg
Department of Physics
Washington University
St. Louis, MO 63110

Thomas Nowak
Department of Chemistry
The University of Notre Dame
Notre Dame, IN 46556

Teresa Gouveia Nunes
Sector De Quimica
L.N.E.T.I.
Estrada Nacional 10
Sacavem 2686, Portugal

Ray L. Nunnally
University of Texas Health
Science Center at Dallas
5323 Harry Hines Blvd., Rm. H1.100
Dallas, TX 75235

F. Omoeyin Ogungbamila
Pharmaceutical Chemistry
University of Ife,
Ile-Ife, QYQ State
Nigeria

Kazuo Ohki
Department of Biochemistry
Gifu University School of
Medicine
Tsukasamachi-40
Gifu, 500, Japan

Keiichi Ohno
Faculty of Engineering
Hokkaido University
Kita 13 Nishi 8, Kita-ku
Sapporo 060, Japan

Pentti Oksman
Department of Chemistry
University of Turku
SE 20500 Turku 50, Finland

Myra T. Olm
129 Penn Lane
Rochester, NY 14625

Krzysztof Olszewski
Clinical Radiospectroscopy Lab.
Polna 33
60-535 Poznan, Poland

Akira Omachi
Dept. of Physiology and Biophysics
University of Illinois Chicago
P.O. Box 6998
Chicago, IL 60680

James C. Orr
Professor of Biochemistry
Faculty of Medicine
Memorial University
St. John's NFLD
Canada A1B 3V6

Mary Osbakken
Radiology and Medicine
Departments
The Milton S. Hershey
Medical Center
P.O. Box 850
Hershey, PA 17033

Martin E. Packard
Varian Associates
611 Hansen Way
Palo Alto, CA 94303

Lakshman Pandey
Department of Physics
University of Alberta
Edmonton, Alberta,
Canada T6G 2J1

Enrique Pantoja
Wright State University
School of Medicine
Radiological Sciences Dept.
F. White Center for Ambulatory Care
3640 Colonel Glenn Road
Dayton, OH 45435

Joseph J. Patroni
Botany Department
University of W. Australia
Nedlands, 6009
West Australia

William Pavlicek, M.S.
The Cleveland Clinic Foundation
Medical Magnetic Resonance 8176
9500 Euclid Avenue
Cleveland, OH 44106

Hartwig Peemoeller
Univ. of New Brunswick
Physics Department
P.O. Box 4400
Fredericton, NB, Canada E3B 5A3

David H. Peyton
Biochemistry Department
Cornell University Medical Center
1300 York Avenue
New York, NY 10021

Harry Pfeifer
WB Experimentalphysik, Sektion Physik
Karl-Marx-Universitat
Linnestrasse 5
7010 Leipzig, Germany

Martin A. Phillippi
Clorox Technical Center
P.O. Box 493
Pleasanton, CA 94566

William D. Phillips
Chairman
Department of Chemistry
Washington University
St. Louis, MO 63110

Rajasekharan P. Pillai
LCMB, Gerontology Res. Center
National Institute on Aging
Baltimore City Hospitals
Baltimore, MD 21224

Mik M. Pinter
Department of Physics
University of Waterloo
Waterloo, Ontario
Canada N2L 3G1

Y. Pocker
Department of Chemistry
University of Washington
Seattle, WA 98195

Istvan Pocsik
Central Res. Inst. for Physics
P.O. Box 49
H1525 Budapest, Hungary

Carl F. Polnaszek
Dept. Of Chemistry
University of Minnesota
139 Smith Hall
Minneapolis, MN 55455

Charles P. Poole, Jr.
Department of Physics & Astronomy
University of South Carolina
Columbia, SC 29208

Andrew L. Porte
Department of Chemistry
The University of Glasgow
Glasgow G12 8QQ, Scotland

Michael A. Porubcan
Chemistry
E.R. Squibb & Sons
P.O. Box 4000
Princeton, NJ 08540

B.S. Prabhananda
Chemical Physics Group
Tata Institute of Fundamental
Research
Homi Bhabha Road
Bombay 400 005 India

Matti Punkkinen
Wihuri Physical Laboratory
University of Turku
20500 Turku 50, Finland

Ian L. Pykett
Advanced NMR Systems, Inc.
30 Sonar Drive
Woburn, MA 01801

A. Quintanilha
Lawrence Berkeley Laboratory
University of California
Berkeley, CA 94720

J. Ramakrishna
Physics Department
Indian Institute of Science
Bangalore 560012, India

D. Ramaswamy
Central Leather Research
Institute
Madras 600 020, India

Jack K. Raney
Drug Enforcement Administration
U.S. Department of Justice
Room 500, U.S. Customs House
610 S. Canal Street
Chicago, IL 60607

B.D. Nageswara Rao
Physics Department
Purdue University
1125 East 38th Street
P.O. Box 647
Indianapolis, IN 46223

Pillutla S. Rao
Dept. of Chemistry
Univ. of Saskatchewan
Saskatoon, Saskatchewan
Canada S7N 0W0

A. Ratnaker, Librarian
Raman Research Institute
Sadashivanagar
Bangalore 560 080, India

Alfred G. Redfield
Department of Biochemistry
Brandeis University
Waltham, MA 02254

Dieter Rehder
Department of Chemistry
University of Hamburg
Martin Luther King Platz - 6
D-2000 Hamburg - 13
West Germany

David George Reid
Physical Organic Chemistry
Smith Kline & French Research Ltd
The Fythe, Welwyn Hertfordshire
England AL6 9AR

Jacques Reisse
Chimie Organique (CP 165)
University Libre de Bruxelles
Avenue F. D. Roosevelt, 50
1050 Bruxelles Belgium

David Rice
Department of Chemistry
University of Massachusetts
Amherst, MA 01003

Rex E. Richards
13, Woodstock Close
Oxford OX2 8DB
United Kingdom

Robert M. Riddle
Texaco Inc.
Bellaire Research Laboratories
P.O. Box 425
Bellaire, TX 77401

John D. Roberts
Dept. of Chemistry
California Institute of Technology
Pasadena, CA 91125

Claudio Rossi
Department of Chemistry
University of Siena
Pian dei Mantellini, 44
Siena, Italy 53100

F.H.A. Rummens
Chemistry Department
University of Regina
Regina, Saskatchewan
Canada S4S 0A2

David Bernard Russell
Department of Chemistry
University of Saskatchewan
Saskatoon, Saskatchewan
Canada S7N 0W0

Heinrich Ruterjans
Institute of Biophysical Chemistry
University of Frankfurt
Haus 75A Univ. Klinikum
Theodor Stern-kai 715
Frankfurt Am Main
Munster, West Germany

Paul L. Sagalyn
Department of the Army
Army Materials & Mechanics
Research Center
Arsenal Street, DRXMR-OM
Watertown, MA 02172

Einar Sagstuen
Institute of Physics
University of Oslo
Blindern, Oslo 3, Norway

Thomas St. Amour
25 W. 124 Lacey
Naperville, IL 60540

Yu Yu Samitov
Kazan State University
Department of Chemistry
Kazan, USSR

H.S. Sandhu
Physics Department
University of Victoria
Victoria, B.C.
Canada V8W 2Y2

Peter Sandor
NMR Laboratory
Central Research Institute
of Chemistry
P.O. Box 17
H-1525 Budapest, Hungary

K.P. Sarathy
NMR Facility, Dept. of Chemistry
Auburn University
Auburn, AL 36849

G. Satyanandam
Department of Physics
Nagarjuna University
Nagarjuna Nagar 522 510, India

Tjeerd Schaafsma
Molecular Physics Department
Agricultural University, De Dreyen
Wageningen 6703 BC
The Netherlands

Robert H. Schuler
Radiation Laboratory
University of Notre Dame
Notre Dame, IN 46556

R.E.J. Sears
Department of Physics
North Texas State University
Denton, TX 76203

Raimo Sepponen
Project Manager, Lic. Tech.
Instrumentation Corp. Palomex
P.O. Box 357
Helsinki SF-00101 Finland

Aldo N. Serafini
University of Miami
School of Medicine
Division of Nucl. Medicine, D-57
P.O. Box 016960
Miami, FL 33101

Anthony Serianni
Department of Chemistry
University of Notre Dame
College of Science
Notre Dame, IN 46556

Kenneth L. Servis
Department of Chemistry
University of South California
University Park
Los Angeles, CA 90007

Michael Sevilla
Chemistry Department
Oakland University
Rochester, MI 48063

Nazir Shah
Department of Physics
Peshawar University
Peshawar, Pakistan

Judith G. Shelling
Department of Med. Genetics
University of Toronto
Toronto, Ontario
Canada M5S 1A8

Mary M. Sherman
Chemistry Department
University of Utah
Salt Lake City, UT 84112

Shigezo Shimokawa
Faculty of Engineering
Hokkaido University
Kita-ku Kita 13, Nishi 8
Sapporo 060, Japan

Parvez H. Shirazi
Nuclear Medicine
Lutheran General Hospital
1775 W. Dempster
Park Ridge, IL 60068

Nava R. Shochet
Department of Chemistry, Rm. 663
State University of New York
at Stony Brook
Stony Brook, NY 11794

Leonard S. Singer
Parma Technical Center
Union Carbide Corporation
P.O. Box 6116
Cleveland, OH 44101

Volker Sinnwell
University of Hamburg
Inst. for Organic Chemistry
and Biochemistry
Martin-Luther-King-Platz 6
D-2000 Hamburg 13, West Germany

Charles Pence Slichter
Department of Physics
University of Illinois
1110 W. Green
Urbana, IL 61801

Jakob Smidt
Technische Hogeschool Delft
Laboratorium Voor Technische
Natuukunde
Lorentzweg 1
Postbus 5046 - 2600-GA Delft
Netherlands

Justin P. Smith
9247 NE 32nd
Bellevue, WA 98004

Wladek Sobol
Department of Physics
University of Waterloo
Waterloo, Ontario
Canada N2L 3G1

Pal Sohar
Pharmacochemical Works
Spectroscopic Department
H-1475 Budapest
P.O. Box 100
Hungary

Junkichi Sohma
Faculty of Engineering
Hokkaido University
Kita 13, Nishi 8 Kita-ku
Sapporo 060, Japan

Tran Dinh Son
CEA - Department de Biologie
CEN-SACLAY - BP No. 2
91190 Gif-fur-Yvette
France

Robert A. Spalletta
Department of Physics
& Electronics Engineering
University of Scranton
Scranton, PA 18510

Alberto Spisni
Institute of Biological Chemistry
University of Parma
Via Gramsci 14
Parma, 43100 Italy

C.S. Springer, Jr.
Department of Chemistry
Suny at Stony Brook
Stony Brook, NY 11794

P.R. Srinivasan
Corp. Anal. Services
New England Nuclear
549 Albany Street
Boston, MA 02118

Shanti P. Srivastava
Indian Institute of Petroleum
Dehra Dun 248 005 India

Jan Stankowski
Inst. Molecular Physics
Polish Academy of Sciences
Smoluchowski Street 17/19
60-179 Poznan, Poland

M. Assaf Steinschneider
4354 N. Bell Ave
Chicago, IL 60618

Peter Stilbs
Institute of Physical Chemistry
University of Uppsala
P.O. Box 256
751 01 Uppsala, Sweden

Evelyn R. Stimson
186 Besemer Hill Road
Ithaca, NY 14850

Steven J. Strach
Research School of Chemistry
Australian National University
GPO Box 4
Canberra, ACT 2601 Australia

Richard C. Straight
Research Service (151J)
VA Medical Center
500 Foothill Drive
Salt Lake City, UT 84148

John H. Strange
Physics Laboratory
University of Canterbury
Kent CT2 7NR England

Makiko Sugiura
Kobe Women's College
of Pharmacy
4-19-1 Mopoyamakita-Mach
Higashinada-KU
Kobe 658 Japan

Catherine M. Sultany
Technical Center
Borg-Worner Chemicals
Washington, WV 26181

Andrzej Szyczewski
Institute of Physics
University of Adama Mickiewics
Grunwaldzka 6
60-780 Poznan, Poland

C.P.S. Taylor
Biophysics Department
University of Western Ontario
London, Ontario
Canada N6A 5C1

Piotr Tekely
Institute of Polymer Chemistry
Polish Academy of Sciences
M. Curie-Sklodowskiej 34
PL-41800, Zabrze Poland

Michael S. Tempesta
Department of Chemistry
University of Missouri-Columbia
Columbia, MO 65211

Takehiko Terao
Department of Chemistry
Faculty of Science
Kyoto University
Kyoto 606, Japan

Cung Manh Thong
E.N.S. IC
Lab Chimie Physique
Macromoleculaire
1 Rue Grandville
54000 Nancy, France

Enzo Tiezzi
Istituto di Chimica Generale
Pian die Matellini 44
53100 Siena, Italy

Ms. Frances Tischler
Chemistry Department
Room 1019
The City College of N.Y.
138th and Convent Avenue
New York, NY 10031

Alexander Tkac
Institute of Physical Chemistry
Slovak Technical University
Faculty of Chemical Technology
Janska 1, 812 37 Bratislava
Czechoslovakia

Masahiko Tokita
Department of Physics
Fukuoka Institute of Technology
Wajiro, Higashi-ku
Fukuoka 811-02, Japan

Tadashi Tokuhiro
Bruker Instruments, Inc.
Manning Park
Billerica, MA 01821

F. Toma
Department de Biologie
Centre d'Etudes Nucleaires
de Saclay
B.P. No. 2
91 Gif-sur-Yvette, France

David R. Torgeson
Iowa State University
Ames Laboratory
Ames, IA 50010

Alan S. Tracey
Department of Chemistry
Simon Fraser University
Burnaby, B.C.
Canada, V5A 1S6

Wolfgang E. Trommer
Department of Chemistry
University of Kaiserslautern
6750 Kaiserslautern, F.R.G.
West Germany

Z. Trontelj
University E. Kardelj of Ljubljana
Physics Department
P.O. Box 39
61111 Ljubljana, Yugoslavia

Jean-Pierre Tuchagues
Laboratoire de Chimie
Coordination
205 Route de Narbonne
31400 Toulouse, France

Kamil Ugurbil
Biochemistry and Gray
Freshwater Biol. Inst.
Univ. of Minnesota
Navarre, MN 55392

Paul Ukleja
Physics Department SMU
North Dartmouth, MA 02747

G.C. Upreti
Physics Department
Indian Institute of Technology
Kanpur 208 016 India

Ioan Ursu
National Council for Science
and Technology
1, Piata Victoriei
7121 Bucharest, Romania

Y. Utsumi
M.E. Project Division
Hitachi, LTD
New Marunouchi, Bldg.
1-5-1 Marunouchi, Chiyoda-KU
Tokoyo, Japan

Gianni Valensin
Istituto Chemie Generale
Via Pian Dei Mantellini 44
53100 Siena, Italy

Paul E. Van Hecke
Streeklaan 46
B-3060 Bertem
Belgium

Nuno Vaz
Department of Physics
General Motors Research
12 Mile and Mound Road
Warren, MI 48090

Vincent S. Venturella
Hoffman LaRoche Inc.
Nutley, NJ 07110

J.H. Viljoen
University Library
Private Bag 5036
Stellenbosch 7600, South Africa

Ronald E. Viola
Chemistry Department
University of Adron
Akron, OH 44325

James Visintainer
Research Division
Goodyear Tire and Rubber Co.
142 Goodyear Blvd.
Akron, OH 44316

Jurgen Voitlander
Institut fur Physikalische Chemie
der Universitat Munchen
Sophienstr 11
D-8000 Munchen 2, West Germany

Wolf Von Philipsborn
Institute of Organic Chemistry
University of Zurich
Winterthurekstrasse 190
CH-8057 Zurich, Switzerland

Ney Vernon Vugman
Instituto de Fisica - UFRJ
Bloco A - Centro Tecnologia
Ilha do Fundao - Cidade Universitaria
21944 - Rio de Janeiro - RJ - Brazil

Hiroshi Watari
National Institute for
Physiological Sciences
38 Nishigonaka
Okazaki Aichi, Japan

Tina Weeding
Department of Chemistry
BG-10
University of Washington
Seattle, WA 98195

Felix Wehrli
Manager, NMR Applications
General Elec. Medical Systems
P.O. Box 414
Milwaukee, WI 53201

J.A. Weil
Department of Chemistry
University of Saskatchewan
Saskatoon, Saskatchewan
Canada S7N 0W0

Michael W. Weiner
Associate Professor of Medicine
Chief, Hemodialysis (111J)
VA Medical Center
4150 Clement Street
San Francisco, CA 94121

Alarich Weiss
Institut Fur Physikalische Chemie
Physikalische Chemie III
Technische Hochschule
Petersenstrasse 20
D-6100 Darmstadt
West Germany

Earl B. Whipple
#4 Dwayne Road
Old Saybrook, CT 06475

Andrzej Wieckowski
Institute of Molecular Physics
of the Polish Academy of Sciences
ul. Smoluchowskiego 17
60-179 Poznan 38, Poland

Tadeusz M. Wilczok
Dept. of Biochemistry
and Biophysics
Institute of Medical Chem.
and Physics
Jagiellonska 4
Sosnowiec 41-200, Poland

Ffrancon Williams
Department of Chemistry
University of Tennessee
Knoxville, TN 37996-1600

Virgil L. Williams
Grant Hospital
Loyola University
550 W. Webster
Chicago, IL 60614

Toni Wirthlin
Varian AG
Steinhauserstrasse
CH-6300 Zug
Switzerland

Myron Wojtowycz
Department of Radiology
VA Hospital
Salt Lake City, UT 84148

Hans C. Wolf
Physikalisches Institut 3
Der Universitat Stuttgart
Pfaffenwaldring 57
D-7000 Stuttgart 80
West Germany

Tadeusz Wosinski
Institute of Physics
Polish Academy of Sciences
Al. Lotnikow 32
02-668 Warsaw, Poland

Kurt Wuthrich
Institut fur Molecular Biologie
Und Biophysik, ETH
Honggerberg, Zurich
Switzerland

Herman R. Wyssbrod
Mt. Sinai School of Medicine of the
City University of New York
Department of Physiology & Biophysics
5th Avenue & 100th Street
New York, NY 10029

Philip L. Yeagle
Department of Biochemistry
102 Cary Hall
SUNY, Buffalo
Buffalo, NY 14214

Xu Yuanzhi
Fujian Institute of Res. on
the Structure of Matter
Chinese Academy of Science
Fuzhou, Fujian
China

Ewa Zajaczkowska-Terpinska
Faculty of Chemistry
Politechnika Warszawa
Poland

Henry M.K. Zeidan
Chemistry Department
Atlanta University
233 Chestnut Street, S.W.
Atlanta, GA 30314

Alex von Zelewski
Institute of Inorganic Chemistry
University of Fribourg
Boulevard de Perolles
CH-1700 Fribourg
Switzerland

CALENDER OF FORTHCOMING CONFERENCES IN MAGNETIC RESONANCE

May 27-June 7, 1985 SUMMER SCHOOL in BASIC NMR will be held prior to the Ninth Waterloo NMR Summer Institute (see below for additional details).

June 10-17, 1985 NINTH WATERLOO NMR SUMMER INSTITUTE will be held at the University of Waterloo, Waterloo Ontario, Canada. Lectures will be held on nuclear spin thermodynamics, rf pulse technology, two dimensional NMR, spin polarization spectroscopy, and on applications in biophysics and solid state physics. For additional information, contact

Cathy Waimsley
Admin. Director
NMR Summer Insitute
Department of Physics
University of Waterloo
Waterloo Ontario
Canada N2L3G1

July 8-12, 1985 7th INTERNATIONAL MEETING on NMR SPECTROSCOPY will take place at Cambridge University, University Chemical Laboratory, Lensfield Road. Seven symposia are planned: NMR in bioorganic chemistry, New experimental techniques, NMR in industry, Solid state NMR, in vivo NMR, NMR in inorganic chemistry, Large molecule NMR. Further details may be obtained from:

Dr. John F. Gibson,
Secretary (Scientific)
The Royal Society of Chemistry
Burlington House
London W1V 0BN England

July 14-19, 1985 27th ROCKY MOUNTAIN CONFERENCE will be held in Denver, Colorado and will include symposia on EPR and NMR. Contact

Jan Gurnsey
5531 Bitterbush Way
Loveland Colorado
80537

September 30-October 4, 1985 12th FACSS Meeting will sponsor an expanded NMR program, broadly covering fundamental research and new

applications of NMR. It will be held at the Marriott and Adam's Mark Hotels in downtown Philadelphia. Contact:

Rodney D. Farlee
NMR Program Chairman
E. I. DuPont de Nemours & Co., Inc.
Experimental Station
Bldg. 328
Wilmington, DE 19898

November 15-18, 1985 FIRST BEIJING CONFERENCE and EXHIBITION on INSTRUMENTAL ANALYSIS, will be held in Beijing, China. The exhibition will be held November 16-25, 1985. The conference and exhibition sponsored by five chinese academic societies including Spectroscopy at Radio and Microwave Frequencies will hold symposia on NMR, EPR, NQR, Double Resonance, and Multiple Quantum Resonance as well as other aspects of instrumentation. Abstracts should be submitted by March 31, 1985. For further information please contact:

Secretariat of First
Beijing Conference and
Exhibition on
Instrumental Analysis
Room 912
Xi Yuan Hotel
Beijing, China
Tel. 890721 Ext. 912

June 29-July 5, 1986 NINTH MEETING of the INTERNATIONAL SOCIETY OF MAGNETIC RESONANCE will be held at the Hotel Gloria, Rio de Janeiro, Brazil. The meeting will cover the broad field of magnetic resonance, including the theory and practice of nuclear magnetic resonance, electron paramagnetic resonance and nuclear quadrupole resonance spectroscopy. Included will be applications in physics, chemistry, biology and medicine. The meeting will strive to foster interaction among scientists in different fields of magnetic resonance and to encourage interdisciplinary exploration. Information may be obtained from

Dr. Ney Vernon Vugman

Instituto de Fisica
Universidade Federal de Rio de Janeiro
Cidade Universitaria
Bloco A - CCMN
Rio de Janeiro 21945
Brazil

The editor would be pleased to receive notices of future meetings in the field of magnetic resonance so that they could be recorded in this column.

NEW BOOKS

NMR and Macromolecules. ACS Symposium Series 247. James C. Randall, editor. xiv+280 pages. American Chemical Society, 1155 16th St., N.W., Washington, D.C. 20036. 1984. \$34.95.

NMR of Newly Accessible Nuclei, Vol. 1 and 2. Pierre Laslo editor. xviii+298 and 436 pages respectively. Academic Press, 11 Fifth Ave., New York, N.Y. 10003. 1983. Vol. 1 \$59; Vol. 2 \$65.

Theory of NMR Parameters, I. Ando and G. A. Webb. 217 pages. Academic Press, New York. 1983. \$52.

Nuclear Magnetic Resonance Spectroscopy, R. K. Harris, xx+250 pages. Pitman Books, 128 Long Acre, London, WC2E 9AN. 1983.

Phosphorus-31 NMR: Principles and Appli-

cations, D. G. Gorenstein, editor. xiv+604 pages. Academic Press, Orlando, Florida 32887. 1984. \$79.00.

Correlative Neuroanatomy of Computed Tomography and Magnetic Resonance Imaging, J. de Groot, with Catherine M. Mills, Line drawings by L. Lyons. xii+248 pp., Lea and Febiger, Philadelphia, \$45.

Nuclear Magnetic Resonance (NMR), M. A. Hopf & F. W. Smith (Progress in Nuclear Medicine: Vol. 8) viii+248 pp., S. Karger. 1984. \$90.

NMR Spectroscopy, Vol. III, Pal Sohal, Ed. 368 pp. CRC Press. 1984.

Magnetic Resonance: Introduction, Advanced Topics & Applications to Fossil Fuels, L. Petrakis & J. P. Fraissard, eds. Reidel Press (Holland). 1984. \$98.00.

INSTRUCTIONS FOR AUTHORS

Because of the ever increasing difficulty of keeping up with the literature there is a growing need for critical, balanced reviews covering well-defined areas of magnetic resonance. To be useful these must be written at a level that can be comprehended by workers in related fields, although it is not the intention thereby to restrict the depth of the review. In order to reduce the amount of time authors must spend in writing we will encourage short, concise reviews, the main object of which is to inform nonexperts about recent developments in interesting aspects of magnetic resonance.

The editor and members of the editorial board invite reviews from authorities on subjects of current interest. Unsolicited reviews may also be accepted, but prospective authors are requested to contact the editor prior to writing in order to avoid duplication of effort. Reviews will be subject to critical scrutiny by experts in the field and must be submitted in English. Manuscripts should be sent to the editor, Dr. David G. Gorenstein, Chemistry Department, University of Illinois at Chicago, Box 4348, Chicago, Illinois, 60680, USA.

MANUSCRIPTS must be submitted in triplicate (one copy should be the original), on approximately 22 x 28 cm paper, typewritten on one side of the paper, and double spaced throughout. If the manuscript cannot be submitted on computer tapes, floppy disks, or electronically (see below), please type with a carbon ribbon using either courier 10 or 12, gothic 12, or prestige elite type face with 10 or 12 pitch. All pages are to be numbered consecutively, including references, tables, and captions to figures, which are to be placed at the end of the review.

ARRANGEMENT: Considerable thought should be given to a logical ordering of the subject matter and the review should be divided into appropriate major sections, sections, and subsections, using Roman numerals, capital letters, and Arabic numerals respectively. A table of contents should be included.

TABLES: These are to be numbered consecutively in the text with Arabic numerals. Their place of insertion should be mentioned in the

text, but they are to be placed in order at the end of the paper, each typed on a separate sheet. Each table should be supplied with a title. Footnotes to tables should be placed consecutively, using lower case letters as superscripts.

FIGURES are also to be numbered consecutively using Arabic numerals and the place of insertion mentioned in the manuscript. The figures are to be grouped in order at the end of the text and should be clearly marked along the edge or on the back with figure number and authors' names. Each figure should bear a caption, and these should be arranged in order and placed at the end of the text. Figures should be carefully prepared in black ink to draftsman's standards with proper care to lettering (typewritten or freehand lettering is not acceptable). Graphs should include numerical scales and units on both axes, and all figures and lettering should be large enough to be legible after reduction by 50-60%. Figures should be generally placed on sheets of the same size as the typescript and larger originals may be handled by supplying high-contrast photographic reductions. One set of original figures must be supplied; reproduction cannot be made from photocopies. Two additional copies of each figure are required. Complex molecular formula should be supplied as ink drawings.

REFERENCES to the literature should be cited in order of appearance in the text by numbers on the line, in parentheses. The reference list is to be placed on separate sheets in numerical order at the end of the paper. References to journals should follow the order: author's (or authors') initials, name, name of journal, volume number, page, and year of publication. The abbreviation of the journal follows that used in the Chemical Abstracts Service Source Index. Reference to books should include in order: author's (or authors') initials, name, title of book, volume, edition if other than the first, publisher, address, date of publication, and pages.

FOOTNOTES should be used sparingly and only in those cases in which the insertion of the information in the text would break the train of thought. Their position in the text should be marked with a superscript Arabic numeral and the footnote should be typed at the bottom of the

relevant page in the text, separated from the latter by a line.

SYMBOLS AND ABBREVIATIONS: Mathematical symbols should be typewritten wherever possible. Greek letters should be identified in pencil in the margin. In reviews containing a number of mathematical equations and symbols, the author is urged to supply a list of these on a separate sheet for the assistance of the printer; this will not appear in print. Standard abbreviations will follow the American Chemical Society's **HANDBOOK FOR AUTHORS** names and symbols for units.

PERMISSIONS: It is the responsibility of the author to obtain all permissions concerned with the reproduction of figures, tables, etc, from copyrighted publications. Written permission must be obtained from the publisher (not the author or editor) of the journal or book. The publication from which the figure or table is taken must be referred to in the reference list and due acknowl-

edgement made, e.g., reprinted by permission from ref. (00).

REPRINTS: Thirty reprints of a review will be supplied free to its senior author and additional reprints may be purchased in lots of 100

INSTRUCTIONS FOR SUBMITTING MANUSCRIPTS ON COMPUTER TAPES, FLOPPY DISKS OR ELECTRONICALLY: If you have used a word processor to type your manuscript, please forward your manuscript after review and revision, in a computer readable form. Tape should be unlabeled, in a standard IBM format, 1600 BPI, 80x80 blocks and ASCII image. Floppy disks readable on IBM, PDP 11, or MacIntosh personal computers are also acceptable. For direct submission over the phone lines use either 300 or 1200 baud ASCII transmission. Additional details will be provided for the appropriate hand-shake requirements. Please supply us with the code for interpreting superscripts, greeks, etc. on your word processor.

PAPERS TO APPEAR IN SUBSEQUENT ISSUES

Application of Lanthanide Shift Reagents in NMR-Spectroscopy for Studying Organophosphorus Compounds, B. I. Ionin, V. I. Zakharov, and G. A. Berkova, Leningrad Lensoviet Institute of Technology, Leningrad, USSR.

2-Dimensional NMR Spectroscopy of Proteins, J. Markley, Purdue University, West Lafayette, Indiana, U.S.A.

Electron Spin Echo Method as Used to Analyze Spatial Distribution of Paramagnetic Centers, A. M. Raitsimring and K. M. Salikhov, Institute of Chemical Kinetics and Combustion, USSR.

In Vivo Applications of ^{19}F NMR Spectroscopy and Imaging, Alice M. Wyrwicz, University of Illinois, Chicago, Illinois, USA.

Felix Bloch Memorial Lectures, Contributions from V. S. Murty (Indian Institute of Technology), Yuanzhi Xu (Zhejiang University, China), P. Sohar (Budapest, Hungary), I. P. Gerothanassis (University de Lausanne, Switzerland), C. L. Khetrpal and G. Govil for the Ninth International Conference on Magnetic Resonance (India), R. Basosi (Istituto di Chimica Generale, Italy), I. Ursu (Bucharest, Romania), A. Saika (Kyoto University, Japan), E. L. Hahn (Berkeley, U.S.), N. F. Ramsey (Cambridge, U.S.), E. R. Andrew (Gainesville, U.S.), D. Fiat (Chicago, U.S.)

A Simple Description of 2-D NMR, A. Bax,

National Institutes of Health, Bethesda, Maryland, U.S.A.

NMR Studies of Specific Protein Nucleic Acid Interactions, P. Lu, University of Pennsylvania, Philadelphia, Pennsylvania, U.S.A.

NMR Studies of Drug Nucleic Acid Complexes, T. Krugh, University of Rochester, Rochester, New York, U.S.A.

EPR in Pulsed Magnetic Fields, S. J. Witters, University of Leuven, Leuven, Belgium.

^{13}C and ^1H NMR of Intact Tissue, M. Barany and A. Carlos, University of Illinois, Chicago, Illinois, U.S.A.

Proton Detected Heteronuclear NMR, D. Cowburn, Rockefeller University, New York, New York, U.S.A.

Modern Pulse Techniques and their Application in High Resolution NMR, R. Benn, Max-Planck-Institut für Kohlenforschung, Mulheim, West Germany.

EPR Imaging, L. J. Berliner, The Ohio State University, Columbus, Ohio, U.S.A.

NMR-Chemical Microscopy, Laurance D. Hall, University of Cambridge School of Clinical Medicine, Cambridge, England

BULLETIN OF MAGNETIC RESONANCE

*The Quarterly Review Journal of the
International Society of Magnetic Resonance*

VOLUME 7

OCTOBER, 1985

NUMBERS 2/3

CONTENTS Felix Bloch Memorial Issue

PREFACE, D. FIAT, GUEST EDITOR	79
INTRODUCTION, E. R. ANDREW	81
FELIX BLOCH AND MAGNETIC RESONANCE, E.L. HAHN	82
FELIX BLOCH - REMINISCENCES OF A GRADUATE STUDENT, M. PACKARD	90
EARLY HISTORY OF MAGNETIC RESONANCE, N.F. RAMSEY	94
MANY-BODY PERTURBATION STUDY OF ELECTRON CORRELATION EFFECTS ON NMR PARAMETERS, A. SAIKA	100
RECENT NUCLEAR MAGNETIC RESONANCE INVESTIGATIONS IN ROMANIA, I. URSU	105
NUCLEAR AND ELECTRON SPIN RELAXATION TECHNIQUES FOR DELINEATION OF BIOINORGANIC AND BIOLOGICAL ACTIVITIES, R. BASOSI, N. NICCOLAI, E. TIEZZI and G. VALENSIN	119
NMR STUDIES OF MOLECULES DISSOLVED IN CHOLESTERIC LIQUID CRYSTALS, C.L. KHETRAPAL, K.V. RAMANATHAN and M.R. LAKSHMINARAYANA	139
EXCEPTS FROM LETTERS	144
ABSTRACTS OF COMMEMORATIVE LECTURES, A. NESZMÉLYI,	154
P. SOHAR	155
ANNOUNCEMENTS	161
NEW BOOKS	161
INSTRUCTIONS FOR AUTHORS	162
FORTHCOMING PAPERS	164

BULLETIN OF MAGNETIC RESONANCE

*The Quarterly Review Journal of the
International Society of Magnetic Resonance*

Editor:

DAVID G. GORENSTEIN

*Department of Chemistry
Purdue University
W. Lafayette, Indiana 47907
U.S.A*

Editorial Board:

E.R. ANDREW
*University of Florida
Gainesville, Florida, U.S.A.*

ROBERT BLINC
*E. Kardelj University of Ljubljana
Ljubljana, Yugoslavia*

H. CHIHARA
*Osaka University
Toyonaka, Japan*

GARETH R. EATON
*University of Denver
Denver, Colorado, U.S.A.*

DANIEL FIAT
*University of Illinois at Chicago
Chicago, Illinois, U.S.A.*

SHIZUO FUJIWARA
*University of Tokyo
Bunkyo-Ku, Tokyo, Japan*

DAVID GRANT
*University of Utah
Salt Lake City, Utah, U.S.A.*

JOHN MARKLEY
*University of Wisconsin
Madison, Wisconsin, U.S.A.*

MICHAEL PINTAR
*University of Waterloo
Waterloo, Ontario, Canada*

CHARLES P. POOLE, JR.
*University of South Carolina
Columbia, South Carolina, U.S.A.*

JAKOB SMIDT
*Technische Hogeschool Delft
Delft, The Netherlands*

BRIAN SYKES
*University of Alberta
Edmonton, Alberta, Canada*

The *Bulletin of Magnetic Resonance* is a quarterly review journal sponsored by the International Society of Magnetic Resonance. Reviews cover all parts of the broad field of magnetic resonance, viz., the theory and practice of nuclear magnetic resonance, electron paramagnetic resonance, and nuclear quadrupole resonance spectroscopy including applications in physics, chemistry, biology, and medicine. The *BULLETIN* also acts as a house journal for the International Society of Magnetic Resonance.

CODEN: BUMRDT

ISSN: 0163-559X

Bulletin of Magnetic Resonance, The Quarterly Journal of the International Society of Magnetic Resonance. Copyright © 1985 by the International Society of Magnetic Resonance. Rates: Libraries and non-members of ISMAR, \$60.00, members of ISMAR, \$18.00. All subscriptions are for a volume year. All rights reserved. No part of this journal may be reproduced in any form for any purpose or by any means, abstracted, or entered into any data base, electronic or otherwise, without specific permission in writing from the publisher.

Council of the International Society of Magnetic Resonance

E.R. ANDREW, President

C.P. SLICHTER, Vice President

D. FIAT, Secretary-General and Founding Chairman

C.P. POOLE, Jr., Treasurer

E.R. ANDREW
Gainesville

G.J. BENE
Geneve

R. BLINC
Ljubljana

M. BLOOM
Vancouver

W.S. BREY, JR.
Gainesville

V. BYSTROV
Moscow

F. CONTI
Rome

R.R. ERNST
Zurich

D. FIAT
Chicago

S. FORSEN
Lund

S. FUJIWARA
Urawa

M. GOLDMAN
Gif sur Yvette

H.S. GUTOWSKY
Urbana

R.K. HARRIS
Durham

K.H. HAUSSE
Heidelberg

J. HENNEL
Krakow

O. JARDETSKY
Stanford

J. JEENER
Brussels

V.J. KOWALEWSKI
Buenos Aires

P.C. LAUTERBUR
Stony Brook

E. LIPPMAA
Tallin

A. LOSCHE
Leipzig

P.T. NARASIMHAN
Kanpur

D. NORBERG
St. Louis

H. PFEIFER
Leipzig

W. von PHILIPSBORN
Zurich

A. PINES
Berkeley

L.W. REEVES
Waterloo

R. RICHARDS
Oxford

J. D. ROBERTS
Altadena

J. SMIDT
Delft

J. STANKOWSKY
Poznan

I. URSU
Bucharest

N.V. VUGMAN
Rio de Janeiro

H.C. WOLF
Stuttgart

The aims of the International Society of Magnetic Resonance are to advance and diffuse knowledge of magnetic resonance and its applications in physics, chemistry, biology, and medicine, and to encourage and develop international contacts between scientists.

The Society sponsors international meetings and schools in magnetic resonance and its applications and publishes the quarterly review journal, *The Bulletin of Magnetic Resonance*, the house journal of ISMAR.

The annual fee for ISMAR membership is \$20 plus \$18 for a member subscription to the *Bulletin of Magnetic Resonance*.

Send subscription to:

International Society of Magnetic Resonance
Professor Charles P. Poole, Jr.
Treasurer
Department of Physics & Astronomy
University of South Carolina
Columbia, South Carolina 29208 U.S.A.

PREFACE

To our great sorrow, Professor Felix Bloch passed away on September 10, 1983. In addition to his many important contributions to the advancement of science, he had been a great humanist and a good friend to many of us. It is well known that Professors Felix Bloch and Edward Mills Purcell shared the 1952 Nobel prize in recognition of their observation of the nuclear magnetic resonance phenomena and for introducing and developing nuclear magnetic resonance. Professor Bloch maintained a continuous interest in nuclear magnetic resonance and its applications, and was very impressed to see the recent utmost important applications of NMR in biology and medicine.

I had known Felix Bloch personally for many years. Initially, I met him at the Weizmann Institute of Science, Rehovot, Israel, at the beginning of my academic career, as he served on the board of Governors of the institute and subsequent to this at scientific meetings. He actively participated in the activities of the International Society of Magnetic Resonance and had been on its Council since its beginning and until the last year of his life. I had consulted him frequently and followed his advice closely. He would find time to answer every letter and to think carefully about the implications of the subject discussed. His greatness was shown in his modesty and in fulfilling all duties, never feeling that he had or deserved some special privilege.

This special issue contains the ISMAR tribute to Professor Bloch — The Felix Bloch Commemorative Lectures — held at many institutes and universities throughout the world. The first part opens with an article written by Erwin Hahn who spent many years with Felix Bloch. The article is based upon a commemorative lecture given at the American Physical Society in Washington, D.C. in April 1984. Next are some reminiscences of Martin Packard who was the first graduate student of F. Bloch and who also participated in his pioneering studies. An article by N. Ramsey describing the early history of magnetic resonance precedes a description by I. Ursu of recent nuclear magnetic resonance investigations in Romania. A paper by A. Saika presented at the 22nd NMR Symposium at Kyoto University in Japan, a paper by R. Basosi, N. Niccolai, E. Tiezzi and G. Valensin, and an article by C. Khetrapal, K. Ramanathan and M. Lakshminarayana conclude the first section of this issue. The second part of our special issue contains excerpts from letters and abstracts received from organizers and

participants of the commemorative lectures.

The following is a short description of the Felix Bloch Commemorative Events:

— on November 15, 1983, "The 22nd NMR Symposium" was held at Kyoto University Japan. J. Sohma and his colleagues organized the event, and A. Saika presented a lecture. The paper is included in this issue.

— On January 17, 1984, "The Analytical Conference" of the Hungarian Chemical Society was held in Budapest, and P. Sohar delivered a brief curriculum vitae of Felix Bloch and presented a talk entitled "Structure determination by NMR."

— A ten-week course from February to April 1984 was organized by L. Conti for undergraduate and graduate students in "Physical Chemistry of Solids" and dedicated to the memory of Felix Bloch at the Institute of General and Inorganic Chemistry at the University of Rome.

— On March 17, 1984 at a "Felix Bloch Commemorative Session" of the Romanian National Committee for Physics, I. Ursu presented a paper at the National Center for Physics in Bucharest. The paper is included in this issue.

— On April 4, 1984. A Memorial Symposium in honor of F. Bloch was sponsored by the School of Pharmacy and the College of Science of the University of Siena. About fifty people attended the meeting which provided discussions on the theoretical and practical aspects of magnetic resonance. The following presentations were given:

"The contribution of Felix Bloch to the understanding of electron and nuclear relaxation phenomena," E. Tiezzi

"A multifrequency ESR approach in the electron spin relaxation studies on copper complexes in solution," R. Basosi

"A multinuclear NMR study of dipolar relaxation parameters: internuclear distances in biomolecular solutions," N. Niccolai and

"NMR relaxation investigations of drug-receptor site interactions," G. Valensin.

Selected portions of these papers are presented as a single article in this issue.

— On April 12, 1984, "Modern NMR Spectroscopy," a session of the Committee of Molecular Structure of the Hungarian Academy of Sciences took place in Budapest with invited lectures by K. Tompa, A. Neszmelyi and P. Sohar. The following presentations were given:

"Nuclear spin tomography," K. Tompa

"Determination of carbon-carbon couplings and some other new high-resolution techniques for direct measurement of topology of organic molecules in solution," A. Neszmelyi and

"Up-to-date NMR methodology in structure elucidation," P. Sohar The abstracts of Drs. Neszmelyi and Sohar are included in this issue.

— On *June 12, 1984*, "The Felix Bloch NMR Symposium" organized by the Polish Biophysical Society and the Institute of Biochemistry occurred at the University of Wroclaw. Eighty scientists participated and K. Maskos and J. Hennel presented the following papers:

"The History of the NMR phenomenon and the Work of Felix Bloch," K. Maskos

"New methods in NMR — Zeugmatography and NMR in the Zero-field." J. Hennel

— On *September 15, 1984*, a one-day symposium on "Magnetic Resonance" held in memory of Professor Bloch at the Indian Institute of Technology in Madras included the paper by V. S. Murty, "Principles of Nuclear Induction."

— On *September 25, 1984* at the Indian Institute of Science in Bangalore, a Winter School on Biological Applications of Magnetic Resonance was dedicated to F. Bloch. The inaugural lecture, "Movement of NMR from physical phenomenon to chemistry, biology, and medicine," was given by E. D. Becker of the National Institutes of Health, Bethesda, Maryland, USA. A brief write-up by C. L. Khetrapal and G. Govil in regard to the Felix Bloch Memorial Lecture is included.

— In *autumn of 1984* at the Kazan State University in the USSR, a magnetic resonance seminar took place in which Y. Samitov presented a commemorative lecture entitled "Frequency non-invariability of NMR chemical shifts in exchanging populated systems and its explanation on the basis of F. Bloch's equation."

— A Felix Bloch Memorial Lecture was organized by X. Yuanzhi and held in Zhejiang University in Hangzhou, China with about thirty people in attendance during *October, 1984*.

— A two-term course on magnetic resonance theories has been organized at the Institute of Physical Chemistry of the Slovak Technical University in Bratislava, Czechoslovakia by A. Tkac. The lectures, *begun in 1984 and continuing into 1985*, are being delivered by P. Pelikan for scientists and advanced students devoted to the memory of Felix Bloch.

— *During 1985* on the occasion of the 150th anniversary of the founding of the Institute of Physics at Karl-Marx-University in Leipzig, A. Losche is to present an historical review of the last century with recognition and appreciation of the work of Felix Bloch.

We thank Mrs. Lore C. Bloch for her support and suggestion to use one of her favorite photographs of her late husband.

Daniel Fiat

It is a privilege to write an introduction to this special issue of the *Bulletin* in which Professor Fiat has collected together the Felix Bloch Commemorative Lectures.

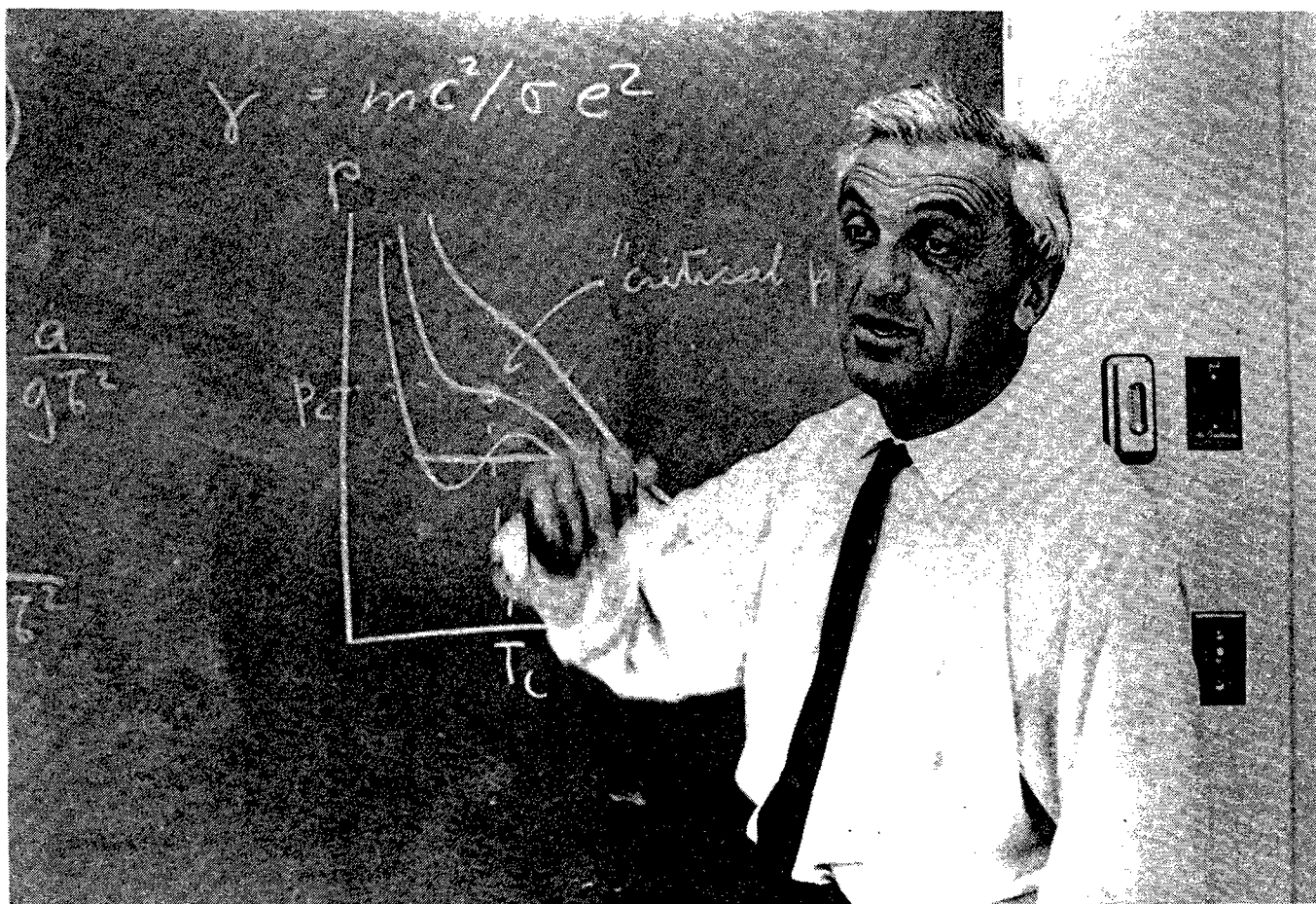
Professor Bloch was one of the great physicists of our time who made many fundamental contributions to Physics. He and Professor Purcell and their colleagues first discovered and demonstrated nuclear magnetic resonance. Now, forty years later, we see what a tremendous impact his discovery has had on Physics, Chemistry, Biology, and Medicine. He made many further contributions to NMR over the years and retained a close interest to the end of his life.

I first met Professor Bloch when I was a graduate student in Cambridge, England and he gave a lecture on NMR (or Nuclear Induction as he then called it) to the Royal Society in London

in 1948. The following year, while doing a post-doctoral year with Professor Purcell at Harvard, I had the good fortune to visit Professor Bloch's laboratory in Stanford, and I kept in touch with him ever since. He participated in the formation of ISMAR in Israel in 1971 and played a most valuable advisory role in the Society's affairs since then. Shortly before his death in 1983 he convened a meeting to assist in the further development of the Society, leading to the new ISMAR Constitution agreed later that year.

Scientists everywhere and ISMAR members in particular have reason to remember gratefully Professor Bloch as a scientist and friend and this issue is our contribution to his memory.

E. Raymond Andrew
President, ISMAR



PROFESSOR FELIX BLOCH

FELIX BLOCH AND MAGNETIC RESONANCE

Erwin L. Hahn

*Physics Department
University of California
Berkeley, California 94720*

Presented at the Felix Bloch Memorial Symposium
American Physical Society
April 25, 1984
Washington D.C.*

Among the versatile and fundamental contributions of Felix Bloch to physics, the science of magnetic resonance in condensed matter, also introduced independently by the Purcell Harvard group, was essentially the crowning achievement of his career. The background for the early investigations of the Stanford group in what was then called "nuclear induction" must be viewed in the context of Bloch's early scientific career. In his early youth it was unheard of to think of making an assured living as a theoretical physicist, so a proper career to choose was engineering, and he became a student of engineering in the Institute of Technology in Zurich. He quickly became bored of these studies, and against the advice of his professors switched to physics. He was aware that only fanatics do theoretical physics and was told that he would probably starve at it if he was mediocre. As a young physicist, eager to capitalize on all the new physics which could be solved by the new quantum mechanics, Bloch made a grand tour of studies at prominent centers of European physics before World War II. He interacted with veritable Who's Who of 20th century physicists - Bohr, Schrödinger, Pauli, Debye, Heisenberg, Kramers, Fokker, Ehrenfest and Fermi. Very soon afterward in the early 1930's, Bloch acquired an eminent stature of his own in the physics of solids. Beginning in 1928 to the time of his death in 1983, his papers ranged through a remarkable range of subjects. Leaving out his magnetic resonance publications, they included radiation

damping in quantum mechanics, the periodicity of electrons in crystals and metals, susceptibility and conductivity in metals, ferromagnetism, charged particle stopping power, quantum electrodynamics, x-ray spectra, x-ray and Compton scattering, Auger effect, beta decay and superconductivity. What was most important in Bloch's future development was his decision to leave Europe in 1934 and to begin his career at Stanford where he eventually began to do experimental physics. The seed of his magnetic resonance or "nuclear induction" idea stemmed from his interest in the neutron. I quote from Bloch's words in his magnetic resonance Nobel Lecture, as follows: "The idea that a neutral elementary particle should possess an intrinsic magnetic moment had a particular fascination for me --- It seemed important to furnish a direct experimental proof for the existence of the magnetic moment of the free neutron." In 1936 Bloch published a paper on the magnetic scattering of neutrons in which he suggested that a beam of slow neutrons in passing through iron would experience a highly localized interaction with the iron atoms. He predicted that neutron spins would become polarized as well as scattered, leading to the present day methods of neutron magnetic scattering. His thinking about magnetic resonance began by his conception of a resonance depolarization experiment in which a polarized neutron beam was passed through space with spins parallel to a strong constant magnetic field H .

As acknowledged in 1938 by Rabi and collaborators, Bloch apparently, along with Gorter, had the magnetic resonance principle in mind, with Bloch interested in carrying out neutron spin resonance. Of course Rabi first accomplished the experiment in 1938 with a molecular

*The author is grateful to Carson Jeffries and Martin Packard for access to source material concerning F. Bloch.

Aug. 4 1945.

Magnetic induction B_n due to nuclear spin orientation:

Consider H_2O (ice) with density ≈ 1 . The number n of protons per cc. is then given by

$$\underline{n} = 2 \times \frac{6 \times 10^{23}}{18} = \underline{6.7 \times 10^{22}}$$

The nuclear moment M_n per cc. at temperature T in a field H is then

$$M_n = \mu_n \frac{e^{\frac{H\mu_p}{kT}} - e^{-\frac{H\mu_p}{kT}}}{e^{\frac{H\mu_p}{kT}} + e^{-\frac{H\mu_p}{kT}}} = \mu_n \tanh \frac{H\mu_p}{kT} \approx n \frac{H\mu_p^2}{kT}$$

$$\text{Now } \mu_p = \text{proton moment} = 2.8 \frac{eh}{4\pi M_p c} = 2.8 \times \frac{4.8 \times 10^{-10} \times 6.5 \times 10^{-27}}{4\pi \times 1.6 \times 10^{-24} \times 3 \times 10^{10}} \\ = 1.4 \times 10^{-23}$$

Therefore with $H = 10^4$ G ; $T = 300$:

$$\underline{M_n^p} = 6.7 \times 10^{22} \frac{10^4 \times 9 \times 10^{-46}}{4 \times 10^{-14}} = \underline{3.4 \times 10^{-6} \text{ G}}$$

$$\text{and } \underline{B_n^p} = 4\pi M_n = \underline{4 \times 10^{-5} \text{ G}}$$

$$\text{For } D_2O \text{ we have } \mu_D = -.8 \times \frac{eh}{4\pi M_D c} = -\frac{.8}{2.8} \times 1.4 \times 10^{-23}$$

$$\underline{M_n^D} = \mu_D n \frac{e^{\frac{H\mu_D}{kT}} - e^{-\frac{H\mu_D}{kT}}}{e^{\frac{H\mu_D}{kT}} + 1 + e^{-\frac{H\mu_D}{kT}}} \approx \frac{2}{3} n \frac{H\mu_D^2}{kT} \\ = \frac{2}{3} \left(\frac{4 \times 10^{-24}}{1.4 \times 10^{23}} \right)^2 M_n^p = \frac{32}{600} M_n^p = \frac{32 \times 1.2}{900} \times 10^{-6} = \underline{2.0 \times 10^{-7} \text{ G}}$$

$$\text{and } \underline{B_n^D} = 4\pi \times 2.0 \times 10^{-7} = \underline{2.2 \times 10^{-6} \text{ G}}$$

Figure 1. Calculations of nuclear Boltzmann factors from original notes of F. Bloch.

(9) Thus $\bar{F} = \frac{2\pi\mu}{R} 2 \times 4.6 = \frac{2\pi\mu}{R} \times .92$
 Also
 The induced signal is (with $N = \text{no. of turns}$)

$$V = \frac{300 N \omega \bar{F}}{c}$$

$$= 10^{-8} \times 8 \times 2\pi \times 8.7 \times 10^6 \cdot \frac{2\pi \times 4.3 \times 10^{-7}}{.4} \times .92$$

$$= 2700 \times 10^{-8} = 2.7 \times 10^{-5}$$

With a $Q = 100$ we should get for
 the signal

$$V_s = QV = 2.7 \times 10^{-3} = \underline{\underline{2.7 \text{ millivolts}}}$$

$$= \underline{\underline{2.7 \text{ millivolts}}}$$

Better method of calculation see p. 116!!!

Figure 2. First estimates of the nuclear induction signal from original notes of F. Bloch.



Figure 3. F. Bloch, H. Staub, and W. Hansen viewing a homemade oscilloscope in the early 50's.

beam. Bloch thereafter acknowledged Rabi's magnetic resonance principle to flip the neutron spin, and in 1940 in collaboration with Luis Alvarez at Berkeley, the neutron moment was measured to an accuracy of 1%. This accuracy was determined by flip coil measurements, which could not be better than 0.4%. Bloch's first notion, which he quickly abandoned as too awkward, was to improve the accuracy of this measurement by calibrating the magnetic field by a molecular beam technique. Bloch began to wonder whether it might be possible to measure the magnetic resonance of nuclei in ordinary condensed matter? He was unaware that Gorter had failed in 1936 and in 1942 to carry out such an experiment in a crystal. This is not surprising since Bloch was not a conscientious surveyor of the literature. He preferred to rediscover and work things out for himself -- a marked characteristic of his independent personality. Nor was he aware of the experiments contemplated or initially carried out on nuclear adsorption at Harvard.

Bloch began from first simple principles to calculate the voltage that would be induced in an inductance by the precessing macroscopic magnetization due to protons in 1 mL of water at room temperature, subjected to a strong field H and a perpendicular r.f. field H_1 . (See Figures 1 and 2). He stated to me personally and to others, on querying him about his train of thought then, that he was amazed how such a simple calculation, taking into account a small Boltzmann factor (of the order 10^{-6}), could give such large voltage signals of the order a millivolt from nuclear induction, well above amplifier noise. He recalled, having confirmed ample nuclear signal size, that the worry of long thermal equilibrium relaxation times might cause failure to see any signal whatsoever. As I proceed further on, this concern about relaxation will be brought out.

The first attempt to measure nuclear induction took place in the fall of 1945, after Bloch returned to Stanford from wartime service at the Radio Research Laboratory in Cambridge, Massachusetts, where he worked on radar scattering and theory of the magnetron. With his student Martin Packard and colleague W. W. Hansen, an apparatus was assembled, with Bloch working on the magnet and Packard and Hansen assembling the radio transmitter and receiver. In those days the physics apparatus at Stanford was in a sorrowfully primitive state with none of the elegant equipment Bloch and Hansen were accustomed to during their research sojourns elsewhere during the war. The Stanford physics basement was cluttered with antique x-ray



Figure 4. M. Packard, R. Sands and F. Bloch.

apparatus -- and that was about it. For the nuclear induction experiment they used a rather primitive lecture demonstration magnet (Figure 5) with current supplied by the small Stanford cyclotron.

They first failed repeatedly in their search for resonance signals at the field supposedly adjusted to the correct value of 1826 gauss for proton resonance at 7.76 MC. In fact, returning to the worry about thermal equilibrium, the sample of water was allowed to sit in the magnetic field all day to make certain that enough macroscopic magnetization would build up to provide a signal before making a search. Little did they know that they had to wait only about 3 seconds for protons to relax in water. Finally something happened after they switched off the magnet one day (sometime after Christmas, 1945) to see what was wrong. A signal blip appeared on the scope unexpectedly. They saw their first adiabatic fast passage signal by dropping the magnetic field through the resonance condition $\omega = \gamma H$. It was quickly confirmed that the signal could be improved by using a paramagnetic iron nitrate solution to shorten the relaxation time. Now nuclear induction was established as a reality. After this success Bloch gave a colloquium lecture while Martin Packard valiantly tried to reproduce the experiment on the lecture table in front of the audience, but he

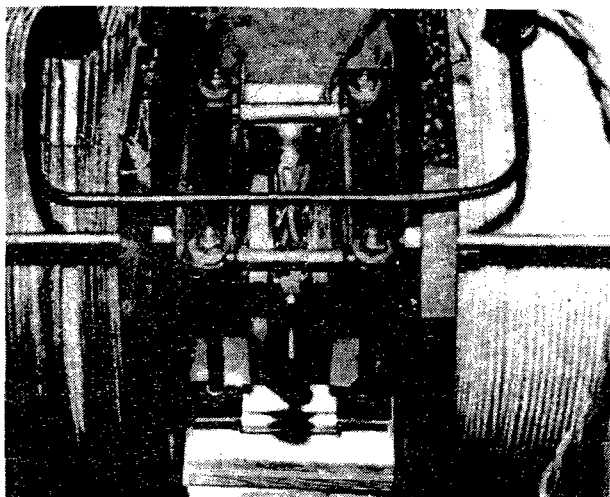


Figure 5. Lecture demonstration magnet used to obtain the first nuclear induction signal.

couldn't find the signal -- the spins were still shy about exposing themselves to the public, having been left alone in their incoherent privacy for an eternity.

These preliminary results, reported in 1946, were followed by Bloch's famous paper on Nuclear Induction in which the phenomenological theory of macroscopic spin dynamics was given. It is of historical interest again to reproduce a certain page (Figure 6) of Bloch's original notebook. This shows clearly his reasoning in arriving at what are now the standard dynamical equations of nuclear magnetic resonance, and the famous transverse T_2 and longitudinal T_1 relaxation times.

A few weeks after the first successful experiments at Stanford, Bloch received the news that a closely related discovery had been made simultaneously at Harvard. Their discoveries were announced in the same issue of *Physical Review*, January 1946. For a brief period of time it was thought that possibly these two investigations were dealing with different things. Finally it was realized the two experiments were observing the same phenomena from different points of view. Bloch's approach was in terms of dynamic macroscopic voltage signals induced by precession and the Faraday effect, whereas the Purcell group description was in optical terms of

quantum mechanical susceptibility and absorption.

Many new findings developed in the years to follow. The concept of motional narrowing in liquids developed explicitly from the Harvard group. Their style focused on microscopic effects of local fields, line widths and shapes, and effects of fluctuations of local fields upon the magnetic resonance signal and its relaxation. When nuclear induction signals in liquids were first investigated at Stanford, their observed line widths, which were predominantly caused by magnetic field inhomogeneity, were interpreted in the beginning to be due to dipolar broadening by neighboring spins in the sample. The germ of motional narrowing was of course finally evident to the Stanford group, since the effect of long relaxation times was included in the Bloch equations. The Stanford group interest, however, was more in the measurement of spins and moments. The Bloch method of crossed-coils was adapted quite efficiently to the search for new resonances which W. W. Hansen had in mind as a master project, interrupted, however, by his untimely death. With Nicodemus and Staub, Bloch returned to his old interest in the neutron, and made a precision measurement of its magnetic moment by observing in the same field two precession frequencies, that of a beam of neutrons in vacuum, and that of protons in water. Later tritium (^3H) was measured by Levinthal, and Packard worked on the precise moment of ^2H . Warren Proctor developed a search NMR spectrometer, and he began to measure the spins and moments of a large number of nuclei. In the course of these searches it was inevitable for Proctor and Yu that they should discover the chemical shift -- the same nucleus in different compounds has a different resonance frequency because contributions of the bonded electrons to the effective field at the nucleus. This shift was also discovered independently by Dickenson at MIT in the laboratory of Francis Bitter. Proctor and Yu observed the NMR shift of nitrogen-14 in NH_4NO_3 dissolved in water: one nitrogen resonance came from the NH_4 group, shifted from a second nitrogen resonance in the NO_3 group. This effect excited Bloch very much at first, thinking that perhaps there existed stable nuclear isomers that had slightly different properties. The other possibility of course was that it could be just a nasty diamagnetic chemical shift which would not and did not excite him. After it was confirmed as chemical in origin the shift did not command Bloch's interest as fundamental in his list of priority problems in physics. To confirm whether or not the two nitrogen resonances

(103) This means, that averaging over broadening results in a "dying out" of m_x and m_y of as $e^{-t/T'}$.

The same does not hold for m_z which is essentially diagonal. Another way of saying the same thing is, that to change m_z requires an energy $H_0 m_z$ which has to be supplied from the thermal agitation (the lattice) whereas, to change m_x or m_y (with constant m_z) requires no energy.

It seems therefore pretty clear, that the eqns on page 77 etc. have to be modified into:

$$\dot{m}_z = g [\vec{H} \times \vec{m}]_z + A (m_0 - m_z)$$

$$\dot{m}_x = g [\vec{H} \times \vec{m}]_x + B m_x$$

$$\dot{m}_y = g [\vec{H} \times \vec{m}]_y - B m_y$$

where $\frac{1}{A} = T =$ ordinary relaxation time

$$\frac{1}{B} = T' = \frac{1}{2\pi \times \text{nuclear level spread } (4\nu)}$$

Figure 6. Formulation of Bloch equations from original notes of F. Bloch.

were not isomers, Bloch telephoned Segre at Berkeley and asked to borrow a little ^{15}N . If the two resonances were not present in ammonium nitrate made up with ^{15}N , then the explanation would be nuclear instead of chemical. Finally the sample arrived and proved again to give two resonances. Thus the matter of chemical shift was a new complicating correction factor which had to be taken into account in measuring magnetic moments.

The above episode was an example of how Bloch was really not enthusiastic about

analyzing the numerous side effects brought in by the many body effects of local fields in condensed matter that could not be comprehended without an involved series of empirical measurements. I remember distinctly the time when Dick Norberg and I were in Felix's office, pouring out our resonance research results to him, Norberg on metals, and I with chemical echo modulation effects. Bloch said: "Norberg, you should be a metallurgist, and Hahn, you should be a chemist!"



Figure 7. M. Packard and R. Varian.

In 1950 Bloch and Jeffries measured precisely the proton magnetic moment in units of the nuclear magnetic by observing in the same field the NMR and cyclotron resonance of protons using a small anti or inverted cyclotron technique. The body of data obtained by all these measurements was ultimately applied to the nuclear shell model of Mayer and Jensen.

Arnold, Dharmati and Packard observed in a very uniform magnetic field, resolution of hyperfine proton resonances in C_2H_5OH , an effect observed by Gutowsky and Slichter in the steady state, and independently by myself in terms of modulation beats of spin echoes. The existence of these fine structure effects together with the chemical shift serve as the basis of high resolution NMR as it exists today. The enterprise of high resolution NMR instrumentation was pioneered by the Varian Company, and now has spread as an analytic technique throughout the world. Very good scientists, a number of whom came from Bloch's NMR group, worked for



Figure 8. F. Bloch in a debating mood, with E. Ginzton.

Varian in those early days which gave the company the research thrust that enabled it to produce the first efficient instrumentation for analytic NMR chemistry.

At this point I would like to interject some particular remarks about the Bloch equations. The Bloch equations have had wide application to a number of physical effects which do not necessarily involve gyromagnetic spins. They apply directly to any two quantum level or equally spaced quantum level system, and are particularly useful in predicting effects involving electric dipole laser resonance phenomena.

Numerous effects in quantum optics are analogs of spin resonance phenomena discovered in former days and are often predicted by Bloch equations. Although considerations of propagation and fluorescence are not present in NMR cavity resonance experiments, there remain a host of similar effects in the time and frequency domain that also appear in quantum optics.

Although the original phenomenological Bloch equations work very well for fluids, in many cases they are not rigorous for all systems, particularly in solids. Nevertheless, the Bloch formulation has stimulated new statistical investigations with the density matrix that are more rigorous for the particular system under investigation. Exceedingly useful is the property that

the Bloch equations enable predictions of nonlinear quantum macroscopic phenomena that no amount of fastidious quantum mechanical perturbation theory could predict as handily.

Personally it was my good fortune and privilege to study under Felix Bloch as a postdoctoral student during the two years 1950 to 1952. It was in his nature to have a profound influence on his students. His love for physics took a high priority in his life, which induced him continually to avoid the impediments of formal rules of bureaucratic restraints that prevented him from doing things for himself. He always invited others to share in his search for answers, and did not distance himself from anyone who would join him in the search, regardless of his or her status. What many of his students gained from him intellectually was often merged with his advice and counsel. Felix was a devoted family man, and not incidentally, he was also an accomplished pianist. With his good wife Lore and the family, the invitations to participate in activities of family life, with musicals, hikes and parties, were all occasions indeed memorable, giving

positive incentive and enjoyment in learning physics from Felix.

The legacy of contributions to science by Felix Bloch was already a monument to him while he was alive. Among his versatile contributions to physics I have emphasized his work on magnetic resonance. The application and impact in particular of the science of NMR now involves the activities of thousands of research people in solid state physics, analytical chemistry, and most recently of clinicians in the medical world who apply the technique for imaging the human body for medical diagnosis. Not long before his death Felix indicated to me as well as to others that the extension of magnetic resonance to humanitarian practical use was of great satisfaction to him,

Felix Bloch is among the Greats in the history of science, affecting many who never met him, a living influence for them and a personal one for those of us who were fortunate to have known him, and who shall remember him with affection and gratitude.

FELIX BLOCH
Reminiscences of A Graduate Student

Martin Packard

*Varian Associates
Palo Alto, California*

My first meeting with Professor Bloch was shortly after V-J Day on a hot afternoon in the fall of 1945. We met in his sparse, high ceiling, cool office in the old physics corner at Stanford University where he described with the elegant use of chalk and blackboard a new and exciting but simple concept — Nuclear Induction. The blackboard and his unconscious cross temple stroking of his forelock were to remain an important part of communications on this concept which won him, along with Edward Purcell, a Nobel Prize in 1952, and won me a Ph.D. in physics in 1949.

After an hour or two of discussion about the project, we agreed that I should come to Stanford as a Ph.D. candidate, working with Bloch and Hansen on the yet untested but carefully researched idea of Nuclear Induction. Stanford was a little more informal in those days. I became the first postwar Physics graduate student without filling out forms or submitting transcripts. This unstructured environment was the mark of a Country and University in transition, and was most conducive to rapid progress.

My introduction to Felix Bloch came through Dr. Daniel Alpert, my group leader at Westinghouse where I had worked on passive microwave devices prior to being assigned to the Manhattan Project at Berkeley. Alpert's major professor was Prof. William Hansen and he had worked with Bloch as well. He thought that Bloch and I might form a symbiotic relationship — my experimental skills and Bloch's theoretical concepts.

The Physics Department basement — or for the theoretical students, the Physics attic — was to become an exciting environment, due largely to the backlog of ideas and the quality of the staff — F. Bloch, D. Webster and P. Kirkpatrick, followed soon by W. Hansen, and later E. Ginzton and L. Schiff. The graduate students were more mature than usual and technically skilled, especially in electronics. Conversely, some of the students had forgotten what they had learned of classical and quantum physics.

In the fall of 1945 the Stanford Physics Department was a mess. Much of the basement had been devoted to X-ray research and was reminiscent of a rabbit warren with hutches

constructed of chicken-wire and lead, interconnected by a random network of forgotten wires. Local Indian relics were stored in one of the enclosures. One was wondered if the bones were the remains of an unlucky graduate student. None of this disorder seemed to trouble Bloch. We evoked squatters rights, and I chose the old upstairs klystron laboratory. (I still wonder whether the correlation between creativity and surroundings is negative or positive.)

Ours was a cross-cultural relationship, which melded under the urgency of demonstrating Nuclear Induction ahead of omnipresent competitors. My culture, which was primarily experimental, was derived from Westinghouse Research where I worked under E. U. Condon, and was modified slightly at Ernest Lawrence's laboratory in Berkeley. Felix, as I addressed him, came from a theoretical background with the basic culture of Bern and Zurich.

Never did our Western familiarities and informalities appear to bother Felix or his wife, Lore. It was not until much later that I learned how long it takes the Swiss to be on a first-name basis. On the other hand, he retained a few residual European customs, which we accepted but with small internal grumblings. One of these was the extended midday dinner. We soon learned that this was not idle time and that conversations which were interrupted at the end of the morning would be continued late in the afternoon, sometimes past our dinner time. One notable example of this creative time was Bloch's invention of the spinning sample for high resolution NMR which came as he was stirring his midday tea.

Although there was a drive for progress, this was implicit and formal meetings were never held between Bill Hansen, Felix and myself. A division of labor was tacitly understood and the work went on independently. Bill Hansen worked on the crosscoil assembly, which was used for decoupling the strong transmitter field from the receiver; Felix modified and calibrated an ancient, small lecture electromagnet, with special transformer pole pieces and a field sweep; and I built the rf circuitry and visual display.

Progress during the first three months seemed slow. There was no infrastructure

comparable to that at Westinghouse or Berkeley. However, the two skilled machinists, Bert and John, were most helpful in building complex parts or in teaching us how to bend metal or grind tool bits. Teaching responsibilities also interfered with research. Felix was sensitive to the material needs of graduate students, and so I was paid as a teaching assistant for a freshman physics course. Since I had been away from freshman physics so long, preparation time was longer than if I had been teaching, e.g., Laplace transforms, but Felix never complained.

Nevertheless, the apparatus did come together and, as with all systems, some backtracking was required. Hansen's original kinematic design, which used an ingenious design of flexible wires, was abandoned in favor of his newly invented paddle for flux steering.

By the Christmas holidays everything seemed to be in order. Barbara and I decided to drive to Oregon to visit my parents, whom I hadn't seen during the war years. Felix expressed mild disappointment but not anger, at the delay. During my six-year stint at Stanford I cannot recall that he ever spoke harshly or was not considerate of his graduate students.

This is not to say that Felix avoided controversy or did not speak on issues that he felt important. I felt squeamish about his participation in the early political infighting which surfaced at selected weekly seminars. Later on he expressed strong opposition to the organization of Physics at Stanford, a problem which continued for a long time.

Felix was a superb theoretician with considerable physical insight. I quickly appreciated his skills without knowing of his previous work; e.g., Bloch walls in ferromagnetics. Prior to my coming to Stanford, he had fully developed his phenomenological equations of NMR on purely theoretical grounds. The equations were never modified, only interpreted. Felix preferred to think about Nuclear Induction in classical terms, which he justified as being the expectation values of the quantum mechanical model.

Felix was a master of the art of keeping important terms and dropping the insignificant ones. It is hard to know how, but he managed to impart this instinct to his students. Perhaps the absence of computers or even hand-cranked Monroe calculators brought out this ability.

He welcomed the interplay between his theory and the experiment. This was well exemplified by the first observations of the Nuclear Induction phenomenon. His original belief was that the static dipolar interaction between protons in our water sample would give

a long thermal relaxation time T_1 , and a very short transverse T_2 .

This understanding dictated the details of the experiment; namely, that the radiofrequency (rf) fields should be very strong, the order of a few Gauss, and that the sample must be pre-polarized in a strong magnetic field for many hours. For the soaking, Felix assembled a small outrigger pole piece in the fringing field of the cyclotron magnet, where the sample was left for more than 24 hours.

Initial observations at the proper magnetic field were disappointing. Almost in desperation we raised the field well above Bloch's calibrated value and turned off the magnet power supply, which added a linear sweep on top of the small sine wave sweep. I happened to see a signal which entered from the right and disappeared to the left, much as a radar signal on an A-scope. Having once seen the signal we very quickly improved it, noting that relaxation times were moderate and that our original instrument design was excessive.

After our success, we left the dark, cold and clammy Cyclotron laboratory for the Blochs' pleasant house, where we shared our euphoria and celebrated Lore's birthday or near birthday with a glass of wine. Felix had expressed his hope to bring Lore a Nuclear Induction signal as a birthday present.

Felix immediately reviewed his equations and explained what we had seen. The transverse relaxation times had been much longer than expected and the longitudinal T_1 much less than expected, due to the rapid tumbling of the water molecules. Felix explained as a matter of fact that the physics of liquids was very difficult compared to solids or gases. The shape which we saw was explained by the Bloch equations and was labeled "rapid passage," as it was neither a dispersion curve, which we had expected, nor a simple absorption curve.

This explanation of the experimental data by the Bloch equations gave me great respect for them, and for their creator. (It is now too late, but I wish I had understood from Felix how he built such a simple, but valid model. Did he introduce the relaxation times as exponentials because of analytical simplicity or did he recognize the similarity to stochastic collisions in optical spectroscopy?)

Jargon was readily accepted by Felix. He invented the term "rabbit ears" for one particularly stubborn problem and was quite comfortable with terms borrowed from radar, an acceptance lacking by purists in the German language.

Felix was always generous with sharing

credit with coworkers and never wished to be an author as the Director of the laboratory. The first experimental paper on Nuclear Induction was authored by F. Bloch, W. Hansen, and M. Packard; however, the accompanying theoretical paper bore only his name. The first paper on chemical shifts was written by W. Proctor and F. Yu. The paper on chemical shifts in protons was by J. Arnold, S. Dharmatti and M. Packard. With Bloch, there never was a problem about the order of the authors, they were just listed alphabetically. Felix was equally generous in acknowledging me and other colleagues at talks which he gave many years after the original work.

We had many social discussions, particularly as our wives often sat together with the Bloch children while we spent the evening in the laboratory. Felix was well read, broadly educated in a classical European manner, and was an excellent piano player which he shared with us occasionally.

Felix did not appear to be the athletic type, however he did from time to time ride his bicycle from their simple house on Emerson street in Palo Alto to the Physics Department, and did take occasional outings to the beach at Carmel. (We still have a lovely bowl that he and Lore brought to us.) Nevertheless, he described his earlier experiences in rock climbing in Switzerland. One of his very difficult climbs ended with a fall and a broken leg. While skiing together at Los Alamos, where we went to measure tritium, I was amazed to see him making a graceful Tellemark, a turn which was new to me, a self taught skier from the Northwest.

Felix Bloch's major scientific interest and thrust was in measuring nuclear magnetic moments of the isotopes as a basis for understanding nuclear forces, which he considered to be the "central problem" of physics. Prior to the war he had measured the neutron moment in terms of the cyclotron resonance with Prof. Louis Alvarez at UC, Berkeley.

During a concert at Cambridge where he worked in Prof. Frederick Terman's laboratory, he considered the way to measure magnetic resonance in matter of normal density. This would make it possible to measure magnet moments in terms of the proton moment without the uncertainty of field calibration. At the time, a magnetic field could not be calibrated to better than 1/10th of a percent. His ideas were sharpened at Cambridge. The experimental techniques, concepts of signal-to-noise, and other practical matters were developed in conversations with Bill Hansen. In the tradition of most

scientists, these matters were discussed only with collaborators and not potential competitors.

Even though much of the early gestation of Nuclear Induction occurred while he was at Harvard and very close to Edward Purcell, they had no interaction. Both groups performed the experiment independently and did not learn of the other's work until the arrival of the Physical Review.

Bloch was always very quick to grasp new concepts and to synthesize them into his own understanding. I had used a symmetry criteria at Westinghouse to measure precision frequencies of cavities and sought to apply this to measuring the magnet moments. Felix thought about this briefly and agreed that that was indeed a valid criteria. He understood and taught us the subtleties of precision and accuracy during many discussions at the blackboard.

In view of Bloch's ability to handle new concepts, it was somewhat surprising to me that there was not instant recognition on the part of either Bloch or Purcell that the two groups were viewing the same phenomenon, even though the apparatus and the theoretical description were much different. Bloch had approached Nuclear Induction on the basis of classical phenomenological equations, while Purcell's group followed a spectroscopic model. The Stanford group initially observed dispersion, using a strong radiofrequency field, while the Harvard group's apparatus was phased to observe absorption in the presence of very weak fields.

It is surprising to me how long early impressions persist. Many years passed before most physicists and chemists accepted nature's view of the commonality of the two approaches. Nevertheless, I was recently asked by a foreign scholar whether Varian Associates' instruments used the Purcell or the Bloch technique.

Bloch coined the term Nuclear Induction, which gradually became displaced by NMR. I felt like a traitor when at Varian we adopted NMR. Confusion still exists in the nomenclature of electron magnetic resonance, chemists seem to like ESR while physicists tend to use the older EPR.

The very first NMR experiments were inexpensive and were, I believe, financed by the Physics Department. I purchased the electronics, which consisted of a Dumont oscilloscope (just like the one I had used at Westinghouse); a few vacuum tubes, some discreet components, a chassis or two, and panels. After the initial success, additional funds were provided by the Office of Naval Research (ONR) to extend the technique to the measurement of magnetic

moments of other isotopes. Happily, the details of this support were invisible to me. I have no recollection of being asked to prepare proposals, budgets, or write reports; Felix either handled this himself or left it up to Anna Laura Berg, our administrative, secretarial, 4 o'clock coffeemaker staff.

This support of basic research by the ONR returned a huge yield to the DOD and to society. No one at that time had any inkling that Nuclear Induction would lead to magnetometers used to hunt submarines or become a major tool for scientists. NMR has become the most important spectroscopic tool for structural and organic chemists; biologists use NMR to study the conformation of DNA; and physicians like the superior diagnostic images of NMR.

Felix was proud but not ostentatious about his role in NMR. During the last few years of his life, Felix was fond of telling that his finger was the first in vivo specimen. I suspect that not even history will ever clarify whether it was the Professor's or the graduate student's finger which was first placed in the Nuclear Induction probe.

Early ONR support enabled the laboratory to become more consolidated, adding additional people and new experimental apparatus. Teaching Assistants became Research Assistants. Under Prof. Hansen's guidance, a Bitter Magnet was designed and built with the expectation that a nearly automatic machine could be designed for searching out and cataloging all the isotopes that had spins. This turned out to be impractical, so magnetic moments were measured isotope by isotope by successive graduate students.

Bloch's foremost interest was in the physics of NMR and phenomena which its use could explain. While he did not enthusiastically support the chemist's interest, neither did he belittle it or interfere with research in his laboratory on chemically oriented problems. This was a lesson he taught me well: a great researcher has humility about his views of what the future may bring.

Felix was a dedicated teacher with exceptional abilities. His lectures were well prepared

but not sterile. Even though he reviewed his lecture notes carefully before class, he sometimes needed to share with us his thought processes as he reconstructed the logic or worked through a difficult chain of the mathematics. I felt that this was an important part of his pedagogical style, and was much better than one visiting professor who presented beautiful stress free lectures, which were so easy to follow that little was remembered.

The classroom work was important, but I feel that our almost daily discussions at the laboratory blackboard were the hallmark of a marvelous teacher. He instigated occasional tutorial sessions to insure our progress towards the Department Oral examination which was the prelude to the final goal. I remember well his asking me to explain internal reflection of light and kindly helped me by elucidating how the light must be attenuated exponentially outside the surface.

His writing was lucid, but sometimes had a slight Swiss accent. This created some anxiety for me and for my wife who was the typist, because after he would return my thesis with revisions, I in turn would change it back. Happily for all of us, including the onlooking graduate students, the series finally converged and my thesis was signed on the day of the birth of our first child.

Dan Alpert had been right. Felix and I formed a symbiotic relationship, which was beneficial to both of us and to society. But sadly it did not last over the years, since Professor Bloch chose estrangement with many of his students; an estrangement which was never reconciled. The reason is unfathomable to me, but seemed linked to his consulting agreement with Varian Associates Inc.

Nobel Laureate Felix Bloch was Switzerland's greatest native physicist. He brought to Leland Stanford Jr. University not only fame but a classical approach to physics and the love of teaching. It was my privilege to have studied under him, and it is my hope that his style of teaching and his approach to physics will be carried on.

EARLY HISTORY OF MAGNETIC RESONANCE

Norman F. Ramsey

*Lyman Laboratory of Physics
Harvard University
Cambridge, Massachusetts 02138*

INTRODUCTION

In the title of this report, emphasis should be given to the word *early*. Some readers may even believe that "Pre-History" would be a better title than early history. The report will cover the period from 1921 to the first nuclear resonance absorption experiments of Purcell, Torrey and Pound and the first nuclear induction experiments of Bloch, Hansen and Packard even though from some points of view the history of magnetic resonance can be said to begin with the experiments that end this report.

My interest in the history of magnetic resonance began with preparations for my Ph.D. final examination in 1939. Since mine was the first Ph.D. thesis based on nuclear magnetic resonance, I feared that my examining committee would ask searching questions as to the origins of the ideas of magnetic resonance and of the molecular beam technique we used to detect the resonance transitions.

EARLIEST SEARCH FOR A DEPENDENCE OF MAGNETIC SUSCEPTIBILITY ON FREQUENCY

The earliest reported search for a dependence of magnetic susceptibility on frequency was carried out by Belz(1) in 1922 for solutions of a variety of paramagnetic salts. No frequency dependence was found. Acting on a suggestion of Lenz and Ehrenfest, G. Breit(2) searched for a frequency dependence of the magnetic susceptibility of various paramagnetic substances but found no dependence on frequency. Perhaps this disappointment contributed to Breit's decision to concentrate in theory, where he later had such a productive career.

SPACE QUANTIZATION WHEN DIRECTION OF MAGNETIC FIELD CHANGES

The origins of the molecular beam magnetic resonance method can be traced back to early theoretical speculations and experiments on the

change in the quantum mechanical space quantization when the direction of a magnetic field is changed. The problem was first posed and partially solved in 1927 by C. G. Darwin(2) and his analysis was subsequently improved by P. Gutinger(3), E. Majorana(4), and L. Motz and M. Rose(4).

In the period 1931-33 several experiments in Otto Stern's laboratory in Hamburg successfully measured the changes in the space quantization when the direction of the magnetic field was changed. The experiments of Phipps and Stern(5) and Frisch and Segre(6) partly agreed with the best theory and partially disagreed. I. I. Rabi(7) pointed out that the discrepancy between theory and experiment was due to the neglect of nuclear spins in previous theories. Although the magnetic moment of the electron is about 2000 times larger than the typical nuclear magnetic moment, the angular momenta are comparable in size and at the low fields used in some of the experiments the nuclear spin angular momenta were tightly coupled to the electron spin making large effects on the observations. In all of these experiments the direction of the field was changed in space as the atoms went by. Since the atoms had a thermal velocity distribution the frequency components were different for different velocities, so on averaging over the velocity distribution, no sharp resonances were either anticipated or observed. Rabi(8) and Schwinger(9) in 1937 calculated the transition probability for molecules that passed through a region in which the direction of the field varied rapidly.

FIRST ATTEMPT TO OBSERVED NUCLEAR MAGNETIC RESONANCE IN CONDENSED MATTER

In 1936 with calorimetric techniques, C. J. Gorter(10) successfully observed a frequency dependence of the paramagnetic relaxation of a number of alums. He found that the observed effects depended on the frequency, ν , as ν^x where x was a number, usually between 1 and 2. No resonance effects were observed. Gorter(10)

also utilized the same calorimetric method in an attempt to look at ^7Li nuclear magnetic resonance in LiCl and for an ^1H resonance in AlK alum but found no such resonance. The following year, Lasarew and Schubnikowt(21) showed at low temperature that the nuclear magnetic moments in solid hydrogen contributed significantly to the observed static magnetic susceptibility of solid hydrogen.

In an experiment reported in 1942 subsequent to the successful molecular beam nuclear magnetic resonance experiments described in the next two sections, Gorter and Broer(10) attempted to observe nuclear magnetic resonance in powders of LiCl and KF , but no resonance was observed. It is still a mystery as to why Gorter did not detect a resonance. In part he suffered from a poor choice of material since R. V. Pound much later showed that pure crystalline LiF has an unusually long nuclear spin-lattice relaxation time. However, that alone does not explain the failure of Gorter's inspired experiments since at a much later date N. Bloembergen found one of Gorter's original crystals and was able to observe an NMR signal with it even though the relaxation time was large. The most likely explanation for the failure of Gorter's experiments was an unfavorable signal-to-noise ratio in his apparatus. It is of interest to note that the first appearance of the phrase "nuclear magnetic resonance" in a publication title is in Gorter's 1942 paper, but he attributes the coin- ing of this phrase to I. I. Rabi.

TRANSITIONS INDUCED BY PASSAGE OF MOLECULES THROUGH DIFFERENTLY ORIENTATED MAGNETIC FIELDS

While Gorter was pursuing his unsuccessful NMR experiments, I. I. Rabi was independently studying transitions induced when atoms or molecules in a molecular beam traversed a region in space of space in which the directions of the magnetic field change successively. In his brilliant 1937 theoretical paper entitled "Space Quantization in a Gyating Magnetic Field", Rabi(8) assumed for simplicity that the field was oscillatory in time even though the initial application was to a field varying along the beam rather than oscillatory with time. As a consequence, all the formulae in that paper are applicable to the resonance case with oscillatory fields and the paper, without alteration, provides the fundamental theory for present molecular beam magnetic resonance experiments as well as for other experiments with magnetic resonance.

MOLECULAR BEAM MAGNETIC RESONANCE

While writing his paper on the gyrating field, Rabi discussed with some of his colleagues the possibility of using oscillatory rather than space varying magnetic fields, but Rabi's laboratory had a full program of important experiments which did not require oscillatory fields, and no experiments utilizing oscillatory fields were started during the first six months following the submission of Rabi's theoretical paper on the gyrating magnetic field. In September 1937, C. J. Gorter visited Rabi's laboratory(12) and described his brilliantly conceived but experimentally unsuccessful efforts to observe nuclear magnetic resonance in lithium fluoride, as described in Gorter's publications of the previous year(10). The research efforts in Rabi's laboratory at Columbia University were soon directed primarily toward the construction of molecular beam magnetic resonance experiments with oscillator driven magnetic fields. Two successful magnetic resonance devices were soon constructed by Rabi(13,14), Zacharias(13,14), Millman(13), Kusch(13), Kellogg(14), and Ramsey(14, 15). A schematic view(13) of the method is shown in Figure 1. In these experiments the atoms or molecules were deflected by a first inhomogeneous magnetic field and refocused by a second one. When the resonance transition was induced in the region between the two inhomogeneous fields, the occurrence of the transition could easily be recognized by the reduction of intensity associated with the accompanying failure of refocusing. For transitions induced by the radiofrequency oscillatory field, the apparent frequency was almost the same for all molecules independent of molecular velocity. As a result, when the oscillator frequency was equal to the Larmor angular frequency ω_0 of a nucleus, a sharp resonance was obtained where

$$\omega_0 = \gamma_I H_0 \quad (1)$$

is the angular precession frequency of a classical magnetized top with the same ratio γ_I of magnetic moment to angular momentum when in a magnetic field H_0 . Figure 2 shows the first reported nuclear magnetic resonance curve; the curve was obtained with a beam of LiCl molecules(13).

Kellogg, Rabi, Ramsey, and Zacharias(14, 15) soon extended the method to the molecules H_2 , D_2 and HD for which the resonance frequencies depended not only on eqn. 1 but also on

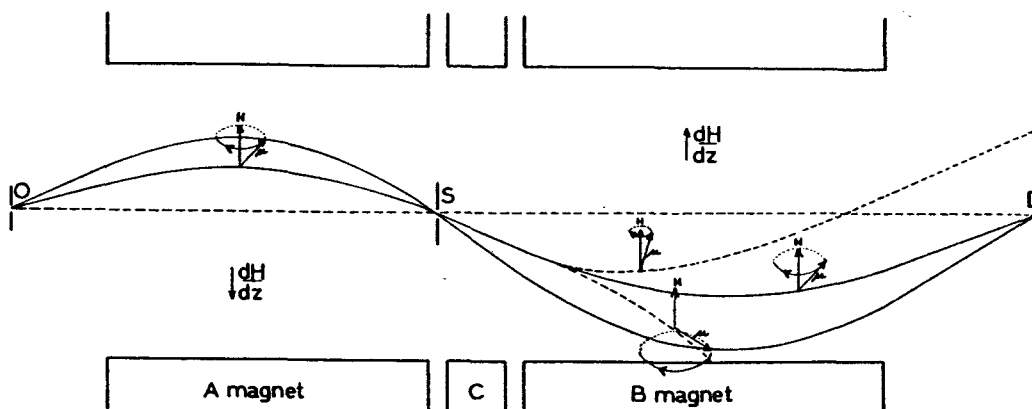


Figure 1. Schematic diagram(13) showing the principle of the first molecular beam magnetic resonance apparatus. The two solid curves indicate two paths of molecules having different orientations that are not changed during passage through the apparatus. The two dashed curves in the region of the B magnet indicate two paths of molecules whose orientation has been changed in the C region so the refocusing is lost due to the change in the component along the direction of the magnetic field.

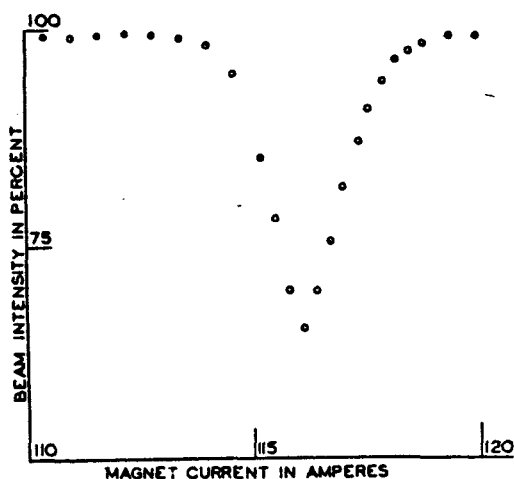


Figure 2. Curve showing refocused beam intensity at various values of the homogeneous field. One ampere corresponds to about 18.4 Gauss. The frequency of the oscillating field was held constant at 3.518×10^6 cycles per second.

internal interactions within the molecule. The transitions in this case occurred whenever the oscillatory field was at a Bohr angular frequency

for an allowed transition

$$\hbar\omega = E_i - E_f \quad (2)$$

For the first time the authors described their results as "radiofrequency spectroscopy". The radiofrequency spectrum for H_2 is shown in Figure 3.

The first molecular beam magnetic resonance experiments were with $^1\Sigma$ molecules for which the primary interactions were those of the nuclear magnetic moments in external magnetic fields, but in 1940 Kusch, Millman and Rabi(16, 17) first extended the method to paramagnetic atoms and in particular to $\Delta F = \pm 1$ transitions of atoms where the relative orientation of the nuclear and electronic magnetic moments were changed, in which case the resonance frequencies were determined dominantly by fixed internal properties of the atom rather than by interactions with an externally applied magnetic field.

In 1949, N. F. Ramsey(18,20) invented the separated oscillatory field method for magnetic resonance experiments. In this new method, the oscillatory field, instead of being distributed throughout the transition region, was

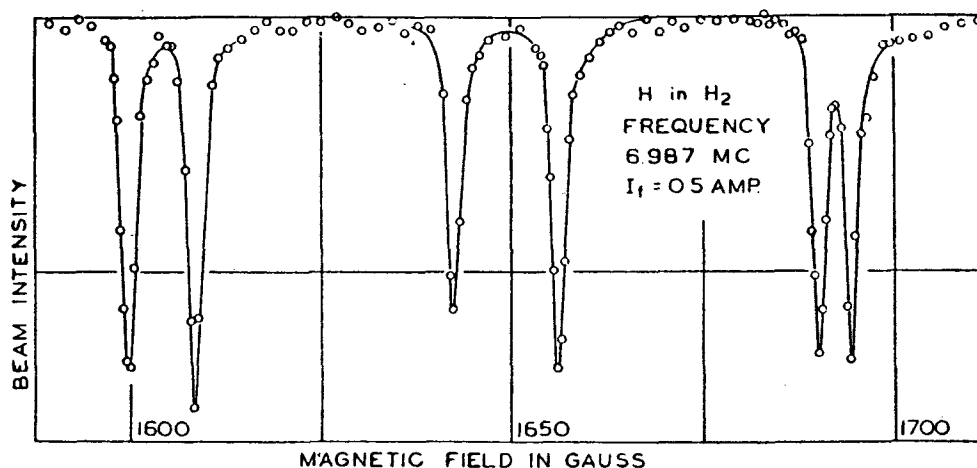


Figure 3. Radiofrequency spectrum of H_2 in the vicinity of the proton resonance frequency(14). The resonance frequencies are primarily determined by the interaction of the proton magnetic moment with the external magnetic but the state of different m_I and m_J are displaced relative to each other by the different values of the nuclear spin-nuclear spin interaction energies and of the spin-rotational interaction.

concentrated in two coherently driven oscillatory fields in short regions at the beginning and end of the resonance region. In an alternative version of the same method, the coherent oscillatory fields are applied in two short pulses -- at the beginning and end of the observation time. The method has the following advantages(20): (1) the resonances are 40% narrower than even the most favorable Rabi resonances with the same length of apparatus; (2) the resonance are not broadened by field inhomogeneities; (3) the length of the transition region can be much longer than the wavelength of the radiation, provided that the two oscillatory field regions are short, whereas there are difficulties with the Rabi method due to phase shifts when the length of the oscillatory region is comparable to the wave length; (4) the first-order Doppler shift can mostly be eliminated when sufficiently short oscillatory field regions are used; (5) the sensitivity of the resonance can be increased by the deliberate use of appropriate relative phase shifts between the two oscillatory fields; and (6) with short lived states the resonance width can be narrowed below that expected from the lifetime of the state and the Heisenberg uncertainty principle if the separation of the oscillatory fields is sufficiently great that only molecules living

longer than average in the excited state can reach the second oscillatory field before decaying.

Essentially the same magnetic resonance technique as developed by Rabi for measuring nuclear magnetic moments with a molecular beam was used by Alvarez and Bloch(21) to measure the magnetic moment of the neutron with a neutron beam. Since the first publication on the neutron magnetic resonance studies was published about two years after the first molecular beam magnetic resonance papers appeared, it is often considered that the neutron studies of Alvarez and Bloch were merely adaptations of the resonance methods developed by Rabi and his associates. However, Alvarez recently has told me that Bloch had thought of doing the neutron beam magnetic resonance experiment before either Alvarez or Bloch had heard of the molecular beam magnetic resonance experiments of Rabi and his associates. It must have been a bitter disappointment to Bloch and Alvarez to learn that their clever idea for magnetic resonance had been anticipated by Rabi and his associates. It is to their credit that they did not let this disappointment blight their research careers; instead each went on to win separate Nobel Prizes for subsequent research.

Work on both molecular beam and neutron

beam magnetic resonance experiments were interrupted by World War II. In 1944 Rabi and Ramsey spent one evening together in Cambridge, Massachusetts, planning possible post-war research experiments. Two ideas emerged as leading candidates. One was to use the molecular beam magnetic resonance method to measure the hyperfine separation in atomic hydrogen since a presumably exact theoretical calculation of this separation existed. This experiment was eventually carried out and led to the first indication of an anomalous magnetic moment of the electron. The other idea was to detect the existence of nuclear magnetic resonance transitions by their effect on the oscillator. To our pleasant surprise, the signal-to-noise calculations were favorable and we became quite enthusiastic about the possibility. We then realized that we were merely reinventing Gorter's nuclear magnetic resonance experiments and that those experiments had failed for unknown reasons. We, therefore, decided that efforts in that direction should be given a low priority compared to the various molecular and atomic beam experiments, including the one on the atomic hydrogen hyperfine separation.

ELECTRON PARAMAGNETIC RESONANCE EXPERIMENTS IN CONDENSED MATTER

In addition to his unsuccessful efforts to observe nuclear magnetic resonance, Gorter(10) successfully observed paramagnetic relaxation in condensed matter. However, his attempts to observe an electron paramagnetic resonance failed. The first successful paramagnetic resonance experiments in condensed matter were those of Zavoisky(23). His observed paramagnetic resonance with CrCl_3 is shown in Figure 4, was first reported in a 1944 Ph.D. thesis, and several years elapsed before there was widespread recognition of his accomplishment. Shortly after Zavoisky's pioneering work, observations of electron paramagnetic resonances were made by Cummerow and Halliday (24) and others.

NUCLEAR MAGNETIC RESONANCE EXPERIMENTS IN CONDENSED MATTER

Following World War II, two groups in the United States sought to develop nuclear magnetic resonance experiments with condensed matter. One was E. M. Purcell, N. G. Torrey and R.V. Pound(25) at Harvard University and the other was F. Bloch, W. Hansen and M. E.

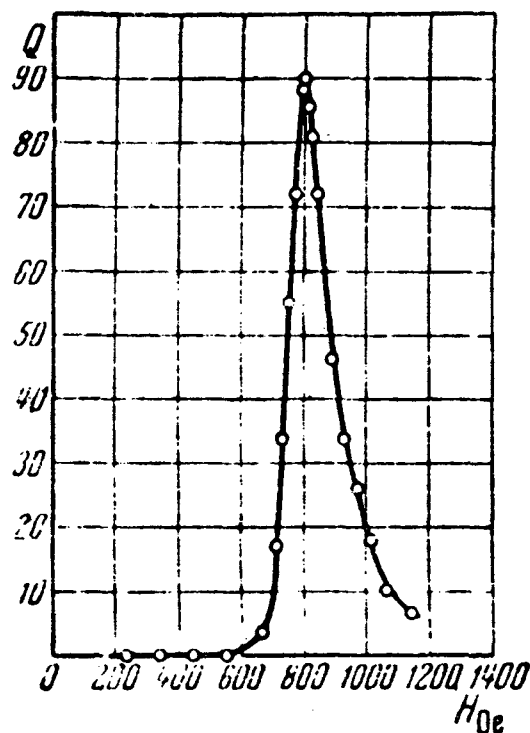


Figure 4. Electron paramagnetic resonance curve obtained by Zavoisky(23) with CrCl_3 . The microwave radiation wavelength was $\lambda = 13.70$ cm and $T = 298$ K.

Packard(26) at Stanford University. Each group had different reasons for being willing to proceed with its experiments despite the failure of Gorter's earlier experiments.

In the case of Purcell, Torrey and Pound(25) they were initially unaware of Gorter's work when they first started their experiment. When Rabi learned of their plans and pointed out to Purcell that Gorter's experiment was similar and had failed, Purcell was disappointed by the news but felt that the work on the new experiment had already gone so far that it should be completed, particularly since their extensive theoretical calculations of relaxation and other feasibility requirements appeared favorable. Purcell and his associates observed the absorption in the resonance circuit and devoted considerable attention to problems of signal size and noise. On December 24, 1945 their letter(25) was received

by the Physical Review announcing the successful observation of nuclear magnetic resonance absorption of the protons in a paraffin filled 30 MHz resonant cavity whose output was balanced against a portion of the signal generator output. When the magnetic field passed through resonance, an unbalanced signal 20 times noise was observed.

When Bloch, Hansen and Packard (26) started their experiments, they were fully aware of Gorter's experiments but they were encouraged to proceed because they thought they knew the source of the previous failure and a means for overcoming it. They believed that Gorter's experiment had failed because the thermal relaxation time T_1 was much longer than Gorter had allowed for. To overcome this difficulty they proposed to put their water sample in a strong magnetic field for several days to allow the nuclear spin system to reach thermal equilibrium. They in fact did so: when their apparatus was all ready for a first test they inserted the water in the high field and before attempting a careful search for a resonance Bloch went off on a ski trip to allow the system to come to equilibrium. When he returned he and his associates found the desired resonance after some initial searching, but they also found that the relaxation time was short and not long. Instead of waiting several days to begin their observations, a few seconds would have sufficed. The detection method of Bloch, Hansen and Packard(26) was rather different from that of Purcell, Torrey and Pound(25). Instead of observing the absorption signal with a single coil, they used two orthogonal coils and picked up the signal induced in the second coil by the coherently precessing nuclei driven by the first coil. For this reason they called their experiments nuclear induction. A letter(26) announcing their successful experiment was received by the Physical Review on January 29, 1946.

From the time of these experiments onward, developments in magnetic resonance occurred at a rapid pace. For this reason, I have chosen that time to bring to an end this account of the early history of magnetic resonance.

REFERENCES

- ¹ M. H. Belz, *Phil. Mag.* **44**, 479 (1922) and G. Beit, *Comm. K. Lab.* 168c (1926).
- ² C. G. Darwin, *Proc. Roy. Soc.* **117**, 258 (1927).
- ³ G. Gutinger, *Zeits. f. Physik* **73**, 169 (1931).
- ⁴ E. Majorana, *Nuovo Cimento* **9**, 43 (1932) and L. Motz and M. E. Rose, *Phys. Rev.* **50**, 348 (1936).
- ⁵ T. E. Phipps and O. Stern, *Zeits. f. Physik* **73**, 185 (1931).
- ⁶ O. Frisch and E. Segre, *Zeits. f. Physik* **80**, 610 (1933).
- ⁷ I. I. Rabi, *Phys. Rev.* **49**, 324 (1936).
- ⁸ I. I. Rabi, *Phys. Rev.* **51**, 652 (1937).
- ⁹ J. Schwinger, *Phys. Rev.* **51**, 645 (1937).
- ¹⁰ C. J. Gorter, *Physica* **3**, 503, 995 and 1006 (1936) and C. J. Gorter and I. J. F. Broer, *Physica* **9**, 591 (1942).
- ¹¹ R. V. Pound, *Phys. Rev.* **81**, 156 (1951).
- ¹² Rabi(13) refers to the visit of Gorter in a footnote to the first paper experimentally demonstrating a successful molecular beam magnetic resonance and Gorter 29 years later published an article giving his own somewhat different recollections of the same visit [*Physics Today* **20**, 76 (Jan. 1967)].
- ¹³ I. I. Rabi, J. R. Zacharias, S. Millman and P. Kusch, *Phys. Rev.* **53**, 318 (1938) and **55**, 526 (1939).
- ¹⁴ J. M. B. Kellogg, I. I. Rabi, N. F. Ramsey and J. R. Zacharias, *Phys. Rev.* **55**, 729 (1939); **57**, 728 (1939); and **57**, 677 (1940).
- ¹⁵ N. F. Ramsey, *Phys. Rev.* **58**, 226 (1940).
- ¹⁶ P. Kusch, S. Millman and I. I. Rabi, *Phys. Rev.* **57**, 765 (1940).
- ¹⁷ S. Millman and P. Kusch, *Phys. Rev.* **57**, 438 (1940).
- ¹⁸ N. F. Ramsey, *Phys. Rev.* **76**, 966 (1949).
- ¹⁹ N. F. Ramsey and H. B. Silsbee, *Phys. Rev.* **84**, 506 (1951).
- ²⁰ N. F. Ramsey, *Physics Today* **33**, 25 (July 1980).
- ²¹ L. Alvarez and F. Bloch, *Phys. Rev.* **51**, 11 (1940).
- ²² J. E. Nafe, E. B. Nelson and I. I. Rabi, *Phys. Rev.* **71**, 914, (1947) and **73**, 718 (1948).
- ²³ E. K. Zavoisky, Ph.D. Thesis 1944 and *J. Phys. USSR* **9**, 211 and 245 (1945) and **10**, 197 (1946).
- ²⁴ R. L. Cumberow and D. H. Halliday, *Phys. Rev.* **70**, 483 (1946).
- ²⁵ E. M. Purcell, H. G. Torrey and R. V. Pound, *Phys. Rev.* **69**, 37 (1946).
- ²⁶ F. Bloch, W. Hansen and M. E. Packard, *Phys. Rev.* **69**, 127 (1946).
- ²⁷ B. G. Lasarew and L. W. Schubnikow, *Phys. Zeits. Sowjet.* **11**, 445 (1937).

MANY-BODY PERTURBATION STUDY OF ELECTRON CORRELATION EFFECTS ON NMR PARAMETERS*

A. Saika

Department of Chemistry
Faculty of Science
Kyoto University
Kyoto 606, Japan

	Page
I. Introduction	100
II. Nuclear Spin-spin Coupling	100
III. Nuclear Magnetic Shielding	103
IV. Conclusions	104
References	104

I. INTRODUCTION

NMR is routinely used as an indispensable research tool in present-day chemical laboratories because a wide variety of parameters can be extracted from the response of an ensemble of nuclear spins to a resonant excitation. Among them, the chemical shift in nuclear magnetic shielding and the electron-coupled nuclear spin-spin coupling are direct measures of the change in chemical environment around the nuclei concerned. Consequently, the accumulation of shift and coupling data allows us to use the shift and nuclear spin-spin coupling as empirical parameters in rapid identification of the molecular species present. Theoretically, they can be expressed as a sum of first- and second-order properties, thus reflecting the details of the static and dynamic electronic structure of molecules.

In this review, we wish to report on electron correlation effects on these magnetic properties. Diagrammatic many-body perturbation theory (MBPT) (1,2) is employed to analyze the effects since the method is most unbiased, allowing us to make order-by-order evaluation of the correlation effects.

II. NUCLEAR SPIN-SPIN COUPLING

To begin with, we will discuss the nuclear spin-spin coupling, since it is expected to be more sensitive to electron correlation and involves more problems. In the early days, Ramsey (3), followed by many others, resorted to a "mean excitation energy" approximation. When the numerator changes sign with each excitation in the second-order perturbation formula, however, the approximation may give erroneous results. In fact some coupling constants were calculated with wrong signs. Later, Pople and Santry (4) took explicit account of excited states to remedy the defect of the mean excitation energy approximation, but they utilized only the lowest virtual orbital in evaluating the perturbation formula. We then extended the procedure to include higher virtual orbitals with no sense of convergence noted (5), suggesting the necessity of employing amply extended basis sets, particularly for the Fermi contact interaction. Furthermore, the functions of both the ground and the excited states should be equally well correlated one way or another. Since full configuration interaction (CI) calculations to incorporate electron correlation into both states are unlikely to be feasible for molecules of general interest, MBPT may offer some advantages. It gives correlation corrections order by order as Feynman diagrams, each of which is expressed in terms of single-particle states. Thus, the total correlated wave functions of neither the ground nor the

*Presented at the 22nd NMR Symposium at Kyoto on November 15, 1984 as a special memorial lecture for Felix Bloch.

Table 1. Fermi contact contribution to HD (in Hz).

Contributions	Ordinary MBPT	FF MBPT
Zeroth-order	12.4	54.3 (=CHF)
First-order	9.4	
Second-order	6.3	-15.4
Third-order		-1.7
Total sum	28.1	37.2
Best estimated		40. ^a

^aReference 13. SD (single and double excitation) CI in reference 12 gives 41.8 Hz, which is exact in the basis set employed, since SD CI is exact for a two-electron system.

Table 2. Nuclear magnetic shielding (in ppm) of HF.

Gauge Origin	$F_{\sigma\parallel d}$	$F_{\sigma\perp d}$	$F_{\sigma\perp p}$	F_{σ}	$H_{\sigma\parallel d}$	$H_{\sigma\perp d}$	$H_{\sigma\perp p}$	H_{σ}
CHF MBPT	481.8	482.4	-103.1	413.5	44.05	1.56	17.66	27.50
Zeroth order	481.8	482.4	-38.62		44.05	1.56	11.96	
First order			-26.37				3.53	
Second order F			-14.46				1.18	
CHF type			-16.31				1.24	
non-CHF type	-0.54	-0.23	1.85		0.41	1.34	-0.06	
Total sum	481.3	482.2	-79.45	428.9	44.46	2.90	16.67	27.89
CHF MBPT	481.8	467.3	-91.93	410.9	44.05	140.7	-113.8	32.58
Zeroth order	481.8	467.3	-11.00		44.05	140.7	-90.50	
First order			-33.74				-17.75	
Second order H			-22.68				-2.34	
CHF type			-22.20				-4.20	
non-CHF type	-0.54	-0.38	-0.48		0.41	-0.19	1.86	
Total sum	481.3	466.9	-67.42	426.8	44.46	140.5	-110.6	34.75

excited states are required.

An MBPT calculation of the coupling constant with an extended basis set was first performed through first order in correlation for the Fermi contact contribution in the HD molecule by Schulman and Kaufman (6). The calculation was extended to second order by Itagaki and Saika (7), but the result with 62 Gaussian type orbitals was still far from convergence as shown in the first column of Table 1.

In this connection, the finite-field many-body perturbation theory (FF MBPT) (8,9) deserves some consideration. The scheme incorporates effects of external perturbations by finite perturbation theory prior to the estimation of correlation effects. The effects of electron correlation are then calculated diagrammatically in terms of the perturbation-adapted single-particle states. Thus, the perturbation-induced relaxation effects (8,9) are taken into account to infinite order, while the true correlation effects are obtained to a finite order by the MBPT approach. Therefore, it provides an efficient means for cases where the effects of external perturbations are quite notable. Indeed, this technique has been successfully applied to electric field properties, reproducing them with sufficient accuracy (8,9).

On the other hand, the FF MBPT method has not been applied to magnetic field properties, because the imaginary nature of magnetic field perturbations requires a much greater computational effort as compared with a real perturbation. For the Fermi contact contribution to nuclear spin-spin coupling, however, FF MBPT calculations can be performed without involving too much labor. Since finite perturbation theory or equivalently coupled Hartree-Fock (10) (CHF) calculations usually overestimate the magnitude of the Fermi contact contribution to nuclear-spin coupling, and the rather large overestimate is likely to originate mainly from the neglect of electron correlation, it is of particular interest to see whether the MBPT approach based on the field-dependent single-particle states can recover a significant portion of the correlation effects. Thus we examined the validity and the tractability of the FF MBPT scheme for the Fermi contact contribution to nuclear-spin coupling, with an example of the hydrogen molecule (11).

The MBPT calculations were performed by computing the field-dependent energy diagrams through third order in electron correlation. To further improve the convergence with

respect to the Fermi contact perturbation, we relaxed the fixed-basis-set approach by optimizing the scaling factor of the orbital exponents in the presence of the Fermi contact perturbation. Since the basis-set problem is extremely acute in the Fermi contact contribution, requiring an amply extended basis set, this approach appears promising and appealing.

In carrying out numerical differentiations of the interaction energy between nuclear spins I_A and I_B expressed as (3)

$$E(I_A, I_B) = h \vec{I}_A \cdot \vec{J}_{AB} \cdot \vec{I}_B, \quad (1)$$

we employed the finite-difference method developed by Kowalewski (12):

$$\begin{aligned} \frac{\partial^2 E(I_A, I_B)}{\partial I_A \partial I_B} \bigg|_{I_A, I_B=0} &= \gamma_A \gamma_B \hbar^2 \frac{\partial^2 E(\mu_A, \mu_B)}{\partial \mu_A \partial \mu_B} \bigg|_{\mu_A, \mu_B=0} \\ &\approx \gamma_A \gamma_B \hbar^2 \frac{E(\mu_A, \mu_B) - E(\mu_A, -\mu_B)}{2\mu_A \mu_B} \end{aligned} \quad (2)$$

The value of μ_A and μ_B was chosen so as to bring the zeroth-order FF MBPT value of J_{AB} into reasonable agreement with the CHF value.

While the uncoupled Hartree-Fock (UCHF) value of 12.4 Hz for the Fermi contact term in HD, corresponding to the zeroth-order value in the ordinary MBPT approach, underestimates the best estimated Fermi contact contribution of 40.0 Hz (13) by 69%, the CHF value of 54.3 Hz, equivalent to the zeroth-order FF MBPT value overestimates it by 36%. This much deviation of even the CHF value is rather unusual in view of small deviations of the CHF values from experiment in the case of the electric dipole polarizability (8,9), magnetizability, and nuclear magnetic shielding (14). Before discussing this point, we shall first analyze the correlation corrections.

We see from the second column of Table 1 that the second-order correction is negative and large, amounting to almost 30% of the zeroth-order value. As for the third-order correction, it is also negative but already fairly small, being only 3% of the zeroth-order value. Furthermore, the final value through third order, 37.2 Hz, is in fair agreement with the best estimated value. This rapid convergence of FF MBPT expansions demonstrates that FF MBPT affords a computationally tractable, efficient scheme of calculating the Fermi contact term. For reasons to be

described in the next section, on the other hand, the CHF method may be a very good approximation in calculating the contributions other than the Fermi contact term.

Finally, we add a transparent physical interpretation of the general overestimate by the CHF method. As given by eqn. 2, the nuclear-spin coupling is proportional to the energy difference between the parallel and antiparallel nuclear-spin states:

$$J_{HD} \propto E(\uparrow\uparrow) - E(\uparrow\downarrow).$$

A positive coupling constant is expected, because the antiparallel nuclear-spin state must be more stable in conjunction with the paired spin state of the bonding electrons. This situation is already realized at the CHF level. Now let us consider the effects of electron correlation. For the parallel nuclear-spin state, α and β electrons have an equal weight on both nuclei similar to the $1\sigma_g$ orbital in the absence of the Fermi contact perturbation. The only difference is that the electron of spin parallel to the nuclear spin, say, the β electron, becomes more diffuse. The difference in the polarization is, however, fairly small and consequently both electrons have a considerable overlap. This leads to a large correlation energy for the parallel nuclear-spin state. For the antiparallel nuclear-spin state, on the other hand, α and β electrons are differently polarized; each electron has a larger density on a proton of opposite spin. Thus, both electrons have a smaller overlap and thereby a smaller correlation energy. The difference in the correlation energies then makes a negative correction

$$(-|E_{\text{corr}}(\uparrow\uparrow)|) - (-|E_{\text{corr}}(\uparrow\downarrow)|) < 0$$

to the overestimated

$$E^{\text{HF}}(\uparrow\uparrow) - E^{\text{HF}}(\uparrow\downarrow),$$

which is ascribable to an unbalance in the left-off electron correlation in the parallel and antiparallel nuclear-spin states. The same argument applies also in cases other than that of directly bonded nuclei.

III. NUCLEAR MAGNETIC SHIELDING

When a magnetic field is applied to an atom or a molecule, currents proportional to the field are induced. These currents may interact with either the applied field or magnetic

nuclei in the system. The former interaction can be observed as the magnetizability and the latter as the nuclear magnetic shielding. Both of them are due to the same induced current as a linear response to the applied field, only their dependences on the distance from the gauge origin being different. Inclusion of a major portion of electron correlation effects on such linear responses is required for the theory to have any predictability. However, the situation with respect to correlation corrections in magnetic cases is much less satisfactory than in electric cases.

Here, we present a systematic study (14) of correlation effects on the nuclear magnetic shielding for the HF molecule as a prototype example of simple diatomic molecules, using MBPT. The Hartree-Fock potential in the absence of the external field is used for generating one-electron states. The result is compared with CHF calculations to assess the validity of the latter approach. The results are summarized in Table 2 (15). First, we briefly touch upon the diamagnetic term and then concentrate on the paramagnetic term.

The CHF method gives no correction to the diamagnetic term, so the second-order correlation correction to it calculated by MBPT is included in the table. It can be seen that the correction is quite small and consequently its contribution to the total shielding is negligible.

The CHF fluorine shielding value agrees satisfactorily with experiment and appears nearly gauge invariant. On the other hand, the proton shielding value shows poor gauge dependence. The values with the gauge origin at the F nucleus may probably be preferable, since F is closer to the centroid of the electronic charge. The apparent good gauge dependence of the fluorine shielding may be due to a fortuitous cancellation, but the details are not fully appreciated yet.

In order to analyze the effects of electron correlation and assess the validity of the CHF approach to nuclear magnetic shielding, we shall examine the MBPT results. The first-order correlation correction corresponds to the first-iterated correction by the CHF method. As exemplified by the perpendicular component of the paramagnetic fluorine shielding, the particle-hole ladder type diagram makes a dominant contribution of -29.00 ppm. The dominance of ladder-type diagrams for nuclear magnetic shielding continues to hold for higher orders. Diagrams contained in the CHF iteration were termed the

apparent correlation effects by Sadlej (9).

Non-CHF diagrams, which were termed the true correlation effects by Sadlej (9), first appear in second order. Among the second-order non-CHF diagrams, each diagram having two one-electron operators attached to the same loop is large. In magnitude, some of them being even larger than ladder-type diagrams. Those diagrams having large values individually are nearly cancelled by one another's counterpart for $F_{\sigma\perp}P$. Although patterns of cancellation are somewhat different depending upon the molecules, it still holds good that the second-order non-CHF diagrams make an inappreciable contribution to nuclear magnetic shielding. Since the nature of operators other than the Fermi contact interaction in nuclear spin-spin coupling is similar to that of the nuclear magnetic shielding operators, non-CHF diagrams are expected to make only a trivial contribution also to nuclear-spin coupling except the Fermi contact term.

The fluorine chemical shift between HF and F_2 is a classic problem of the chemical shift first qualitatively discussed 30 years ago (16). We analyze the problem here in terms of diagonal ladder diagrams. In HF, major contributions to the paramagnetic term come from the interactions of the highest occupied 1π orbital with the 4σ and 5σ orbitals, which correspond to the counterclockwise currents of the π orbital around the angular node precisely at the fluorine nucleus. Excitation from the 3σ orbital to the 2π , 3π , and 6π orbitals gives rise to clockwise currents around F, leading to the diamagnetic term. The above diagrammatic picture is too simplified in the sense that the large off-diagonal contributions are neglected, but may still help our understanding. In the case of F_2 , the $1\pi_u-3\sigma_u$ pair makes a conspicuous paramagnetic contribution, corresponding to the paramagnetic currents in the simple atomic model (16).

IV. CONCLUSIONS

Effects of electron correlation on the nuclear magnetic shielding and the nuclear spin-spin coupling have been analyzed by comparing MBPT and CHF results. MBPT expansion through second order in electron correlation with reference to the Hartree-Fock Hamiltonian in the absence of the external fields shows that diagrams not included by the CHF method make only a small net contribution for these properties except the Fermi contact nuclear-spin coupling. Therefore, the CHF method is

expected to provide a viable and reliable tool for calculating them. However, it generally overestimates the Fermi contact term. The overestimate originating from the unbalanced incorporation of electron correlation can be efficiently and systematically corrected by the FF MBPT approach.

ACKNOWLEDGMENTS

I would like to acknowledge the indispensable cooperation of the coworkers both cited and not cited in the references. The services of the Computer Centers at Kyoto University and the Institute for Molecular Science are gratefully appreciated.

REFERENCES

- ¹K. A. Brueckner, *Phys. Rev.* **97**, 1353(1955).
- ²J. Goldstone, *Proc. R. Soc. (London) Ser. A* **239**, 267(1957).
- ³N. F. Ramsey, *Phys. Rev.* **91**, 303(1953).
- ⁴J. A. Pople and D. P. Santry, *Mol. Phys.* **9**, 311(1964).
- ⁵Y. Kato and A. Saika, *J. Chem. Phys.* **46**, 1975(1967).
- ⁶J. M. Schulman and D. M. Kaufman, *J. Chem. Phys.* **53**, 477(1970).
- ⁷T. Itagaki and A. Saika, *J. Chem. Phys.* **71**, 4620(1979).
- ⁸R. J. Bartlett and G. D. Purvis III, *Phys. Rev. A* **20** 1313(1979).
- ⁹A. J. Sadlej, *J. Chem. Phys.* **75**, 320(1981).
- ¹⁰R. McWeeny, *Phys. Rev.* **126**, 1028(1961); R. M. Stevens, M. Pitzer, and W. N. Lipscomb, *J. Chem. Phys.* **38**, 550(1963).
- ¹¹M. Iwai and A. Saika, *Phys. Rev. A* **28**, 1924(1983).
- ¹²J. Kowalewski, A. Laaksonen, B. Roos, and P. Siegbahn, *J. Chem. Phys.* **71**, 2896(1979).
- ¹³W. T. Raynes and N. Danteli, *Chem. Phys. Lett.* **94**, 558(1983) gives 40.6 Hz for the coupling at equilibrium. If we simply subtract 0.6 Hz for the noncontact terms estimated by J. M. Schulman and W. S. Lee, *J. Chem. Phys.* **73**, 1360(1980), we obtain 40.0 Hz for the Fermi contact term at equilibrium.
- ¹⁴M. Iwai and A. Saika, *J. Chem. Phys.* **77**, 1951(1982).
- ¹⁵Reprinted from part of Table II in ref. 14 by permission of the American Institute of Physics.
- ¹⁶A. Saika and C. P. Slichter, *J. Chem. Phys.* **22**, 26(1954).

RECENT NUCLEAR MAGNETIC RESONANCE INVESTIGATIONS IN ROMANIA
-A Felix Bloch Commemorative Lecture*-

Ioan Ursu

*National Center for Physics
P.O. Box 5206
Magurele-Bucharest, Romania*

If one accepts science as a part of frontier life, that is — as strife and struggle, there seems to be no better and dignified way of paying tribute to pathfinders than talking of plain hard work. At four decades since its discovery, nuclear magnetic resonance spectroscopy is an almost basic tool, a most remarkable one, exceedingly pervasive by now in an astounding variety of fields. It is, perhaps, only its belonging to the high technology realm that hinders an even wider and quicker dissemination of its power in all the many areas of human endeavour where "knowing why" is an irreducible prerequisite of "knowing how."

The discovery by Bloch of magnetic resonance phenomena in 1945 had indeed a great impact on various branches of science like physics, chemistry, life sciences, etc. Today its applications range from fundamental research in physics (materials science, solid state structure, phase transitions, very low temperatures, etc., chemistry (molecular structure, chemical reactions), biology-biophysics (water and ionic diffusion across membranes, drug-membrane interactions, water ordering in biological systems) to many applied fields like the chemical industry — where it became a routine quality control technique, or agriculture (determination of content of oil, water or proteins in seeds and other products) or geology and oil technology (magnetometry, among others). Today one witnesses the penetration of NMR into clinical investigations, as a most fascinating and sophisticated development: the NMR imaging of the depths of the human body.

A glimpse at the whole development of the NMR field can bring us to better understand and properly appreciate the importance of Bloch's brilliant discovery that, in his original papers of

1946, he had called "nuclear induction." It should be stressed that many of the actual NMR achievements that followed over the years were proposed and predicted by Felix Bloch in these papers.

At the beginning of his research activity (Leipzig), he started as a theorist, developing the theory of electron conduction in metals. Later, in the U.S.A., he entered experimental physics, proposing a novel method for measuring the neutron magnetic moment (1936); the relevant experiment was carried out successfully in 1939. In fact, the ideas propelling this experiment induced him into believing that the change in orientation of nuclear magnetic moments should yield a measureable voltage signal in bulk matter. He proved it to be a fact after the war (1945) (1), when the radiofrequency techniques had been brought to an advanced level. In 1946 he published the extended paper on the theory of "nuclear induction" (2), followed by a second one (3), presenting the experimental evidence of the phenomenon.

Typically, Bloch acted as a brilliant theorist who had to grow as an ingenious experimentalist. It is interesting to note that this quality of the "father" of NMR eventually developed into a distinctive pattern of all subsequent important developments in NMR, related to such concepts and methods as spin temperatures, relaxation in solids, slow motions, double resonances, spin echos, multiple pulses, etc.; those who developed theories were eager to, and decisively instrumental in implementing the appropriate experimental approach to both prove them and put them to work.

Back to Bloch's first theoretical paper on NMR, it must be pointed out that, beside giving solution to the equations of the magnetization motion in the presence of the radiofrequency fields, he also recognized the importance of "thermal agitation" and "internuclear interaction" in shaping the NMR signal. In this context he gave a correct qualitative interpretation of the nuclear spin-lattice and spin-spin relaxation times T_1 and T_2 respectively, as characterizing

*Delivered at the Felix Bloch Commemorative Session of the Romanian National Committee for Physics on 17 March 1984, at the National Center for Physics, Magurele-Bucuresti.

the response of the spin system reaching thermal equilibrium. He also devised the phenomenological equations describing the change of magnetization due to relaxation processes. These equations, combined with the equation of motion of nuclear magnetization under the influence of magnetic fields lead to the famous Bloch equations. It is worth noting that such equations proved to describe a wider range of phenomena than NMR. The quantum mechanics calculation of the relaxation process in liquids fully proved the correctness of the relaxation equations introduced by Bloch (in solids only the "longitudinal" equation was confirmed). These theories revealed the connection between T_1 , T_2 and the molecular motion in liquids and solids.

Determination of the temperature dependence of T_1 and T_2 became a powerful method to investigate molecular motion, thus confirming a prediction of Bloch's in his theoretical paper (1946). It should be noted that, in its conclusive lines, this paper hinted also at other important future developments in NMR, such as access to very low temperatures, the advent of new high precision magnetometers, or the use of paramagnetic impurities.

Bloch made an early observation that the paramagnetic impurities "in small percentage essentially act as catalysts and do not otherwise affect the nucleus under consideration." The full application of this idea, with most positive results, was only recently recognized when the paramagnetic impurities were used to label the intracellular or extracellular water in biological systems. This method, successfully applied in the case of erythrocyte membranes and phospholipid vesicle membrane, made possible the NMR investigation of water transport across the biological membranes and permitted the study of drug effects on membrane permeability or the change of permeability due to pathological alterations of the cells. The dynamic polarization of nuclei — that stands today as a valuable asset in both theoretical and experimental nuclear physics — is also worth highlighting in the fallout of the original recognition by Bloch of the potential importance of paramagnetic ions in a sample.

Today NMR — and all kinds of magnetic resonance techniques for that matter — is an established field, proud of its identity and prominence. Existence of the International Society of Magnetic Resonance — the ISMAR, and of AMPERE — the Atoms et Molecules par Etudes Radio-Electriques — ring the sound of a worldwide community and interaction. Our International Summer School of Magnetic Resonance in Mangalia, Romania (1969), that has grown since

into a series of regular AMPERE schools and colloques held in various countries over the Continent, and also the XVIth Congress AMPERE held in Bucharest (1970) — the first Colloque of this organization to be upgraded to a Congress — convincingly prove its importance.

The beginning of research on magnetic resonance phenomena in our country dates back to 1956 - 1957. A major impetus to this work came from meeting the discoverer of NMR in Princeton during my stay there. At this commemoration of Felix Bloch I must say that I owe much of my enduring involvement with magnetic resonance to meeting him in Princeton, thus getting first-hand insight into the matter, a flavor of how much can be done on it and an opening to how it can be done. His research style and work helped inspire us to establish in this country an active school of magnetic resonance, now endowed with modern labs and gathering fine experts in Bucharest, Cluj, Iassy, Timisoara, not to speak of the commercial facilities available for an increasing number of customers in industry, agriculture, health care, over the country.

It is with all of this in mind that I would like to speak now of some of our current work. I have neither the intention to give here a comprehensive historical appraisal of all our work over the years, nor am I able to cover the whole range of topics and projects under way. Compiling an exhaustive list of references would hardly help the scope of this commemorative lecture either; such lists are available from several review papers and books (4-7), most of them related to our work in Bucharest and Cluj. Because of my belief that NMR is now an established science, I will describe only two topics that I find both relevant and that we are *now* working on. These are (i) nuclear spin-spin and spin-lattice relaxation in UF_6 — an isotope effect investigation; and (ii) nuclear spin-spin and spin-lattice relaxation in 1-X-adamantanes — the molecular dynamics in the vicinity of order-disorder phase transitions.

We shall be dealing, therefore, mainly with results of nuclear spin-lattice relaxation experiments on some molecular crystals. Recall that, as in many other fields, Bloch's and Purcell's ideas regarding the relaxation process in solids have found application in the investigation of molecular motion in this class of compounds. The NMR experiments were essential to determine the motional properties of the plastic phase in molecular crystals and helped in the understanding of the order-disorder phase transition in such compounds.

More recently, interest in such NMR

investigations has increased once high resolution-very cold neutron experiments proved feasible and the theory of structural phase transition was developed for molecular crystals. This trend allowed a comparison of NMR and cold neutron data and a better understanding of the mechanism of molecular motion in different phases of molecular crystals.

NUCLEAR SPIN-SPIN AND SPIN-LATTICE RELAXATION IN UF_6 - AN ISOTROPIC EFFECT INVESTIGATION

Utilization of NMR techniques in order to perform isotopic assays of ^{235}U in the various chemical environments that accompany this relevant isotope all along its intricate path in the nuclear industries has long been seen as a challenge worth study in our labs in Bucharest and Cluj (8-14). The work was naturally targeted on UF_6 - a compound of great importance in the nuclear fuel cycle (15).

Addressing head-on this task can hardly yield results of any practical value: direct detection of ^{235}U by NMR is difficult indeed, due to the low sensitivity of this nucleus - 2×10^{-5} relative to protons at equal magnetic field; it would thus require very high fields and a large data acquisition capability. Direct detection would then appear as a time-consuming, infrastructure-intensive method - a fact that can make it prohibitive for current applications in nuclear technology.

To circumvent this difficulty, we proposed an indirect method that uses the detection of ^{19}F . The presence of ^{235}U is detected through recording changes in the ^{19}F spin-spin relaxation time T_2 that is due to ^{19}F - ^{235}U indirect-scalar interactions. Such interactions, modulated by the strong quadrupolar relaxation of ^{235}U leads to an additional relaxation mechanism for ^{19}F . One can expect the effect is stronger in the liquid phase, where the dipolar interactions and the chemical shift anisotropy are reduced.

Samples and Experimental Procedure

Samples of uranium hexafluoride with different degrees of ^{235}U enrichment ranging from $I = 0.005$ to $I = 0.93$ were obtained from two different sources.

Two sets of samples were supplied by British Nuclear Fuels Ltd. at nuclear purity and one set was prepared in our laboratory. The preparation methods were different for these two sources (10). For the home-made set the procedure kept the concentration of paramagnetic impurities at

the lowest possible level, in order to minimize their effects on T_2 of ^{19}F . The use of three sets of samples allowed us to set an upper limit of the errors introduced by paramagnetic impurities.

The NMR equipment used in this experiment was a variable frequency Bruker pulsed spectrometer (SXP 100). The same spectrometer was used in the FT mode, in order to obtain high resolution spectra of ^{19}F .

The spin-lattice relaxation times T_{1Z} and T_{1D} were measured with the usual sequences (16-21): $[(\pi/2)_0 - \tau - (\pi/2)_0]$ and $[(\pi/2)_0 - T_2 - (\pi/4)_{90} - \tau - (\pi/4)_{90}]$ - respectively. In the case of liquid samples T_2 was measured using the CPMG sequence (16).

Results and Discussion

The isotope effects are clearly observed in the liquid phase of UF_6 . Figure 1 shows the dependence of T_2 on ^{235}U enrichment at differ-

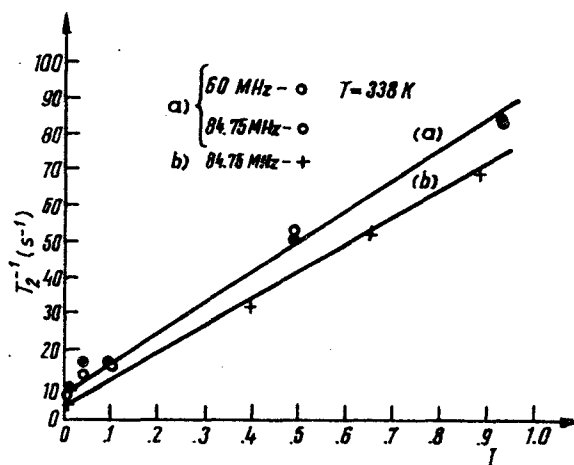


Figure 1. ^{19}F transverse nuclear magnetic relaxation rate (T_2^{-1}) versus ^{235}U enrichment in liquid UF_6 at $T = 338$ K: a) the BMF -samples measured at $H_0 = 60$ MHz and 84.75 MHz; b) the home-made samples measured at $H_0 = 84.75$ MHz.

ent temperatures. It should be noted that the relaxation rate T_2^{-1} at the highest enrichment is about 13 times shorter than that at natural abundance of ^{235}U . The experimental points lie on straight lines, indicating that the spin-spin relaxation time T_2 of ^{19}F depends linearly on

the ^{235}U enrichment. This dependence was found in all three sets of samples used in the experiment. The relaxation times T_2 measured at two different frequencies were identical within the limit of experimental errors.

These results were confirmed through a complementary approach, by high resolution ^{19}F spectra in liquid UF_6 . The spectra show a single line with no fine structure for all samples (Figure

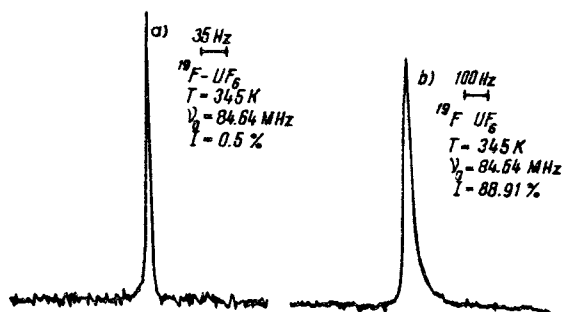


Figure 2. ^{19}F high resolution NMR spectra in liquid UF_6 recorded at $H_0 = 84.63$ MHz and $T = 345$ K. Spectra (a) and (b) correspond to the samples with the enrichments $I = 0.007$ and $I = 0.84$, respectively.

2). The presence of the ^{235}U isotope induces only a strong line broadening. At a high enrichment the linewidth reaches a value of 36 Hz, i.e. an increase by a factor of 9 as compared to the linewidth of the natural abundance samples (≈ 4 Hz). The spin-lattice relaxation time T_1 shows a weak dependence on I (Figure 3a, b) and no significant frequency dependence, even in the case of the highest enrichment.

The spin-lattice relaxation of the Zeeman reservoir (T_{1Z}) and of the dipolar reservoir (T_{1D}) were measured as a function of temperature and enrichment in the solid phase of UF_6 (Figure 4a, b). No isotope effect on the relaxation rates was detected. The temperature dependence and the activation energy ($E_a = 0.71$ eV) found in the solid phase of UF_6 are in agreement with previous results obtained on natural UF_6 (22).

Relaxation Mechanisms

Previous investigations of UF_6 (at natural abundance of ^{235}U) (23) have determined that

the main relaxation mechanism in the liquid phase of this compound is due to the spin-rotational interaction (SR), whereas in the solid phase the chemical shift anisotropy (CS) provides the dominant mechanism. In both cases the dipole-dipole interaction (DD) provides only a negligible contribution.

In these studies the F-U interactions were not taken into account, since ^{235}U was at very low concentration and ^{238}U has no magnetic moment.

When ^{238}U is replaced by ^{235}U , the nuclear ^{19}F - ^{235}U indirect-scalar interactions become important and they may create a new relaxation path for ^{19}F .

For the relaxation rates T_L^{-1} ($L = 1, 2$) of ^{19}F -nuclei in liquid UF_6 we may consider the following equation:

$$T_L^{-1} = (T_L^{-1})_{\text{SR}} + (T_L^{-1})_{\text{CS}} + (T_L^{-1})_{\text{DD}} + (T_L^{-1})_{\text{Q}}$$

$(T_L^{-1})_{\text{Q}}$ accounts for the quadrupole relaxation process and is due to the large quadrupole moment of ^{235}U .

The first three contributions do not explain the enrichment effect and should be discarded on the following grounds:

- the theoretical predictions for the frequency and temperature dependence of the relaxation rates T_1^{-1} and T_2^{-1} (8, 23) as determined by the chemical shift anisotropy or the dipole-dipole interactions are contrary to the experimental data;
- the relaxation through spin-rotational interaction might explain the observed temperature and frequency dependence. However, since the change in the inertial momentum of the UF_6 molecule is negligible when ^{235}U replaces ^{238}U , the relaxation rate due to this mechanism should not change significantly and, therefore, it cannot explain the enrichment dependence.

Since the quadrupole momentum of ^{235}U is relatively large, any distortion of the UF_6 molecule leads to a large quadrupole interaction (24). Reorientation of the UF_6 molecules provides a very strong relaxation mechanism for the ^{235}U nuclei through their quadrupole interaction with the electric field gradients within the molecules. If τ_q is the appropriate correlation time for the reorientation, $e^2 q Q / \hbar$ is the quadrupole coupling constant and η is the asymmetry parameter, then the relaxation times of ^{235}U -nuclei in the extreme narrowing limit are given by (25):

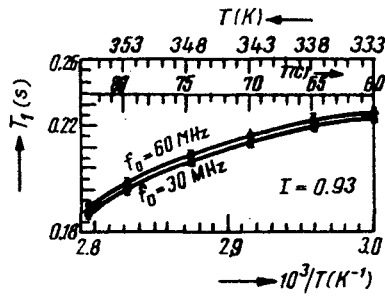
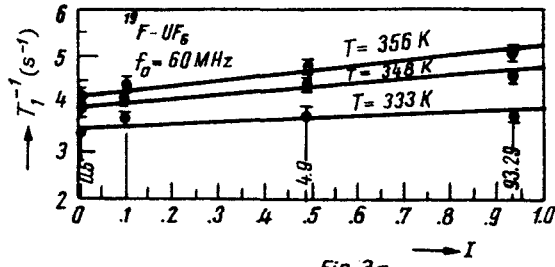


Fig. 3 b

Figure 3. a) Longitudinal relaxation rate T_1^{-1} of ^{19}F in UF_6 vs. enrichment at three different temperatures and b) T_1^{-1} vs. T^{-1} at two different measuring frequencies for the highest enrichment.

$$T_{LQ}^{-1} = (1/98)(1+\eta^2/3)(eqQ/h)^2\tau_q.$$

The rapid relaxation of the uranium nuclei induces rapidly fluctuating magnetic fields at the fluorine nuclei sites through the indirect-scalar coupling JIS ; this mechanism has been described in (25) as a type II scalar relaxation process. The contributions to the ^{19}F relaxation rates are:

$$(T_1^{-1})_Q = (21/2)J^2 \frac{T_{1U}}{1+(\omega_F - \omega_U)^2 T_{1U}^2} \quad (1)$$

$$(T_2^{-1})_Q =$$

$$(21/4)J^2 \left[T_{1U} + \frac{T_{1U}}{1+(\omega_F - \omega_U)^2 T_{1U}^2} \right] \quad (2)$$

As $\omega_U \ll \omega_F = 5 \times 10^8 \text{ s}^{-1}$ and T_{1U} is presumably longer than 10^{-8} s , the relation $(\omega_F - \omega_U)^2 T_{1U}^2 \gg 1$ holds and eqns. 1 and 2

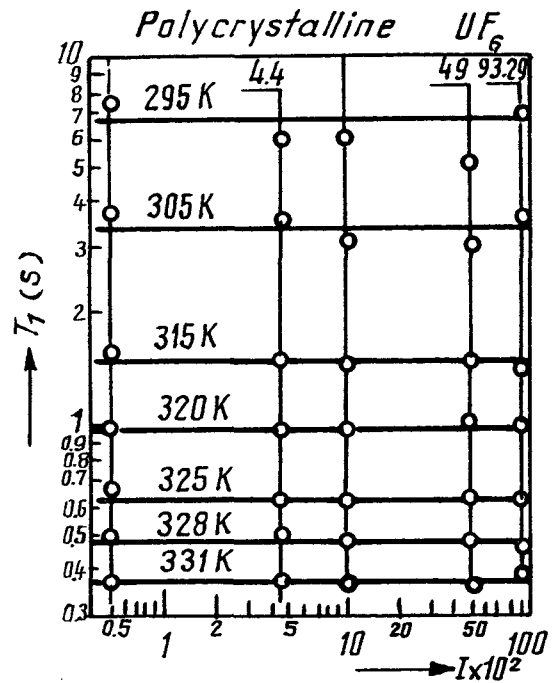


Fig. 4 a

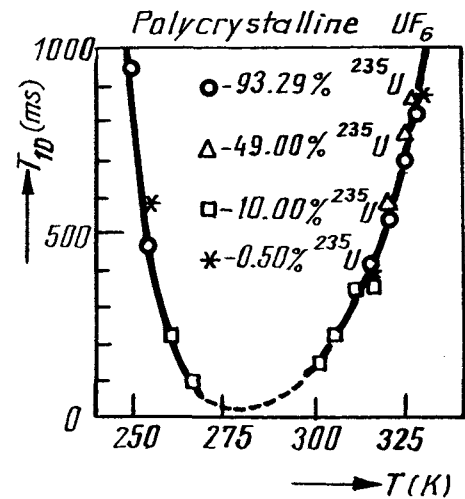


Fig. 4 b

Figure 4. a) ^{19}F longitudinal relaxation time T_1 in solid UF_6 at 60 MHz and b) ^{19}F high field dipolar relaxation in solid UF_6 at 60 MHz as a function of temperature.

have the approximate form:

$$(T_1^{-1})_Q = 0, \quad (3)$$

$$(T_2^{-1})_Q = (1029/2)J^2[(1+\eta^2/3)(eqQ/h)^2]\tau_q^{-1}$$

Eqn. 3 explains why T_1^{-1} does not depend on the presence of ^{235}U while T_2^{-1} depends on it via $(T_2^{-1})_Q$ contribution. The temperature dependence predicted by eqn. 3 is correct as long as the usual assumption $\tau_q = \tau_q^0 \exp(E_a/kT)$ is valid. One should note that in the limiting cases $I = 0$ and $I = 1$, the relaxation rates are $(T_L^{-1})_0 = (T_L^{-1})_{\text{SR}}$ and $(T_L^{-1})_1 = (T_L^{-1})_{\text{SR}} + (T_L^{-1})_Q$. These values are obtained from Figure 1 by extrapolation:

$$(T_2^{-1})_0 = 4.2 \text{ s}^{-1} \quad (T_2^{-1})_1 = 78.4 \text{ s}^{-1}$$

For intermediate enrichments $I = x$, xN molecules will relax with $(T_L^{-1})_1$ and the others $(1-x)N$ with $(T_L^{-1})_0$. In this case, if there is no intermolecular exchange the decay of ^{19}F -transverse magnetization should be the sum of two time-dependent exponentials with decay constants $(T_2^{-1})_0$ and $(T_2^{-1})_1$ and the FT spectra should be the superposition of two lines with different line broadenings.

For all values of I we have observed only a single exponential decay and FT spectra do not reveal the superposition of two lines. Consequently, we concluded that in the liquid phase of UF_6 an intermolecular mechanism spreading magnetic information over the whole nuclear magnetic system should exist. In this case one observes a single exponential decay (a single line in the FT spectrum) with an effective relaxation rate:

$$(T_2^{-1})_{\text{eff}} = (1-I)(T_2^{-1})_{\text{SR}} + I(T_2^{-1})_Q \quad (4)$$

Eqn. 4 gives a reasonable explanation of the linear dependence of the observed relaxation rate T_2^{-1} on the ^{235}U enrichment.

Since we found that $(T_2^{-1})_{\text{SR}} \ll (T_2^{-1})_Q$ from eqn. 4, it follows that for a relatively high enrichment ($I \geq 0.8$),

$$(T_2^{-1})_{\text{eff}} \approx I(T_2^{-1})_Q \sim \tau_q$$

The semilogarithmic plot of $(T_2^{-1})_{\text{eff}}$ against T^{-1} at $I = 0.89$ is linear (Figure 5), with an activation energy $E_a = 0.072 \text{ eV}$ — a value close to that found in natural UF_6 (23) using T_1 measurements. This indicates that the quadrupole relaxation of ^{235}U in liquid phase of UF_6 involves the same type of molecular collisions

(i.e. the same correlation time) as the spin-rotation

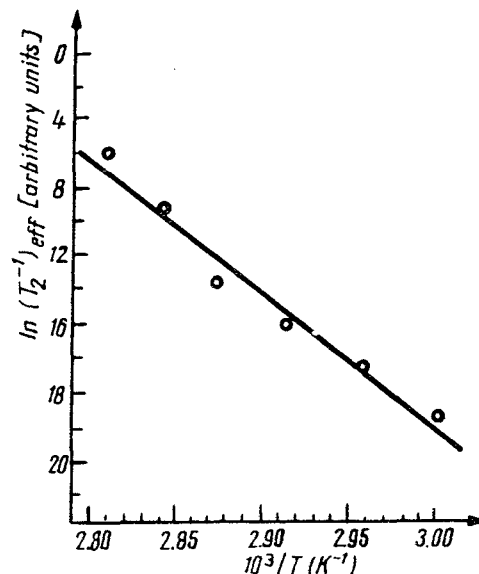


Figure 5. Semilogarithmic plot of the $(T_2^{-1})_{\text{eff}}$ relaxation rate versus the reciprocal temperature.

tional mechanism.

The quadrupolar mechanism assumed above is confirmed by the high resolution spectra. The nuclear scalar coupling ^{19}F - ^{235}U should lead to a multiplet structure. In the case of a sample with $I = 0.89$ the ^{19}F spectrum should reveal a central line corresponding to molecules with ^{235}U ($S = 0$) and eight symmetrical satellites of about the same intensity corresponding to the molecule with ^{235}U ($S = 7/2$). Experimentally this pattern could not be detected, since the rapid fluctuation of ^{235}U -magnetic moment induced by the strong quadrupolar relaxation leads to the collapse of the multiplet structure, the emerging spectrum being a single broad line (Figure 2).

We note that in similar compounds, such as MoF_6 and WF_6 the coupling constant J is 47 Hz and 44 Hz respectively (26).

Assuming that J is about the same for UF_6 too, one can obtain the order of magnitude of T_{1U} from eqn. 3. Using $(T_2^{-1})_Q = 78 \text{ s}^{-1}$ and $J = 47 \text{ Hz}$ one obtains $T_{1U} \approx 6 \times 10^{-3} \text{ s}$ and $J T_{1U} = 0.3 < 1$.

The absence of a narrow line due to the ^{235}U -molecules suggests again the existence of a

mechanism to convey the magnetic information between ^{235}U and ^{235}U molecules. Such a mechanism may be generated either by an intermolecular indirect-scalar interaction F-U, or by an intermolecular atomic exchange. The latter possibility is suggested by the fact that it was observed in compounds of the form UR_4 (27).

The relaxation rates T_{1Z}^{-1} and T_{1D}^{-1} in the solid phase of UF_6 do not depend on ^{235}U isotopic abundance (9). The frequency and temperature dependence agrees with previous results on natural UF_6 (22). The dominant relaxation mechanism is due to the modulation of the anisotropic chemical shift by the molecular reorientations.

NMR spectra and longitudinal relaxation rates of ^{19}F isotope in saturated vapors of uranium hexafluoride have been measured as a function of ^{235}U enrichment, temperature and Larmor frequency (13, 14). The linewidth and T_1 values show a pronounced dependence on ^{235}U enrichment. The temperature dependence of longitudinal relaxation rate in saturated vapors of UF_6 (0.7% ^{235}U) is similar to that of other molecular compounds (SF_6 , WF_6 , MoF_6 , etc.). The " T_1^{-1}/ρ " law is not recognized in the case of enriched UF_6 . This fact, corroborated with the homogeneous broadening of ^{19}F absorption line in the high temperature domain, proves that ^{19}F - ^{235}U scalar coupling modulated by time-fluctuating quadrupole interaction of U is the dominate relaxation mechanism.

Summing up the results we arrive at the following conclusions:

- (a) the isotope effect, studied for the first time on UF_6 follows a linear dependence of the ^{19}F transverse relaxation rate on the U-enrichment in the liquid phase of UF_6 ; a similar isotope effect was observed in UF_6 saturated vapors;
- (b) the frequency and temperature dependence as well as the isotope effect can be explained by taking into account the selective contribution of the quadrupole relaxation of the ^{235}U nuclei to the relaxation rates T_1^{-1} and T_2^{-1} of F-nuclei.
- (c) this contribution is dominant over dipole-dipole and spin-rotational interactions for the transverse relaxation rate. Our data allowed a study of the temperature dependence of the quadrupolar contribution. The activation energy obtained from these data is very close to that found through T_1 measurements in natural UF_6 . Therefore, we conclude that the quadrupole relaxation of ^{235}U is generated by the same type of molecular collisions as in the case of the

spin-rotational mechanism;

(d) the high resolution spectra of ^{19}F show a collapse of the multiplet structure, thus confirming the assumed model;

(e) the existence of a single transverse relaxation rate at different enrichments suggests the presence in the liquid phase of an intermolecular mechanism that spreads magnetic information over the entire system of spins;

(f) under certain conditions (inter alia — availability of a small specialized spectrometer) the isotope effect may be used as a fast NMR method to determine the ^{235}U -isotopic abundance.

Our current work aims at (i) a fully developed theory of the isotope effect in NMR on gaseous UF_6 and (ii) establishing whether or not an isotope effect is identifiable in the solid phase of UF_6 ; to this end, the use of nuclear double resonance is envisaged. These topics, which are potentially relevant for monitoring production and safeguards in some nuclear industries, enjoy also the interest and support of the International Atomic Energy Agency.

NUCLEAR SPIN-SPIN AND SPIN-LATTICE RELAXATION IN 1-X-ADAMANTANES — MOLECULAR DYNAMICS IN THE VICINITY OF ORDER-DISORDER PHASE TRANSITION

The molecular crystals may be characterized by strong intramolecular forces of covalent nature and weak intermolecular forces. As a consequence, the molecules in crystals behave like rigid bodies executing librations and/or reorientation jumps against the weak intermolecular forces.

For many purposes these forces were successfully described by atom-atom interaction potentials of the exponential-6 type function (28).

Many molecular crystals undergo structural phase transitions. A special class of them are the molecular crystals with a plastic phase. This class has a very low fusion entropy indicating that the crystal has lost a part of ordering already before the melting point. The low fusion entropy is due to the fact that in the plastic phase the crystal is orientationally disordered (i.e. the molecules may occupy several orientations in the crystal).

At lower temperature the plastic crystals undergo a solid-solid phase transition with an orientational ordering of the molecules in the low temperature phase.

The studies of these phase transitions,

undertaken by different methods (X-ray, NMR, neutron diffraction) on some compounds considered as models (adamantane, NH_4Cl , CH_4) has established that the transition is of a dynamical type. Therefore the investigation of molecular motion above and below the transition temperature is essential in order to describe the mechanism of such transitions.

The great variety of results regarding the properties of plastic phases (e.g. entropy of transition, plastic range) in different compounds could not be reconciled through attempts to relate in an empirical way the measured quantities with the shape and symmetry of free molecules (29, 30). On the other hand, theoretical calculations have shown that such differences as those between adamantane ($\text{C}_{10}\text{H}_{16}$) and hexamethylenetetramine ($\text{C}_6\text{H}_{12}\text{N}_4$), molecules with similar structure and shape, could not be explained only by the variation of atom-atom potentials due to the replacement of C by N (28).

All of these results suggest that, in order to reveal the role played by different factors, a valuable approach is to study a group of similar compounds with slightly different molecular properties — like the molecular symmetry, electric dipole or the nature of the substituent.

In order to provide, through such an approach, some new information about the molecular motion and the order-disorder phase transition, we undertook an NMR investigation of 1-Cl, 1-Br, and 1- NH_2 -adamantanes (31, 32). Their molecular structures are closely related to each other and to that of adamantane (T_d symmetry). On the other hand, when scanning the above sequence of compounds one notes that some of their properties depart gradually from those of adamantane; thus

- (i) the symmetry is increasingly lower: the first two compounds (C_{3v} molecules) have only one C_3 -molecular symmetry axis, while the third compound has no molecular symmetry axis at all (Figure 6);
- (ii) the Van der Waals radii are increasingly larger, as well as the electric dipole;
- (iii) the atom-atom potential is gradually changed.

Experimental Results

The temperature dependence of the proton spin-spin relaxation time (T_2), of the spin-lattice relaxation of the Zeeman reservoir (T_{1Z}) and of the dipolar reservoir (T_{1D}) on powder samples are shown in Figures 7, 8a, b, c. T_2 was defined as the time when the FID signals decay to half of their initial values.

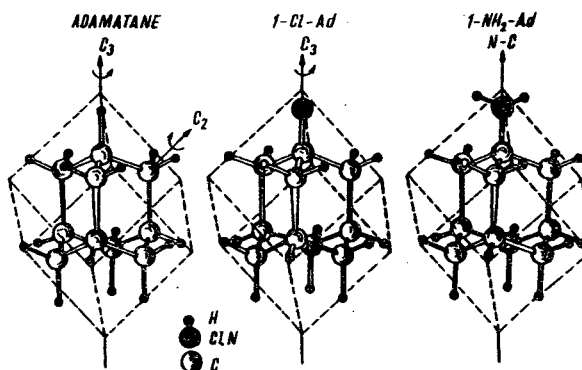


Figure 6. Molecules of adamantane, 1-Cl, 1-Br and 1- NH_2 -adamantanes.

The main results may be summarized as follows:

1. In each of the three compounds there is a certain temperature T_I where T_2 becomes shorter, indicating a motional line-narrowing process. For 1-Cl and 1-Br-ad, these temperatures coincide with the reported transition temperatures determined by d.s.c. measurements (29).

2. At the same temperatures T_{1Z} has a strong anomalous decrease (or increase). Below these temperatures, the temperature dependence of T_{1Z} is of V-type (B.P.P), indicating a relaxation process due to an energy-activated molecular motion. The activation energy and the correlation times were obtained from a least squares fit of experimental data (solid lines in Figure 8) to the usual expression of T_{1Z} :

$$T_{1Z}^{-1} = C \left[\frac{\tau_c}{1 + (\omega_0 \tau_c)^2} + \frac{4\tau_c}{1 + 4(\omega_0 \tau_c)^2} \right] = C f(\tau_c) \quad (5)$$

and $\tau_c = \tau_0 \exp(E_a/kT)$.

The same procedure was used in the high temperature phase (α -phase) of 1-Cl-ad which displays a T_{1Z} minimum in this phase too. 1-Br-ad and 1- NH_2 -ad do not have such a minimum in the α -phase and no independent information about τ_0 and C could be obtained if one

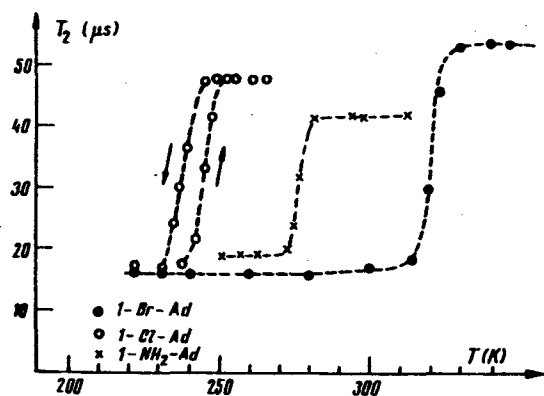


Figure 7. Temperature dependence of T_2 .

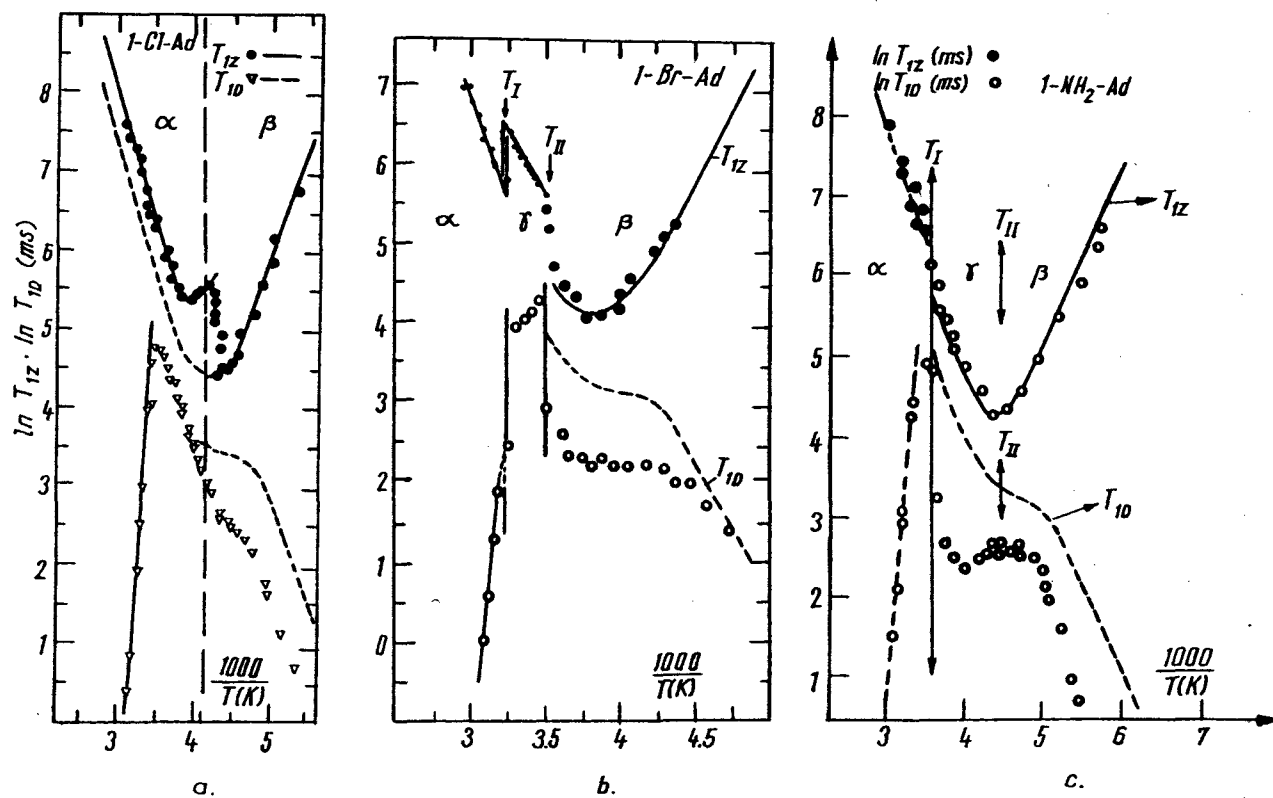


Figure 8. Semilogarithmic plot of T_{1X} (●) and T_{1D} (○) versus T^{-1} . The solid and dashed lines are a least squares fit of eqns. 5 and 6 to experimental data.

TABLE 1

	Ordered β -phase		Disordered α -phase					
	τ_o (s)	E_a	$d^*(s)$	$d_o(s)$	E_a	E_D	$T_m - T_I$	Γ
1-Br-Ad.	$8 \cdot 10^{-16}$	7.4	$7 \cdot 10^{-3}$	10^{-21}	8.5	27	86	3.17
1-Cl-Ad.	$8.3 \cdot 10^{-15}$	6.85	$10 \cdot 10^{-3}$	$10^{-21.8}$	6.85	29	198.3	4.23
1-NH ₂ -Ad.	$6.9 \cdot 10^{-15}$	5.4	$27 \cdot 10^{-3}$	$2 \cdot 10^{-18}$	5	23	209	4.6
Adamantane	10^{-15}	6.5	$1.6 \cdot 10^4$	$1.6 \cdot 10^{-21}$	3	36	331.4	12

* Calculated at $T = 312$ K with p of a f.c.c. structure.

Fusion temperatures T_m taken from Ref. 29 and adamantane data from Ref. 35

E_a and E_D are given in Kcal/mol.

TABLE 2

	$(K_n)_{ij}$	$(K_3)_{ij}$	$K_n \sim \sum_{i < j} (K_n)_{ij}/S$	$K_3 \sim \sum_{i < j} (K_3)_{ij}/S$
A	$(1 - 3\cos^2 \theta_{ij})^2 / 4r_{ij}^6$	$(\frac{1}{8}\sin^4 \theta_{ij} + \frac{1}{4}\sin^2 \theta_{ij}) / r_{ij}^6$	0.3	0.185
B	$(1 - 3\cos^2 \theta_{ij})^2 / 4r_{ij}^6$	$\frac{1}{8}\sin^4 \theta_{ij} / r_{ij}^6$	0.3	0.555
C	$(1 - 3\cos^2 \theta_{ij})^2 / 4r_{ij}^6$	$(\frac{1}{4}\sin^4 \theta_{ij} + \frac{8}{3}\sin^2 \theta_{ij}) / r_{ij}^6$	0.3	0.12
D	$(1 - 3\cos^2 \theta_{ij})^2 / 4r_{ij}^6$	$(\frac{1}{8}\sin^4 \theta_{ij} + \frac{7}{72}(1 - 3\cos^2 \theta_{ij})^2 + \frac{1}{18}) / r_{ij}^6$	0.3	0.222
E	$K_{ij}(\text{isotropic}) = r_{ij}^{-6}$		$K(\text{iso}) \sim \sum_{i < j} K_{ij}(\text{iso})/S = 1$	
C ₃	$K_{ij}(C_3) = 1 - \frac{1}{4}(1 - 3\cos^2 \theta_{ij})^2 / r_{ij}^6$		$K(C_3) \sim \sum_{i < j} K_{ij}(C_3)/S = 0.7$	

θ_{ij} is the angle between C_3 -symmetry axis of molecule and the vector r_{ij} connecting the spins i and j .

relies only on T_1 data.

3. For all three compounds, T_{1D} in the high temperature phase is much shorter than T_{1Z} and has a reversed temperature dependence. The low values of T_{1D} and the high activation energy E_D indicate that the relaxation mechanism of the dipolar reservoir in the α -phase is due to a slow-motion process.

Below the phase transition temperature T_I the dipolar relaxation time T_{1D} has a totally different temperature dependence, one that is much more reflective of a fast molecular reorientation mechanism. If the dipolar reservoir is relaxed by the same molecular motion as the Zeeman reservoir, then an approximate expression of T_{1D} is given by (33):

$$T_{1Z}^{-1} = C[\tau_c + \frac{3\tau_c}{1 + (\omega_0\tau_c)^2} + \frac{6\tau_c}{1 + 4(\omega_0\tau_c)^2}] \quad (6)$$

The relaxation times T_{1D} , given by eqn. 6, are shown as dashed lines in the γ -phases. T_{1D} was calculated using E_a , τ_0 and C obtained from T_{1Z} data. The experimental values are systematically lower than the values predicted by eqn 6, even for low temperatures.

4. The phase transition at T_I is accompanied by thermal hysteresis of the relaxation times in the case of 1-Cl, and 1-Br-ad. There is no such effect in the case of 1-NH₂-ad.

5. The NMR relaxation data clearly show that there is a second phase transition in 1-Br-ad at $T_{II} = 253$ K. There is also evidence that a second transition might take place at $T_{II} = 217$ K in 1-NH₂-ad too. The phases between T_I and T_{II} were labeled at α -phase.

Some of the experimental results are given in Table 1.

Discussion

The high values of T_2 in α -phases of all these compounds correspond to a motional line-narrowing process. If we assume a Gaussian line, the values of T_2 can be exactly related to the second moment M_2 . On this assumption for 1-Cl, 1-Br and 1-NH₂-ad, we obtained for $M_2(\alpha)$ the values 0.88, 0.72, and 1.09 G² respectively.

The low values of M_2 (the expected values of the rigid second moment is about $M_{2R} \approx 20$ G²) in α -phases can be explained only by either a isotropic reorientation of the molecule, or by a jump reorientation about several axes. The increase of M_2 (decrease of T_2) below T_I ($M_2(\beta) = 7.0, 7.5, 5.4$ G²) reflects a restricted molecular motion in (α)-phases. The number of

orientations the molecule may take in the β -phase decreases, and the second moment is no longer averaged to zero (the intramolecular part of it). Nevertheless, the motion in the β -phase produces a significant reduction in the second moment. The values of T_2 and its temperature dependence above and below T_I prove that the molecules lose a part of their degree of orientation as the α - β transition takes place — which agrees with the high entropy of transition found by d.s.c. measurements (29) in 1-Cl and 1-Br-ad.

Usually, for molecules which possess a symmetry axis (e.g. the adamantane or NH₄Cl) the reorientation takes place about these axes and the molecule fluctuates between *indistinguishable* orientations, even at a very low temperature. In the case of 1-Cl-ad and 1-Br-ad the molecule (C_{3v}) has a C_3 -symmetry axis. The reorientation about this axis leads only to a partial reduction in the second moment. The strong decrease of M_2 in the β -phase can be explained by the set-in of a new molecular motion that, alone or combined with the reorientation about the C_3 -axis, strongly reduces the effective dipolar interactions. Since the molecule has no other symmetry axes, we assume the new motion that sets-in in the α -phase to be a jump reorientation of the molecule between several *distinguishable* orientations (the C_3 -axis changes its orientation in time). On the other hand, the gap between T_{1Z} above and below T_I in 1-Cl-ad can be explained only by a decrease (a factor of 4) in the α -phase, of the the parameter C in eqn. 5.

In order to explain these results we have proposed (32) the following model:

(a) the molecule performs two independent jump reorientations: one about the C_3 -axis with correlation time τ_3 , the other between n distinguishable orientations with correlation time τ_n ;

(b) the fluctuations between distinguishable orientations are allowed only in the α -phase. This reorientation process slows down in the vicinity of T_I and disappears in the α -phase leading to an orientational ordering in this phase.

Calculations of correlation functions according to this model lead to the following form of T_{1Z} (32):

$$T_{1Z}^{-1} = K_3 f(\tau_3) + K_n f(\tau_n) + K f(\tau)$$

with $\tau^{-1} = \tau_3^{-1} + \tau_n^{-1}$.

This model allowed us to test different possibilities of reorientation in the α -phase, on the assumption of a f.c.c. structure. The results are given in Table 2 for the following cases:

A. four reorientations parallel to (111, -111, 1-11, -1-11) directions;

- B. eight orientations parallel to the three-fold cubic axes;
- C. four orientations parallel to (111, -1-11, -11-1, 1-1-1);
- D. six orientations parallel to (100, -100, 010, 0-10, 001, 00-1)
- E. isotropic reorientation and C_3 — the case when the reorientation takes place only about a C_3 -symmetry axis of the molecule (the case of β -phases).

From all these possibilities, the most appropriate one to account for the experimental results in 1-Cl-ad is the case A, since assuming $\tau_n(\alpha) \ll \tau_3(\alpha)$ it gives

$$C(\beta) : C(\alpha) \approx K(C_3) : K_3 = 3.85$$

which is indeed very close to the reported value of 4. According to this result, the phase transition does not change essentially the C_3 -reorientations, but strongly changes τ_n (i.e. the intermolecular potential barrier which opposes the reorientations between distinguishable orientations).

Due to the high activation energy and the low values of T_{1D} at high temperatures, we are lead to identify the slow-motion process that relaxes the dipolar reservoir as being the translational diffusion of molecules.

The strong-collision theory (34) relates the mean time of molecular jumps to a vacancy τ_d to T_{1D} by

$$T_{1D}^{-1} = 2(1 - p)\tau_d^{-1}.$$

The temperature dependence of T_{1D} shows that τ_d is of the form $\tau_d = \tau_{d0} \exp(E_D/kT)$.

The values of τ_{d0} and E_D are given in Table 1 assuming a f.c.c. structure for all compounds ($p = 0.223$ (35)).

Finally, we mention that we did not try at present to give a full interpretation of T_{1D} results in β -phases. One reason is that the form of eqn. 6 of T_{1D} is valid only when the dipolar energy resides in intermolecular dipolar interaction (33). Nevertheless, in the γ -phase of 1-Br-ad this approximation is valid and we assumed it true below T_{II} , at least in its vicinity. The lower value of $(T_{1D})_{\text{exptl.}}$ is caused by an additional relaxation mechanism which we assume to be due to the dipolar proton-bromine coupling. Its contribution to the relaxation rate shown in Figure 9 was obtained as

$$(T_{1D}^{-1})_Q = (T_{1D}^{-1})_{\text{exptl}} - (T_{1D}^{-1})_{\text{rotation}}$$

Assuming a short relaxation time for the

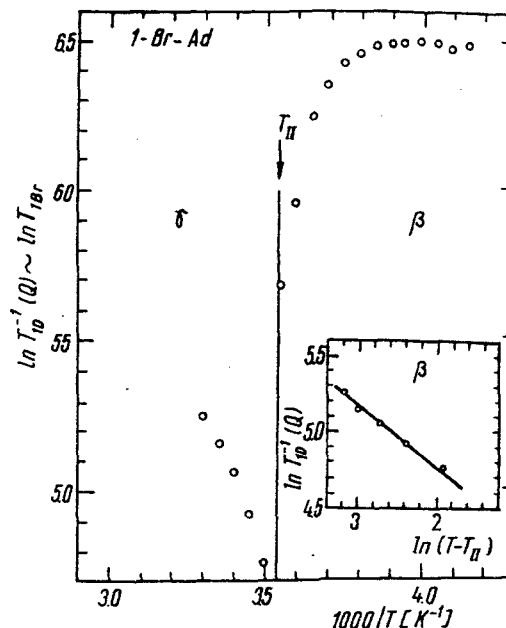


Figure 9. Temperature dependence of $(T_{1D}^{-1})_Q$ in the vicinity of T_{II} for 1-Br-adamantane.

quadrupole nucleus Br ($T_{1Br} < T_2$), the weak collision theory predicts $(T_{1D}^{-1})_Q \sim T_{1Br}$. The temperature dependence of $(T_{1D}^{-1})_Q$ reflects that of T_{1Br} . Above T_{II} , T_{1Br} decreases as $T_{1Br} \sim (T - T_{II})^\beta$ with $\beta = 0.43$. Below T_{II} , T_{1Br} has a large increase and tends to reach a plateau. The temperature dependence of T_{1Br} displays a critical behavior similar to that found in some ferroelectrics (36). A check of this rather speculative result may be provided by a direct measurement of T_{1Br} .

Finally, we observed that this is a correlation between the reorientation motion and the translational diffusion. Clear evidence for this correlation is obtained if one introduces the parameter $\Gamma = E_a(\text{rotation})/E_D(\text{diffusion})$. Experimentally one finds (see Table 1) that the plastic range ($T_m - T_c$) is a decreasing function of Γ . This result agrees with the prediction of the theory developed by L. M. Amzel and L. N. Becka (37) which establishes the connection between the translational disorder (fusion, T_m) and the orientational ordering (solid-solid) transition, T_I in a

molecular crystal. Although this theory may give a qualitative explanation of our data, it is not entirely adequate for this class of compounds, since the activation energy E_D as measured by the NMR method is different from the diffusion used in ref. (37). In fact, E_D is the sum of two contributions: the activation energy of migration E_m . Only the last term is taken into account in ref. (37).

Summing up, we arrive at the following conclusions:

1. The temperature dependences of T_2 , T_{1Z} and T_{1D} show that all three investigated compounds undergo an orientational order-disorder phase transition at T_I .

2. In the high temperature disordered phase (α -phase) the molecule should reorient between several distinguishable orientations. At the same time the molecules perform strong translational diffusion. The molecular motion process in this phase is similar to that found in the disordered phase of adamantane, placing this phase in the class of plastic phases.

A model of motion was introduced based on T_{1Z} data in 1-Cl-ad. According to this model, the isotropic motion is very improbable in the disordered phase.

3. The $\alpha \leftrightarrow \beta$ (γ) transition is accompanied by a "freezing-in" of the reorientation between distinguishable orientations ($\tau_n \rightarrow \infty$) and a blocking of translational diffusion.

4. In the low temperature phase (β) the molecules continue to reorient between a reduced number of orientations. The results in 1-NH₂-adamantane show that such a motion exists even when the molecule has no symmetry axis. In fact, it can be argued (38) that 1-NH₂-ad has an effective C_3 -axis (C-N) since the two protons of the NH₂ group have a negligible effect on the intermolecular potential.

5. When compared to adamantane, the results obtained on the compounds under consideration in this section show that substituents produce a shift towards high temperatures of transition and a reduction of the plastic range ($T_m - T_c$). The high symmetry of adamantane molecule allows it to preserve a high possibility of reorientation in the ordered phase (35). At the transition point the second moment is not changed, which is not the case for 1-Cl, 1-Br, and 1-NH₂-adamantanes.

Faithful to my original claim of selective description, let me choose a single theme for a concluding remark. As it happens with many mature fields in physics, NMR today is moving in two directions: increased sophistication/increased relevance. While these may come

together, more often than not they may not.

The first trend is encouraged heavily by both the rapid progress of the instrumentation (increased availability and large-scale automation of standard equipment and novel, improved ones) and the vast possibilities of associating various kinds of resonance techniques (ENDOR, nuclear-nuclear double resonance, solid effect, optical-nuclear double resonance, etc.). Ever better hardware creates addiction; temptation is great, particularly where the high technology is readily accessible. There is little doubt that magnetic resonance studies facilitated by mere possession of diverse and effective instrumentation will eventually yield new results — just as access to personal computers opened new prospects to approaching stability theory (turbulence, strange attractors, etc.) On the other hand, there is even less doubt that a careful selection of jobs to be assigned to NMR — and other resonance techniques — can only maximize the scientific and practical benefits of the efforts and cost invested in them. With few exceptions — and NMR tomography is, of course, a strikingly good example of the best in hardware and software development — I do not feel that everything has yet been done to complete this process.

Admittedly, the topical sampling in this lecture may not be the most convincing one. Yet, we do hope to improve ourselves in being able to pick the most relevant issues and to give them the most technically appropriate and cost-effective treatment.

As I knew him, I am sure that Felix Bloch would have liked it.

And I am confident that, together, we can do it.

REFERENCES

- ¹ F. Bloch, *Phys. Rev.* **69**, 127 (1946).
- ² F. Bloch, *Phys. Rev.* **70**, 460 (1946).
- ³ F. Bloch, W. U. Hansen, and M. Packard, *Phys. Rev.* **70**, 474 (1946).
- ⁴ I. Ursu, *La Résonance Paramagnétique Electronique*, Dunod, Paris, 1968.
- ⁵ I. Ursu, *Rezonanta Magnetica in Compusi cu Uraniu* (Magnetic Resonance in Uranium Compounds, in Romanian), Academiei, Bucharest, 1979; *Magnytny Rezonants v Sovedineniyap Urana*, Energoatomizdat, Moscow, 1983 (updated edition, in Russian).
- ⁶ A. T. Balaban, M. Banciu, and J. Pognany, *Aplicatii ale Metodelor Fizice in Chimia Organica* (Physics Methods in Organic Chemistry, in Romanian), Stiintifica si Enciclopedica, Bucuresti, 1983.

- ⁷P. Draghicescu, *Rev. Roum. Phys.* **6**, 567 (1969).
- ⁸I. Ursu, D. E. Demco, V. Simplaceanu, and N. Vilcu, *Rev. Roum. Phys.* **19**, 8 (1974).
- ⁹I. Ursu, D. E. Demco, V. Simplaceanu, and N. Vilcu, *Rev. Roum. Phys.* **22**, 705 (1977).
- ¹⁰I. Ursu, D. E. Demco, M. Bogdan, Al. Darabant, P. Fitori, R. Grosescu, and N. Vilcu, *Rev. Roum. Phys.* **27**, 451 (1982).
- ¹¹I. Ursu, D. E. Demco, and R. Lungu, *Rev. Roum. Phys.* **23**, 787 (1978).
- ¹²I. Ursu and D. E. Demco, *RAMIS-International Conference*, Poznan, 1978.
- ¹³I. Ursu, D. E. Demco, M. Bogdan, P. Fitori, and Al. Darabant, Preprint *CNF*, CS-7 (1983).
- ¹⁴I. Ursu, D. E. Demco, P. Fitori, and M. Bogdan, abstracts, *ISMAR-Chicago Conference* (1983).
- ¹⁵I. Ursu, *Fizica si Tehnologie Materialelor Nucleare (Physics and Technology of Nuclear Materials*, in Romanian), Academiei, Bucharest, 1982.
- ¹⁶S. Meiboom and D. Gill, *Rev. Sci. Instrum.* **29**, 688 (1958).
- ¹⁷D. E. Demco, V. Simplaceanu, and I. Ursu, *J. Magn. Reson.* **13**, 310 (1974).
- ¹⁸D. E. Demco, P. Van-Hecke, and J. Waugh, *J. Magn. Reson.* **16**, 467 (1974).
- ¹⁹D. E. Demco, V. Simplaceanu, and I. Ursu, *First Specialized Coll. AMPERE*, Krakow (1973).
- ²⁰D. E. Demco, V. Simplaceanu, and I. Ursu, *Rev. Roum. Phys.* **19**, 613 (1974).
- ²¹J. Jeener and P. Broekaert, *Phys. Rev.* **157**, 232 (1967).
- ²²R. Blinc, E. Pirkmajer, I. Zupancic, and P. Rigny, *J. Chem. Phys.* **43**, 3417 (1965).
- ²³P. Rigny and J. Virlet, *J. Chem. Phys.* **47**, 4645 (1967).
- ²⁴W. H. Zachariasen, *The Transuranium Elements*, McGraw Hill Book Co., New York, 1949.
- ²⁵A. Abragam, *The Principles of Nuclear Magnetism*, Oxford Univ. Press, London, 1961.
- ²⁶P. Rigny and A. Demortier, *C. R. Acad. Sc., Paris*, t. 263, 1408 (1966).
- ²⁷T. H. Siddall and W. E. Steward, *J. Chem. Soc., Chem. Commun.* **14**, 922 (1969).
- ²⁸C. A. Fyfe and D. Harold-Smith, *Can. J. Chem.* **54**, 769 (1976).
- ²⁹T. Clark, T. McO. Knox, H. Mackle, and M. A. McKerverey, *J. Chem. Soc., Faraday I*, **73**, 1224 (1977).
- ³⁰J. B. Guthrie and J. P. McCulloch, *J. Phys. Chem. Solids* **18**, 28 (1961).
- ³¹I. Ursu, R. Grosescu, M. Lupu, and E. Cornilescu, *Rev. Roum. Phys.* **28**, 253 (1983).
- ³²I. Ursu, R. Grosescu, M. Lupu, and M. Lazarescu, *Rev. Roum. Phys.* **28**, 789 (1983).
- ³³M. Punkkinen, *Ann. Acad. Fenn. A VI* **385**, 3 (1972).
- ³⁴C. P. Slichter and D. C. Aillion, *Phys. Rev.* **135**, A 1099 (1964).
- ³⁵A. H. Resing, *Mol. Cryst.* **9**, 101 (1969).
- ³⁶R. Blinc, J. Pirs, and S. Zumer, *Phys. Rev.* **8**, B 15 (1973).
- ³⁷L. M. Amzel and L. N. Becka, *J. Phys. Chem. Solids* **30**, 521 (1969).
- ³⁸R. Grosescu, A. Vasilescu, M. Lupu, and I. Ursu (to be published).

NUCLEAR AND ELECTRON SPIN RELAXATION TECHNIQUES FOR DELINEATION OF BIOINORGANIC AND BIOLOGICAL ACTIVITIES

R. Basosi, N. Niccolai, E. Tiezzi and G. Valensin

*Department of Chemistry
Piano dei Mantellini
44 - 53100 Siena Italy*

	Page
I. Introduction	119
II. Conformational analysis from ^{13}C - ^1H selective NOE	120
III. ^1H NMR relaxation investigations of ligand-receptor interactions	129
IV. Biomolecular structure and dynamics of liquid phase metal complexes by computer aided multifrequency ESR	131
A. Electron Spin Relaxation of Copper in solution. Multifrequency ESR in the determination of rigid limit magnetic parameters	132
B. Multifrequency ESR of CuBIm complex in solution	134
C. Multifrequency ESR and nuclear relaxation of Cu(II)-(L-Histidine) ₂ complex in solution	137
References	138

I. INTRODUCTION

The history of biological applications of electron and nuclear magnetic resonance spectroscopies is almost as long as that of the techniques themselves. The first magnetic resonance experiments were in fact, published (1,2) a few years before the first biological applications were devised (3). The development of the field of magnetic resonance is however a typical example of how an original discovery in the field of physics can become of widespread applicability in several research areas of chemistry, biology and, more recently, medicine. The reasons for such rapid development and widespread interest are to be found in the close correlation between magnetic resonance parameters and molecular features. It has been stated, for instance, that nuclear magnetic resonance yields the same information for liquids as X-ray spectroscopy does for solids.

Three approaches have been given particular prominence in the field of biological applications of magnetic resonance: (i) investigation of the preferred conformations in solution of biologically active molecules; (ii) delineation of the receptor interactions of effector molecules; (iii) analysis of the structural and dynamic features of complexes of metal ions with biomolecules. Conformational analysis in solution can be aided by several NMR approaches, among which the measurements of the nuclear Overhauser

enhancements (NOE) are by far the most exploited, yielding information on the through-space dipolar connectivities and/or the molecular dynamics of the investigated system (4).

In the case of ^{13}C - $\{^1\text{H}\}$ NOE's, both 1D (5,6) and 2D (7) methods have been proposed as alternative approaches. However, no quantitative analysis in terms of heteronuclear distances has been so far performed. Such analysis will be described in this review for carbonyl carbons in a wide range of molecular systems (8-10) in order to test the reliability and to define the limits of the method of obtaining heteronuclear distances from selective proton-carbon NOE's observed in 1D ^{13}C spectra.

The NMR spectrum of a macromolecule is usually a broad envelope which seldom allows one to observe any individual resonance lines. Moreover it often happens that a small quantity of the macromolecule, insufficient to give a strong resonance absorption, can be isolated. Consequently the problem of studying interactions between a small ligand and its macromolecular receptor has then to be approached by observation of any changes in the NMR parameters of the ligand caused by the presence of the macromolecule. Exchange between at least two environments, free (f) and bound (b) to the macromolecule, must then be considered in developing theoretical equations for the NMR parameters of the ligand; namely either

chemical shift or relaxation rates have been shown (11, 12) to be a function of the rate of chemical exchange. Occasionally it may be possible to detect the resonances of the bound ligand directly, but generally the concentration of the macromolecule, and hence of the bound ligand, will be small and this detection will be difficult. If however the rate of chemical exchange between the bound and free environments is fast with respect to either the difference in chemical shift or the nuclear relaxation rate, then the observed NMR parameters will be a weighted average of those in each environment and thus information on the bound resonance signals can be gained in the bulk.

Paramagnetic metal complexes found in or interacting with biological system have been extensively investigated by magnetic resonance researchers. The study of copper in metalloproteins or small complexes has attracted widespread interest in part because of the unique opportunity of gaining detailed information on the electronic structure of copper containing systems, using parameters deduced from optical spectroscopy and from ESR spectroscopy.

There are only two metal ions, VO^{2+} and Cu^{2+} , where this approach is possible at any temperature and degree of motion, and of these Cu^{2+} is by far of greater biological significance.

A primary tool in the examination of the structure of many copper complexes as well as of their chemical and biological reactions has been ESR spectroscopy of frozen samples. Although immobilized phase ESR spectroscopy has provided very fruitful insight into the biological behavior of these complexes, it is limited by the change in temperature and physical state of the system which affects the biological significance of the model. An alternative is to run room temperature, solution ESR measurements. The advantage is that spectral conditions match reaction conditions. This may be particularly important in the study of cellular reactions, for interactions of membranes and complexes which alter the motional properties of the paramagnetic species. The apparent disadvantage is the relative lack of information in the room temperature ESR spectrum, due to the motional averaging of the magnetic parameters associated with the principal magnetic axes.

However, in principle this problem can be minimized by multifrequency ESR analysis used in combination with other complementary procedures such as computer simulation of spectra, isotopic selective substitution and nuclear paramagnetic relaxation measurements.

The rationale for multifrequency analysis is

that fitting ESR spectra at several frequencies using the same spin Hamiltonian input parameters is a very stringent requirement which ensures an unambiguous characterization of the system under study and the relaxation mechanisms involved.

Conformational Analysis from ^{13}C - ^1H Selective NOE

The selective heteronuclear NOEs were generated by the pulse sequence described in Figure 1. The selective low-power decoupler pulse had, typically, a duration of 5-10 times the relaxation time of the irradiated proton. The delay D1 allows complete recovery of ^{13}C longi-

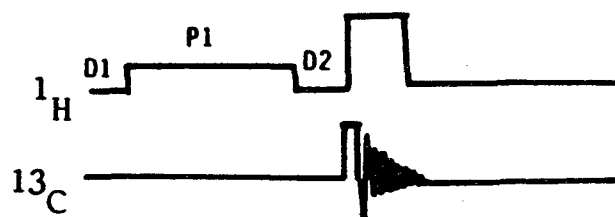


Figure 1. The pulse sequence used for obtaining the selective heteronuclear NOE's.

tudinal magnetizations. The delay D2 allows proper switching of the decoupler between the low power and high power modes.

The nuclear Overhauser effect, which occurs whenever spectra are recorded under conditions of continuous broad-band proton decoupling (BB), causes intensity changes of the peaks.

For ^{13}C nuclei, these range from 1.988 to 0.153 in the $(\omega_{\text{H}} + \omega_{\text{C}})^2 \tau^2 \ll 1$ and $\omega_{\text{C}} \tau_{\text{C}} \gg 1$ limits, respectively, provided that the nuclear spin-lattice relaxation process of carbon nuclei is overwhelmingly dominated by proton carbon dipolar interactions. In general, for a given $I = 1/2$ nucleus:

$$\text{NOE}_X(\text{BB}) = (I_z - I_0)/I_0 = \frac{\gamma_{\text{H}}}{\gamma_{\text{X}}} \frac{W_2 - W_0}{2W_1 + W_2 + W_0 + W^*} \quad (1)$$

where γ is the magnetogyric ratio, I_z and I_0 are the peak intensities measured under continuous

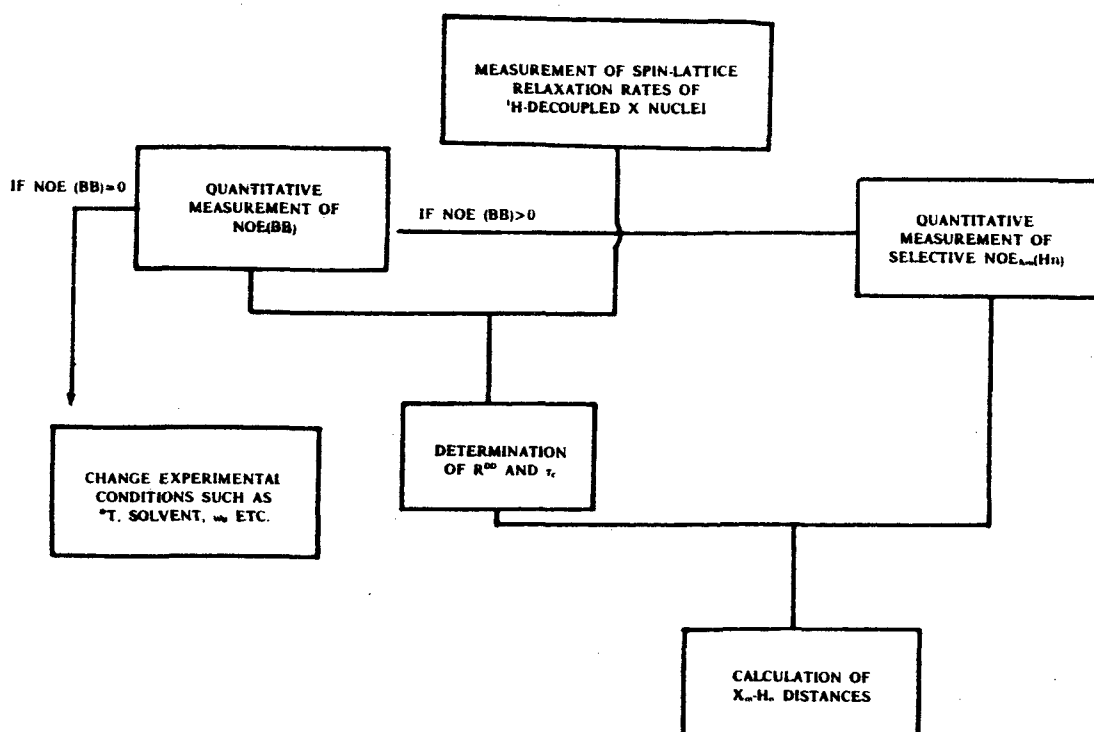


Figure 2. The strategy for obtaining information on molecular structure and dynamics from a combined analysis of selective NOEs and spin-lattice relaxation times.

and gated decoupled conditions, W 's are the transition probabilities which determine the relaxation of the X nucleus and W^* accounts for relaxation contributions other than the ^1H - ^{13}C dipolar one.

As previously suggested in ^1H - ^1H NOE analyses (13,14), for a nucleus X surrounded by i protons eqn. 1 can be rewritten as:

$$\text{NOE}_X(\text{BB}) = \frac{\sum_i \sigma^i X}{R_X} \quad (2)$$

where $\sigma^i X$ is the i th cross-relaxation contribution and R_X is the spin-lattice relaxation rate of the nucleus X , measured in the absence of cross-relaxation with the dipolarly coupled protons. This relaxation rate is the one routinely measured under BB conditions.

Upon selective presaturation of a proton H_a which dipolarly interacts through space with a

^{13}C nucleus C_b at a distance r_{ab} , its resonance experiences a NOE given by:

$$\text{NOE}_{C_b}(H_a)R_{C_b} = \gamma_H \sigma^{ab} / \gamma_C R_{C_b} \quad (3)$$

It follows that:

$$\text{NOE}_{C_b}(H_a)R_{C_b} = \frac{\hbar^2 \gamma_H^2 \gamma_C}{10 r_{ab}^6} \left\{ \frac{6\tau_c}{1 + (\omega_H + \omega_C)^2 \tau_c^2} - \frac{\tau_c}{1 + (\omega_H - \omega_C)^2 \tau_c^2} \right\} \quad (4)$$

Thus, by combining selective NOE measurements and spin-lattice relaxation rates, information on single proton-carbon distances can be obtained in two different ways:

a) the ratio method: when the saturation of H_a gives NOEs on two or more carbon resonances, internuclear distances can be calculated from the following relationship:

Table 1. ^{13}C relaxation parameters measured for compound 1.

C_n	ppm ^a	$R_{C_n}^b$	$\text{NOE}_{C_n}(\text{BB})^c$	$\chi_{C_n}^{\text{DD}}^d$	R^{DD}/m^e
5	168.44	0.09	1.06	0.53	----
1	156.00	0.25	1.19	0.59	----
3	133.62	1.74	1.84	0.92	1.60
4	118.66	0.10	1.30	0.65	----
2	115.21	1.72	1.94	0.97	1.66
6	64.66	2.22	1.95	0.98	1.09
7	53.45	1.61	1.90	0.95	0.76
8	49.67	0.81	2.04	1.02	0.27
9	14.57	0.38	1.67	0.84	0.10

a) ppm from internal TMS; b) ^{13}C spin-lattice relaxation rates in s^{-1} ; c) non-selective NOEs; d) fractional effectiveness of ^1H - ^{13}C dipole-dipole relaxation mechanism; e) $R^{\text{DD}}/m = (R_{C_n} \times \chi_{C_n}^{\text{DD}})/m$ is the dipolar contribution to the spin-lattice relaxation rate measured for carbon n which has m attached protons.

Table 2. ^{13}C relaxation parameters measured for compound 2.

C_n	ppm ^a	$R_{C_n}^b$	$\text{NOE}_{C_n}(\text{BB})^c$	$\chi_{C_n}^{\text{DD}}^d$	R^{DD}/m^e
8	168.73	0.16	1.30	0.65	----
5	165.19	0.08	1.00	0.50	----
1	143.52	0.19	1.23	0.62	----
2	130.01	1.66	1.87	0.94	1.56
4	123.87	0.11	1.22	0.61	----
3	118.09	1.69	1.99	1.00	1.69
6	60.17	1.11	1.84	0.92	0.51
9	23.97	0.63	1.74	0.87	0.18
7	14.00	0.51	1.89	0.95	0.16

a), b), c), d) and e) see note of Table 1.

Table 3. Selective NOEs and internuclear distances calculated for 1.

C_n (Hm)	NOE_{C_n} (Hm)	r_{C_n-Hm}	
		r_o^a	r_1^b
C_1 (NH ₂)	0.96 ^c	1.92	1.81
C_1 (H ₂)	0.56 ^c	2.11	1.99
C_2 (H ₂)	1.87	1.07	1.05
C_3 (H ₃)	1.67	1.07	1.07
C_4 (H ₃)	0.95 ^c	2.11	2.12
C_5 (H ₃)	0.39 ^c	2.72	2.50

a) Distances calculated from Dreiding models (in Å); b) distances calculated according to method 1 described in the text (in Å); c) these NOEs, observed in single carbons, derive from a simultaneous irradiation of two equivalent protons. Hence, they have been divided by two to yield correct internuclear distances (see text).

Table 4. Selective NOEs and internuclear distances calculated for 2.

C_n (Hm)	NOE_{C_n} (Hm)	r_{C_n-Hm}	
		r_o^a	r_1^b
C_8-H (N)	0.27	2.08	2.15
C_1-H (N)	0.37	2.08	1.98

a), b) and c) see the note of Table 3.

$$\frac{\text{NOE}_{\text{C1}(\text{H}_a)\text{R}_{\text{C1}}}}{\text{NOE}_{\text{C2}(\text{H}_a)\text{R}_{\text{C2}}}} = \frac{r_{\text{C2H}_a}^6}{r_{\text{C1H}_a}^6} \quad (5)$$

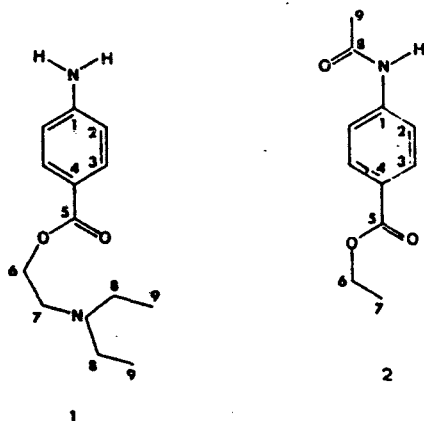
provided that one of the two distances is known and the same correlation time, τ_c , modulates the dipolar interaction of H_a with C1 and C2 atoms. With this method, structural information can be obtained without having any "a priori" estimate of τ_c .

b) the absolute method: on the basis of eqn. 4, r_{ab} can be calculated if the correlation time is known. This correlation time can be evaluated from the dipolar contribution of the spin-lattice relaxation rates of protonated carbons.

In general, the experimental strategy shown in Figure 2. has been followed in order to obtain structural and dynamic information from the measured relaxation parameters.

It should be noted that a simultaneous irradiation on n equivalent protons yields a n times larger selective NOE, provided that the same correlation time and internuclear distance control all the n X-H dipolar interactions.

Two molecular systems of different size and spectral complexity are here analyzed. In the first case, two small organic compounds have been studied:



Their ^{13}C spin-lattice relaxation rates R_{Cn} , and the non-selective NOEs, $\text{NOE}(\text{BB})$, have been measured (see Tables 1 and 2 respectively). These data suggest the following conclusions on relaxation mechanisms and molecular dynamics of 1 and 2: i) in both molecules protonated carbons exhibit $\text{NOE}(\text{BB})$'s very close to $\gamma_{\text{H}}/2\gamma_{\text{C}}$ indicating that their relaxation pathways are dominated by the dipolar interaction with the

bound proton(s) and that this relaxation mechanism has to be modulated by correlation times which satisfy the extreme narrowing conditions: $(\omega_{\text{H}} + \omega_{\text{C}})^2 \tau^2 \ll 1$. ii) Quaternary carbons have a much slower relaxation rate and a fractional effectiveness of the dipolar mechanism, $\text{X}_{\text{DD}}^{\text{DD}}$, which ranges from 0.5 to 0.65. These $\text{X}_{\text{DD}}^{\text{DD}}$ values, calculated from $\text{NOE}(\text{BB})/1.99$ ratios, indicate that the dipolar-mechanism still plays a significant role in the relaxation of these carbon nuclei.

NOEs built up by the selective proton presaturations in the range of 5.5-8.5 ppm have been measured for compounds 1 and 2 and their values are reported in Tables 3 and 4 respectively. It is interesting to note that in 1 the strong dipolar interaction $\text{C}_2\text{-H}_2$ and $\text{C}_3\text{-H}_3$ are J modulated. This J modulation ($^1\text{J}_{\text{C}_2\text{H}_2} = 156$; $^1\text{J}_{\text{C}_3\text{H}_3} = 163$ Hz) can be explained by considering that $^{13}\text{C}\text{-}^1\text{H}$ dipolar interactions occur at the frequency of the ^{13}C satellite proton resonances. The J modulation is not observed for the other $\text{NOE}_{\text{Cn}(\text{Hm})}$'s due to the small coupling constants involved and to the low resolution of the frequency dependence study shown in Figure 3. For a quantitative evaluation of this J modulated selective NOEs a sum of the two maxima is needed. On the other side, the selective Overhauser enhancements observed on C_1 , C_4 and C_5 upon selective irradiation of amino and H_3 protons have to be divided by two. Indeed in these three cases the distance between the simultaneously excited equivalent protons and the considered carbons are the same; then the observed NOEs must be divided by two to determine the contribution from one proton, so as to deduce the correct C-H distance. Internuclear distances can be evaluated by using the absolute method, provided that a suitable τ_c can be determined. This can be done by analyzing the dipolar contribution of the ^{13}C spin-lattice relaxation rates of protonated carbons (15). From $(\text{R}_{\text{DD}}/\text{m})$'s reported in Table 1, effective correlation times can be calculated. In particular, by assuming $r_{\text{C}_2\text{H}_2} = r_{\text{C}_3\text{H}_3} = 1.07$ Å, a correlation time $\tau_c = 6.1 \pm 0.2 \times 10^{-11}$ s can be estimated. The same value for τ_c has been found for compound 2. Once the correlation times have been defined, the absolute method previously described can be used to obtain proton-carbon distances, reported as r_i 's in Tables 3 and 4.

The distances so calculated show a good agreement with the corresponding distances estimated from Dreiding models (r_0 's in Tables 3 and 4). Of particular interest are the distances involving aminic or amidic proton(s): these groups occur in a wide variety of important

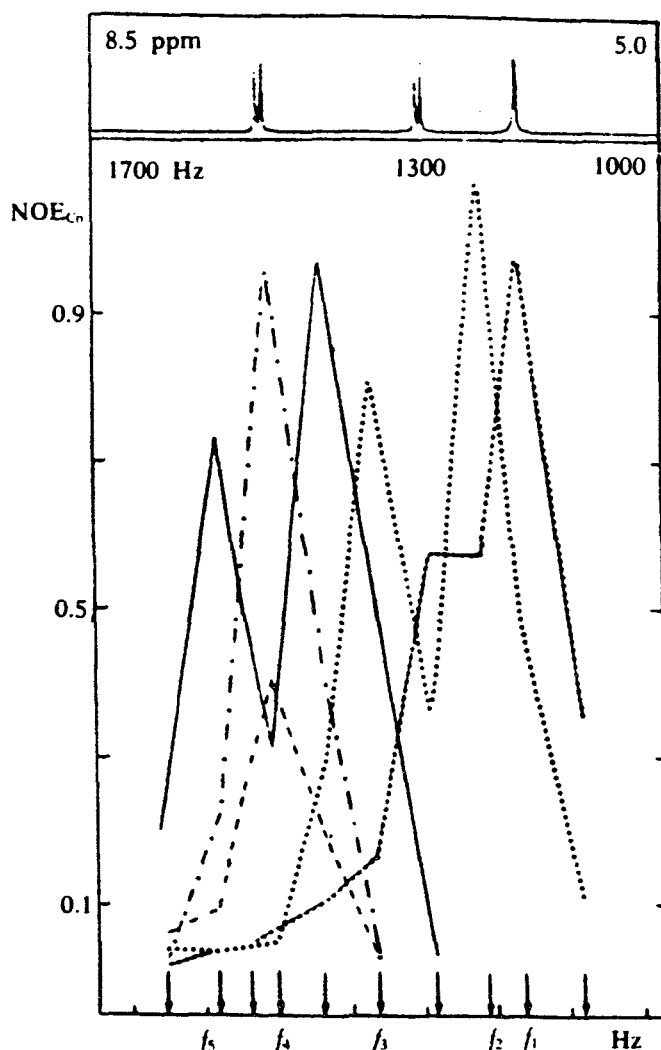


Figure 3. Frequency dependence of selective NOEs observed on C_1 (—), C_2 (.....), C_3 (— — —), C_4 (— · — · —) and C_5 (— · — · —) ^{13}C resonance of *I*, upon the decoupler settings indicated by the arrows. The top insert shows the irradiated region of the proton spectrum.

classes of organic molecules.

The fact that r_0 's are close to the corresponding r_1 's suggests that a suitable τ_c has been chosen for the calculations and a good accuracy in internuclear distance measurements can be achieved, if NOEs and R 's are carefully determined and a reasonable selectivity of the

decoupler pulse can be obtained. This was not the case for the irradiation of H_2 and H_3 in *2*, where the presence of a more strongly coupled H_2 - H_3 system ($\delta/J = 26$ and 3.8 in *1* and *2* respectively), has the consequence that the J modulation of selective NOEs did not yield sharp maxima as for compound *1*. A quantitative treatment of selective NOEs in strongly coupled systems is, therefore, more complex and this constitutes actually a limit of the method.

As an example of a more complex molecular system, gramicidin S has been investigated. This cyclic decapeptide in DMSO solution does not show very significant NOE(BB)'s at room temperature, suggesting that a long correlation time modulates the ^1H - ^{13}C dipolar interactions. Therefore, all the NMR measurements for the decapeptide were run at 80°C . In these experimental conditions and in the applied frequency range of proton selective irradiation, many selective NOEs are observed, see Figure 4.

For discriminating between real and spill-over generated selective

The on-resonance excitation of amide protons always yields large NOEs on the geminal carbonyl carbons, which can be used for carbon resonance assignments but do not contain any structural information.

Furthermore, several conformationally dependent NOEs were observed on: a) Phe $\text{C}=\text{O}$ upon selective irradiation of Val NH (this NOE is characteristic of the peptide β turn structure); b) Phe $\text{C}=\text{O}$ upon irradiation of Orn NH_2 due to the formation of a side chain-backbone hydrogen bond; c) Leu $\text{C}=\text{O}$ and Val $\text{C}=\text{O}$ upon irradiation of Leu NH, consistent with the Φ and Ψ angles of the Leu residue and with the presence of a transannular hydrogen bond characteristic of the gramicidin S antiparallel D pleated sheet conformation. All the proton-carbon distances shown in Figure 5 are calculated from the observed selective NOEs on gramicidin S ^{13}C resonances using eqn. 4 and a $\tau_c = 3.5 \times 10^{-10}$ s.

From the experimental results reported above it is apparent that a combined analysis of selective NOEs and spin-lattice relaxation rates can yield powerful structural information and heteronuclear distances. For this type of structural approach the selection of the experimental conditions has a critical importance due to the NOE dependence on ω_0 , τ_c and, hence, on temperature, viscosity and molecular size. The proton decoupler selectivity may cause spillover and, therefore, a difficult interpretation of experimental data of molecules whose proton spectrum is not well spread out in the region of interest.

Table 5. Nonselective (R^{NS}) and selective (R^S) longitudinal relaxation rates of the phenyl protons of Glycyl-L-tyrosine bound to Zn-carboxypeptidase A

Freq- quency (MHz)	[Enzyme] (mM)	[Gly-Tyr] (mM)	Tyr $H_{\epsilon\epsilon}$			Tyr $H_{\delta\delta}$		
			R^{NS} (s^{-1})	R^S (s^{-1})	R^{NS}/R^S	R^{NS} (s^{-1})	R^S (s^{-1})	R^{NS}/R^S (s^{-1})
90	0	43.	1.19	0.76	--	1.56	1.11	--
90	0.66	43.	1.28	1.39	0.17	1.72	2.00	0.20
90	0	22.	1.14	0.84	--	1.51	1.06	--
90	0.83	22.	1.35	2.04	0.21	1.78	2.50	0.22
270	0	43.	0.65	0.51		1.19	1.06	
270	0.66	43.	0.78	0.85		1.19	1.43	
270	0	10.	0.64	0.53		1.13	0.94	
270	0.16	10.	0.69	0.77		1.13	1.26	

Note, T = 274 K.

Table 6. Nonselective and selective spin-lattice rates of colchicine 0.1 mol dm^{-3} at pH = 7.0 after the addition of 0.1 mL of different biological preparations.

Preparation added	H_{11}		H_1		H_2		H_6	
	R^{NS}	R^S	R^{NS}	R^S	R^{NS}	R^S	R^{NS}	R^S
-----	1.29	0.89	2.96	2.07	3.95	2.72	4.35	3.02
DPPC vesicles	1.31	1.18	3.08	2.78	3.97	3.65	4.31	3.97
Rbc 4%	1.42	1.51	3.01	3.48	4.07	4.56	4.36	5.13
Rbc ghost 4%	1.34	1.21	3.06	2.81	4.01	3.72	4.30	3.89

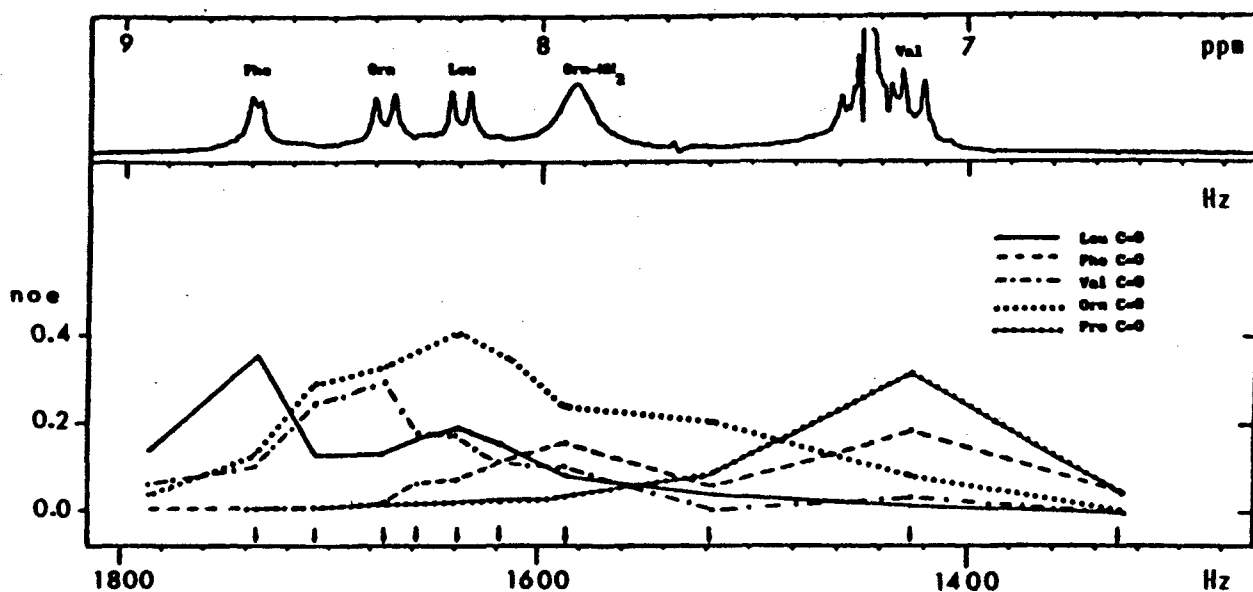


Figure 4. The frequency dependence of selective NOEs on proton chemical shift observed for gramicidin S in DMSO at 50.3 MHz and 80° C.

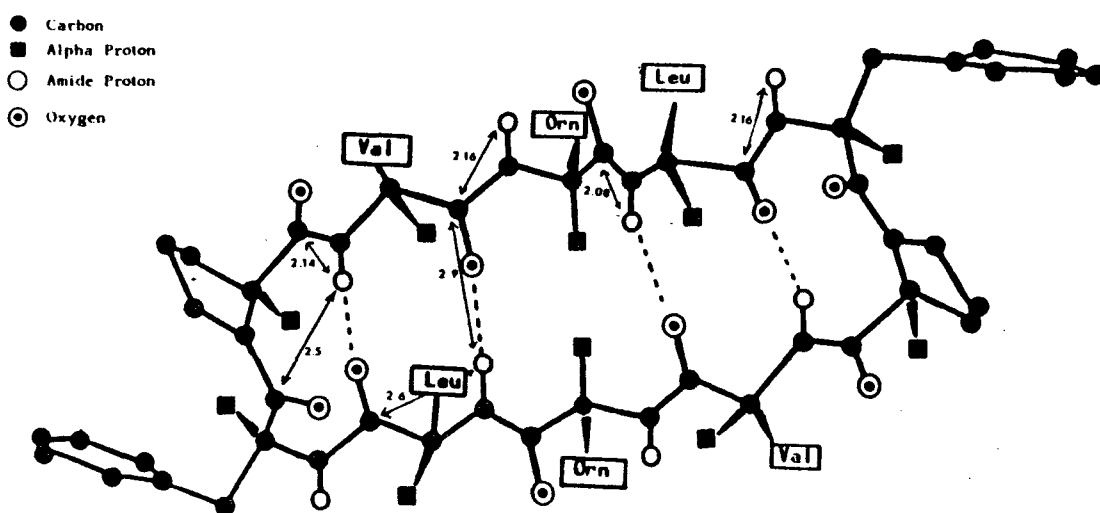


Figure 5. The solution structure of gramicidine S. The arrows indicate the detected ^1H - ^{13}C dipolar couplings and the corresponding internuclear distance are shown. Overhauser effects, only NOE maxima obtained under on-resonance irradiation, are taken into account.

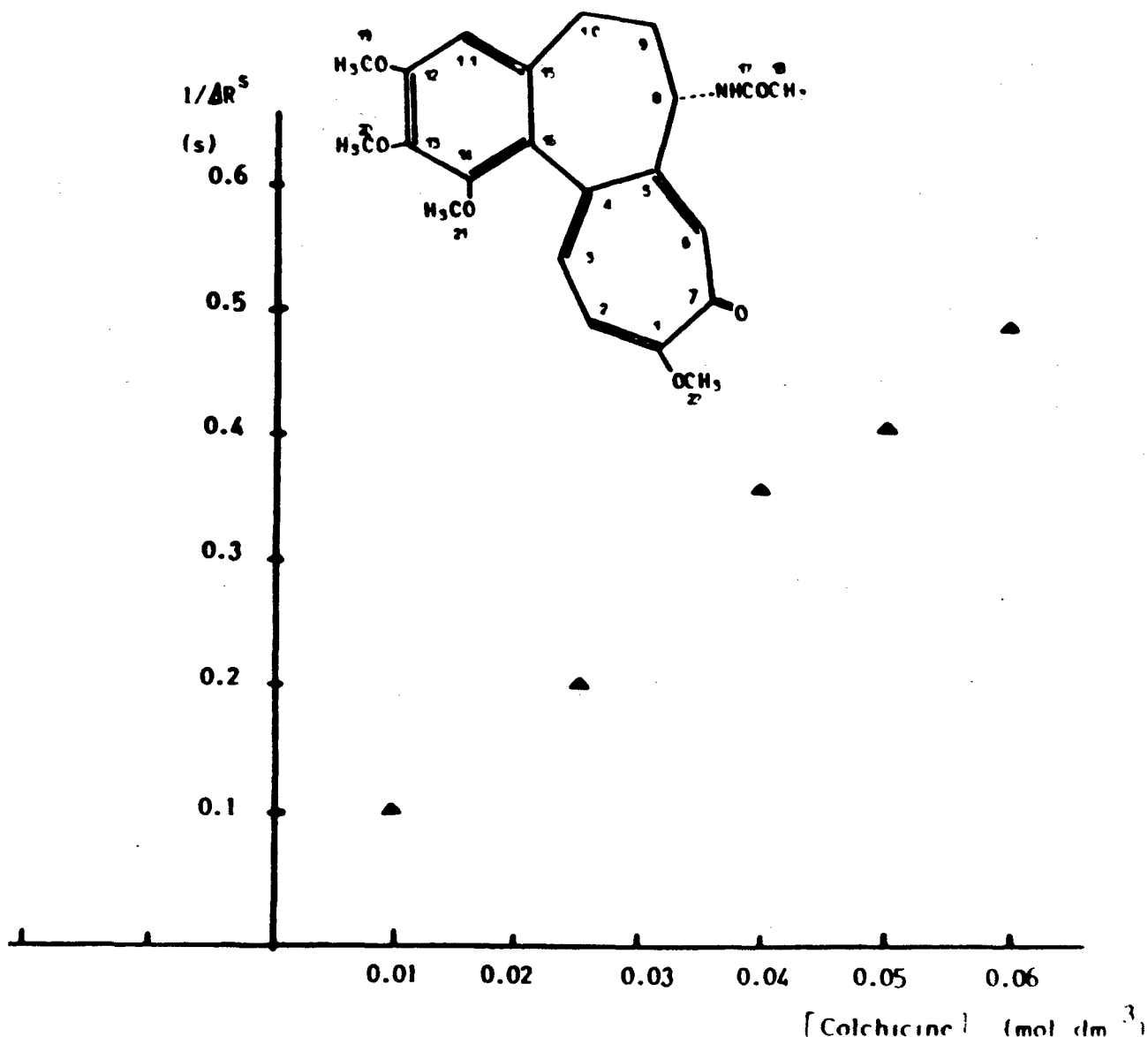


Figure 6. $1/\Delta R^2$ vs. colchicine for the H_2 proton in the presence of red blood cells. pH = 7.0, T = 298 K.

Then, 2D heteronuclear NOE spectra can be comparatively analyzed, even though their quantitative interpretation is not straightforward.

II. 1H NMR RELAXATION INVESTIGATIONS OF LIGAND-RECEPTOR INTERACTIONS

The applicability of the NMR approach to investigations of ligand-receptor interactions suffers from the following drawbacks:

1) The amount of ligand bound may be too

small to be detected, such that under conditions of slow exchange no effect on the bulk resonance will be observed.

2) Conditions of fast exchange may not apply to all the resonances, since they may have different relaxation times and chemical shifts in the bound site.

3) The observed parameter may be intrinsically insensitive to the presence of the macromolecule.

The third point needs further discussion since it represents the reason why diamagnetic

systems have been up to now neglected and why the method of selective irradiation has been shown (16-20) to allow a very suitable approach to diamagnetic ligand-receptors pairs. In fact, if two environments are assumed, a fast exchange rate yields the following equation.

$$M_{\text{obs}} = p_f M_f + p_b M_b \quad (6)$$

where M is a generalized NMR parameter, f and b refer to the free and bound environments and the p 's are the fractions of ligand molecules ($p_f + p_b = 1$). Since p_b must be usually kept very small ($p_b \ll 1$, $p_f \approx 1$), the NMR approach is feasible only provided M_b is quite different from M_f . If the M is the chemical shift, observation of any effect practically occurs only in the presence of nearby paramagnetic centers within the molecule. If M is the spin-lattice relaxation rate (the spin-spin relaxation rate will not be considered here since many complications arise in the measurements), the relaxation mechanism as well as the modulation of the relaxing field must be considered. In the most frequent case of protons relaxed by intramolecular ^1H - ^1H dipolar interactions the spin-lattice relaxation rate can be expressed as a sum of interactions extended to all the actual spin-pairs (13)

$$R_{1i} = \sum_{j \neq i} \rho_{ij} + \sum_{j \neq i} \sigma_{ij} \quad (7)$$

ρ_{ij} and σ_{ij} , named the direct and cross relaxation terms of any spin i dipolarly coupled to a spin j , depend upon the transition probabilities among the four energy levels ($\alpha\alpha$, $\alpha\beta$, $\beta\alpha$, $\beta\beta$):

$$\rho_{ij} = 2W_1 + W_2 + W_0 \quad (8)$$

$$\sigma_{ij} = W_2 - W_0 \quad (9)$$

where W_1 is the single quantum transition probability ($\alpha\beta \longleftrightarrow \beta\beta$, $\alpha\alpha \longleftrightarrow \beta\alpha$), W_0 is the zero-quantum transition probability ($\alpha\beta \longleftrightarrow \beta\alpha$, and W_2 is the double quantum transition probability ($\alpha\alpha \longleftrightarrow \beta\beta$). The explicit forms of ρ_{ij} and σ_{ij} in the case of intramolecular dipolar interactions are:

$$\rho_{ij} = \frac{\hbar^2 \gamma_H^4}{10r_{ij}^6} \left[-\frac{3\tau_c}{1+\omega^2\tau_c^2} + \frac{6\tau_c}{1+4\omega^2\tau_c^2} + \tau_c \right] \quad (10)$$

$$\sigma_{ij} = \frac{\hbar^2 \gamma_H^4}{10r_{ij}^6} \left[\frac{6\tau_c}{1+4\omega^2\tau_c^2} - \tau_c \right] \quad (11)$$

where r is the interproton distance, ω is the proton Larmor frequency and τ_c the motional

correlation time. Substitution of eqns. 9 and 10 into eqn. 7 yields, for a given spin pair:

$$R_{1i} = \frac{3\hbar^2 \gamma_H^4}{10r_{ij}^6} \left[\frac{\tau_c}{1+\omega^2\tau_c^2} + \frac{4\tau_c}{1+4\omega^2\tau_c^2} \right] \quad (12)$$

Since binding to a macromolecular receptor slows down the reorientational motions to the $\omega\tau_c \gg 1$ region, where $f(\tau_c)$ is very small, the spin-lattice relaxation rate of the bound ligand will be large only in cases where the relaxation mechanism has changed, which, as a matter of fact, has limited the applicability of relaxation studies to paramagnetic systems.

However, when selective irradiation is used to excite the spin i such that the spins j are not perturbed eqn. 7 is modified as follows (21):

$$R_{1i}^S = \sum_{j \neq i} \rho_{ij} \quad (13)$$

and, as a consequence,

$$R_{1i}^S = \frac{\hbar^2 \gamma_H^4}{10r_{ij}^6} \left[-\frac{3\tau_c}{1+\omega^2\tau_c^2} + \frac{6\tau_c}{1+4\omega^2\tau_c^2} + \tau_c \right] \quad (14)$$

in such a case, even if the relaxation mechanism does not change, entering the slow motion region does not alter the direct dependence of R_{1i}^S on τ_c and thus the selective relaxation rate of the bound ligand is expected to be quite different from that of the free ligand in solution. It follows that selective irradiation of properly chosen spin systems within relatively small "NMR visible" biomolecules allows detection of binding to macromolecular receptor without requiring insertion of paramagnetic spin probes.

As an example, binding of the substrate glycyl-tyrosine to the Zn-enzyme carboxypeptidase can be tested as shown in Table 5 (16). Selective irradiation of whichever doublet within the AA'BB' spin system of the aromatic ring yields changes in R^S in the range 40-100% depending upon the Larmor frequency; whereas changes in R^{ns} (=non-selective) are negligible, especially at high frequency (16).

The method of selective irradiation can then be exploited to detect binding to ill-defined receptors within biological preparations, such as blood or whole cell samples. In Table 6 the effect of adding different samples to a solution of colchicine (a well known anti-mitotic and tumor-inhibiting alkaloid) are reported. It is evident that only binding may be responsible for the observed enhancement of R^S , since no change in viscosity, such that molecular motions are slowed down by more than one order of magnitude, can be demonstrated.

Once the ligand-receptor binding has been isolated, as in the case of colchicine interacting with erythrocytes (RBC), details of the interaction can be gained by proper changes in the experimental variables, such as pH, temperature, concentration etc. In particular titration of the R^S enhancement vs. the ligand concentration allows evaluation of the apparent association constant K_{ass} . For a 1:1 interaction the binding equilibrium can be schematized as;



The apparent equilibrium constant is given by:

$$K = \frac{[RBC-C]/[C][RBC]}{[RBC-C]} = \frac{[RBC-C]}{[C]\{[RBC]_0 - [RBC-C]\}} \quad (16)$$

where $[C]$ is the concentration of free colchicine and $[RBC]_0$ represents the initial concentration of red blood cells.

The fraction of bound colchicine, p_b , is given by:

$$p_b = \frac{[RBC-C]}{[C] + [RBC-C]} \approx \frac{[RBC-C]}{[C]} \quad (17)$$

Eqn. 16 can be rearranged in the following way:

$$[RBC-C] = K[C][RBC]_0 / \{1 + K[C]\} \quad (18)$$

Substituting eqn. 18 into eqn. 6 and 17 yields:

$$1/\Delta R^S = (1/K + [C])/R_b^S [RBC]_0 \quad (19)$$

Eqn. 19 states that extrapolating the plot of $1/\Delta R^S$ vs. $[C]$ to zero allows evaluation of K ($1/\Delta R^S$ is zero when $[C] = -1/K$). A typical plot is shown in Figure 6 for the H_2 proton of colchicine: the linear relationship is evident, allowing straightforward extrapolation to $1/\Delta R^S = 0$.

III. BIOMOLECULAR STRUCTURE AND DYNAMICS OF LIQUID PHASE METAL COMPLEXES BY COMPUTER AIDED MULTIFREQUENCY ESR

Most conventional ESR is linear and "approximately" CW, operating at around 9 GHz, the X-band microwave region, and employing 100 kHz field modulation. However, since the resonance conditions can be fulfilled for a variety of frequency-field combinations, many other

frequencies are possible.

In the case of copper complexes (22) multifrequency ESR can: (i) be used to study frequency effects on relaxation times and linewidths; (ii) provide a critical test of theoretical simulations; (iii) provide a means to increase spectral resolution by varying the interplay of Zeeman and hyperfine interaction (e.g. to separate the spectra of different species); (iv) be used to study higher order and state mixing effects. Microwave frequency is thus an important experimental parameter.

Increasingly, application of ESR is demanding a detailed consideration of spectral profiles, rather than simply the positions and intensities of the lines. This has led to greater use of computer simulation in interpreting the spectra.

A simulated spectrum will be in the best agreement with an experimental one if the parameters used in calculating the simulated spectrum are adjusted so that the least squares quantity is minimized. With this kind of approach subjective judgements in the evaluation of "goodness of fit" can be eliminated.

Computer simulation when used alone is a quite efficient tool for ESR spectral analysis, but when used in combination with isotopic selective substitution and multifrequency ESR results in a synergistic effect yielding a complete and precise description of the system under study (23). In fact, even when the study is limited to the less complicated room-temperature spectra the use of isotopically pure samples is recommended because in so doing the time necessary for spectral simulation is minimized.

In a bioinorganic system involving a paramagnetic center like copper ion, further information on the molecular structure and dynamics can be provided by the combined use of ESR and FT-NMR. It is well known that the transverse and longitudinal relaxation times are shortened by interaction with a paramagnetic species such as a transition metal ion. The selective variation of the T_1 's and T_2 's in the same ligand molecule depend on the distance from the metal and on the ESR hyperfine coupling constant according to the Solomon-Bloembergen equation (24, 25). The interpretation is correct provided that exchange between free and coordinated ligands is rapid on the NMR time scale.

The selective broadening of the ligand NMR peaks after the addition of the paramagnetic metal ion probe provides independent information about the assignment of the binding sites. Furthermore nuclear relaxation rates of the 1H and ^{13}C nuclei of the ligand allows us to infer about dynamic and structural properties. In fact the

dipolar and the scalar I.S. interactions become the most effective relaxation mechanism whenever fast exchange conditions between bulk and bound ligand hold. As a consequence a paramagnetic contribution to the nuclear relaxation rates can be measured in the following way:

$$\begin{aligned} 1/T_{ip} &= 1/T_{i(\text{metal})} - 1/T_{i(\text{blank})} \\ &= f/T_{iM} \quad (i=1,2) \end{aligned} \quad (20)$$

where $T_{i(\text{metal})}$ and $T_{i(\text{blank})}$ are the experimental relaxation times after and before the metal addition respectively. When Cu(II) is the paramagnetic probe the following simplified Solomon-Bloembergen equation holds:

$$1/T_{2M} = KA^2\tau_e \quad 1/T_{1M} = K'\tau_c/r^6 \quad (21)$$

That is to say the paramagnetic contribution to transverse relaxation rate (T_{2p}^{-1}) is determined only by the scalar interaction, whereas the paramagnetic contribution to the longitudinal relaxation rate (T_{1p}^{-1}) arise from the dipolar interaction only. It is noteworthy that the (T_{1p}^{-1}) contributions depend (as concerns nuclei in the same complex) upon the distance r between the ligand nuclei and the metal ion.

The independent check by means of the FT-NMR technique gives direct information on the ligand in most cases; whereas the ESR spectra gives straightforward evidence of the metal-ligand bond by means of the Fermi contact interaction between the unpaired electron of the copper atom and the ligand nuclei.

The interplay of multifrequency ESR, computer simulation, isotopic substitution, together with the difference in the time scale for ESR and NMR can provide a deep insight into the relaxation mechanisms and the molecular structure and dynamics of copper complexes in solution.

Although some examples will be presented in detail, the material described is by no means comprehensive, as the topic reviewed has become such a broad area of study. Rather we have tried to provide information from our work and experience that we hope will be of general interest.

A. Electron Spin Relaxation of Copper in Solution. Multifrequency ESR in the Determination of Rigid-limit Magnetic Parameters.

The ESR linewidth for Cu(II) in solution can be attributed to the incomplete averaging out of

the spin Hamiltonian parameters (anisotropic g factor and hyperfine coupling A) by the tumbling motion (26-28).

The theory of relaxation mechanisms governing the ESR lineshape has been refined to a very satisfactory level for the motionally narrowed limit (29-34).

The general theories of magnetic resonance (35) predict modification of the position of hyperfine lines (second order shift(s) in ESR spectra as a result of the effects of the line broadening and relaxation mechanisms (35-37).

As these shifts have usually been considered small, compared to the linewidths, they have invariably been neglected (38, 39). However, second-order shifts become quite significant at lower microwave frequency and they can readily provide direct information on the magnetic parameters in the liquid phase at room temperature.

The second-order shifts vary within an appreciable range with an inflection in a plot of the dynamic second-order shifts as a function of rotational correlation time, when $\omega\tau_R = 1$; where ω is the microwave frequency. Dynamic second-order shift effects are expected to be pronounced at low microwave frequencies in systems with large hyperfine interactions, such as square-planar Cu^{2+} complexes. Furthermore, they give observable effects at X and Q band.

The rationale for combining lineshape and frequency shift measurements was developed by Hyde and Froncisz (22), reformulating in Kivelson's notation, the expression of Bruno (40) for the dynamic second-order frequency shifts in the fast tumbling limit.

A complete treatment of the non-secular contributions to the spin Hamiltonian (using a perturbation approach) definitely demonstrated the reliability of a general theory for complexes displaying axial magnetic tensors with $S = 1/2$ over the expanded range of the motional region ($\tau_R = 10^{-11} - 5 \times 10^{-8}$ s) (41). The dynamic second-order frequency shifts can be explicitly included in computer simulation programs.

In a recent paper (42) an unambiguous, rigorous way has been found to extract all of the necessary magnetic parameters in the fluid phase by a combination of multifrequency ESR spectroscopy and computer simulation. The approach depended critically on the analysis of dynamic second-order frequency shifts. Previously, the only approach was to freeze the sample and extract the magnetic parameters from analysis of the frozen solution powder pattern. This is undesirable for many reasons. Vanngard (43) called attention to changes in

Table 7. Magnetic parameters of $^{63}\text{Cu}(\text{dte})_2$.

	Error from Gof		77 K	
	298 K Data	Analysis	67%	33%
g_{iso}	2.0440	± 0.0003		
g_{\perp}	2.015	± 0.003		
g_{\parallel}	2.102	± 0.006	2.118	2.130
Δg	0.087	± 0.008		
a_{iso}	-229.0 MHz	± 2 MHz		
A_{\perp}	-90.3 MHz	± 12 MHz		
A_{\parallel}	-506.3 MHz	± 24 MHz	-495 MHz	-459 MHz
ΔA	-416.0 MHz	± 36 MHz		
τ_R	75 ps	± 15 ps		

Table 8. ESR parameters for CuBIm .

	g_{\parallel}	g_{\perp}	Δg	g_{iso}	A_{\parallel} (MHz)	A_{\perp} (MHz)	ΔA (MHz)	A_{iso} (MHz)	τ_R (ps)
A_{iso} Room Temp.: Best fit for -1/2, +1/2, +3/2 lines	2.20	2.03	0.171	2.09	-651.7	+48.3	-700	-185	250
Best fit for +3/2 line	2.20	2.03	0.171	2.09	-651.7	+48.3	-700	-185	275
Frozen: Simulated data	2.210	2.039	0.171	2.096	-549	-48.	-501	-215	

coordination that can occur. Other authors (44) observed a temperature dependence of equilibrium between two species. Aggregation can occur (45) and often tedious empirical approaches to get good glasses must be employed. In water, freezing can change the local pH (46) and Wilson and Kivelson (47) found that the isotropic g and A values of copper acetylacetonate are actually temperature dependent. All of these complications can be avoided by exploitation of multifrequency ESR of copper complexes.

What has been done thus far in this area is limited to rather small complexes that tumble sufficiently rapidly in solution that motional narrowing theory can be used. However the Freed theory of slow tumbling ESR spectra based on the stochastic Liouville equation would allow the approach to be extended to systems where the rotational correlation time is 100 times greater, permitting experiments on larger complexes and in more viscous environments. This extension will permit systems of real biological interest to be investigated.

The very complex expression for the linewidths of copper complexes developed by Kivelson permits in principle by suitable detailed analysis the determination of all spin Hamiltonian input parameters. However, the dominant terms are all proportional to the rotational correlation time, τ_R , and, in the real world of noise and experimental error, the less dominant terms are extremely difficult to measure. Thus one cannot possibly obtain uniquely both the correlation time and the spin Hamiltonian input parameters.

A suitable formulation of dynamic second-order shift contributions to the position of the lines of Copper are given in:

$$\begin{aligned} \Delta B(M_I) = & \hbar/g\beta_a \{ [M_1^2 - I(I+1)]a^2/2\omega_0 - \\ & [B_0^2(\Delta\gamma)^2 f/15\omega_0 + 7(\Delta A)^2 I(I+1)f/90\omega_0 + \\ & 2M_1 B_0 \Delta\gamma \Delta A f/15\omega_0 - M_1^2 (\Delta A)^2 f/90\omega_0] \} \end{aligned} \quad (22)$$

where:

$$\Delta A = (A_{\parallel} - A_{\perp})(\text{rad s}^{-1}), \Delta g = g_{\parallel} - g_{\perp},$$

$$\Delta\gamma = (\Delta g\beta_e)\hbar, \omega_0 = 2\pi\nu_0,$$

$$a = (1/3)(2A_{\perp} + A_{\parallel}),$$

$$u = 1/(1 + \omega_0 \tau_R^2), \text{ and } f = \omega_0^2 \tau_R^2 u,$$

$$\Delta g_{1,\parallel} = g_{1,\parallel} - 2.0023.$$

At low microwave frequency second-order effects have to be reconsidered. dominant terms are proportional not to τ_R but to τ_R^2 . If dynamic second-order shifts can be measured, then a full solution leading to a unique determination of all spin-Hamiltonian input parameters and also the rotational correlation time can be determined.

From a computer simulation of dynamic shifts developed as a function of microwave frequency and rotational correlation time, it was apparent that the shifts should in fact be readily determinable. However, always in the real world systematic errors in the experiment, noise, background contamination and omission of subtle effects in the theoretical formulation makes things more difficult. What eventually was done was to extract all of the linewidths and all of the line positions with respect to DPPH at five widely varying microwave frequencies (1.19, 2.51, 3.44, 9.12 and 34.7 GHz) using a low molecular weight complex $\text{Cu}(\text{dte})_2$ in toluidine at room temperature.

A two step approach for determining directly at room temperature the spin Hamiltonian input parameters (g_{iso} , a_{iso} , Δg and ΔA) and correlation time (τ_c) in the motional narrowing limit, was developed. In the first stage an interplay of experimental and algebraic approaches yielded initial values, and in the second stage these values were refined by full computer simulation of the spectra and evaluated by an objective goodness-of-fit procedure.

With these values and errors a full blown comparison of simulated and experimental spectra was undertaken. All of the spectral data points were used rather than just the points corresponding to widths and positions, resulting in what must be considered excellent agreement (see Figure 7).

A conscientious approach to error determination from the small residual differences was undertaken, and what is thought to be a new branch of computer aided ESR spectroscopy is introduced: "Sensitivity Analysis." Using only simulated spectra, the change in a spectrum when only one parameter is changed is studied using least squares analysis. this is done for every input parameter at every microwave frequency. Not surprisingly, high frequencies are best for Zeeman terms and low frequencies for hyperfine terms. This sophisticated analysis led eventually to the data and errors shown in Table 7. These errors are less than any others that have ever been assigned in the history of copper ESR spectroscopy of frozen solutions of copper complexes. It is noteworthy from Table 7 that magnetic parameters obtained from analysis of

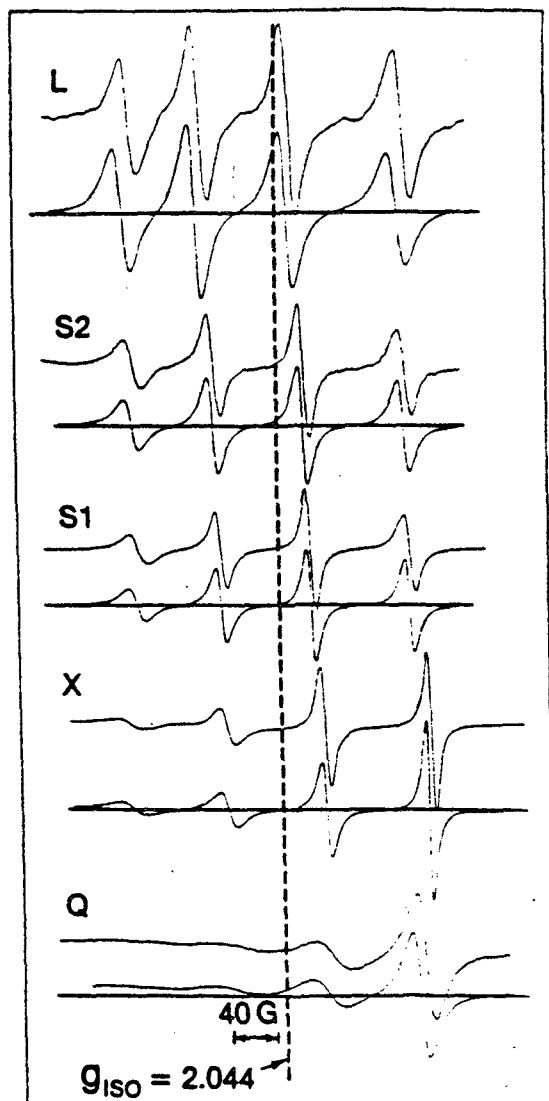
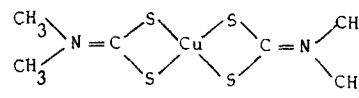


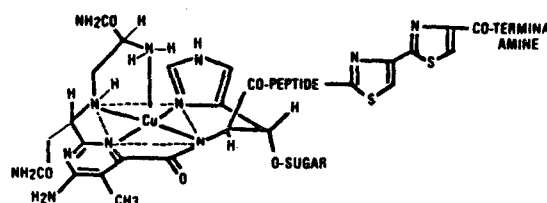
Figure 7. Experimental and simulated room temperature spectra for $^{65}\text{Cu}(\text{dte})_2$ in o-toluidine using the input parameters given in Table 7 at five different microwave frequencies (1.19, 2.50, 3.44, 9.12, 34.7 GHz).

frozen solution spectra bear little resemblance to the values obtained from liquid phase analysis, confirming our previous considerations.



B. Multifrequency ESR of CuBlm Complex in Solution

CuBlm is an active antitumor agent currently used clinically whose mechanism of action has not been fully resolved (48).



The aim of this report is to characterize the copper complexes of Blm from the room temperature data using a strategy based on multifrequency ESR spectroscopy combined with computer simulation of the spectra. Room temperature EPR data only provide new information concerning the coordination mode of the drug to the metal ion, but provide new information concerning the dynamic motion of the complex.

It has been shown that the fast tumbling theory of Kivelson can be used for copper complexes with molecular weights as high as 1600, the molecular weight of CuBlm, if an optimum frequency is available (22).

It was anticipated that the ESR data for CuBlm at low frequency (4 GHz) could be analyzed by the fast tumbling theory. In addition, the intermediate size of the complex might model some of the constraints anticipated for the cupric ion bound to higher molecular weight proteins.

The strategy for data analysis in the present study has been to focus on the high field lines (the $+1/2$ line at X-band and the $+3/2$, $+1/2$, and possibly the $-1/2$ line at S-band) and to use

computer simulations based on Kivelson's fast tumbling theory to determine a set of ESR parameters consistent with the room temperature data. Initial values for Δg , ΔA , and g_{iso} are taken from the frozen solution data (see Table 8). A_{iso} is estimated from the experimental data taken at low frequency (42) following "Sensitivity Analysis" previously discussed in Section IV.A. The correlation time τ_R and each of the parameters in the calculation are systematically varied until a best fit is obtained.

The configuration of the copper complex of the glycopeptide bleomycin, CuBlm, is presumed to be pyramidal square planar from a previous X-ray structural determination of a fragment of cupric bleomycin.

Computer simulations of the room temperature spectrum using parameters from the frozen CuBlm data also suggest that the ESR parameters for CuBlm vary upon going from the immobile to the mobile state (Table 8).

At room temperature, the fast tumbling theory appears to dominate the X-band spectrum for the $+1/2$ line and the S-band spectrum for the $+3/2$, $+1/2$, and possibly the $-1/2$ lines.

A decrease in A_{iso} for CuBlm in the liquid state can be directly surmised from the low frequency S-band spectrum for which three of the four cupric hyperfine lines are partially resolved (Figure 8). Computer simulated spectra indicate that the absolute value of $A_{||}$ increases about 100 MHz and the value of A_{\perp} may change sign for CuBlm in the liquid state.

The parameters can be used to measure the extent of ionic bonding (α) and the extent of the contact term (k) from the eqns. 23 and 24.

$$A_{||} = P[-k - 4\alpha^2/7 + (g_{||} - 2.0023) + 3(g_{\perp} - 2.0023)/7] \quad (23)$$

$$A_{\perp} = P[-k + 2\alpha^2/7 + 11(g_{\perp} - 2.0023)/14] \quad (24)$$

where P is taken as $350 \times 10^{-4} \text{ cm}^{-1}$ (44). The symmetry is assumed to be tetragonal with the unpaired hole in the $d_{x^2-y^2}$ orbital (49).

A comparison of the ionic bonding (α) and the contact term (k) between the parameters emphasizes the effect of the changes in $A_{||}$ and A_{\perp} described in Table 8. The ionic bonding increases ($\alpha_{\text{frozen}} = 0.85$ and $\alpha_{\text{r.t.}} = 1.0$) and the contact term decreases ($k_{\text{frozen}} = 0.34$ and $k_{\text{R.T.}} = 0.25$).

Simulations using a rotational correlation time of about 250 psec indicate that CuBlm may not be spherical in the liquid phase.

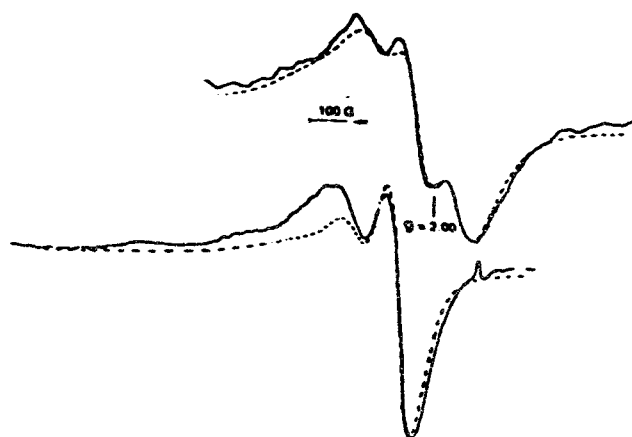


Figure 8. S-band (3.46 GHz) (upper) and (X-band) (lower) ESR spectra for $^{65}\text{CuBlm}$ in D_2O . Dashed lines are computer simulated spectra for room temperature data which gave the best fit for the $M_I = 3/2$ line.

If CuBlm were spherical, the rotational correlation time would be expected to be greater than 1000 psec for a molecular weight of 1600. The resolution of the cupric hyperfine structure is sensitive to τ_R for given ESR parameters, ΔA , A_{iso} , g_{iso} , and Δg . The low value for τ_R suggests that CuBlm is not spherical but rather cigar shaped or even more likely, CuBlm has segmented flexibility and rotates about a hinge. Three sections linked together may be the peptide moiety, the disaccharide group, and the metal binding site region of Blm. The metal binding site is dominated by the motion of the fast component of the inertial tensor which would account for a value of τ_R which is smaller than anticipated for a sphere.

Furthermore, it is argued from an analysis of the cupric hyperfine coupling constants given in Table 8 and the bonding parameters previously defined that the CuBlm structure opens up at room temperature and that the cupric ion is displaced from the square plane (50).

C. Multifrequency ESR and Nuclear Relaxation of Cu(II)-(L-Histidine)₂ Complex in Solution

Structural features of low molecular weight Cu(II) complexes have been extensively investigated with special emphasis on their biochemical role. The binding mode of L-His in the Cu(II)(L-His)₂ complex is however still controversial although several investigations have been carried out (51, 52). Here we present the results of NMR and ESR experiments from which the structure and dynamics of the complex are suitably delineated. The assumptions have been made that L-His retains approximately the same configuration as that found in the complex in the solid state and that the Solomon-Bloembergen approach can suitably account for the observed nuclear relaxation rates.

A multifrequency ESR approach combined with computer fitting (Figure 9) was used to gain information on the magnetic spin Hamiltonian parameters and on the rotational correlation time.

The nuclear relaxation rates were measured for both protons and carbons of the His molecule at increasing Cu(II) concentrations (Table 9) (53). The correlation time for the dipolar interaction was evaluated by using the crystallographic distances for the Cu-C_α vector and was found consistent with that obtained by ESR analysis within the experimental error ($\tau_c = 0.8\text{--}2.0 \times 10^{-10}$ s).

The value for the correlation time was then used to get the number of imidazole moieties in the copper coordination sphere using equations given in Section IV.

It became apparent (53) that ¹³C data can be interpreted in terms of a mixture of two complexes such that 24% of Cu(II)(L-His)₂ complex contains histidines bound in the histamine-like way, while the remaining 76% contains one L-His molecule bound in the histamine-like way and the other L-His bound in the glycine-like way.

The evaluation of advantages and limits of each approach leads to the conclusion that only by combining evidence from several independent techniques is it possible to obtain a thorough comprehension of both structural and dynamic features of these complexes.

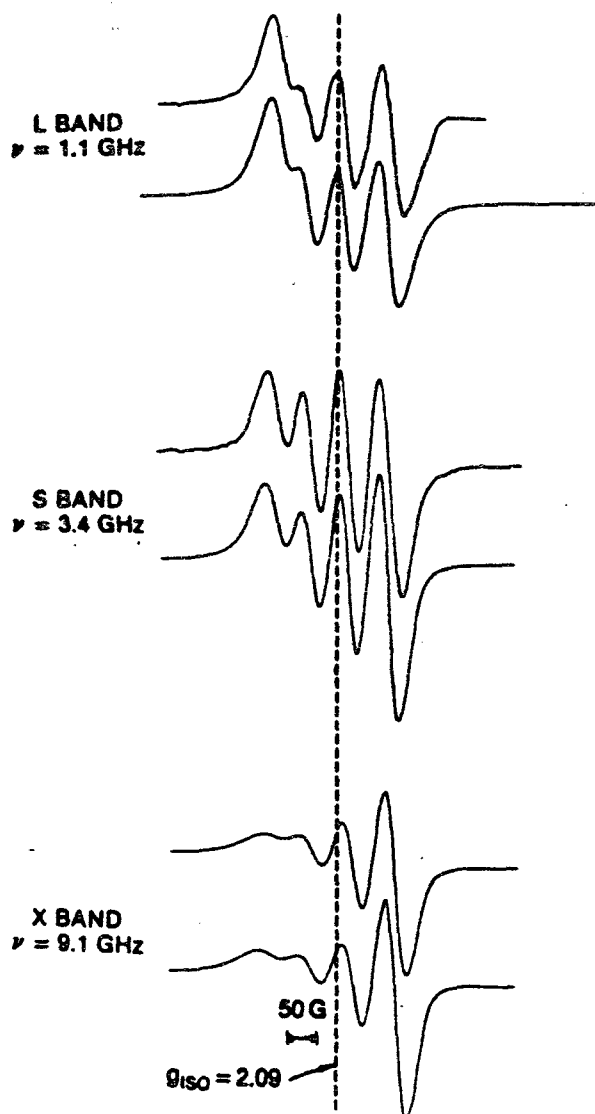


Figure 9. Experimental (top) and simulated (bottom) L-band ($\omega = 7.54 \times 10^{-1}$ rads⁻¹) S-band ESR spectra of Cu(II)(L-His)₂ complex in H₂O solution pH = 7.3 at 298 K. The [L-His] concentration is 0.1 mol dm⁻³ and [Cu²⁺] is 8×10^{-3} mol dm⁻³.

Table 9. Paramagnetic nuclear relaxation rates of ^1H and ^{13}C nuclei of L-His in D_2O in the presence of Cu^{2+} ions at $\text{pH} = 7.0$ and $T = 298 \text{ K}$.

	[LL-His] (mol dm $^{-3}$)	[Cu $^{2+}$] (mol dm $^{-3}$)	$T_{1\rho}^{-1}$ (s $^{-1}$)	$T_{2\rho}^{-1}$ (s $^{-1}$)
H $_2$	0.1	5×10^{-5}	0.78	2.10
H $_4$	0.1	5×10^{-5}	0.18	3.06
H	0.1	5×10^{-5}	0.67	2.13
N $\beta_1\beta_2$	0.1	5×10^{-5}	0.45	3.46
COO $^{-2}$	0.2	5×10^{-5}	0.45	4.82
C	0.2	5×10^{-5}	0.55	4.98
C β	0.2	5×10^{-5}	0.09	1.12
C $_5$	0.2	5×10^{-5}	0.53	5.42
C $_4$	0.2	5×10^{-5}	0.13	1.29
C $_2$	0.2	5×10^{-5}	0.87	7.75

REFERENCES

- ¹F. Bloch, *Phys. Rev.* **70**, 460; F. Bloch, W. W. Hansen and M. Packard, *Phys. Rev.* **70**, 474 (1946).
- ²E. M. Purcell, H. C. Torrey and R. V. Pound, *Phys. Rev.* **69** (1946).
- ³C.B. Bratton, A. L. Hopkins and J. W. Weinberg, *Science* **147**, 738 (1965).
- ⁴D. Doddrell, V. Glushko and A. Allerhand, *J. Chem. Phys.* **56**, 3683 (1972).
- ⁵J. Uzawa and S. Takeuchi, *Org. Magn. Reson.* **11**, 502 (1978).
- ⁶M. F. Aldersley, F. M. Dean and B. F. Mann, *J. Chem. Soc., Chem. Commun.*, 107 (1983).
- ⁷P. Rinaldi, *J. Am. Chem. Soc.* **105**, 5167 (1983).
- ⁸N. Niccolai, E. Tiezzi and C. Rossi, *Nuovo Cimento* **3D**, 993 (1984).
- ⁹N. Niccolai, C. Rossi, V. Brizzi and W. A. Gibbons, *J. Am. Chem. Soc.* **106**, 5732 (1984).
- ¹⁰N. Niccolai, A. Sega, M. Scotton and C. Rossi, *Gazz. Chim. Ital.*, in press.
- ¹¹T. J. Swift and R. E. Connick, *J. Chem. Phys.* **37**, 307 (1962).
- ¹²R. Luz and S. Meiboom, *J. Chem. Phys.* **40**, 2686 (1964).
- ¹³J. H. Noggle and R. E. Schirmer, in *The Nuclear Overhauser Effect*, Academic Press, New York, 1971.
- ¹⁴C. R. Jones, C. T. Sikakana, S. Hehir, M. C. Kuo and W. A. Gibbons, *Biophys. J.* **24**, 815 (1978).
- ¹⁵A. Allerhand, D. Doddrell and R. A. Komorosky, *J. Chem. Phys.* **55**, 189 (1971).
- ¹⁶G. Valensin, T. Kushnir and G. Navon, *J. Magn. Reson.* **46**, 23 (1982).
- ¹⁷G. Valensin, A. Casini, A. Lepri and E. Gaggelli, *Biophys. Chem.* **17**, 297 (1983).
- ¹⁸G. Valensin and P. E. Valensin, *Magn. Reson. Med.* (1985), in press.
- ¹⁹I. Barni Comparini, E. Gaggelli, N. Marchettini and G. Valensin, *Biophys. J.* (1985) in press.
- ²⁰G. Valensin, A. Lepri and E. Gaggelli, *Biophys. Chem.* (1985) in press.
- ²¹R. Freeman, H. A. O. Hill, B. L. Tomlinson and L. D. Hall, *J. Chem. Phys.* **61**, 4466 (1974).
- ²²J. S. Hyde and W. Froncisz, *Ann. Rev. Biophys. Bioeng.* **11**, 391 (1981).
- ²³W. E. Antholine, R. Basosi, J. S. Hyde, S. Lyman and D. H. Petering, *Inorg. Chem.* **23**, 3543 (1984).
- ²⁴I. Solomon, *Phys. Rev.* **99**, 559 (1955).
- ²⁵N. Bloembergen and L. O. Morgan, *J. Chem. Phys.* **34**, 842 (1961).
- ²⁶H. M. McConnell, *J. Chem. Phys.* **25**, 709 (1956).
- ²⁷B. R. McGavey, *J. Phys. Chem.* **60**, 71 (1956).

- ²⁸N. Bloembergen, E. M. Purcell and R. V. Pound, *Phys. Rev.* **73**, 679 (1948).
- ²⁹D. Kivelson, *J. Chem. Phys.* **27**, 1987 (1957).
- ³⁰D. Kivelson, *J. Chem. Phys.* **33**, 1094 (1960).
- ³¹D. Kivelson, *J. Chem. Phys.* **41**, 1904 (1964).
- ³²R. Wilson and D. Kivelson, *J. Chem. Phys.* **44**, 154 (1966).
- ³³P. W. Atkins and D. Kivelson, *J. Chem. Phys.* **44**, 169 (1966).
- ³⁴D. Kivelson, in *Electron Spin Relaxation in Liquids*, L. T. Muus and P. W. Atkins, Eds., Plenum Press, New York, 1972, pp. 213-77.
- ³⁵F. Bloch, *Phys. Rev.* **102**, 104 (1956).
- ³⁶A. G. Redfield, *J. Res. Develop.* **1**, 19 (1957).
- ³⁷A. Abragam, in *The Principles of Nuclear Magnetism*, Oxford Univ. Press, Oxford, 1970.
- ³⁸G. K. Fraenkel, *J. Chem. Phys.* **42**, 4275 (1965).
- ³⁹G. K. Fraenkel, *J. Phys. Chem.* **71**, 139 (1967).
- ⁴⁰G. V. Bruno, J. K. Harrington, M. P. Eastman and J. Eastman, *J. Phys. Chem.* **81**, 1111 (1977).
- ⁴¹R. F. Campbell and J. H. Freed, *J. Phys. Chem.* **84**, 2668 (1980).
- ⁴²R. Basosi, W. E. Antholine, W. Froncisz and J. Hyde, *J. Chem. Phys.* **81**, 4849 (1984).
- ⁴³T. Vanngard, in *Biological Applications of Electron Spin Resonance*, H. M. Swartz, J. R. Bolton and D. C. Borg, Eds., Wiley, New York, 1972, p. 423.
- ⁴⁴K. E. Falk, E. Ivanova, B. Ross and T. Vanngard, *Inorg. Chem.* **9**, 556 (1970).
- ⁴⁵J. S. Leigh and G. H. Reed, *J. Phys. Chem.* **75**, 1202 (1971).
- ⁴⁶Y. Oriti and M. Morita, *J. Biochem., Tokyo* **81**, 163 (1977).
- ⁴⁷R. Wilson and D. Kivelson *J. Chem. Phys.* **44**, 4445 (1966).
- ⁴⁸D. H. Petering, W. E. Antholine and L. A. Saryan, in *Synthesis and Properties of Antitumor Agents and Interferon-inducing Agents*, Ottenbrite and Butler, Eds., Marcell Dekker, New York, 1984, pp. 203-46.
- ⁴⁹A. H. Maki and McGarvey, *J. Chem. Phys.* **29**, 31 (1958).
- ⁵⁰W. E. Antholine, G. Riedy, J. S. Hyde, R. Basosi and D. H. Petering, *J. Biomol. Struct. and Dynamics*, **2**, 469 (1984).
- ⁵¹B. A. Goodman, D. B. McPhail and H. K. J. Powell, *J. Chem. Soc., Dalton Trans.*, 822 (1981).
- ⁵²N. Camerman, J. K. Fawcett, T. P. A. Kruck, B. Sarker and A. Camerman, *J. Am. Chem. Soc.* **100**, 2690 (1978).
- ⁵³G. Valensin, R. Basosi, W. E. Antholine and E. Gaggelli, *J. Inorg. Biochem.* **23**, 125 (1985).

NMR STUDIES OF MOLECULES DISSOLVED IN CHOLESTERIC LIQUID CRYSTALS

C.L. Khetrapal¹, K.V. Ramanathan¹ and M.R. Lakshminarayana²

1. Indian Institute of Science, Bangalore 560012, India.

2. University of Agricultural Sciences, Bangalore 560065, India.

ABSTRACT

The results obtained from NMR spectroscopy of molecules oriented in cholesteric liquid crystals are presented. The advantages, limitations and future prospects of using cholesteric materials as orienting media for NMR experiments have been discussed with emphasis on our own recent work.

I. INTRODUCTION

Though thermotropic nematic and lyotropic mesophases have been widely used as solvents in NMR experiments (1,2) comparatively much less work has been reported on cholesteric materials. On the other hand, since such materials exhibit remarkable unusual properties leading to novel technological applications, the interest in such studies has enhanced in recent times. One of the reasons for the scarce use of the cholesteric materials as orienting media particularly in the proton NMR experiments lies in the difficulty in orienting them and in obtaining sharp lines. However, the experiments demonstrating that suitable mixtures of cholesteric materials provide sharp lines in proton NMR spectroscopy (3-5) promise new applications.

Studies on orientation of optically active compounds, translational diffusion, deuteron magnetic resonance of deuterated molecules dissolved in cholesteric liquid crystals and their mixtures with nematics and the determination of molecular geometry have all been reported.

The purpose of this short review is to present a critical evaluation of the results and the prospects of the use of cholesteric materials as anisotropic media in NMR experiments. Though reports on the study of spin-lattice relaxation times T_1 and $T_{1\rho}$ and self diffusion studies (6), the induced cholesteryl lyotropic mesophases (7,8) and the orientational order in cholesteric liquid crystals (9-12) are available, they are not included here since the review is restricted to small molecules dissolved in cholesteric liquid crystals.

II. STUDY OF OPTICALLY ACTIVE COMPOUNDS

Distinct NMR spectra for d and l enantiomers have been observed for optically active molecules dissolved in optically active cholesteric liquid crystals (3). This is due to the fact that the degree of order of the solute molecules differs for the d and l geometry. The results have been demonstrated for racemic 3,3,3-trichloropropylene oxide dissolved in a mixture of cholesteryl chloride and cholesteryl myristate.

The experiments clearly demonstrate the use of cholesteric mesophases for the study of optically active compounds in order to obtain separate information on the \underline{d} and the \underline{l} forms. Such information cannot be had from nematic and lyotropic mesophases. The potentials of such experiments have yet to be exploited.

III. STUDY OF TRANSLATIONAL DIFFUSION

Translational diffusion coefficient of small molecules such as methane and dichloromethane dissolved in five cholesteric mixtures of alkyl cyanobicyclohexane and cholesteryl chloride have been measured in the temperature range of 25°C to 75°C using pulse gradient spin echo method (13). For cholesteric phases, it is expected that the diffusion coefficient along the pitch (D_{\parallel}) is different from that orthogonal to it (D_{\perp}). Further, NMR investigations in pure neat cholesterics indicate that D_{\parallel} is proportional to the square of the pitch (14-16); the relation has also been derived (17) using simple random walk model for cholesteric liquid crystals. The studies, therefore, provide a method for the determination of the pitch of the helix. NMR has also been used to determine the pitch in a cholesteric lyomesophase formed by adding \underline{l} -alanine to a solution of disodiumchromoglycate in water (18).

In mixture of the nematic liquid crystal ZLI-1167 (aternary eutectic mixture of propyl, pentyl and heptyl bicyclohexyl carbonitrile) containing 20% cholesteryl chloride with a

pitch of 2.2 μ , $D_{\perp} / D_{\parallel} \approx 1.1$ for both methane and dichloromethane has been obtained. The Arrhenius activation energies for the diffusion constants are determined as 6-7 KCal/mole. The diffusion coefficients are found to be independent of the pitch i.e. the cholesteryl chloride concentration.

IV. DEUTERON MAGNETIC RESONANCE OF MOLECULES DISSOLVED IN CHOLESTERIC LIQUID CRYSTALS

Deuteron magnetic resonance is particularly a useful technique for the study of the orientation of the molecules dissolved in liquid crystals exhibiting cholesteric and blue mesomorphism (19,21). Both the line separations and the shapes of the quadrupole splittings have been interpreted. The features of the cholesteric phase spectra and of the molecules dissolved therein indicate that the ordering of the phase is incomplete. This is illustrated by the observations of the asymmetry of the quadrupole split doublet components of partially deuterated liquid crystals and the weak inner doublets in the spectra of the dissolved deuterated probe molecules such as benzene- d_6 . The blue phase spectra exhibit features which are distinctly different from those of cholesteric and isotropic phases. They are consistent with the fact that the phase consists of cholesteric-like chiral segments with elementary units arranged in cubic symmetry. The dimensions of the elementary units are of the order of the cholesteric phase pitch length. It may be mentioned that the studies of the blue phase have also been undertaken

using fluorine and proton NMR spectroscopies but due to lower magnetic fields used and the smaller anisotropic interactions of the ^{19}F and the ^1H , the blue phase spectra consisting of broad and isotropic-like signals were obtained (10).

The deuterium NMR spectra of deuterated molecules dissolved in mixtures of opposite handed chirality have also attracted attention (20,21). The NMR spectra of such compensated cholesteric mixtures providing media with very large pitch exhibit sharp lines characteristic of high ordering without any contribution due to randomly oriented domains. The spectra of benzene- d_6 , acetonitrile- d_3 and chloroform- d have thus been studied. The influence of the addition of the nematic liquid crystals such as MBBA [N-(p-methoxybenzylidene)-p'-n-butylaniline], S-1114 [trans-4-pentyl-4(4-cyanophenyl)-cyclohexane] and ZLI-1167 on the deuterium NMR spectra of the deuterated molecules (C_6D_6 , CD_3CN , CDCl_3) dissolved in the compensated cholesteric mixtures consisting of 1:0.74 weight ratio of cholesteryl chloride to cholesteryl nonanoate has also been examined. Upto about 30 weight percent of MBBA, only one quadrupole split doublet of the dissolved probe molecule is observed. Around 30 weight percent and above, two quadrupole split doublets (Fig.1) start appearing. Though a doubling of the quadrupole doublet is also observed in mixtures with S-1114 beyond a certain concentration, no such effect

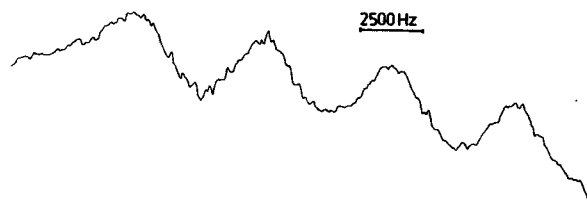


Fig.1. 41.44 MHz Deuterium NMR spectrum of C_6D_6 dissolved in a mixture of cholesteryl chloride : cholesteryl nonanoate : MBBA in the weight ratio of 1:0.73:0.73.

Solute Concentration : 2.7 weight percent

Temperature : 17°C

No. of Scans : 32,000

is noticeable in mixtures with ZLI-1167. However, addition of ZLI-1167 to the mixture containing the compensated cholesteryl mixture and MBBA sharpens both the doublets (Fig.2). The

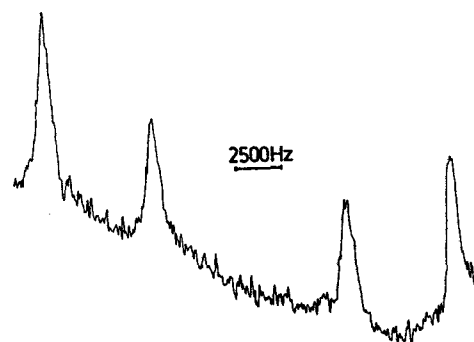


Fig.2. 41.44 MHz Deuterium NMR spectrum of CDCl_3 dissolved in mixture of ZLI-1167, cholesteryl chloride, Cholesteryl nonanoate and

MBBA in the weight ratio of 1:0.075:0.055:0.43.

Solute Concentration : 4.6 weight percent

Temperature : 20°C

No. of Scans : 1,28,000

exact explanation and the possible applications of such experiments are being explored.

V. DETERMINATION OF GEOMETRY OF MOLECULES DISSOLVED IN CHOLESTERIC LIQUID CRYSTALS

The only compound studied in a cholesteric liquid crystal solution for the determination of molecular structure is acetonitrile (5). The proton NMR spectrum of ^{13}C -acetonitrile including the ^{13}C -satellites in the natural abundance of ^{13}C has been investigated in a 1:0.74 weight ratio of cholesteryl chloride to cholesteryl nonanoate. The spectrum with a linewidth at half height of 4 Hz (Fig.3) was obtained. The r_α -structure

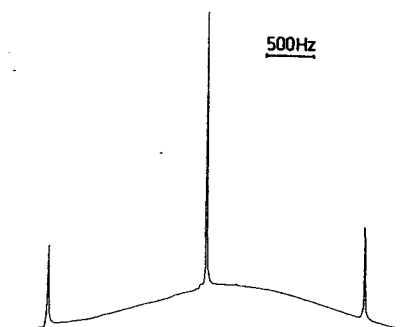


Fig.3. 270 MHz proton NMR spectrum of CH_3CN dissolved in a mixture of cholesteryl chloride and cholesteryl nonanoate in the weight ratio of 1:0.74.

Solute Concentration : 5 weight percent

Temperature : 34°C

No. of Scans : 28

of acetonitrile has thus been determined. The r_α value of the HCH bond angle has been obtained as 109.2°. This agrees well with the microwave value of 109.3° (22).

It has thus been concluded that the cholesteric liquid crystals can be used as convenient solvents in NMR spectroscopy. They provide sharp lines with widths comparable to those in normal thermotropic nematic solvents. Due to the different solubility properties of the cholesteric and the nematic liquid crystals, the results certainly promise the enhancement of the scope of the NMR spectroscopy of oriented systems. The study of a variety of optically active compounds in such solvents may be of future interest. Though the solvent effects on the structure of molecules dissolved in such mesophases have yet to be explored, the indication from the first reported study are that the effects may be of the same order of magnitude as in the case of normal nematics.

REFERENCES

1. C.L. Khetrapal and A.C. Kunwar, in *Adv. Liq. Cryst.* (Ed. G.H. Brown), Vol.6, Academic Press, New York (1983).
2. J.W. Emsley and J.C. Lindon, *NMR spectroscopy using liquid crystal solvents* Pergamon, Oxford, 1975.

3. E. Sackmann, S. Meiboom and L.C. Snyder, J.Am.Chem. Soc. 90, 2184 (1968).
4. E. Sackmann, S. Meiboom and L.C. Snyder, J.Am.Chem. Soc. 89, 5981 (1967).
5. C.L. Khetrapal and K.V. Ramanathan, Chem.Phys.Lett. (in the press).
6. M. Vilfan R. Blinc, J. Dolinsek, M. Ipavec, G. Labajnar and S. Zumer, J.Physique 44, 1179 (1983). R.Y. Dong, M.M. Pintar and W.F. Forbes, J.Chem.Phys. 55, 2449 (1971).
7. M.R. Alcantara, M.V.M.C. De Melo, V.R. Paoli and J.A. Vanin, Mol.Cryst.Liq. Cryst. 95, 299 (1983).
8. M.R. Alcantara, M.V.M.C. De Melo, V.R. Paoli and J.A. Vanin, Mol.Cryst.Liq. Cryst. 90, 335 (1983); M.R. Alcantara et al., Mol.Cryst.Liq.Cryst. 107, 359 (1984).
9. P.J. Collings, S.I. Goss and J.R. McColl, Phys.Rev. 11A, 684 (1975), P.J.Collings and J.R. McColl, J.Chem.Phys. 69, 3371 (1978).
10. P.J. Collings, T.J. McKee and J.R. McColl, J.Chem.Phys. 65, 3520 (1976).
11. N.C. Shivaprakash and J.S. Prasad, J.Chem.Phys. 76, 866 (1982).
12. P.J. Collings, J.Chem.Phys. 79, 3605 (1983).
13. M.E. Moseley, R. Poupko and Z. Luz, Mol.Cryst.Liq. Cryst. 95, 279 (1983).
14. Z. Yaniv, G. Chidichimo, N.A.P. Vaz, and J.W. Doane, Phys.Lett. 86A, 297 (1981).
15. G. Chidichimo, Z. Yaniv, N.A.P. Vaz and J.W. Doane, Phys.Rev.A, 25, 1077 (1982).
16. N.A.P. Vaz, G. Chidichimo, Z. Yaniv and J.W. Doane, Phys.Rev.A, 26, 637 (1982).
17. G. Karakostas and D.S. Moroi, Phys.Lett. 87A, 101 (1981).
18. D. Goldfarb, M.E. Moseley, M.M. Labes and Z. Luz, Mol.Cryst.Liq.Cryst. 89, 119 (1982).
19. E.T. Samulski and Z. Luz, J.Chem.Phys. 73, 142 (1980).
20. Z. Luz, R. Poupko and E.T. Samulski, J.Chem.Phys. 74, 5825 (1981).
21. C.L. Khetrapal, K.V. Ramanathan and M.R. Lakshminarayana (unpublished).
22. C.C. Costain, J.Chem.Phys. 29, 864 (1958).

Excerpts from letters

- from Erwin Hahn, University of California at Berkeley, He expressed his wish that the speech presented at the APS Meeting in April 1984, Washington, D.C. "be known to everybody in NMR" for the reason that although "the account is one which is somewhat personal,"..."yet gives a history of the discoveries which lead up to what NMR is today." The write up gives "the human side of how Felix Bloch was involved in the evolution of NMR."
- from Junkichi Sohma, Hokkaido University, Sapporo, Japan. Dr. Sohma's complete letter follows this section.
- from Pal Sohar, Pharmacochemical Works, Budapest, Hungary. A Bloch Memorial Lecture was presented by Dr. Sohar at the Analytical Conference of the Hungarian Chemical Society, and the introductory part will be published in "Magyar Kemikusok Lapja" in Hungarian. "A second Bloch Memorial Meeting was held at the Hungarian Academy of Sciences. A brief survey of F. Bloch's scientific activity was read by G. Varsanyi, Chairman of the Working Committee of Molecular Structure of the Hungarian Academy of Sciences."
- from Luigi G. Conti, University of Rome, Italy. Dr. Conti's complete letter appears at the end of this section.
- from Ioan Ursu, University of Bucharest, Romania. Dr. Ursu's letter also appears at the end of this section.
- from Riccardo Basosi, Enzo Tiezzi, and Gianni Valensin, University of Siena, Italy. "We would like to express our sincere condolences for Professor F. Bloch passing away and we strongly agree that his pioneer work in the magnetic resonance field deserves to be honoured with a tribute of lectures in all the universities where a strong program in magnetic resonance exists. With this in mind, we were able to get the Faculties of Sciences and Farmacy of the University of Sienna in sponsoring the organization of a commemorative lecture in honor of Felix Bloch with a proper introduction on his important contribution to the advancement of science."
- from Karol Maskos, University of Wroclaw, Poland. "I am glad to inform you that on June 12, this year we have organized /Polish Biophysical Society and Institute of Biochemistry University of Wroclaw/ a minisymposium in memory of Felix Bloch - The Felix Bloch NMR Symposium. There was about 80 participants of this meeting. Professor Jack W. Hennel from Krakow was talking about new methods in NMR i.e.: Zeugmatography and NMR in the zero-field and I gave the lecture on the history of the NMR phenomenon and the Felix Bloch works."

- from V.S. Murthy, Indian Institute of Technology, Madras, India. Dr. Murthy expressed with extreme sorrow the passing away of Professor Felix Bloch and informed us of plans for holding a one-day seminar in honor of F. Bloch on 15.9.1984.
- from C.L. Khetrapal, Indian Institute of Science, Bangalore, India and G. Govil, Tata Institute of Fundamental Research, Bombay, India. Dr. Khetrapal and Dr. Govil's write up of the inaugural lecture of the Winter School held in Bangalore is reprinted in full at the end of this section.
- from Yu Yu Samitov, Kazan State University, USSR. "I want to inform you that in one year time from Professor Felix Bloch death, one of the 1984 autumn meetings of Kazan State University (Magnetic Resonance Seminary, Yu Yu Samitov, Chairman) will be devoted to Professor Felix Bloch's Commemorative Lecture. Usually this seminary collects a lot of different academicians and students of the Institute of Kazan."
- from Xu Yuanzhi, Zhejiang University, Hangzhou, China. Dr. Yuanzhi's tribute to Professor Bloch appears after this section.
- from Alexander Tkac, Slovak Technical University, Bratislava, Czechoslovakia. Dr. Tkac's comments on the course dedicated to Felix Bloch appears after this section.
- from Artur Losche, Karl-Marx-University, Leipzig, German Democratic Republic. Dr. Losche's letter follows this section.

FACULTY OF ENGINEERING
HOKKAIDO UNIVERSITY
SAPPORO, 060 JAPAN

Jan. 11, 1984

Prof. D. Fiat
Chairman
International Society of
Magnetic Resonance
Medical Center,
University of Illinois
P. O. Box 6998
Chicago, Ill. 60680
U.S.A.

Dear Prof. Fiat:

In your letter dated of November 4, 1983 you suggested a Felix Bloch Commemorative Lecture held in a number of institutes and universities.

My colleagues in Japan and I were glad to take your suggestion and decided to have a Felix Bloch Commemorative Lecture in the 22nd NMR Symposium held in Kyoto 14-16 November 1983. Although NMR Symposium is not an institute, exactly speaking, the Symposium sponsored by Chemical Society of Japan and other academic institutions is the best organization for the Commemorative Lecture, we believe. We would like to ask you to admit the lecture given in the Symposium for commemoration of Bloch as the F. Bloch Commemorative Lecture.

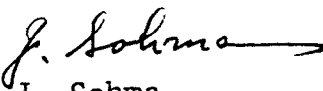
The lecture was given by Dr. Aporo Saika, Professor of chemistry, Kyoto University in the 2nd day of the 22nd NMR Symposium, 15 November 1983. The title was "Many-Body Perturbation Theoretic Study of Electron Correlation Effects on NMR Parameter".

Admitted as the Felix Bloch Commemorative Lecture in Japan, the lecture delivered by Professor Saika will be printed as a special issue of the Bulletin of Magnetic Resonance.

Please make a direct contact with Professor Saika on his manuscript of the lecture. His adress is as follows

Professor A. Saika
Faculty of Science
Kyoto University,
Kyoto 606, JAPAN

Sincerely yours,


J. Sohma



UNIVERSITÀ DEGLI STUDI DI ROMA
FACOLTÀ DI SCIENZE MATEMATICHE, FISICHE E NATURALI

ROMA, 31 May 1985
Città Universitaria - Tel. 490.324

ISTITUTO DI CHIMICA GENERALE ED INORGANICA

Professor Daniel Fiat
International Society of Magnetic Resonance
University of Illinois at Chicago
Health Sciences Center, MSA-E207, Box 6998
Chicago, Illinois 60680, U.S.A.

Dear Daniel,

In answer to your letter of 21 May, 1985, I'll try to give some details of the course I kept in the Spring of 1984 together with its motivation.

I was introduced to magnetic resonance by George Murray at Pennstate in 1959. He had just returned to the U.S. from Oxford, still fresh of his first European experience, and I was living fully my American adventure. In spite of his young age, George was already an expert both in high resolution and wide-line NMR. At that time I believed that NMR was just a technique, like X-ray diffraction and gas chromatography, fields already familiar to me. Very early I learnt that nuclear magnetism, especially solid-state NMR, embraced a large body of interdisciplinary physics, so that it could be considered the ideal subject in order for students to grasp the subtlety and variety of science.

My course "Physical Chemistry of Solids", dedicated to the memory of Felix Bloch, and given from February to April 1984 at the University of Rome for undergraduates and graduate students of Chemistry, Earth Sciences and Physics, was centered on magnetic resonance in solids. The course was conceived so that at the end of it the students could understand in all details some research work (not fully published yet!) done in the Institute of General Chemistry. To this end the course was divided into ten parts: mathematics, groups and crystallography, elasticity, dislocations, X-ray diffraction, NMR, diffusion and defect thermodynamics, magnetism, radiation effects, electron microscopy, and dependence of strain on crystal size. The chapter on the dependence of strain (or lattice parameter) on crystal size contained all the research work referred to above. The course ended with this chapter; the last section of it presented a short discussion of nuclear magnetism in small crystals. The course was thirty hours long (three hours a week). On the average ten references were given per chapter.

Hoping that this information can be useful to you, I remain

very sincerely yours

Luigi G. Conti

C.N.R. Senior Research Staff Member

Prof. Ioan Ursu,
National Council for Science and Technology
1, Piata Victoriei, 71202 Bucharest,
Romania

Prof. Daniel Fiat,
University of Illinois at Chicago
Medical Center, P.O. Box 6998
912 S. Wood St., 2nd Floor N.
60680 Chicago
U.S.A.

10 February, 1984

Dear Professor Fiat,

On March 17, the Romanian National Committee for Physics will hold a Felix Bloch Commemorative Session. I have it organized along your suggestion and also giving expression to my high esteem and praise for the NMR founder that I had the privilege to meet when in USA, in the fifties. In fact, I want to thank you for kindly inviting me to be a part in this international act of commemoration.

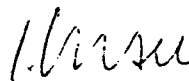
Enclosed is the lecture I intend to deliver on this occasion. I would be much gratified indeed if this could be published in the Bulletin of Magnetic Resonance, as you have told me. With this prospect in mind, and relying upon your opinion as colleague and friend, I am open to your appraisal of the paper and suggestions as to how to improve, if need will be, its ability to serve its purpose.

Please be informed that the revised manuscript of my paper "EPR of Uranium Ions" has been sent to Dr. David Gorenstein for publication, as we had agreed.

I hope this letter finds you in good health and as active as ever. I also hope you have received my previous letter, and am looking forward to hearing from you on the few matters raised there.

Wishing you all the best, I remain,

Sincerely yours,



Ioan Ursu

Felix Bloch Memorial Lecture

C.L. Khetrapal
Indian Institute of Science, Bangalore-560 012, India

and

G.Govil
Tata Institute of Fundamental Research, Bombay-400 005.

The International Society of Magnetic Resonance wrote to us to organise a Felix Bloch Memorial Lecture in honour of the "Father" of NMR during the year 1984. We felt that the most appropriate forum for such an event would be the XI International Conference on Magnetic Resonance in Biological systems held in Goa, India or its satellite event namely the Winter School on Biological Applications of Magnetic Resonance held in Bangalore during September 1984. Dr.E.D. Becker of the National Institutes of Health, Bethesda, Maryland, USA was approached to deliver such a lecture. Dr. Becker was kind enough to accept the invitation. Since the idea of such a lecture was to provide an overview of the development of NMR with special contributions of (the late) Professor Bloch, it was felt that the Winter School in Bangalore would be a better forum. It was felt that this would give an opportunity to the younger generation of Scientists from India and abroad to know about the developments and potentials of NMR.

Dr. Becker gave the lecture on September 25, 1984 at the Indian Indian Institute of Science, Bangalore, as the inaugural lecture of the Winter School. The title of the lecture was "Movement of NMR from physical phenomenon to chemistry, biology and medicine". Dr. Becker very nicely described the entire development of the field in about one hour. He started the lecture with the discovery of the phenomenon by Professor Bloch

and others and continued upto the latest developments including medical and the biomedical applications - He mentioned that NMR started as a technique in the hands of physicists for the precise determination of nuclear magnetic moments in mid 1940's, was potentially utilized by the chemists starting from 1950's, the biophysicists, biochemists, biologists and physicians joined the "gange" in 1970's with the developments of the Fourier-transform techniques, high field superconducting magnets, other advancements in the magnet technology and the availability of fast dedicated computers; the biomedical applications may dominate the field in the future.

The lecture was attended by about 150 scientists from India and abroad. The audience was heterogeneous group of scientists working in various branches of science including medicine. It provided an excellent opportunity to know about the developments and potentials of NMR in various branches of science.

THE GREAT SCIENTIST, PROFESSOR FELIX BLOCH
WILL LIVE TOGETHER WITH US FOREVER

Professor Felix Bloch, the great founder of NMR experiment and theory and the outstanding scientist has gone away with us for one year. We commemorate him with deep sorrow feelings and highest reverence.

Although no one of us who has seen him, yet any people who have only elementary knowledge of NMR, all know prof. F. Bloch to be the principal originator of magnetic resonance theory, and the earliest scientist discovering the phenomenon of NMR.

In recognition of his prominent contribution to NMR theory and its application, he was awarded the Nobel Prize in physics in 1952. He still untirely made his greatest contribution for development of magnetic resonance spectroscopy until his heart stopped to pulsate.

He left an unevaluable and precious wealth for us. When we are engaged in the research of magnetic resonance, the name of Bloch will always hover in our mind, whether in a smooth case or in a dilemma. His intellectual legacy has become a source of force to surmount the difficulty on the marching road of our research work.

Every time when I have a course of lectures on magnetic resonance, I always tell my students the brilliant name of F. Bloch, and praise his immortal exploit and achievement in magnetic resonance field, just as I lectured in the course of " Practical ESR Spectroscopy " at Qinghua University in 1983 and at Zhejiang University recently.

We Chinese colleagues mourn the greatest scientist, prof. F. Bloch. He will be lived in our heart forever.

Xu Yuanzhi
Prof. of physical Chemistry
Zhejiang University
Hangzhou, China.

SLOVENSKÁ VYSOKÁ ŠKOLA TECHNICKÁ V BRATISLAVE

NOSITEĽKA RADU REPUBLIKY

CHEMICKOTECHNOLOGICKÁ FAKULTA, Jánska ul. 1, 812 37 Bratislava
Katedra fyzikálnej chémie

Professor Daniel Fiat
Secretary General of ISMAR
University of Illinois at Chicago
Health Sciences Center
MSA-E207, P.O.Box 6998
Chicago, Illinois 60680
U.S.A.

Vaša značka

Naša značka

Vybavuje

Bratislava
January 23, 1985

Vec:

Dear Professor Fiat,

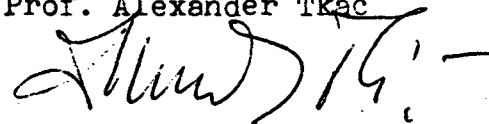
I thank you for the informing Bulletin concerning the activities of ISMAR in the last year. I can only add our modest contribution by organizing a two-term course of magnetic resonance fundamental theories for scientists and advanced students devoted to the memory of Professor Bloch. This course held at our Institute of Physical Chemistry of Slovak Technical University in Bratislava will be continued also in the next half-year. The lectures were delivered by our much experienced theoretical quantum chemist Dr. Peter Pelikán.

In the sence of your short comment - please consider this as my request for waiver of dues for the year 1985 /currency exchange difficulties/. Many thanks !

I wish to your admirable care of ISMAR much success and many creative ideas in the new year, and personally for you and your family good health and happiness.

Sincerely yours,

Prof. Alexander Tkáč



Prof. Dr. A. Lösche
Sektion Physik
Karl-Marx-Universität
DDR - 701 Leipzig
Linnéstraße 5

Leipzig, 29.1.1984.

Dr. Daniel Fiat
University of Illinois
Chicago Health Sciences Center
MSA-E207 P.O.Box 6998
Chicago, Illinois 60 680
U.S.A.

Dear Daniel,

I thank you very much for your New Year's Greetings and the informations concerning the ISMAR.

When I came back from an Ampere-Colloque ~~fr~~ on the isle of Crete, I heard that Felix Bloch died. We are very sad; we admire him because of his firmness at the beginning of the Hitler era and were hoping to see him once again in Leipzig. You know, that Bloch came to Leipzig, invited by Debye, who was before professor of theoretical physics in Zurich and got 1928 in Leipzig the chair of experimental physics. Bloch followed him but here he turned to Heisenberg and was one of his most famous students. Next year we have the 150 th anniversary of the foundation of the institute of physics at our university. At this occasion, we shall give a historical review of the last century, and also an appreciation of Felix Bloch.

With the best wishes for you and your family -I think good wishes are useful all over the year, not only at the beginning - I remain with

kind regards

sincerely yours

A. Lösche

Measurement of ^{13}C - ^{13}C coupling constants and a few other related methods in high resolution NMR spectroscopy for the direct determination of topology of unknown organic molecules in solution

by A. Neszmélyi

Central Research Institute for Chemistry,
Hungarian Academy of Sciences,
H-1025 Budapest, Pusztaszeri ut 59/67, Hungary

Abstract of the lecture given memoriam F. Bloch,
on 12 April 1984.

After 40 year of its discovery, NMR measurements -both for liquids and solid samples in the high resolution mode - are based on sophisticated pulse sequences realized under computer control on high field, superconducting-magnet spectrometers.

These experimental conditions are drastically different from those of the early pioneering times in NMR, still the theoretical description and simulation of a specific NMR experiment by modern density matrix methods is very close in its conception to the original ideas of F. Bloch formulated first in his famous equations.

Unparalleled in the history of spectroscopy, high resolution NMR was the first method enabling us to measure molecular connectivity in a direct way using naturally labelled compounds in ^{13}C -NMR. In cases where X-ray techniques is not applicable the $^1\text{J}_{\text{CC}}$ network and the related relayed coherence transfer mechanism is the only way to choose for unknown organic structures if simpler methods fail. Results of the author have been also reported.

Up-to-date NMR-techniques in structure determination.

P. Sohár

EGIS Pharmaceuticals, Spectroscopic Department, H-1475
Budapest, P.O.Box 100, Hungary

Abstract of the commemorative lecture dedicated to the memory
of Felix Bloch, on 12 April 1984.

By the spread of computer controlled high field FT spectrometers equipped with superconducting magnets and using complex pulse trains for getting high resolution spectra, NMR spectroscopy reborn in the last decade reinforcing its fundamental importance in the research of chemical structure determination. Some of the earlier techniques of NMR that were generally inaccessible, became routine nowadays and completely new methods were developed. The present paper surveys some of the up-to-date NMR methods commonly used for structure elucidation in organic chemistry, using examples from the authors' own works.

1. Gated heteronuclear double resonance (DR) were used for measuring carbon-hydrogen coupling constants without loss of intensity enhancement by NOE. On the basis of high direct $^1J(C,H)$ values (see Fig.1.) the structure of compound 1 containing cyclopropyl ring was proved, which formed unexpectedly upon 1,5-addition in the following reaction instead of 2 (1,2-adduct) or of 3 (ring closing product of 2).

2. Homonuclear DR experiment (Fig. 2) made possible the correct assignment of 5,8, 4,4' and 6,7 signal pairs of compound 4 and consequently the determination of its endo-endo configuration and preferred conformation containing a more shielded equatorial proton in Pos. 4. relative to its axial pair H-4'. This unusual relation between geminal cyclohexil-like proton shifts may be caused by the anisotropy of the phenyl ring in the preferred conformation [1].

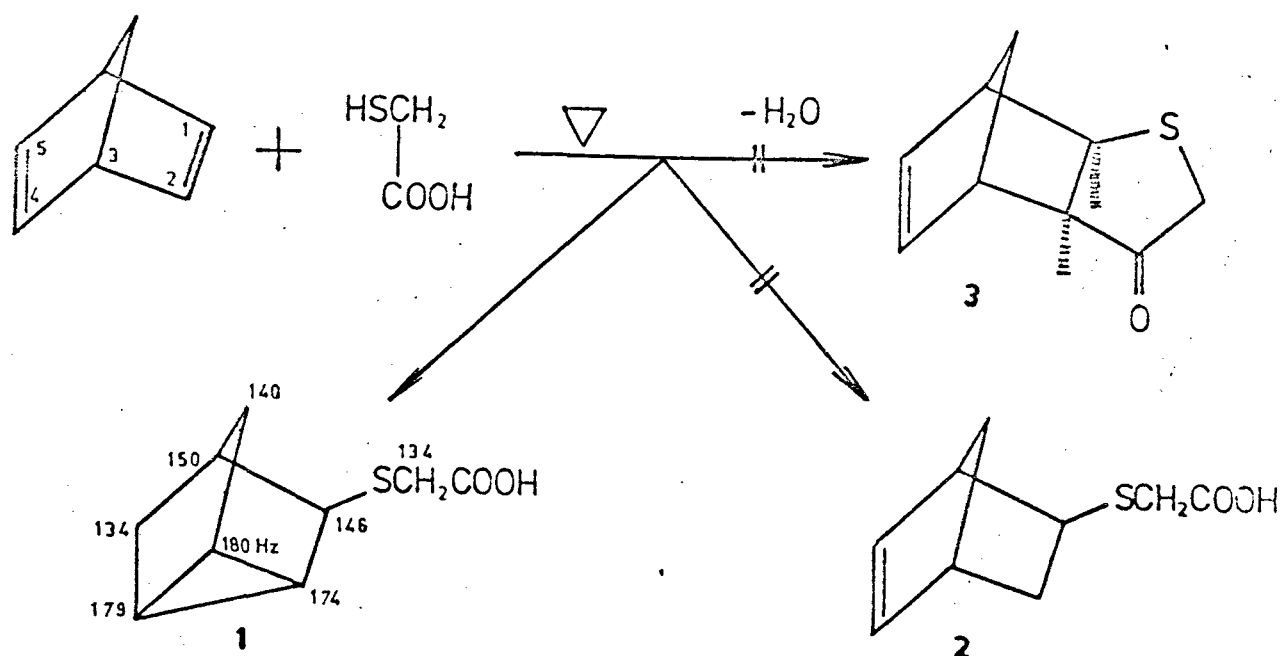


Fig. 1. Synthesis of compound 1 and the $^1\text{J}(\text{C},\text{H})$ coupling constants in Hz.

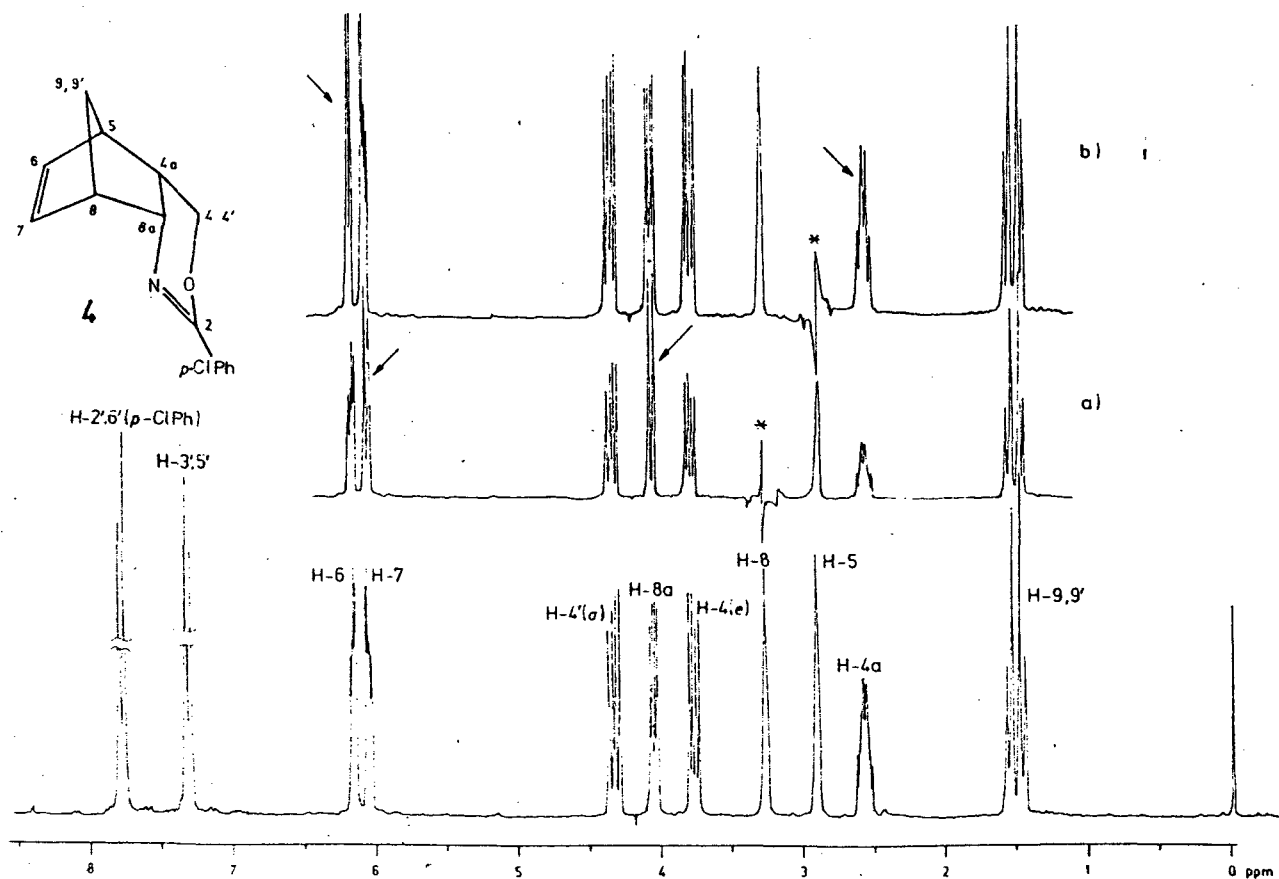


Fig. 2. ^1H NMR spectrum of 4 at 250 MHz. Double resonance spectra, saturating the $\text{H}-8$ (a) and $\text{H}-5$ (b) signals, respectively.
* Saturated signal; / signal changed by saturation.

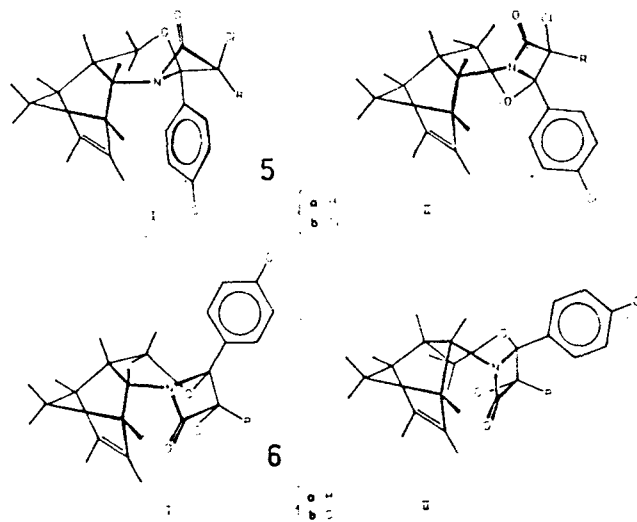


Fig. 3. Stable conformers of compounds 5 and 6.

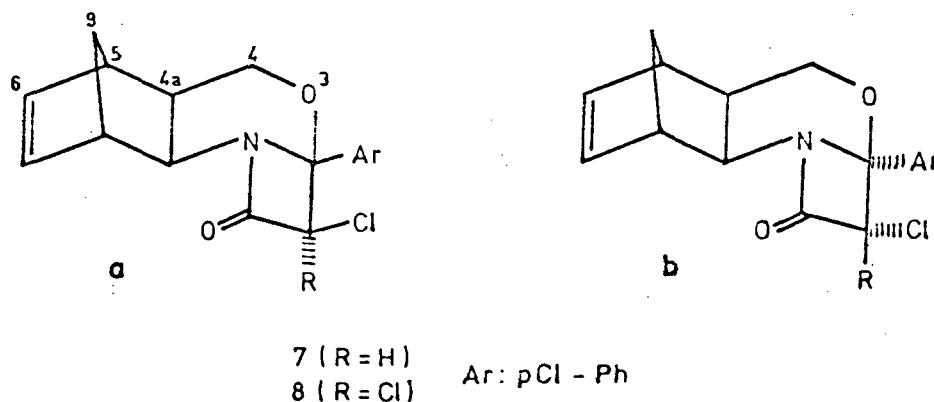


Fig. 4. Stereostructure of diastereomeric azetidinones 7a,b and 8a,b.

3. Stereostructure (Fig. 3) of anellation isomeric β -laktams 5,6 prepared from the reaction of 4 with chloro- and dichloro-acetyl chlorid were determined making use of differential NOE (DNOE) measurements [1]. In case of 7 and 8 analogues (Fig. 4) the main component was isolated from the two-component product of the cycloaddition. The computer of the Bruker WM-250 FT-spectrometer was utilized and the spectra of the pure main-products multiplied by an appropriate factor were subtracted from the spectra of the isomeric mixtures, to obtain the spectra of the minor components. The spectrum parameters derived in this way enabled to clear the configuration and conformation of the individual diastereomeric azetidinones 7a,b and 8a,b [2].

4. DEPT experiment made possible to identify solvent peak overlapped carbon resonance lines e.g. for compound 9 and

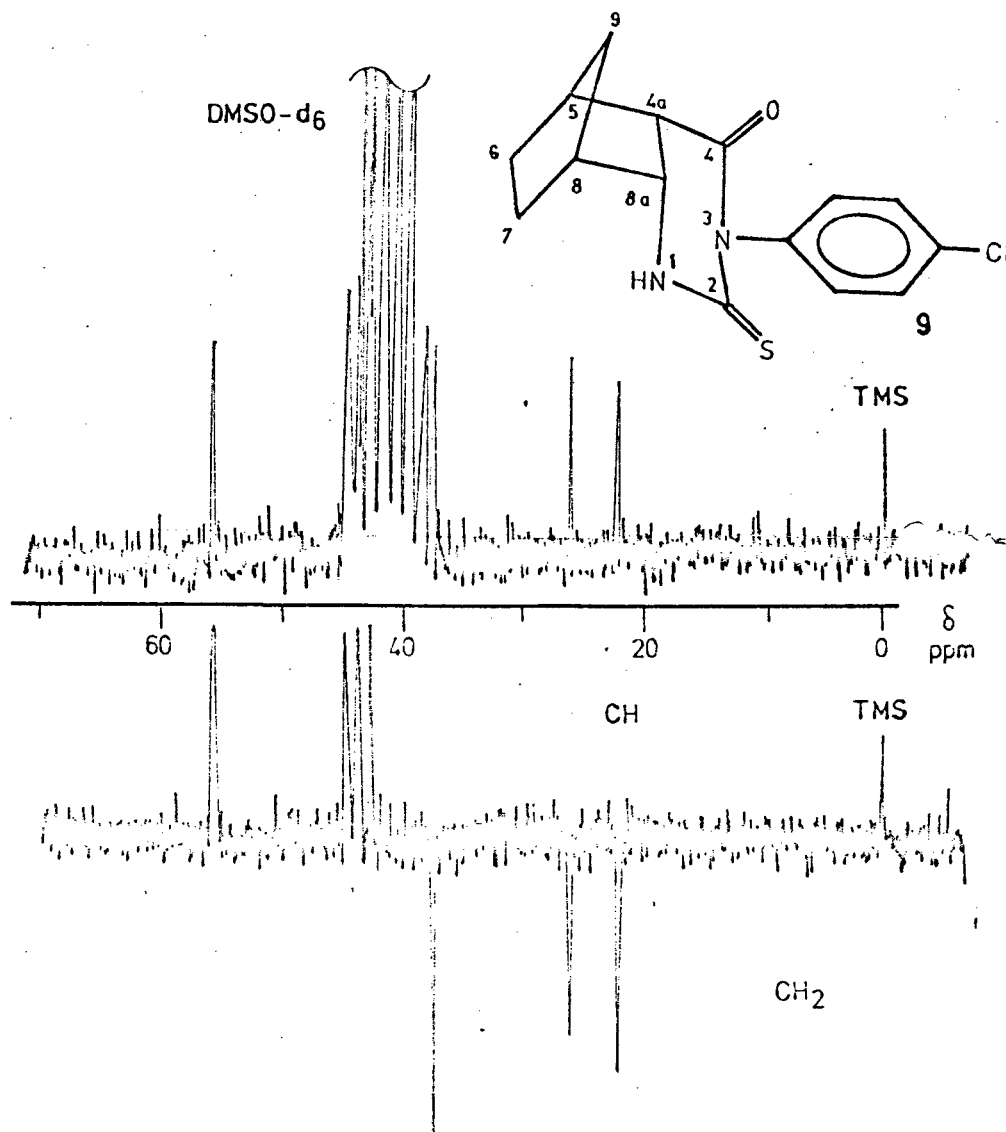


Fig. 5. The ^{13}C NMR spectrum of compound 9 and the DEPT experiment.

simultaneously to prove the assignments of individual lines by stating the order of the corresponding carbon atoms (Fig.5).

5. The structure of 1:3;2:4;5:6-tri-O-isopropylidene-D-glucitol (10), which was proposed earlier to be the 1:2,3:5,4:6-analogue, was re-determined by ^1H NMR measurement at 250 MHz [3]. The assignment were proved by DR experiments. Using the spectral parameters as starting values, the theoretical spectrum of the eight skeletal protons was constructed and the chemical shifts and proton-proton coupling constants were calculated by iteration (RMS: 0.014) using the PANIC program of Bruker AG. The good agreement for the calculated and experimental spectra can be seen from Fig. 6.

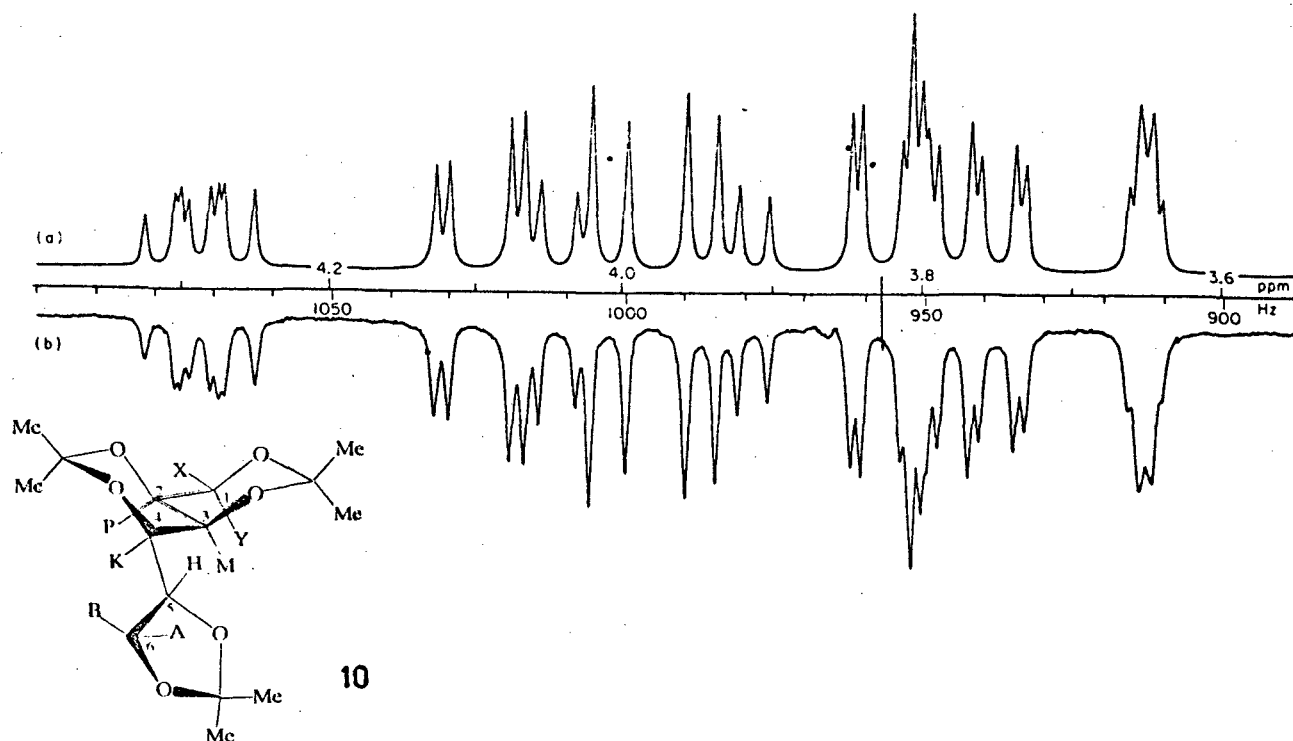


Fig. 6. (a) Calculated and (b) experimental ^1H NMR spectra of the skeletal protons in compound 10. For the calculated spectrum, after four iteration cycles, a line width of 0.7 Hz was applied for constructing a Lorentzian line-shape spectrum.

6. Cinnamaldehyde and nitroethanol give a cyclic hemiacetal, which exists as a mixture of two diastereomers. After dissolving in CDCl_3 the ratio of the components changes from approximately 10:1 to 3:2 in a few days. The ethyl acetal of this hemiacetal (11) is stereohomogeneous, and the ethoxy group is axial to the pyran ring owing to the anomeric effect. This configuration was proved by two-dimensional NMR measurement [4] permitting separate observation of the originally overlapping multiplets and direct reading the proton-proton coupling constants (Fig. 7).

REFERENCES

1. P. Sohár, G. Stájer and G. Bernáth.: Configuration and NMR Study of Tricyclic Oxazines Fused to a Norbornene or Norbornane Skeleton. *Org. Magn. Resonance*, 21, 512. (1983).
2. P. Sohár, G. Stájer, I. Pelczer, A. E. Szabó, J. Szúnyog and G. Bernáth.: Synthesis and NMR study of Norbornane/Norbornene-fused Tetracyclic Azetidinones. *Tetrahedron*, In Press.
3. P. Sohár and J. Kuszmann.: Reinvestigation of the Structure of 1:3,2:4,5:6-Tri-O-isopropylidene-D-glucitol by ^1H NMR Spectroscopy at 250 MHz. *Org. Magn. Resonance*, 21, 694 (1983).

4. P. Sohár, Gy. Mikite, I. Pelczer, Á. Kovács and A. Kis-Tamás.:
 Configurational Analysis of Diastereomeric Open-Chain and
 Cyclic Nitro-Substituted Diols by NMR Spectroscopy.
 Org. Magn. Resonance, 22, 710 (1984).

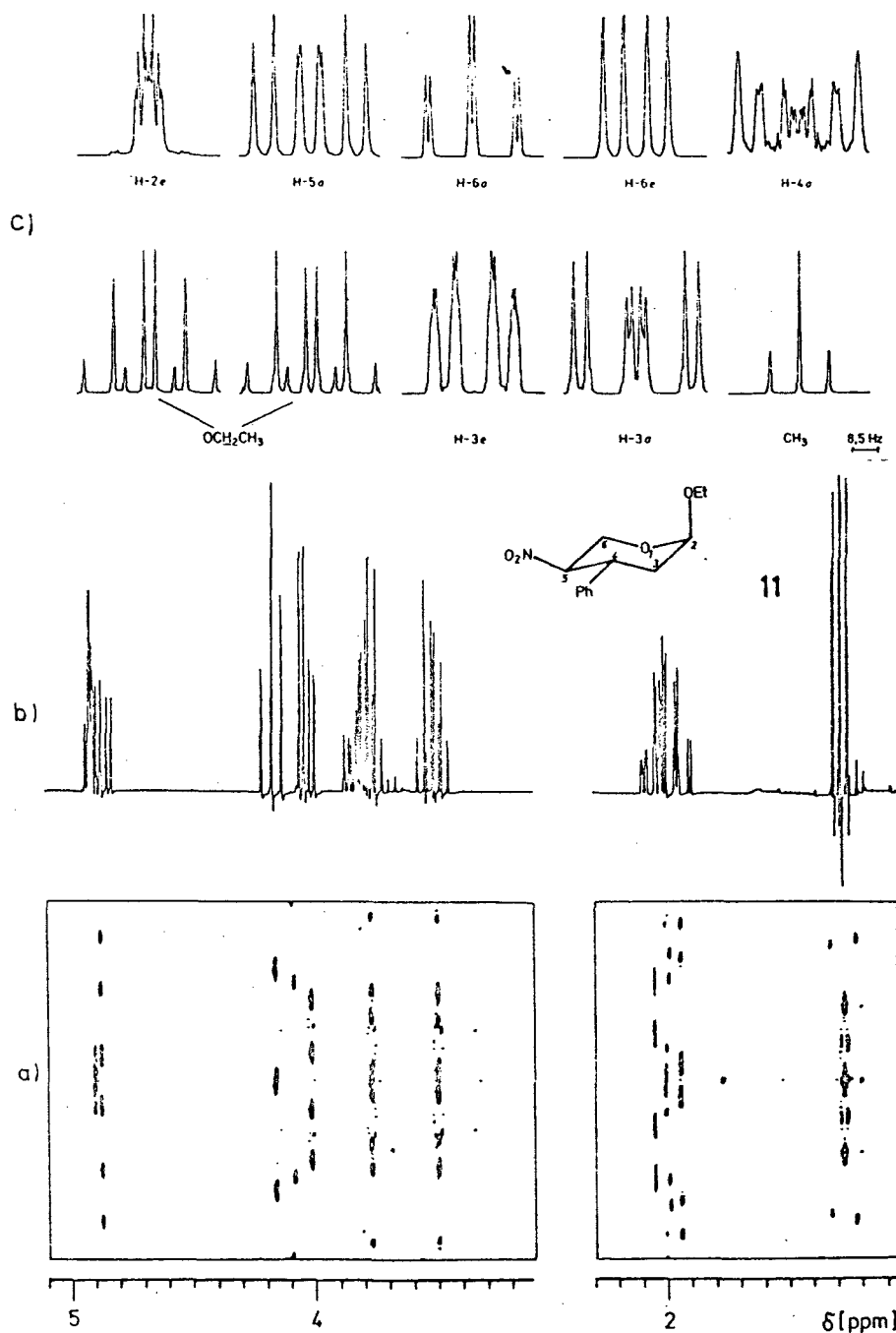


Fig. 7. (a) J-resolved ^1H 2D NMR spectrum of compound 11 at 250 MHz; (b) resolution-enhanced 1D spectrum with partly overlapping multiplets; (c) Cross-section (columns) of the 2D matrix from the J-resolved ^1H 2D NMR spectrum (separated multiplets of the individual hydrogens).

CALENDER OF FORTHCOMING CONFERENCES IN MAGNETIC RESONANCE

November 15-18, 1985 **FIRST BEIJING CONFERENCE and EXHIBITION on INSTRUMENTAL ANALYSIS**, will be held in Beijing, China. The exhibition will be held November 16-25, 1985. The conference and exhibition sponsored by five chinese academic societies including Spectroscopy at Radio and Microwave Frequencies will hold symposia on NMR, EPR, NQR, Double Resonance, and Multiple Quantum Resonance as well as other aspects of instrumentation. Abstracts should be submitted by March 31, 1985. For further information please contact:

Secretariat of First
Beijing Conference and
Exhibition on
Instrumental Analysis
Room 912
Xi Yuan Hotel
Beijing, China
Tel. 890721 Ext. 912

June 29-July 5, 1986 **NINTH MEETING of the INTERNATIONAL SOCIETY OF MAGNETIC RESONANCE** will be

held at the Hotel Gloria, Rio de Janeiro, Brazil. The meeting will cover the broad field of magnetic resonance, including the theory and practice of nuclear magnetic resonance, electron paramagnetic resonance and nuclear quadrupole resonance spectroscopy. Included will be applications in physics, chemistry, biology and medicine. The meeting will strive to foster interaction among scientists in different fields of magnetic resonance and to encourage interdisciplinary exploration. Information may be obtained from

Dr. Ney Vernon Vugman
Instituto de Fisica
Universidade Federal de Rio de Janeiro
Cicade Univeritaria
Bloco A - CCMN
Rio de Janeiro 21945
Brazil

The editor would be pleased to receive notices of future meetings in the field of magnetic resonance so that they could be recorded in this column.

NEW BOOKS

NMR and Macromolecules. ACS Symposium Series 247. James C. Randall, editor. xiv+280 pages. American can Chemical Society, 1155 16th St., N.W., Washington, D.C. 20036. 1984. \$34.95.

NMR of Newly Accessible Nuclei, Vol. 1 and 2. Pierre Laslo editor. xviii+298 and 436 pages respectively. Academic Press, 11 Fifth Ave., New York, N.Y. 10003. 1983. Vol. 1 \$59; Vol. 2 \$65.

Theory of NMR Parameters, I. Ando and G. A. Webb. 217 pages. Academic Press, New York. 1983. \$52.

Nuclear Magnetic Resonance Spectroscopy, R. K. Harris, xx+250 pages. Pitman Books, 128 Long Acre, London, WC2E 9AN. 1983.

Phosphorus-31 NMR: Principles and

Applications, D. G. Gorenstein, editor. xiv+604 pages. Academic Press, Orlando, Florida 32887. 1984. \$79.00.

Correlative Neuroanatomy of Computed Tomography and Magnetic Resonance Imaging, J. de Groot, with Catherine M. Mills, Line drawings by L. Lyons. xii+248 pp., Lea and Febiger, Philadelphia, \$45.

Nuclear Magnetic Resonance (NMR), M. A. Hopf & F. W. Smith (Progress in Nuclear Medicine: Vol. 8) viii+248 pp., S. Karger. 1984. \$90.

NMR Spectroscopy, Vol. III, Pal Sohad, Ed. 368 pp. CRC Press. 1984.

Magnetic Resonance: Introduction, Advanced Topics & Applications to Fossil Fuels, L. Petrakis & J. P. Fraissard, eds. Reidel Press (Holland). 1984. \$98.00.

INSTRUCTIONS FOR AUTHORS

Because of the ever increasing difficulty of keeping up with the literature there is a growing need for critical, balanced reviews covering well-defined areas of magnetic resonance. To be useful these must be written at a level that can be comprehended by workers in related fields, although it is not the intention thereby to restrict the depth of the review. In order to reduce the amount of time authors must spend in writing we will encourage short, concise reviews, the main object of which is to inform nonexperts about recent developments in interesting aspects of magnetic resonance.

The editor and members of the editorial board invite reviews from authorities on subjects of current interest. Unsolicited reviews may also be accepted, but prospective authors are requested to contact the editor prior to writing in order to avoid duplication of effort. Reviews will be subject to critical scrutiny by experts in the field and must be submitted in English. Manuscripts should be sent to the editor, Dr. David G. Gorenstein, Chemistry Department, University of Illinois at Chicago, Box 4348, Chicago, Illinois, 60680, USA.

MANUSCRIPTS must be submitted in triplicate (one copy should be the original), on approximately 22 x 28 cm paper, typewritten on one side of the paper, and double spaced throughout. If the manuscript cannot be submitted on computer tapes, floppy disks, or electronically (see below), please type with a carbon ribbon using either courier 10 or 12, gothic 12, or prestige elite type face with 10 or 12 pitch. All pages are to be numbered consecutively, including references, tables, and captions to figures, which are to be placed at the end of the review.

ARRANGEMENT: Considerable thought should be given to a logical ordering of the subject matter and the review should be divided into appropriate major sections, sections, and subsections, using Roman numerals, capital letters, and Arabic numerals respectively. A table of contents should be included.

TABLES: These are to be numbered consecutively in the text with Arabic numerals. Their place of insertion should be mentioned in the

text, but they are to be placed in order at the end of the paper, each typed on a separate sheet. Each table should be supplied with a title. Footnotes to tables should be placed consecutively, using lower case letters as superscripts.

FIGURES are also to be numbered consecutively using Arabic numerals and the place of insertion mentioned in the manuscript. The figures are to be grouped in order at the end of the text and should be clearly marked along the edge or on the back with figure number and authors' names. Each figure should bear a caption, and these should be arranged in order and placed at the end of the text. Figures should be carefully prepared in black ink to draftsman's standards with proper care to lettering (typewritten or freehand lettering is not acceptable). Graphs should include numerical scales and units on both axes, and all figures and lettering should be large enough to be legible after reduction by 50-60%. Figures should be generally placed on sheets of the same size as the typescript and larger originals may be handled by supplying high-contrast photographic reductions. One set of original figures must be supplied; reproduction cannot be made from photocopies. Two additional copies of each figure are required. Complex molecular formula should be supplied as ink drawings.

REFERENCES to the literature should be cited in order of appearance in the text by numbers on the line, in parentheses. The reference list is to be placed on separate sheets in numerical order at the end of the paper. References to journals should follow the order: author's (or authors') initials, name, name of journal, volume number, page, and year of publication. The abbreviation of the journal follows that used in the Chemical Abstracts Service Source Index. Reference to books should include in order: author's (or authors') initials, name, title of book, volume, edition if other than the first, publisher, address, date of publication, and pages.

FOOTNOTES should be used sparingly and only in those cases in which the insertion of the information in the text would break the train of thought. Their position in the text should be marked with a superscript Arabic numeral and the footnote should be typed at the bottom of the

relevant page in the text, separated from the latter by a line.

SYMBOLS AND ABBREVIATIONS: Mathematical symbols should be typewritten wherever possible. Greek letters should be identified in pencil in the margin. In reviews containing a number of mathematical equations and symbols, the author is urged to supply a list of these on a separate sheet for the assistance of the printer; this will not appear in print. Standard abbreviations will follow the American Chemical Society's **HANDBOOK FOR AUTHORS** names and symbols for units.

PERMISSIONS: It is the responsibility of the author to obtain all permissions concerned with the reproduction of figures, tables, etc, from copyrighted publications. Written permission must be obtained from the publisher (not the author or editor) of the journal or book. The publication from which the figure or table is taken must be referred to in the reference list and due acknowl-

edgement made, e.g., reprinted by permission from ref. (00).

REPRINTS: Thirty reprints of a review will be supplied free to its senior author and additional reprints may be purchased in lots of 100

INSTRUCTIONS FOR SUBMITTING MANUSCRIPTS ON COMPUTER TAPES, FLOPPY DISKS OR ELECTRONICALLY: If you have used a word processor to type your manuscript, please forward your manuscript after review and revision, in a computer readable form. Tape should be unlabeled, in a standard IBM format, 1600 BPI, 80x80 blocks and ASCII image. Floppy disks readable on IBM, PDP 11, or MacIntosh personal computers are also acceptable. For direct submission over the phone lines use either 300 or 1200 baud ASCII transmission. Additional details will be provided for the appropriate hand-shake requirements. Please supply us with the code for interpreting superscripts, greeks, etc. on your word processor.

PAPERS TO APPEAR IN SUBSEQUENT ISSUES

Application of Lanthanide Shift Reagents in NMR-Spectroscopy for Studying Organophosphorus Compounds, B. I. Ionin, V. I. Zakharov, and G. A. Berkova, Leningrad Lenseviet Institute of Technology, Leningrad, USSR.

2-Dimensional NMR Spectroscopy of Proteins, J. Markley, Purdue University, West Lafayette, Indiana, U.S.A.

Electron Spin Echo Method as Used to Analyze Spatial Distribution of Paramagnetic Centers, A. M. Raitsimring and K. M. Salikhov, Institute of Chemical Kinetics and Combustion, USSR.

In Vivo Applications of ^{19}F NMR Spectroscopy and Imaging, Alice M. Wyrwicz, University of Illinois, Chicago, Illinois, USA.

EPR Imaging, L. J. Berliner, The Ohio State University, Columbus, Ohio, U.S.A.

NMR-Chemical Microscopy, Laurance D. Hall, University of Cambridge School of Clinical Medicine, Cambridge, England

A Simple Description of 2-D NMR, A. Bax,

National Institutes of Health, Bethesda, Maryland, U.S.A.

NMR Studies of Specific Protein Nucleic Acid Interactions, P. Lu, University of Pennsylvania, Philadelphia, Pennsylvania, U.S.A.

NMR Studies of Drug Nucleic Acid Complexes, T. Krugh, University of Rochester, Rochester, New York, U.S.A.

EPR in Pulsed Magnetic Fields, S. J. Witters, University of Leuven, Leuven, Belgium.

^{13}C and ^1H NMR of Intact Tissue, M. Barany and A. Carlos, University of Illinois, Chicago, Illinois, U.S.A.

Proton Detected Heteronuclear NMR, D. Cowburn, Rockefeller University, New York, New York, U.S.A.

Modern Pulse Techniques and their Application in High Resolution NMR, R. Benn, Max-Planck-Institut für Kohlenfoischung, Mulheim, West Germany.

BULLETIN OF MAGNETIC RESONANCE

*The Quarterly Review Journal of the
International Society of Magnetic Resonance*

VOLUME 7

DECEMBER, 1985

NUMBER 4

CONTENTS

A SIMPLE DESCRIPTION, OF TWO - DIMENSIONAL NMR SPECTROSCOPY, A. BAX	167
ELECTRON SPIN ECHO METHOD AS USED TO ANALYZE THE SPATIAL DISTRIBUTION OF PARAMAGNETIC CENTERS, A. M. RAITSIMRING AND K. M. SALIKHOV	184
INSTRUCTIONS FOR AUTHORS	218

BULLETIN OF MAGNETIC RESONANCE

*The Quarterly Review Journal of the
International Society of Magnetic Resonance*

Editor:

DAVID G. GORENSTEIN

*Department of Chemistry
Purdue University
W. Lafayette, Indiana 47907
U.S.A*

Editorial Board:

E.R. ANDREW

*University of Florida
Gainesville, Florida, U.S.A.*

DAVID GRANT

*University of Utah
Salt Lake City, Utah, U.S.A.*

ROBERT BLINC

*E. Kardelj University of Ljubljana
Ljubljana, Yugoslavia*

JOHN MARKLEY

*University of Wisconsin
Madison, Wisconsin, U.S.A.*

H. CHIHARA

*Osaka University
Toyonaka, Japan*

MICHAEL PINTAR

*University of Waterloo
Waterloo, Ontario, Canada*

GARETH R. EATON

*University of Denver
Denver, Colorado, U.S.A.*

CHARLES P. POOLE, JR.

*University of South Carolina
Columbia, South Carolina, U.S.A.*

DANIEL FIAT

*University of Illinois at Chicago
Chicago, Illinois, U.S.A.*

JAKOB SMIDT

*Technische Hogeschool Delft
Delft, The Netherlands*

SHIZUO FUJIWARA

*University of Tokyo
Bunkyo-Ku, Tokyo, Japan*

BRIAN SYKES

*University of Alberta
Edmonton, Alberta, Canada*

The *Bulletin of Magnetic Resonance* is a quarterly review journal sponsored by the International Society of Magnetic Resonance. Reviews cover all parts of the broad field of magnetic resonance, viz., the theory and practice of nuclear magnetic resonance, electron paramagnetic resonance, and nuclear quadrupole resonance spectroscopy including applications in physics, chemistry, biology, and medicine. The *BULLETIN* also acts as a house journal for the International Society of Magnetic Resonance.

CODEN: BUMRDT

ISSN: 0163-559X

Bulletin of Magnetic Resonance, The Quarterly Journal of the International Society of Magnetic Resonance. Copyright © 1985 by the International Society of Magnetic Resonance. Rates: Libraries and non-members of ISMAR. \$60.00, members of ISMAR, \$18.00. All subscriptions are for a volume year. All rights reserved. No part of this journal may be reproduced in any form for any purpose or by any means, abstracted, or entered into any data base, electronic or otherwise, without specific permission in writing from the publisher.

Council of the International Society of Magnetic Resonance

E.R. ANDREW, President

C.P. SLICHTER, Vice President

D. FIAT, Secretary-General and Founding Chairman

C.P. POOLE, Jr., Treasurer

E.R. ANDREW
Gainesville

G.J. BENE
Geneve

R. BLINC
Ljubljana

M. BLOOM
Vancouver

W.S. BREY, JR.
Gainesville

V. BYSTROV
Moscow

F. CONTI
Rome

R.R. ERNST
Zurich

D. FIAT
Chicago

S. FORSEN
Lund

S. FUJIWARA
Urawa

M. GOLDMAN
Gif sur Yvette

H.S. GUTOWSKY
Urbana

R.K. HARRIS
Durham

K.H. HAUSSER
Heidelberg

J. HENNEL
Krakow

O. JARDETSKY
Stanford

J. JEENER
Brussels

V.J. KOWALEWSKI
Buenos Aires

P.C. LAUTERBUR
Stony Brook

E. LIPPMAN
Tallin

A. LOSCHE
Leipzig

P.T. NARASIMHAN
Kanpur

D. NORBERG
St. Louis

H. PFEIFER
Leipzig

W. von PHILIPSBORN
Zurich

A. PINES
Berkeley

L.W. REEVES
Waterloo

R. RICHARDS
Oxford

J. D. ROBERTS
Altadena

J. SMIDT
Delft

J. STANKOWSKY
Poznan

I. URSU
Bucharest

N.V. VUGMAN
Rio de Janeiro

H.C. WOLF
Stuttgart

The aims of the International Society of Magnetic Resonance are to advance and diffuse knowledge of magnetic resonance and its applications in physics, chemistry, biology, and medicine, and to encourage and develop international contacts between scientists.

The Society sponsors international meetings and schools in magnetic resonance and its applications and publishes the quarterly review journal, *The Bulletin of Magnetic Resonance*, the house journal of ISMAR.

The annual fee for ISMAR membership is \$20 plus \$18 for a member subscription to the *Bulletin of Magnetic Resonance*.

Send subscription to:
International Society of Magnetic Resonance
Professor Charles P. Poole, Jr.
Treasurer
Department of Physics & Astronomy
University of South Carolina
Columbia, South Carolina 29208 U.S.A.

A SIMPLE DESCRIPTION OF TWO-DIMENSIONAL NMR SPECTROSCOPY*

Ad Bax

Laboratory of Chemical Physics
National Institute of Arthritis, Diabetes
and Digestive and Kidney Diseases
National Institutes of Health
Bethesda, Maryland 20205, USA

	Page
I. Introduction	167
A. Sampling Frequency and Sensitivity	168
B. Lineshapes and Transform Techniques	170
C. Two-dimensional Quadrature and Absorption Mode	172
D. Coherence Transfer by Means of Radiofrequency Pulses	173
II. Homonuclear Shift Correlation through Scalar Coupling	175
III. Homonuclear Chemical Shift Correlation through Cross Relaxation	177
IV. Indirect Detection of ^{15}N through Multiple Quantum Coherence	178
V. Discussion	182
References	182

I. INTRODUCTION

The concept of two-dimensional (2D) Fourier transformation in NMR was first introduced by Jeener (1) in 1971. Since that time, several hundred different 2D pulse schemes have been proposed in the literature. The selection of experiments that will be described is based on the insight they provide into the basis and generality of 2D NMR, and also on the importance for solving the most common types of problems.

The experiments that will be described here are (a) 2D homonuclear shift correlation through scalar coupling (COSY), (b) 2D cross relaxation spectroscopy based on the nuclear Overhauser effect (NOESY) and (c) heteronuclear chemical shift correlation of ^1H and ^{15}N chemical shifts

through multiple quantum coherence.

Before addressing those experiments, an introduction into the principles and general aspects of two-dimensional NMR will be presented. The original 2D experiment, proposed by Jeener (1), will be discussed for the simple case of non-coupled nuclear spins, for example, the protons in chloroform. This will illustrate how a 2D Fourier transformation is accomplished and also which type of data presentation (absorptive / dispersive / absolute value) is generally preferable. Jeener's original sequence is depicted in Figure 1. At the end of the preparation period, which is sufficiently long to establish a (close to) thermal equilibrium situation, a 90° pulse applied along the $-y$ axis of the rotating frame (90° $-y$ pulse) rotates the magnetization to a position parallel to the x axis (Figure 2a). The system then evolves (usually in an unperturbed fashion) for a time t_1 , which is generally referred to as the evolution period. During this period the magnetization rotates through an angle $\Omega_1 t_1$, where Ω_1 is the angular rotation frequency of the magnetization considered (Figure 2b). At the end

*Part of this manuscript has been published in the proceedings of the *NATO Advanced Study Institute on NMR in Living Systems*, Sicily, Italy, 1984.

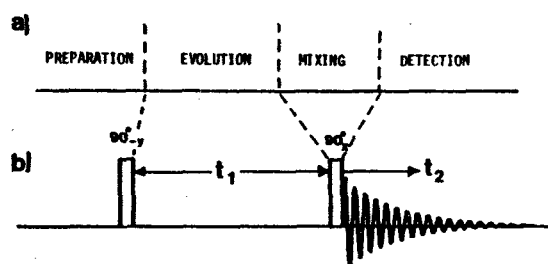


Figure 1. (a) General subdivision of the time axis of a two-dimensional NMR experiment. (b) Pulse scheme of the Jeener experiment.

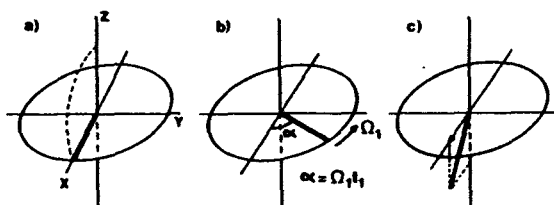


Figure 2. Evolution of the magnetization of a set of isolated spins during the pulse scheme of Figure 1b. (a) The 90°_y pulse rotates the z magnetization to the x axis. (b) During the evolution period, t_1 , the magnetization rotates through an angle $\alpha = \Omega_1 t_1$; (c) The second 90° pulse rotates the transverse magnetization into the xz plane, leaving a transverse component proportional to $\cos(\alpha)$ parallel to the x axis.

of the evolution period, a 90°_x pulse rotates the magnetization into the xz plane (Figure 2c). At this point in time a transverse component proportional to $\cos(\Omega_1 t_1)$ is left parallel to the x axis of the rotating frame. During the detection period, t_2 , a signal $s(t_1, t_2)$ will be detected that is proportional in amplitude to $\cos(\Omega_1 t_1)$. If quadrature detection is employed during the detection period, the signal is described by:

$$s(t_1, t_2) = M_0 \cos(\Omega_1 t_1) \times$$

$$\exp(i\Omega_2 t_2) \exp(-t_1/T_2^{(1)}) \exp(-t_2/T_2^{(2)}) \quad (1)$$

where Ω_1 and Ω_2 denote the angular frequencies of the magnetization during the times t_1 and t_2 , respectively. $T_2^{(1)}$ and $T_2^{(2)}$ are the decay constants of the magnetization during the times t_1 and t_2 . Of course, in this simple experiment, $\Omega_1 = \Omega_2$ and $T_2^{(1)} = T_2^{(2)}$. However in many other experiments this is not necessarily the case, and therefore different labels are used.

Fourier transformation with respect to t_2 of the FID's acquired for the various t_1 values gives a set of spectra with amplitude proportional to $\cos(\Omega_1 t_1)$:

$$s(t_1, \omega_2) = M_0 \cos(\Omega_1 t_1) [A_2(\omega_2) + iD_2(\omega_2)] \exp(-t_1/T_2^{(1)}) \quad (2)$$

where $A_2(\omega_2)$ and $D_2(\omega_2)$ are the absorptive and dispersive parts of the resonance, given by

$$A_2(\omega_2) = T_2^{(2)} / \{1 + [T_2^{(2)}(\omega_2 - \Omega_2)]^2\} \quad (3a)$$

$$D_2(\omega_2) = T_2^{(2)}(\omega_2 - \Omega_2) A_2(\omega_2) \quad (3b)$$

The absorptive parts of a set of those spectra, obtained for different values of t_1 , are sketched in Figure 3a. Cross sections parallel to the t_1 axis through the data matrix of Figure 3a show a cosine modulation with angular frequency Ω_1 , if taken near $\omega_2 = \Omega_2$, and consist of near zero intensity for other ω_2 values. Usually the data matrix of Figure 3a is transposed in the computer memory, in order to facilitate a Fourier transformation with respect to t_1 (Figure 3b). Fourier transformation of those t_1 sections, generally referred to as *interferograms* (2), gives the final 2D spectrum, shown in Figure 3c. Usually such a spectrum is presented as a contour plot (Figure 3d), rather than a stacked line representation, since this simplifies measuring coordinates of the resonance and avoids the possibility of low intensity resonances to be hidden behind intense resonances.

A. Sampling Frequency and Sensitivity

In conventional one-dimensional Fourier transform NMR experiments, the spectral width after Fourier transformation equals $1/(2\Delta t)$, or $\pm 1/(2\Delta t)$ in the case of complex Fourier transformation, where Δt is the time between sampling points. Analogously, if consecutive t_1

values are separated by an amount Δt_1 , this will give a spectral width equal to $1/(2\Delta t_1)$ after Fourier transformation with respect to t_1 .

In a regular one-dimensional Fourier transform experiment, the signal-to-noise ratio for a single time-domain data point can be very poor;

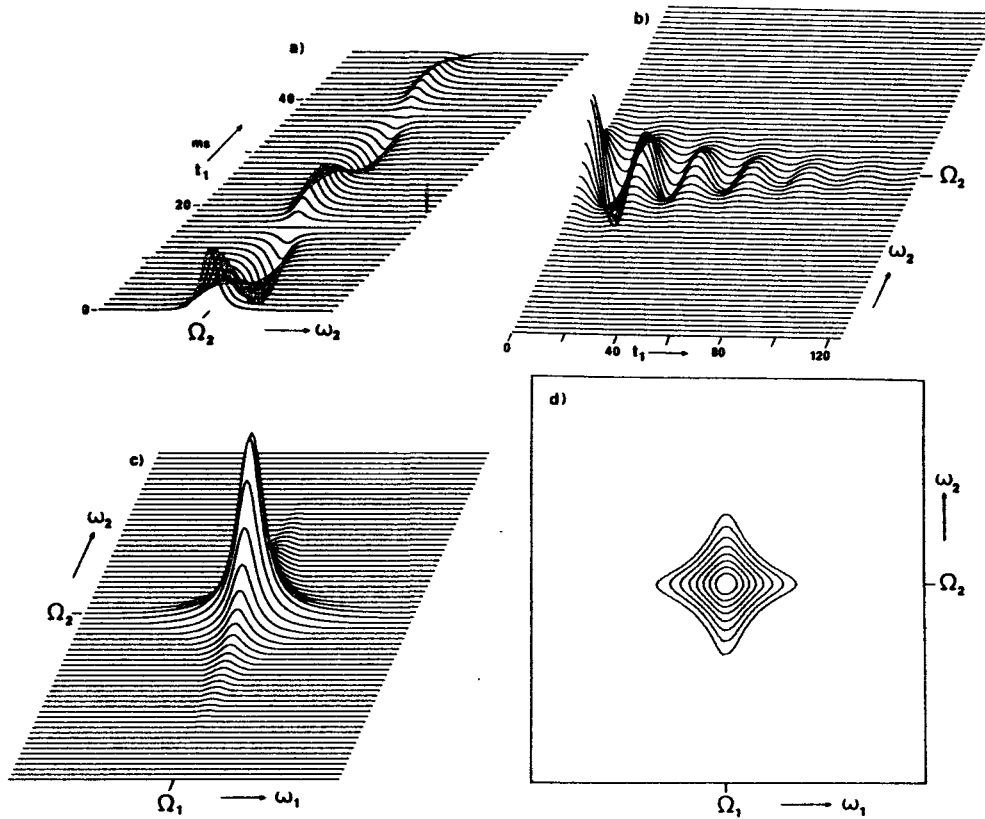


Figure 3. (a) A set of spectra obtained with the sequence of Figure 1b for increasing durations of the evolution period, t_1 . (b) Transposed data matrix of Figure 3a. (c) Fourier transform of the interferograms of Figure 3b resulting in a two-dimensional stacked line spectrum. (d) The spectrum of Figure 3c, represented as a contour plot.

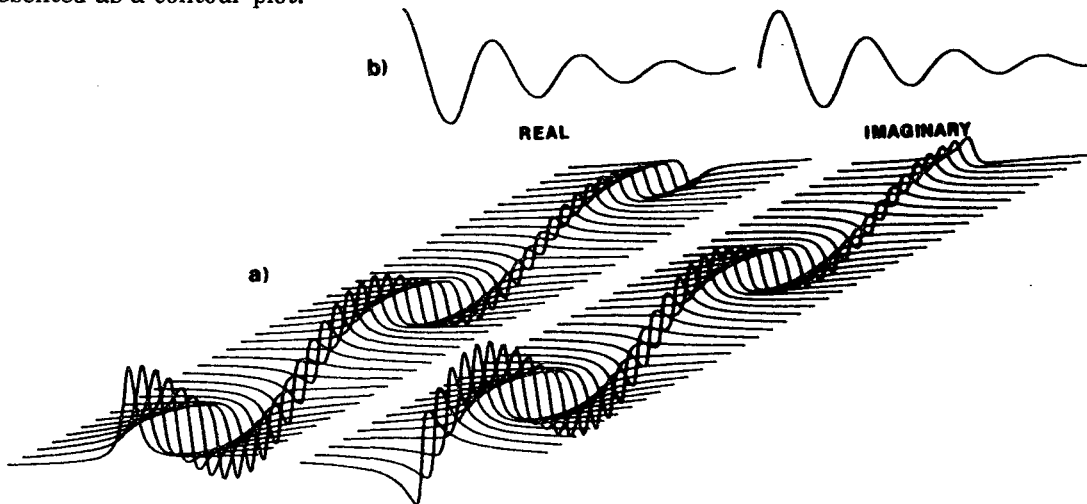


Figure 4. (a) A set of phase-modulated spectra. The phase of the resonance is a linear function of the duration of the evolution period, t_1 . Both the real and imaginary halves of the spectra are shown. (b) Complex interferogram taken at $\omega_2 = \Omega_2$. The first half of the interferogram represents a t_1 section through the real halves of the spectra in Figure 4a, and the second half is the interferogram through the imaginary halves. A quadrature Fourier transform of this complex interferogram determines the sign and the magnitude of the modulation frequency.

however, the Fourier transformation takes the signal energy of all data points and puts it all into one (or several) narrow resonance line(s). Similarly, if for each t_1 value in a 2D experiment a spectrum with poor signal-to-noise ratio is obtained, the second Fourier transformation with respect to t_1 combines the signal energy of a particular resonance from all spectra obtained for different t_1 values, and concentrates it into one narrow line in the 2D spectrum. Therefore, the sensitivity of 2D NMR is not necessarily lower than for the one-dimensional experiment.

In certain types of experiments one tries to transfer magnetization from one resonance to another by means of a coherent process or by means of cross relaxation or chemical exchange (to be discussed later). In this case the sensitivity of 2D NMR can become rather poor if the transfer process is not very efficient (as is the case in coherent transfer through non-resolved couplings or in the case of slow cross relaxation or chemical exchange). However, the analogous one-dimensional experiment also suffers in sensitivity in this case.

If sensitivity is a crucial problem, the two rules that should always be obeyed are:

1. The acquisition time in the t_2 dimension, $t_{2\max}$, should be at least equal to $1.5 T_2$.
2. The acquisition time in the t_1 dimension, $t_{1\max}$, should be chosen as short as possible, i.e. not longer than absolutely necessary to obtain enough resolution in the ω_1 dimension after Fourier transformation. Since the signal decays as a function of the time t_1 , spectra taken for short t_1 values contribute more to the 2D resonance intensity (and sensitivity) than spectra obtained for t_1 values on the order of $T_2^{(1)}$ or longer.

More discussions on sensitivity of 2D NMR can be found in the literature (3-6).

B. Lineshapes and Transform Techniques

The spectrum in Figure 3c represents the cosine Fourier transform with respect to t_1 of the real part of eqn. 2. If interferograms through the real and imaginary halves of the $S(t_1, \omega_2)$ are Fourier transformed separately, this gives:

$$S(\omega_1, \omega_2) = A_1(\omega_1)A_2(\omega_2) + iA_1(\omega_1)D_2(\omega_2) + jD_1(\omega_1)A_2(\omega_2) + jiD_1(\omega_1)D_2(\omega_2) \quad (4)$$

where "j" has the same meaning as "i", but refers to the imaginary data in the F_1

dimension. $A_1(\omega_1)$ and $D_1(\omega_1)$ are defined analogous to eqn. 3. The four terms at the right hand side of eqn. 4 are also known as S^{cc} , S^{cs} , S^{sc} and S^{ss} in the older literature (2,7). Clearly, only one of the four parts (S^{cc}), shows the desirable 2D absorption mode lineshape.

The signal of eqn. 2 is modulated in amplitude by a cosine function. It is impossible to tell from the second Fourier transformation whether the modulation frequency, Ω_1 , is positive or negative. Of course, for this simple case one knows that $\Omega_1 = \Omega_2$, and if quadrature detection during t_2 is employed, the sign of the modulation frequency is determined. However, in many experiments this is not the case and in order to avoid confusion, one has to make sure that all modulation frequencies have the same sign by positioning the transmitter frequency at either the low or high field side of the spectrum. Because of sensitivity considerations, quadrature detection in the t_2 dimension is always necessary, and data storage space is wasted if the transmitter frequency is not set at the center of the spectrum. Also, radiofrequency offset effects may become prohibitively severe in certain types of experiments.

A simple way around this problem is the introduction of artificial phase modulation, to be described below. If a second experiment, " $90^\circ_y - t_1 - 90^\circ_y - \text{acquire}(t_2)$ " is performed, the signal detected in this second experiment will start out along the y axis (at $t_2 = 0$) and is modulated in amplitude by $\sin(\Omega_1 t_1)$:

$$\begin{aligned} s'(t_1, t_2) &= M_0 \sin(\Omega_1 t_1) \exp[i(\Omega_2 t_2 + \pi/2)] \times \\ &\exp(-t_1/T_2^{(1)}) \exp(-t_2/T_2^{(2)}) \\ &= iM_0 \sin(\Omega_1 t_1) \exp(i\Omega_2 t_2) \times \\ &\exp(-t_1/T_2^{(1)}) \exp(-t_2/T_2^{(2)}) \end{aligned} \quad (5)$$

Adding the results of the two experiments, eqns. 5 and 1, directly together and omitting the relaxation terms gives:

$$s^*(t_1, t_2) = M_0 \exp(i\Omega_1 t_1) \exp(i\Omega_2 t_2) \quad (6)$$

Eqn. 6 represents a signal of which the phase at time $t_2 = 0$ is a linear function of the duration of evolution period, t_1 . Fourier transformation with respect to t_2 will yield a resonance at $\omega_2 = \Omega_2$, and with phase $\Omega_1 t_1$:

$$\begin{aligned} S^*(t_1, \omega_2) &= \\ M_0 [\cos(\Omega_1 t_1) A_2(\omega_2) - \sin(\Omega_1 t_1) D_2(\omega_2)] + \end{aligned}$$

$$iM_0[\cos(\Omega_1 t_1)D_2(\omega_2) + \sin(\Omega_1 t_1)A_2(\omega_2)] \quad (7)$$

A set of spectra obtained this way for a series of t_1 values, is sketched in Figure 4. Both the real and imaginary halves of those spectra are shown. An interferogram taken at $\omega_2 = \Omega_2$ does not contain any of the dispersive components since $D_2(\Omega_2) = 0$, and this interferogram is described by:

$$S^*(t_1, \Omega_2) = M_0[\cos(\Omega_1 t_1) + i\sin(\Omega_1 t_1)]T_2^{(2)} \quad (8)$$

where the real part represents the interferogram taken through the real part of eqn. 6, and the imaginary part of eqn. 8 is the interferogram taken through the imaginary parts of the $s^*(t_1, \Omega_2)$ spectra. This complex interferogram is sketched in Figure 4b. A complex Fourier transformation of eqn. 8 can be made, and the sign of the modulation frequency, Ω_1 , is automatically determined. Any interferogram taken at an ω_2 value different from Ω_2 , will have non-zero contributions from $D_2(\omega_2)$, and Fourier transformation with respect to t_1 of this $D_2(\omega_2)$ contribution will yield a resonance in the F_1 dimension that is 90° out of phase relative to the interferogram taken at $\omega_2 = \Omega_2$. The full 2D Fourier transform of eqn. 6 is given by:

$$S^*(\omega_1, \omega_2) = M_0[A_1(\omega_1)A_2(\omega_2) - D_1(\omega_1)D_2(\omega_2)] + iM_0[A_1(\omega_1)D_2(\omega_2) + D_1(\omega_1)A_2(\omega_2)] \quad (9)$$

Clearly, both the real and imaginary part of this function are mixtures of absorption and dispersion. The real part of eqn. 9 is sketched in Figure 5. The resonance shows a so-called "phase twist" lineshape (2), and cannot be phased to the pure absorption mode. In practice, an absolute value mode calculation is usually made before display:

$$\text{Absolute value} = [\text{Re}^2 + \text{Im}^2]^{1/2} \quad (10)$$

Since the tails of an absolute value mode resonance decrease proportional to $1/|\omega - \Omega|$, this resonance shows undesirable tails, decreasing resolution.

Nevertheless, this artificially induced phase modulation is currently the most common way of operation for most 2D experiments. The software of most commercial spectrometers assume data in a 2D experiment to be phase-modulated, and the data matrix transposition routine

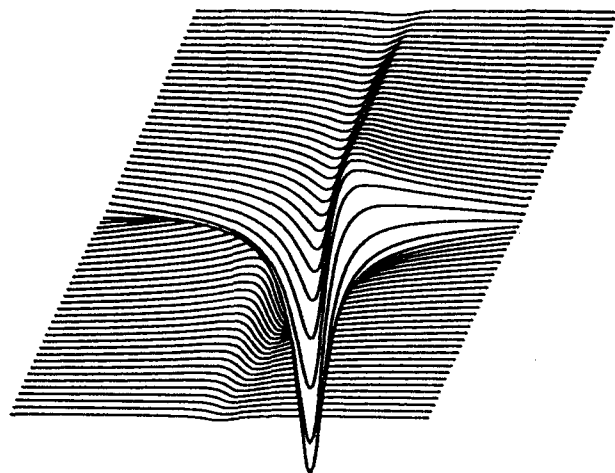


Figure 5. phase-twisted line shape obtained by Fourier transformation with respect to t_1 of the matrix of Figure 4a.

automatically places the imaginary half of the interferogram behind the real half (as depicted in Figure 4b), ready for a second complex Fourier transformation, this time with respect to t_1 .

The strong tailing of the absolute value mode lineshape can be suppressed by the use of appropriate digital filtering. All those filters have in common that they reshape the envelope amplitude of the time domain data to decay in a near symmetrical fashion from the midpoint of the FID (8). Filters commonly used for this purpose are the sine bell function (9), the "pseudo-echo window" (10) and the convolution difference filter (11). Figure 6 compares the contour plots for a regular absolute value mode line-shape, and one that has been obtained after the time domain data were multiplied by a sine bell in both dimensions. Unfortunately, the sensitivity generally suffers severely from the use of such resolution enhancement filtering functions (the COSY experiment, to be discussed later, can under certain conditions be an exception to this rule).

Although phase modulated experiments are experimentally very convenient, sensitivity and resolution suffer. Another disadvantage of artificial phase modulation, not discussed above nor mentioned explicitly in the literature, is that only half of the available signal is used: if the

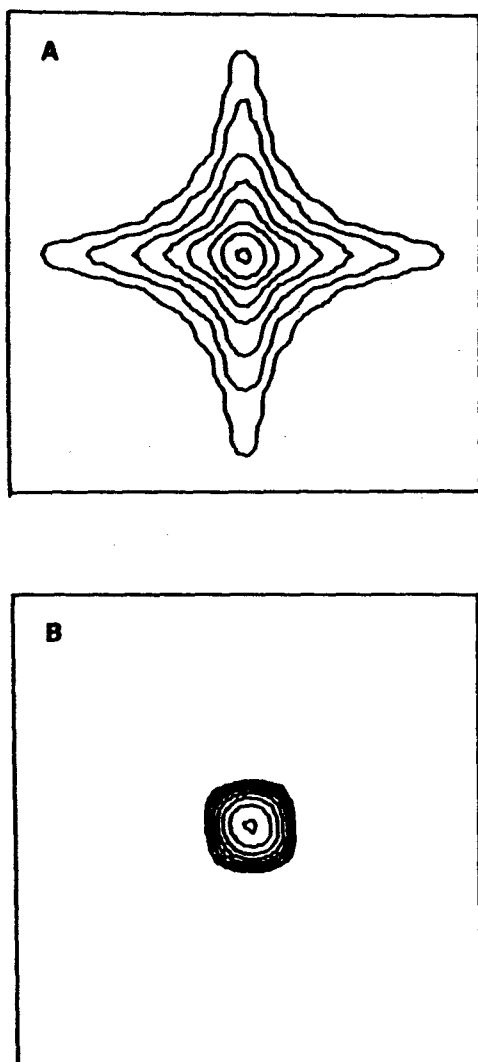


Figure 6. Comparison of the contour plots of absolute value mode line shapes. (a) Line shape obtained after an absolute value mode calculation of a signal that has been multiplied by a negative exponential with a time constant $T_2 = AT/3$, where AT is the duration of the acquisition time. (b) Line shape obtained if the time domain signal is multiplied by a sine bell function. The lowest contour level is taken at 1/12th of the peak height.

difference of the two experiments (eqn. 1 and eqn. 5) were taken, this gives a signal of the shape:

$$s^-(t_1, t_2) = M_0 \exp(-i\Omega_1 t_1) \exp(i\Omega_2 t_2) \quad (11)$$

The noise in eqns. 6 and 11 is in principle independent. If only the sum or the difference is taken, half of the available signal is wasted!

C. Two-dimensional Quadrature and Absorption Mode

As explained above, absorption mode 2D spectra can only be recorded if the transmitter is placed at either the low or high field side of the spectrum. Since data acquisition during t_2 has to be done in quadrature (for sensitivity reasons), this type of experiment is very inefficient as far as data storage is concerned. Also, pulse imperfections due to resonance offset can become severe. A more efficient way to obtain a 2D absorption mode spectrum in 2D quadrature, was first introduced by Muller and Ernst (12) and by Freeman et al. (13) and also by States et al. (14). This so-called hypercomplex Fourier transformation approach will be described below.

Consider again the pulse sequence of Figure 1 and the signal of eqn. 1. A second experiment, $90^\circ_x - t_1 - 90^\circ_x - \text{acquire}(t_2)$, is performed. The signal in the second experiment is initially ($t_2 = 0$) also along the x axis, but is modulated in amplitude by $\sin(\Omega_1 t_1)$. The FID's obtained in the two experiments, $s(t_1, t_2)$ and $s'(t_1, t_2)$, are not co-added this time, but stored in separate locations in memory. Hence, for every t_1 value, two spectra are recorded, one modulated by a cosine and the other one by a sine function. Fourier transformation of the two sets of spectra gives:

$$S(t_1, \omega_2) = M_0 \cos(\Omega_1 t_1) [A_2(\omega_2) + iD_2(\omega_2)] \quad (12a)$$

$$S'(t_1, \omega_2) = M_0 \sin(\Omega_1 t_1) [A_2(\omega_2) + iD_2(\omega_2)] \quad (12b)$$

The simple but crucial trick is to replace the imaginary part of $S(t_1, \omega_2)$ by the real part of $S'(t_1, \omega_2)$, yielding:

$$S^t(t_1, \omega_2) = M_0 \exp(i\Omega_1 t_1) A_2(\omega_2) \quad (13)$$

A set of those spectra is shown in Figure 7. Complex Fourier transformation with respect to t_1 of eqn. 13 gives for the real part:

$$S^t(t_1, \omega_2) = M_0 A_1(\omega_1) A_2(\omega_2) \quad (14)$$

which represents a 2D absorption mode resonance. Undoubtedly this will become the accepted way of data processing for most 2D NMR

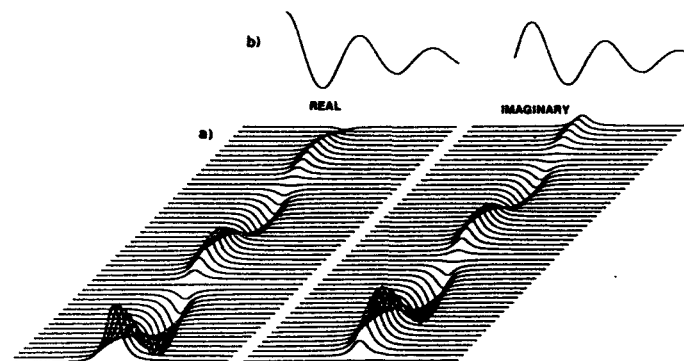


Figure 7. (a) The left halves of the spectra are the absorption parts of the spectra obtained with an experiment where the resonance is modulated in amplitude by a cosine function. The dispersive parts of these spectra have been replaced by the absorptive part of the spectra obtained with a second experiment, where the resonances are modulated in amplitude by a sinusoidal function. (b) Complex interferogram taken at $\omega_2 = \Omega_2$.

experiments in the near future.

A slightly different approach for the same problem of two-dimensional quadrature and absorption mode has recently been proposed by Bodenhausen et al. (15) and is based on an idea first introduced by the Pines group (16). In this so-called TPPI method (Time Proportional Phase Increment), the rf phases of all preparation pulses are incremented by 90° for consecutive t_1 values. This causes the apparent modulation frequency to be increased (or decreased) by $(2\Delta t_1)^{-1}$, and makes it appear that all modulation frequencies are positive (or negative), and therefore allows a real (cosine) Fourier transformation with respect to t_1 . Although, at first sight, the hypercomplex and the TPPI methods seem totally different, a closer analysis shows that the methods are almost identical. Also from

a practical point of view there is little difference: identical size data matrices are required and identical data acquisition times are needed for the two methods, giving indistinguishable resolution and sensitivity in the final spectrum. Comparing the two methods is similar to comparing the different ways in which most commercial spectrometers versus most of the Bruker spectrometers acquire quadrature information in a one-dimensional spectrum. In most spectrometers two data points, containing the x and y information, are sampled simultaneously, whereas in most Bruker spectrometers quadrature information is obtained by sampling at twice the rate, and incrementing the receiver reference phase by 90° for consecutive sampling points, taking only one data point at a time (17).

Lines in an absorption mode spectrum can be so narrow that digitization of the resonances becomes a problem. In this case, the highest point of a resonance in a 2D spectrum can be reduced by as much as 70%, apparently decreasing the intensity of a resonance in a contour plot dramatically. This effect has been observed experimentally. A simple solution to this problem is to zero fill by a number of data points equal to the number of signal-containing data points, prior to Fourier transformation. In absolute value mode spectra, lines are broadened sufficiently by the absolute value mode calculation and use of this zero-filling procedure is therefore usually not essential.

D. Coherence Transfer by Means of Radiofrequency Pulses

Classical vector pictures have been used for over three decades to explain the mechanisms on which many NMR experiments rely (18). However, for a description of most of the newer type pulse sequences, applied to coupled spin systems, straightforward application of those vector pictures leads to erroneous results. Ernst and co-workers (19) and other workers (20,21) have introduced a formalism that does allow the use of vector pictures to analyze the behavior of a coupled spin system. This operator formalism based vector picture is more complicated than is the use of the classical picture based on the Bloch equations, but is much less tedious than use of the density matrix formalism. The new approach will be briefly discussed for a homonuclear weakly coupled two-spin system. Two weakly coupled spins, A and B, will be considered.

The total net magnetization of spin A equals the vector sum of the magnetizations of the two

doublet components (Figure 8). As in the classical vector picture, the vector sum of the two

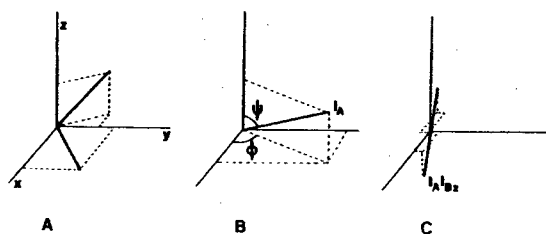


Figure 8. (a) Arbitrary orientation of the two magnetization vectors of the doublet components of nuclei, A. (b) The vector sum of the two doublet components. (c) The difference between the two doublet components, representing antiphase magnetization.

doublet components is represented by a vector I_A that can be decomposed in the standard fashion into its components along the principal axes of the rotating frame (Figure 8b):

$$I_A = \cos(\Psi)I_{Az} + \sin(\Psi)\cos(\phi)I_{Ax} + \sin(\Psi)\sin(\phi)I_{Ay} \quad (15)$$

This vector sum is the sum of the in-phase components of the two doublet magnetization vectors. The antiphase components of the two doublet magnetization vectors do not contribute to I_A in this picture. Since those components are opposite to each other, they do not contribute to macroscopic observable magnetization. Of the antiphase components of spin A, one component corresponds to spin B in the $m=1/2$ spin state, and the other to the $m=-1/2$ state. This antiphase magnetization can then formally be written as $2I_A I_{Bz}$. The factor "2" in this product is needed for normalization. The new formalism treats the individual terms in such a product as normal magnetization, in the classical way.

In order to make the description more explicit: consider the effect of a 90°_x pulse applied to the two-spin system that is initially in thermal equilibrium. The magnetization ($I_{Az} + I_{Bz}$) gets rotated to a position parallel to the -y axis*, and thus creates $-(I_{Ay} + I_{By})$. The magnetization of the two nuclei can be considered separately, and we will concentrate on the fate of the

A spin magnetization. This will rotate with angular frequency, Ω_A , about the z axis and the two doublet components will periodically (with period $1/J$) get in antiphase. These two processes can be considered separately:

$$I_{Ay} \xrightarrow{\Omega_A I_{Az} t} I_{Ay}\cos(\Omega_A t) - I_{Ax}\sin(\Omega_A t) \quad (16a)$$

$$I_{Ay} \xrightarrow{2\pi J I_{Az} I_{Bz} t} I_{Ay}\cos(\pi J t) - 2I_{Ax}I_{Bz}\sin(\pi J t) \quad (16b)$$

$$I_{Ax} \xrightarrow{2\pi J I_{Az} I_{Bz} t} I_{Ax}\cos(\pi J t) + 2I_{Ay}I_{Bz}\sin(\pi J t) \quad (16c)$$

Substitution of eqns. 16b and 16c in 16a then gives the complete evolution of the magnetization. The interesting terms in eqn. 16 are the products $I_{Ax}I_{Bz}$ and $I_{Ay}I_{Bz}$. Consider a 90° pulse applied to such a term:

$$I_{Ax}I_{Bz} \xrightarrow{90^\circ_y} -I_{Az}I_{Bx} \quad (17a)$$

$$I_{Ax}I_{Bz} \xrightarrow{90^\circ_x} -I_{Ax}I_{By} \quad (17b)$$

eqn. 17a shows how antiphase A spin magnetization gets converted into antiphase B spin magnetization by a 90° pulse applied perpendicular to the doublet magnetization vectors. This important result is the basis of Jeener's original experiment when applied to a homonuclear coupled spin system. Eqn. 17b contains the product $I_{Ax}I_{By}$ and is harder to visualize; this term represents so-called two-spin coherence, a combination of zero- and double quantum coherence. The time evolution of the product equals the product of the time evolution of the individual terms; i.e. the time evolution of $I_{Ax}I_{By}$ is given by

$$I_{Ax}I_{By} \xrightarrow{\Omega_A t I_{Az} + \Omega_B t I_{Bz}} [\cos(\Omega_A t)I_{Ax} + \sin(\Omega_A t)I_{Ay}] \times [\cos(\Omega_B t)I_{By} - \sin(\Omega_B t)I_{Bx}] \quad (18)$$

The operator formalism is easily extended to more spins by considering product terms of all spins involved. For a more complete description of this extremely useful formalism, the reader is

*In order to be consistent with conventions used in the paper by Sorensen et al.(19), describing the operator formalism, we adopt here the convention that a 90°_x rotates the magnetization anti-clockwise around the x axis, i.e. from the z to the -y axis.

referred to the literature (19-21).

II. HOMONUCLEAR SHIFT CORRELATION THROUGH SCALAR COUPLING

Jeener's original 2D pulse scheme can be considered as a convenient alternative for the conventional one-dimensional double resonance experiments, and is often referred to as the COSY (CORrelated SpectroscopY) experiment. A complete quantum mechanical description of the experiment was presented by Aue et al.(22) but did not contribute much to the popularity of the experiment. Only in the early 1980's the widespread applicability of this technique was realized (23-27). The basic pulse scheme has already been discussed in the previous sections. Here a $90^\circ_x - t_1 - 90^\circ_\phi - \text{acquire}(t_2)$ pulse scheme is used, where the phase ϕ of the final pulse and the mode of data acquisition are selected as indicated in Table 1. This means that a minimum of four experiments is performed for each t_1 value with the phase of the final 90° pulse incre-

Table 1. Cycling of the phase of the observe pulse, ϕ , and of the receiver in the various steps of the COSY experiment in order to obtain phase modulation and to detect the coherence transfer echo.

Step	ϕ	Receiver
1	x	+
2	y	-
3	-x	+
4	-y	-

mented by 90° each time and data alternately added to and subtracted from memory. This way of phase cycling results in detection of the $s^-(t_1, t_2)$ signal of eqn. 11, often referred to as the coherence transfer echo (28). The occurrence of the echo is easily understood by considering that in eqn. 11, Ω_1 and Ω_2 have approximately the same value (in the laboratory frame). Therefore, at time $t_1 = t_2$, the phase of the magnetization, $\exp[i(\Omega_2 t_2 - \Omega_1 t_1)]$, is to first order

independent of the magnetic field strength, i.e. independent of magnetic field inhomogeneity, and consequently an echo will occur. The entire four-step experiment is often repeated four times with the phases of all radiofrequency pulses and receiver incremented by 90° each time. This additional so-called CYCLOPS cycling (29) eliminates imperfections in the quadrature detection system of the spectrometer which otherwise may cause small mirror image signals about the $\omega_2 = 0$ and $\omega_1 = 0$ axes.

The COSY experiment relies on transfer of magnetization from spin A to spin X by the second 90° pulse in Jeener's experiment, and can only occur if spin A and X are mutually coupled. The mechanism for this magnetization transfer has been discussed in the previous section: eqn. 17a shows how spin A doublet components that are in antiphase with respect to spin X are transferred into X spin doublet components that are in antiphase with respect to spin A. The amount of antiphase A-spin magnetization present before the second 90° transfer pulse depends on $\sin(\pi J_{AX} t_1)$. The magnetization observed during t_2 starts out in antiphase and is proportional to $\sin(\pi J_{AX} t_2)$. The time domain signal for the magnetization transferred from A to X is given by

$$s^-_{AX}(t_1, t_2) = M_0 \sin(\pi J_{AX} t_1) \sin(\pi J_{AX} t_2) \times \exp(-i\Omega_A t_1) \exp(i\Omega_X t_2) \quad (19)$$

Note that for very short t_1 values only very little magnetization is transferred from A to X. Rewriting:

$$\sin(\pi J t) = -i [\exp(i\pi J t) - \exp(-i\pi J t)] / 2 \quad (20)$$

and substitution in eqn. 19 shows that the Fourier transformed signal $S^-(\omega_1, \omega_2)$ will show four peaks at $(\omega_1, \omega_2) = (\Omega_A \pm \pi J_{AX}, \Omega_X \pm \pi J_{AX})$, and that those resonances show antiphase relationships, as schematically indicated in Figure 9. Also indicated in Figure 9 are the "diagonal resonances," due to magnetization that is not transferred from A to X or from X to A, and which are 90° out of phase relative to the cross peaks. It is therefore impossible to phase all resonances in this spectrum simultaneously to the 2D absorption mode (unless the pulse scheme is altered (30)), and an absolute value mode calculation before display is therefore commonly used. The artificial phase modulation scheme

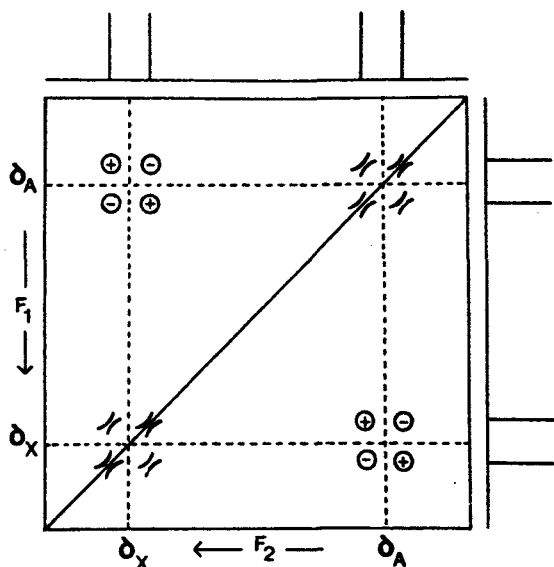


Figure 9. Schematic diagram of the 2D COSY spectra of an AX spin system. The four components of the AX cross multiplet are pairwise in antiphase, whereas the four diagonal multiplet components are 90° out of phase in both dimensions relative to the cross peaks.

(discussed before) therefore does not degrade performance of the experiment very much. Also, since the cross peak time domain signal has an envelope amplitude proportional to $\sin(\pi J_{AX}t_1)\sin(\pi J_{AX}t_2)$, and acquisition times in the t_1 and t_2 dimension are typically 100-300 ms, use of a sine bell digital filter is close to a matched filter for those signals and favors the sensitivity of the cross multiplets, meanwhile cutting down the intensity of redundant diagonal peaks which have a $\cos(\pi J_{AX}t_1)\cos(\pi J_{AX}t_2)$ dependence.

Figure 10 shows the COSY spectrum for a 25 mM solution of amphotericin B in DMSO- d_6 , recorded on a Nicolet 500 MHz spectrometer. 512 t_1 increments of 300 μsec each were used, and 512 complex data points were acquired for each t_1 value. The artificial phase modulation scheme (Table 1) was employed and the total measuring time was 4 h. Note that in the regular one-dimensional spectrum many of the couplings are not or poorly resolved. However, a wealth of cross peaks can be observed in the 2D

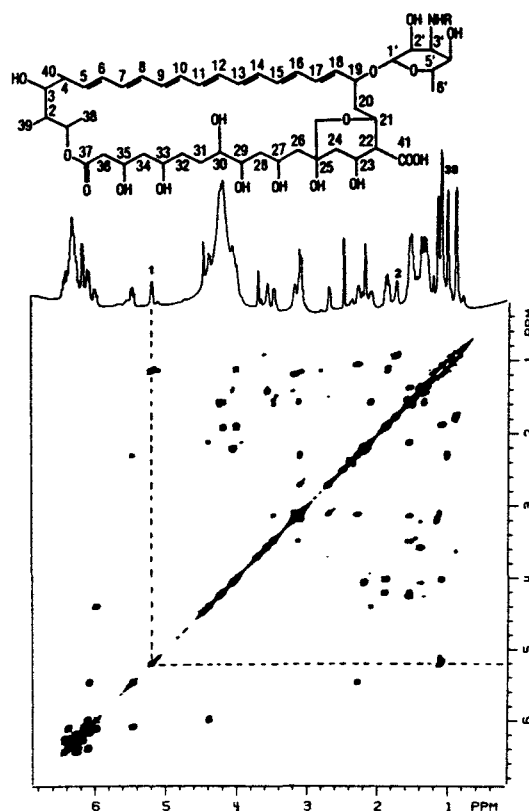


Figure 10. 500 MHz absolute value mode COSY spectrum of a sample of amphotericin B in DMSO- d_6 . 16 experiments were performed for each t_1 value, and the total duration of the experiment was 4 h. A sine bell has been used in both dimensions prior to Fourier transformation.

spectrum. For example, it is seen that proton 1 is coupled to methyl group 38 (broken line in Figure 10).

Many users of the COSY experiment are often puzzled by the absence or low intensity of certain cross peaks. For example, the cross peaks between protons 1 and 2 in Figure 10 have too low an intensity to be observed in the contour plot. In general, it is hard to calculate exactly how intense a cross multiplet will be, but two factors that are of major importance will be mentioned below.

1. A proton that is coupled to a large number of other protons will show rather low

intensity for its individual 1D multiplet components. In the COSY experiment, this low intensity will now be redistributed among all protons to which it is coupled by the mixing pulse, yielding very low intensity for the cross multiplets. The effect is particularly severe for cross peaks between two multiplets that both have a complicated multiplet structure.

2. If transverse relaxation times, T_2 , are short compared with J_{AX}^{-1} , the transferred magnetization in eqn. 19 will never assume a large value and therefore only (vanishingly) low intensity cross peaks can be observed.

From point 1, it is clear that a large coupling does not necessarily give rise to an intense cross peak. However, if acquisition times $t_{1,max}$ and $t_{2,max}$ are chosen short (<100 ms) this will relatively emphasize cross peaks due to large scalar couplings. Recently, it has been shown that if the size of certain couplings can be estimated, a "designer" filter can be used to pick up those missing cross peaks (31).

III. HOMONUCLEAR CHEMICAL SHIFT CORRELATION THROUGH CROSS RELAXATION

In the COSY experiment, magnetization is transferred from one proton to another through the scalar coupling mechanism. This experiment relies on the existence of (partially) resolved scalar couplings. Another way to transfer magnetization between nuclei is the cross relaxation mechanism, which relies on the internuclear dipolar interaction. This mechanism is generally referred to as the nuclear Overhauser effect (NOE). The 2D pulse scheme that is based on the NOE effect is generally known as the NOESY experiment. This experiment was first proposed by Ernst, Jeener et al.(32,33). It is mentioned here that the same experiment can also be used for the investigation of chemical exchange processes. Obviously, no resolved couplings are needed for this experiment; the experiment tends to work very well for macromolecules which have a slow tumbling rate and therefore less ideal averaging of the dipolar coupling mechanism. This is the reason for strong cross relaxation and causes line broadening in the conventional 1D spectrum and also in the 2D spectrum.

The pulse scheme is sketched in Figure 11 and the mechanism on which this 2D experiment relies will be briefly discussed below. Assume for reasons of simplicity that all pulses in the

scheme are applied along the x axis of the rotat-

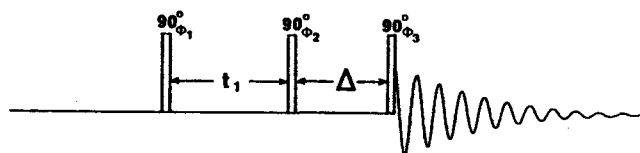


Figure 11. Pulse scheme of the 2D experiment to detect homonuclear cross relaxation and chemical exchange. The phases of the rf pulses, ϕ_1 and ϕ_2 , and of the receiver are cycled according to Table 2, and the results of the odd and even steps are stored in separate locations in memory and processed as described in the text in order to obtain an absorption mode spectrum.

ing frame, and consider a molecule with two spins A and B that have no mutual scalar coupling. The longitudinal magnetization of spin A, just after the second 90° pulse, is given by:

$$M_{zA}(t_1) = -M_{0A} \cos(\Omega_A t_1) \quad (21)$$

During the mixing period of duration, Δ , cross relaxation with spin B takes place, changing the longitudinal B spin magnetization by an amount $C[M_{zA}(t_1) - M_{zB}(t_1)]$ and the A spin magnetization by the opposite amount, where C is a constant depending on the cross relaxation rate, the longitudinal relaxation rates, and the duration, Δ . Just before the final pulse, the longitudinal B spin magnetization is thus given by

$$M_{zB}(t_1) = f[M_{zB}(t_1)] + CM_{zA}(t_1) \quad (22)$$

where $f[M_{zB}(t_1)]$ is a function depending on the relaxation of proton B during the delay, Δ , and on the modulation of the B spin magnetization by the first two pulses in the sequence. It is the second term at the right hand side of eqn. 22 that is the term of interest, since this term is due to cross relaxation from nucleus A to B. The final 90° pulse converts this term into transverse B magnetization which follows from eqns. 21 and 22:

$$s_{AB}(t_1, t_2) = CM_{0A} \cos(\Omega_A t_1) \exp(i\Omega_B t_2) \quad (23)$$

Table 2. Phases ϕ_1 and ϕ_3 of the pulses in Fig. 11 in the various steps of the experiment. Phase ϕ_2 is x for all 16 steps. Data of odd and even steps are stored separately in the computer memory.

Step	ϕ_1	ϕ_3	Receiver
1	x	x	x
2	y	x	x
3	$-x$	x	$-x$
4	$-y$	x	$-x$
5	x	y	y
6	y	y	y
7	$-x$	y	$-y$
8	$-y$	y	$-y$
9	x	$-x$	$-x$
10	y	$-x$	$-x$
11	$-x$	$-x$	x
12	$-y$	$-x$	x
13	x	$-y$	$-y$
14	y	$-y$	$-y$
15	$-x$	$-y$	y
16	$-y$	$-y$	y

This signal is of the same shape as eqn. 1, and 2D Fourier transformation will therefore give a resonance at $(\omega_1, \omega_2) = (\Omega_A, \Omega_B)$. In contrast with the COSY experiment, diagonal and cross peaks in the 2D spectrum will all have the same phase, or exactly opposite phase, depending on the motional correlation time, τ_c . It is therefore strongly desirable to record the spectrum in the absorption mode, using the procedure outlined in Section IC. In order to eliminate transfer through scalar coupling (the COSY mechanism) further phase cycling is necessary. In practice a 16-step sequence (Table 2) is often used and additionally, this 16-step sequence is repeated four times in the CYCLOPS mode (29) in order to eliminate quadrature artifacts. Remaining coherent transfer through zero and triple quantum coherence, that is not cycled out this way can largely be eliminated by random fluctuation of Δ by a small amount (5%), provided that the frequency of this zero or triple quantum coherence is larger than $20/\Delta$ Hz.

If the cross relaxation is slow compared to

the longitudinal relaxation, maximum transfer from spin A to B, and vice versa, occurs for a mixing time on the order of the shortest T_1 of the two spins involved. Hence, from a sensitivity point of view, a mixing time on the order of T_1 is optimum for the detection of cross peaks. However, if one wants to obtain quantitative information about the relaxation rates, one has to consider that the cross peak buildup rate (as a function of Δ) is non-linear (32-36). The simplest way around this problem is to consider only short mixing times, for which the NOE buildup is still in the linear region (35,36), but this approach necessarily leads to smaller cross peaks, i.e. lower sensitivity.

As an example, Figure 12 shows a contour plot of the 2D NOE spectrum of amphotericin B, showing a large number of cross peaks, obtained for a mixing time of 200 ms. Analysis of the cross peak network does not only provide assignment for all ^1H resonances in this compound, additional to that obtained from the COSY spectrum of Figure 10, but also gives information regarding the three-dimensional structure in solution.

IV. INDIRECT DETECTION OF ^{15}N THROUGH MULTIPLE QUANTUM COHERENCE

Detection of ^{15}N shifts is limited by its low NMR sensitivity, which is due to the small and negative value of the magnetogyric ratio and to the low natural abundance (0.37%). The fact that the magnetogyric ratio, γ , is negative can cause signal cancellation in the case of incomplete nuclear Overhauser enhancement. NMR sensitivity is approximately proportional to $\gamma^{5/2}$ (37) and is therefore about a factor of 300 lower for ^{15}N than for protons, which implies a factor of 100000 difference in measuring time. It has been demonstrated that the INEPT experiment (38,39) can alleviate this problem to a certain extent, but nevertheless detection remains difficult. Bodenhausen and Ruben (40) demonstrated that the ^{15}N frequency could be measured indirectly *via* the protons directly coupled to the ^{15}N nucleus. Their rather complicated sequence transfers proton magnetization to the ^{15}N , which then evolves during the evolution period of the 2D experiment, before being transferred back to the protons which are detected during the acquisition time in this experiment. A much simpler alternative, that relies on the same principle as this "Overbodenhausen experiment" has been proposed rather recently (41,42). Experimental results indicate that with this new experiment

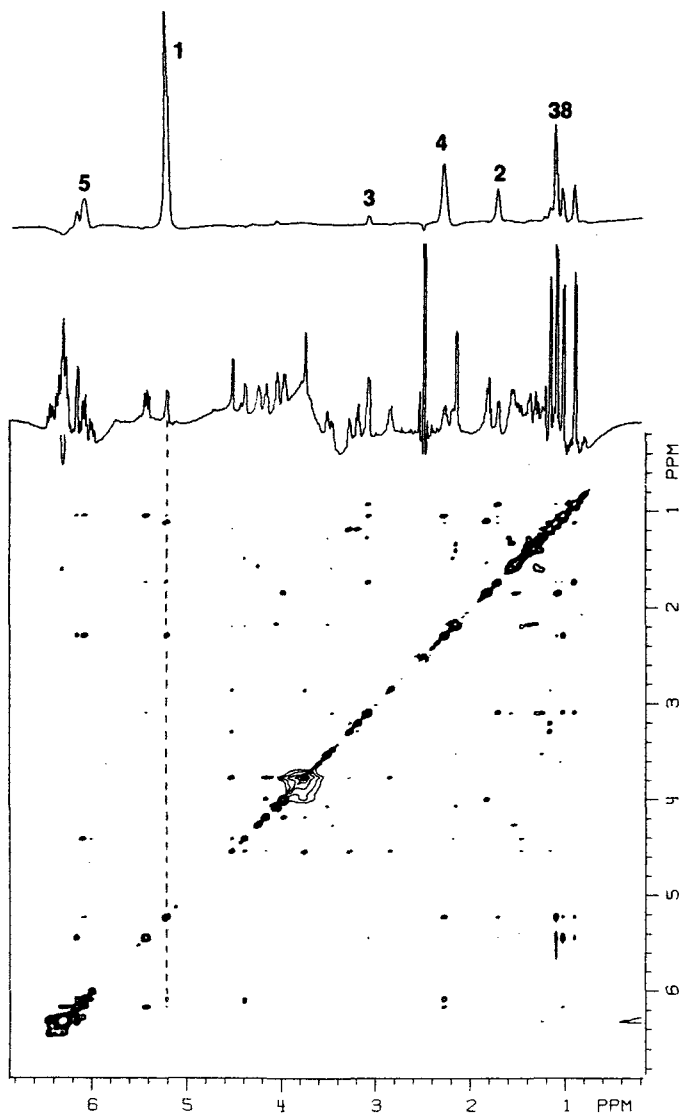


Figure 12. Two-dimensional NOE spectrum of amphotericin B, recorded at 500 MHz, using a mixing time of 200 ms. The top trace displays the cross-section taken through the 2D spectrum at the chemical shift of H1, showing spacial proximity to Me39, Me40, H2, H4, and H5. The cross-peak with H3 (3.12 ppm) is much lower in intensity suggesting a larger distance. The mixing time (200 ms) is not short enough to exclude relayed NOE effects, and quantitative interpretation of cross peak intensities is not feasible from this single spectrum.

the theoretical enhancement factor of 300 really

can be obtained (43). The experiment works only for protonated ^{15}N nuclei. Consider the energy level diagram of an isolated ^1H - ^{15}N pair (Figure 13). The broken lines represent the two (weak)

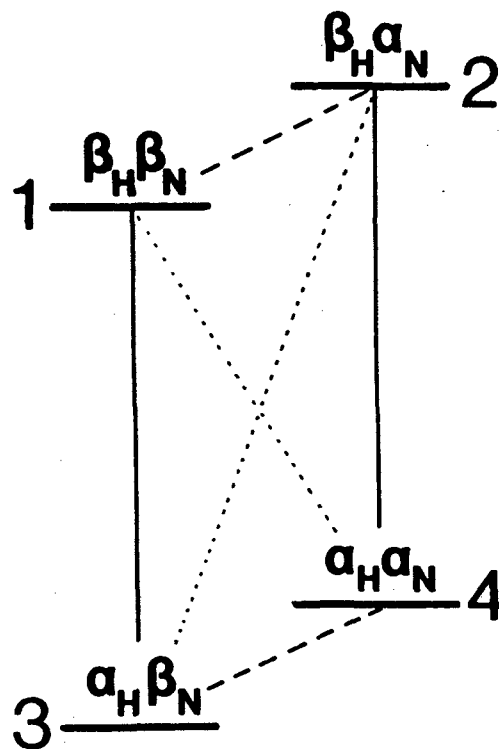


Figure 13. Energy level diagram and wave functions for a ^{15}N - ^1H spin pair. The insensitive ^{15}N resonances (broken lines) are measured indirectly by measuring the zero and double quantum resonances (dotted lines) via the proton resonances (solid lines).

^{15}N transitions. The solid lines represent the (intense) proton transitions. The basic concept of the new experiment is to generate the dotted transitions (zero and double quantum), that resonate with frequencies $\Omega_{\text{H}} \pm \Omega_{\text{N}}$. If those frequencies are measured indirectly, with a 2D experiment, the ^{15}N frequency can be calculated since the proton frequency, Ω_{H} , is known.

The pulse scheme of the experiment is shown in Figure 14. The ^1H 180° pulse at the center of the evolution period and the ^{15}N decoupling during data acquisition are optional and will, at first, not be taken into account. The theory of the

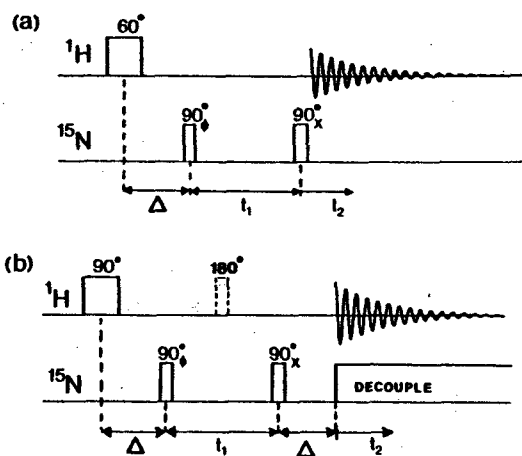


Figure 14. Pulse scheme of the experiment for indirect detection of ^{15}N through multiple quantum coherence. The first pulse applied to the protons can be of the Redfield type or of the 1-3-3-1 type and does not require additional phase cycling. (b) The 180° ^1H pulse applied at the center of the evolution period interchanges zero and double quantum coherence and causes elimination of the ^1H frequency contribution in the F_1 dimension, leading to a regular heteronuclear shift correlation spectrum. The ^{15}N decoupling during acquisition removes heteronuclear coupling from the F_2 dimension and, in principle, doubles the sensitivity of the experiment. In both (a) and (b), the phase of the first 90° ^{15}N pulse is cycled according to Table 3.

experiment is most easily described with the operator formalism, treated in section ID. The proton 90° pulse creates magnetization along the -y axis of the rotating frame, which then evolves for a time Δ :

$$I_{Hy} \xrightarrow{(\Omega_H + 2\pi J_{NH} I_{Hz})\Delta} \{I_{Hy} \cos(\Omega_H \Delta) - I_{Hx} \sin(\Omega_H \Delta)\} \cos(\pi J_{NH} \Delta) + 2\{-I_{Hx} \cos(\Omega_H \Delta) - I_{Hy} \sin(\Omega_H \Delta)\} \sin(\pi J_{NH} \Delta) I_{Nz} \quad (24)$$

If the delay, Δ , is set to $1/(2J_{NH})$, only the second term at the right hand side of expression 24 survives, and a 90°_x ^{15}N pulse applied at this time will generate product terms $I_{Hx}I_{Ny}$ and $I_{Hy}I_{Nx}$. The sine and cosine coefficients will be

Table 3. Phase of the first ^{15}N pulse in the pulse scheme of Fig. 14 and the mode of data collection for detection of the double (DQ) and of the zero quantum (ZQ) component.

Step	ϕ	DQ	ZQ
1	x	x	x
2	y	-y	y
3	-x	-x	-x
4	-y	y	-y

omitted to simplify the expressions. During the evolution period, those product terms evolve according to:

$$I_{Hx}I_{Ny} \xrightarrow{\Omega_H t_1 + \Omega_N t_1} [\cos(\Omega_H t_1) I_{Hx} + \sin(\Omega_H t_1) I_{Hy}] \times [\cos(\Omega_N t_1) I_{Ny} - \sin(\Omega_N t_1) I_{Nx}] \quad (25)$$

The final 90° ^{15}N pulse converts those two-spin coherences back into observable ^1H magnetization. If all terms are taken into account, a 90°_x ^{15}N pulse generates an observable signal:

$$s(t_1, t_2) = M_0 H \exp[i(\Omega_H \pm \pi J_{NH})(t_1 + t_2)] \cos(\Omega_N t_1) \quad (26a)$$

and if the first 90° ^{15}N pulse were applied along the -y axis, the second 90° ^{15}N pulse generates

$$s(t_1, t_2) = M_0 H \exp[i(\Omega_H \pm \pi J_{NH})(t_1 + t_2)] \sin(\Omega_N t_1) \quad (26b)$$

If either of those two signals is used separately to calculate a 2D spectrum, two resonances in

ing the zero and double quantum frequencies, respectively. The results of eqns. 26a and 26b can be combined in the usual fashion (eqns. 6 and 11) to give either the double or the zero quantum frequency in the 2D spectrum. Because the zero quantum resonance in the 2D spectrum

is centered at $(\omega_1, \omega_2) = (\Omega_N + \Omega_H, \Omega_H)$, the computer can subtract a frequency ω_2 from all ω_1 coordinates, to yield a pure chemical shift correlation map, with resonances centered at (Ω_N, Ω_H) . Broad-band ^{15}N decoupling during the detection period can be used to eliminate the effect of heteronuclear coupling in this experiment.

If the first ^{15}N 90° pulse is applied along the $-x$ axis, the signal of eqn. 26a will be detected with opposite sign. Since signals from protons not coupled to ^{15}N will not know about this phase shift and their shape will be unchanged in the two experiments, subtraction of the two experiments will give cancellation of the signals of protons that are not coupled to ^{15}N . Hence, the ^{15}N satellites in the ^1H spectrum can therefore be detected, not hampered by the 600 times stronger signal from protons coupled to ^{14}N . In total four experiments will be performed for every t_1 value, with the phase of the first ^{15}N pulse cycled along all four axes.

As an example, Figure 15 shows the zero and double quantum spectra of a 30 mM solution of α -thymosin, dissolved in 90% $\text{H}_2\text{O}/10\%$ D_2O . Spectra were recorded on a modified Nicolet 300 MHz instrument, and the total measuring time was approximately 12 h. The signals of eqns. 26a and 26b were stored in separate locations and spectrum (a) was computed from the double quantum signals and (b) was computed from the zero quantum signals, using the same two sets of acquired data.

In practice, application of the sequence of Figure 14b can sometimes be more difficult for natural abundance samples than the sequence of Figure 14a. This is due to the high power ^{15}N decoupling during data acquisition, which can cause a slight perturbation of the ^2H lock signal. A very stable lock signal is required to allow complete elimination of the 600 times stronger signal from protons coupled to ^{14}N .

As pointed out in Section I, it is desirable to record spectra in the absorption mode, both from a viewpoint of sensitivity as well as resolution. However, in this experiment the data are truly phase modulated (not artificially induced). Conversion to amplitude modulation is possible by insertion of a 180° pulse at the center of the evolution period (44). However, in the case where the proton also has homonuclear coupling, phase modulation cannot be avoided and pure absorption mode spectra cannot be recorded. A nice feature of the simplest form of the experiment is that it utilizes only one pulse for the observed protons. This pulse can be of arbitrary flip angle; a small flip angle allows a faster repetition rate and consequently will yield somewhat

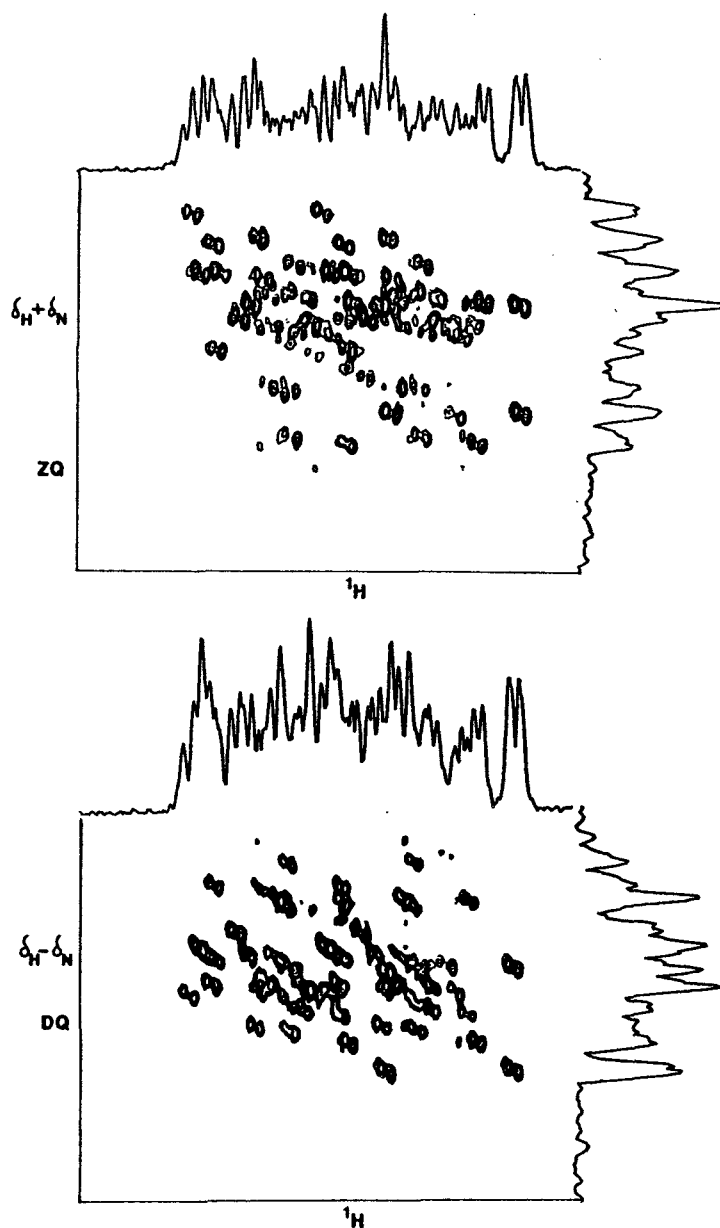


Figure 15. Zero and double quantum natural abundance ^1H - ^{15}N spectra of a 30 mM solution of α -thymosin in H_2O . Spectra were recorded on a modified Nicolet 300 MHz instrument, and both spectra are obtained from the same set of acquired data. The total measuring time was approximately 12 h. The spectra were kindly provided by Dr. David Live and Dr. Donald Davis.

higher sensitivity. More important is the fact that any type of pulse can be used for this proton excitation. For example, a Redfield water suppression or a 1-3-3-1 water suppression pulse

can be used, making it feasible to use this experiment in H_2O solution. Of course, the experiment is not limited to the indirect detection of ^{15}N resonances. The technique has also great promise for metabolic NMR studies in vivo, by using ^{13}C labeled starting material.

V. DISCUSSION

Although only a small number out of the large collection of two-dimensional NMR experiments has been treated here, it will be clear that the 2D approach extends the capabilities of NMR experiments enormously. Many applications of 2D NMR in organic and biochemistry have appeared in the recent literature. On modern NMR spectrometers, utilization of the various two-dimensional experiments has become rather simple by the introduction of suitable support software and spectrometer documentation. The main problem the inexperienced spectroscopist has to face is which experiment to choose and which results to expect. A comprehensive guide on this subject has not yet appeared, but in general it is usually a good idea to apply the standard experiments before attempting to use a more sophisticated version of those experiments. It is expected that the number of experimental pulse schemes still will expand significantly, but once the spectroscopist realizes that all those methods are small variations on the same theme, the collection of 2D experiments will appear less bewildering and practical application of those techniques becomes much simpler.

ACKNOWLEDGMENT

I wish to thank Ingrid Pufahl for typing and editing most of the manuscript. I am also indebted to Dr. David Live and to Dr. Donald Davis for providing the spectra of Figure 15 and to Dr. A. Aszalos for providing the sample of Amphotericin B and for interpretation of the corresponding spectra that resulted in complete assignment of the ^1H spectrum.

REFERENCES

- ¹J. Jeener, *Ampere International Summer School*, Basko polje, Yugoslavia (1971).
- ²G. Bodenhausen, R. Freeman, R. Niedermeyer and D.L. Turner, *J. Magn. Reson.* **26** 133 (1977).
- ³W. P. Aue, P. Bachmann, A. Wokaun and R. R. Ernst, *J. Magn. Reson.* **29**, 523 (1978).
- ⁴A. Bax and T. H. Mareci, *J. Magn. Reson.* **53**, 360 (1983).

- ⁵M. H. Levitt, G. Bodenhausen, and R. R. Ernst, *J. Magn. Reson.* **58**, 462 (1984).
- ⁶D. L. Turner, *J. Magn. Reson.* **58**, 500 (1984).
- ⁷P. Bachmann, W. P. Aue, L. Mueller and R. R. Ernst, *J. Magn. Reson.* **28**, 29 (1977).
- ⁸A. Bax, A. F. Mehlkopf and J. Smidt, *J. Magn. Reson.* **40**, 213 (1980).
- ⁹A. deMarco and K. Wuethrich, *J. Magn. Reson.* **24**, 201 (1976).
- ¹⁰A. Bax, G. A. Morris and R. Freeman, *J. Magn. Reson.* **43**, 333 (1981).
- ¹¹I. D. Campbell, C. M. Dobson, R. J. P. Williams, and A. V. Xavier, *J. Magn. Reson.* **11**, 172 (1973).
- ¹²L. Mueller and R. R. Ernst, *Mol. Phys.* **38**, 963 (1979).
- ¹³R. Freeman, S. P. Kempell and M. H. Levitt, *J. Magn. Reson.* **34**, 663 (1979).
- ¹⁴D. J. States, R. A. Haberkorn and D. J. Ruben, *J. Magn. Reson.* **48**, 286 (1982).
- ¹⁵G. Bodenhausen, H. Kogler and R. R. Ernst, *J. Magn. Reson.* **58**, 370 (1984).
- ¹⁶G. Drobny, A. Pines, S. Sinton, D. Weitekamp and D. Wemmer, *Faraday Div. Chem. Soc. Symp.* **13**, 49 (1979).
- ¹⁷A. G. Redfield and S. D. Kunz, *J. Magn. Reson.* **19**, 250 (1975).
- ¹⁸See, for example, T. C. Farrar and E. D. Becker, *Pulse and Fourier Transform NMR*, Academic Press, New York (1971).
- ¹⁹O. W. Sorensen, G. W. Eich, M. H. Levitt, G. Bodenhausen and R. R. Ernst, *Progr. in NMR Spectroscopy* **16**, 163 (1983).
- ²⁰K. J. Packer and K. M. Wright, *Mol. Phys.* **50**, 797 (1983).
- ²¹F. J. M. van de Ven and C. W. Hilbers, *J. Magn. Reson.* **54**, 512 (1983).
- ²²W. P. Aue, E. Bartholdi and R. R. Ernst, *J. Chem. Phys.* **64**, 2229 (1976).
- ²³A. Bax and R. Freeman, *J. Magn. Reson.* **44**, 542 (1981).
- ²⁴K. Nagayama, A. Kumar, K. Wuethrich and R. R. Ernst, *J. Magn. Reson.* **40**, 321 (1980).
- ²⁵A. Bax, R. Freeman and G. A. Morris, *J. Magn. Reson.* **42**, 164 (1982).
- ²⁶G. Wider, S. Macura, A. Kumar, R. R. Ernst and K. Wuethrich, *J. Magn. Reson.* **56**, 207 (1984).
- ²⁷D. Marion and K. Wuethrich, *Biochem. Biophys. Res. Commun.* **113**, 967 (1983).
- ²⁸A. Bax, *Two-Dimensional NMR in Liquids*, Reidel, Boston, 1982, Chpt. 2.
- ²⁹D. I. Hoult and R. E. Richards, *Proc. Roy. Soc. London, Ser. A.* **344**, 311 (1975).
- ³⁰U. Piantini, O. W. Sorensen and R. R.

Ernst, *J. Am. Chem. Soc.* **104**, 6800 (1982).

³¹A. Bax, R. A. Byrd and A. Aszalos, *J. Am. Chem. Soc.*, **106**, 7632 (1984).

³²J. Jeener, B. H. Meier, P. Bachmann and R. R. Ernst, *J. Chem. Phys.* **71**, 4546 (1979).

³³S. Macura and R. R. Ernst, *Mol. Phys.* **41**, 95 (1980).

³⁴W. Braun, G. Wider, K. H. Lee and K. Wuethrich, *J. Mol. Biol.* **169**, 921 (1983).

³⁵W. Braun, C. Boesch, L. R. Brown, N. Go and K. Wuethrich, *Biochem. Biophys. Acta* **667**, 377 (1981).

³⁶S. Macura, K. Wuethrich and R. R. Ernst, *J. Magn. Reson.* **46**, 269 (1982).

³⁷A. Minoretti, W. P. Aue, M. Reinhold and R. R. Ernst, *J. Magn. Reson.* **40**, 175 (1980).

³⁸G. A. Morris and R. Freeman, *J. Am. Chem. Soc.* **101**, 760 (1979).

³⁹D. P. Burum and R. R. Ernst, *J. Magn. Reson.* **39**, 163 (1980).

⁴⁰G. Bodenhausen and D. J. Ruben, *Chem. Phys. Lett.* **69**, 185 (1980).

⁴¹A. Bax, R. H. Griffey and B. L. Hawkins, *J. Am. Chem. Soc.* **105**, 7188 (1983).

⁴²A. Bax, R. H. Griffey and B. L. Hawkins, *J. Magn. Reson.* **55**, 301 (1983).

⁴³D. H. Live, D. G. Davis, W. C. Agosta and D. Cowburn, *J. Am. Chem. Soc.* **106**, 6104 (1984).

⁴⁴L. Mueller, *J. Am. Chem. Soc.* **101**, 4481 (1979).

ELECTRON SPIN ECHO METHOD AS USED TO ANALYZE THE SPATIAL DISTRIBUTION OF PARAMAGNETIC CENTERS

A. M. Raitsimring and K. M. Salikhov

Institute of Chemical Kinetics and Combustion
Siberian Branch of the USSR Academy of Sciences
Novosibirsk 630090
USSR

	Page
I. Introduction	185
II. Models of Spatial PC Distribution in Solids	186
A. Uniform Volume PC Distribution	186
B. Pair Distribution	186
C. Distributions of the Cluster and "Island" Types	187
D. Surface and Linear Distributions	188
III. Theoretical Principles of Studying Spatial Spin Distributions by ESE Methods	188
A. Mechanism of PC d-d Contribution to ESE Signal Decay	189
B. Paramagnetic Particle Pairs	190
C. Uniform Volume PC Distribution	193
D. Uniform Linear PC Distribution	195
E. Non Uniform PC Distribution	196
IV. Methods of Spatial PC Distribution Analysis in ESE Experiments	198
A. The Inverse Problem of the ESE Method	198
B. Ways of Determining Pair Distribution Functions	198
C. General Methods of Determining the Pair Distribution Function	200
V. Measurements of ESE Signal Decays due to d-d Interactions of PCs. Experimental Data	
Data on Phase Relaxation in Systems with Non Uniform PC Distribution	202
A. Determination of Microwave H_1 Pulse Amplitude in a Spectrometer Cavity at the Location of a Sample	202
B. Separation of Contributions from d-d Interactions, Spin-lattice Relaxation and Electron-nuclear Interactions to the Total ESE Signal Decay Kinetics	202
C. Systems with a Uniform Volume PC Distribution	207
D. Experimental Results on Phase Relaxation at a Uniform PC Distribution	207
VI. Systems with Nonuniform PC Distributions	210
A. Distribution of $Fe^{2+} \cdots R$ Pairs in Alcohol Matrices	210
B. Pairs with Long Relaxation Times	213
C. Some Examples of Investigating Pairs with $W\tau \sim 1$	213
D. Spatial SO_4^- Radical-ion Distribution in Tracks of $T\beta$ -particles	214
VII. Conclusion	215
References	216

LIST OF SYMBOLS

C	— mean volume concentration of spins
g_i	— g-values of the i-th spins
$g(\omega)$	— ESR line shape
$\langle \dots \rangle_{g(\omega)}$	— averaging over ESR line shapes
H_1	— microwave pulse amplitude
$J_B(2W\tau),$ $J_A(2W\tau)$	— functions describing the contributions from spectral and instantaneous diffusion mechanisms to the ESE signal decay of samples of T_1 -type, respectively
$r_{1,2}$	— radius-vector connecting two spins
$n(r)$	— distance distribution function of pairs
$Q_B(\tau W_{\max}),$ $Q_A(\tau W_{\max})$	— functions describing the contributions from spectral and instantaneous diffusion mechanisms to the ESE signal decay for samples of T_2 -type, respectively
T_1	— spin-lattice relaxation times
t_p	— duration of a microwave pulse
$\dot{W} = 1/2T_1$	— spin flip-flop rate
$v(2\tau)$	— ESE signal decay due to dipolar interactions in a pair of spins, or the total ESE signal decay observed experimentally
$v_L(2\tau)$	— ESE signal decay attributed to spin-lattice interaction
$v_{in}(2\tau)$	— ESE signal decay due to dipole-dipole interaction in isolated spots of spin localization
$v_N(2\tau)$	— ESE signal decay due to electron-nuclear coupling
$V(2\tau)$	— ESE signal decay due to dipole-dipole interaction at a certain spatial spin distribution
χ	— linear spin concentration
$\Theta = \gamma H_1 t_p$	— angle of rotation of spins whose Larmor precession frequency coincides with the carrier frequency of microwave pulses
$\Theta(\omega)$	— angle of rotation of spins whose precession frequency is ω -shifted from the carrier frequency
Φ	— angle between $r_{1,2}$ and the external magnetic field direction H_0
τ	— time interval between microwave pulses
τ_0	— "dead" time, a minimum time interval between microwave pulses
$\Phi(W)$	— spin flip rate distribution function

I. INTRODUCTION

Numerous problems in physics, chemistry and biology call for information on spatial distribution of paramagnetic centers (PC) — transition metal ions, their complexes, free radicals, atoms, stabilized electrons, etc. — in solid matrices. This information is indispensable, e.g. for photo- and radiation chemistry: spatial distribution of active intermediates appreciably affects the reaction kinetics and the subsequent product generation. The same information is required to interpret magnetic effects in recombination of radicals and optically detected magnetic resonance spectra. In biological systems it is sometimes necessary to determine PC spacing for solving the problem of localization of electron transfer chains, separations between paramagnetic labels and metal ions that are present in a biopolymer structure, etc.

Electron spin echo (ESE) methods have become effective tools to study spatial PC distributions in solid matrices. Applicability of ESE

methods in this field is based on the fact that ESE signal decays are mainly contributed to by dipole-dipole (d-d) PC interactions which depend on spatial PC distribution. At present a number of techniques of studying spatial PC distributions in solids have been proposed and realized in practice based on the ESE principle.

The present paper reviews the basic methods of ESE investigations of spatial PC distributions and some data obtained mainly within the last few years for particular systems. During this period noticeable progress has been achieved in understanding the pair distribution in various photochemical systems, and interesting results on numerical simulation of radical tracks have been obtained. Moreover, new aspects of theory of ESE signal decay have been recently developed, in particular, theory of ESE signal decay due to dipole-dipole interactions between PCs. Refinements in the theory make it possible to distinguish contributions from different phase relaxation mechanisms to ESE signal decays. The present paper reviews only the main

theoretical results, whereas detailed discussion of previously developed theories can be found in the literature (1-3). Recent theoretical investigations have supplemented the existing ESE theory and specified some quantitative characteristics of well-studied systems.

The review embraces seven sections. Section II presents some model spatial PC distributions. Theoretical results on PC d-d interaction effects upon ESE signal decay are summarized in Section III. Section IV is devoted to methods of analyzing experimental data with the aim of obtaining information on spatial PC distributions. In Section V some general problems are considered arising in experiments on d-d interactions. Lastly, data on spatial PC distributions in concrete systems are described in Section VI, and Section VII concludes the discussion.

II. MODELS OF SPATIAL PC DISTRIBUTION IN SOLIDS

In the present review only magnetically diluted systems are considered. The spatial distribution of PCs stabilized in solids can be diversified depending on the way of preparing the sample and the technique of PC introduction or generation. Therefore, though not aimed at describing ESE signal decays for all spatial distributions, we believe it to be expedient to consider some sufficiently simple plausible cases which can serve as models for real systems.

A. Uniform Volume PC Distribution

At a random uniform distribution all lattice points of a solid can be occupied by PCs with equal probability. In this case, the spatial distribution is fully determined by the only parameter: the mean PC concentration $C = N/V$, where N is the overall number of spins in the sample, V is the sample Volume. Figure 1 furnishes an example of a uniform distribution in a two-dimensional lattice. The PC coordinates are randomly distributed within the range 0-1. A uniform PC distribution can be observed in a number of cases. It seems to be realized in crystals doped with small amounts of a substance during their growth, in fast-frozen glassy solutions of paramagnetic complexes and stable free radicals.

The initial nonuniform distribution in samples can be made uniform by a special treatment considered in Section V.

The simplest cases of the variety of nonuniform PC distributions are as follows.

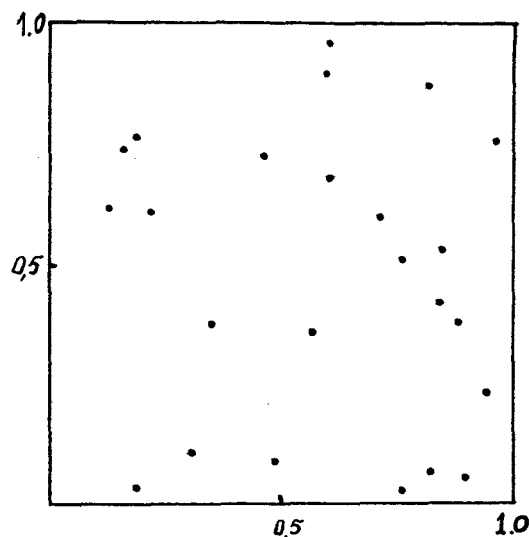


Figure 1. Random distribution of paramagnetic centers in a two dimensional lattice.

B. Pair Distribution

The PC distribution in pairs is of practical importance. For instance, PC pairs are generated in initial stages of low-temperature photolysis (4), as well as under radiolysis in solids, the PC generation probability being the higher the harder the irradiation (5). The separation and the relative orientation of PCs inside pairs can be either fixed or somehow distributed. Numerous examples of pairs with fixed partner separations have been considered in the literature (4). In the general case, PC pairs show a certain variability of the partner separation and relative orientation. The relative PC location can be determined by the pair distribution function $n(r)$. The quantity $n(r)dr$ is the statistic weight of the pair subensemble, with the radius-vector between the partners in a pair ranging within $(r, r+dr)$. When partners are located isotropically, the pair distribution function depend only on the partner separation and assumes the form

$$n(r)dr = 4\pi n(r)r^2 dr. \quad (1)$$

PC pairs in turn can be distributed either uniformly or nonuniformly throughout the sample. In the following systems PC pair distributions are uniform and thus can be fairly well described by

the mean pair concentration, Figure 2 showing an example of such distributions.

C. Distributions of the Cluster and "Island" Types

In some cases PCs can be stabilized in solids in groups or clusters (see Figure 3). Distributions of the cluster type are realized most likely in coils of macromolecules with paramagnetic

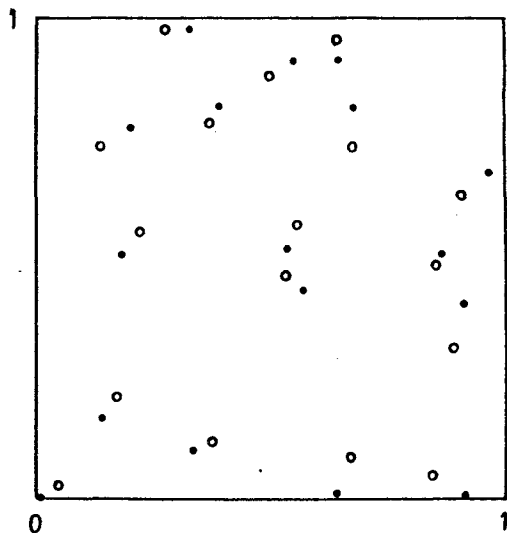


Figure 2. Random uniform distribution of pairs in a two-dimensional lattice.

labels, in artificial liposomes with paramagnetic ions and stable radicals introduced into them, in small metal particles with conduction electrons originating in specially prepared alkaline-halide crystals (6).

Similar distributions can arise under ionizing irradiation with an intermediate linear energy transfer; the so-called blobs and short tracks (5), regions of high radical concentration. Nonuniform PC distributions can also result from structural irregularities in solids. Freezing solutions can lead to macro- and microscopic stratification of phases. In this case, paramagnetic admixtures or radiation-generated PCs occupy not the whole volume but certain regions, phases or microphases, or are stabilized at definite structural inhomogeneities. Inhomogeneous structure characterizes systems of biological origin which exhibit, as a rule, nonuniform PC

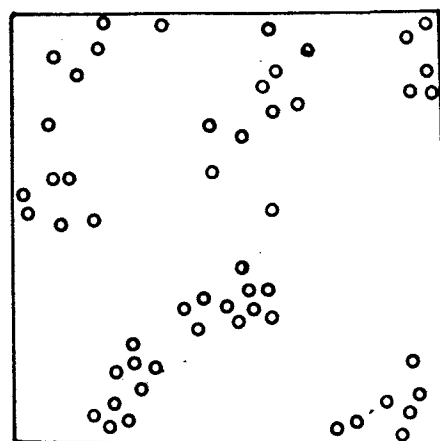


Figure 3. Cluster distribution of paramagnetic centers.

distributions (7).

When PCs make small groups, the distribution should be called of the cluster type. The notation of mean concentration is hardly applicable to such systems, and the spatial distributions should be described through the relative particle location in a cluster. If the number of PCs in a group is sufficiently great (let this case be referred to as island distribution), it seems to be possible to introduce the notion of local PC concentration inside an island as

$$C_i = N/V_{st} = CV/V_{st}, \quad (2)$$

where V is the sample volume, V_{st} is the volume wherein PCs are stabilized.

It is necessary to note an interesting feature of the nonuniform distribution resulting from either structural inhomogeneities or nonequivalency of various stabilization sites in a solid lattice. Let us assume that free radicals which are generated in a solid can be distributed and moved only along the lattice dislocation axis. This distribution is obviously nonuniform since the lattice points remote from dislocations are inaccessible for PCs. At the same time, in magnetic resonance experiments this distribution can be manifested as a uniform distribution since the effective mean PC spacing can be manifested as a

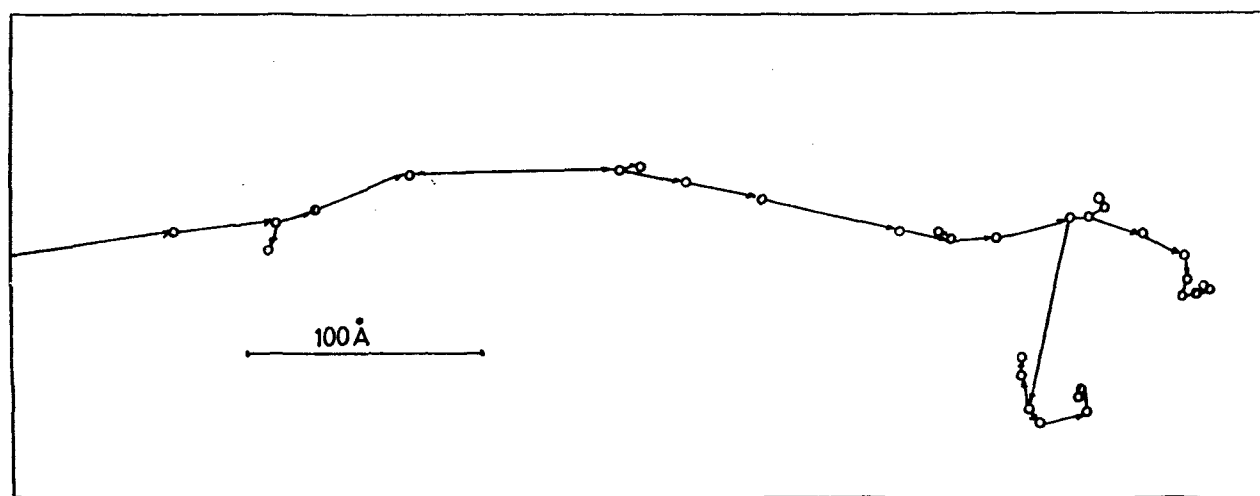


Figure 4. Spatial positions of ionizations induced by an electron with the initial energy of 1 keV calculated by Monte-Carlo method. The way of generating such tracks is described in detail in ref. 24 from which the present figure is taken.

uniform distribution since the effective mean PC spacing can be equal to the mean spacing at a uniform PC distribution and thus the d-d interaction is the same in both cases. The nonuniformity of the above distribution is manifested in magnetic resonance only at great occupation numbers of stabilization sites considered, i.e. as the spin concentration in the sample increases.

The possibility of imitating a uniform distribution must be taken into account in studying spatial PC distribution by analysis of the spin d-d interaction effects observed in experiment.

D. Surface and Linear Distributions

Interesting cases of PC distribution are PC stabilization either on a solid surface or along lines (dislocations, polymer chains, ionizing particle tracks). These distributions can be in turn either uniform or nonuniform. An example of nonuniform distribution is that of ionization points along a low-energy electron shown in Figure 4. In solid matrices ions are transformed into radicals that are stabilized in the vicinity of ionization points.

Thus, we have mentioned some possible PC distributions in solids, the borders between them being, however, not strict. For instance,

spin-labeled DNA and biopolymers can vary their configuration from a blob (cluster distribution) to a line depending on external conditions; ionizing particles may simultaneously create pairs, clusters and island of PCs. An increase in the number of radicals in irradiated systems can result in both uniform due to overlapped tracks and nonuniform distribution due to occupation of accessible stabilization sites.

Below we consider the way of determining the type of one or another distribution and its details by experimental data on ESE.

III. THEORETICAL PRINCIPLES OF STUDYING SPATIAL SPIN DISTRIBUTIONS BY ESE METHODS

A spatial PC distribution can be in principle determined by studying the contribution from the PC d-d interaction to the spin dynamics. There is a great variety of spectroscopic manifestations of d-d interactions in magnetic resonance experiments. For instance, in the case of a PC pair with $1/2$ spin, a fixed partner separation $r_{1,2}$ and a fixed relative orientation $r_{1,2}$ relative to an external magnetic field H_0 ($\Theta_{1,2}$ angle), the d-d interaction splits the ESR spectral lines into two components with the splitting equal to

$$\Delta = (3/2)\gamma\hbar(1-3\cos^2\Theta_{12})r_{12}^{-3}, \quad (3)$$

where γ is the gyromagnetic ratio for the PC. The partner separation can be determined from the angular dependence of Δ on $\cos\Theta_{12}$. As one more example, it is possible to mention the static dipolar broadening of ESR lines in systems with uniform PC distributions. For particles with 1/2 spins it is (8)

$$\Delta\omega_{1/2} = (4\pi^2/9\sqrt{3})\gamma^2\hbar C. \quad (4)$$

This relation shows that measurements of the dipolar broadening of ESR lines makes it possible to determine the concentration of PCs stabilized in a solid; such measurements were carried out in a number of works (4). However, it is extremely difficult to experimentally measure the d-d interaction contribution to the ESR line broadening and shape in magnetically diluted solids since the linewidth in such systems is chiefly conditioned by not d-d interactions but some other factors: g-tensor anisotropy, isotropic and anisotropic hyperfine interactions, and external field inhomogeneities. In the case of free radicals stabilized in a solid matrix, the ESR linewidth is 1–10 G, while the dipolar broadening, according to eqn. 4, equals a fraction of a Gauss at a typical particle concentration of 10^{18} cm $^{-3}$.

Being insensitive to nonhomogeneous broadening (9), the ESE method can be successfully employed to eliminate the masking effect of this broadening and to distinguish the contribution from comparatively weak d-d interactions to the spin dynamics.

A. Mechanism of PC d-d Contribution to ESE Signal Decay

Quite a number of investigators contributed to the development of theoretical and experimental principles of the ESE method and its application to various problems in chemistry, physics, and biology. Among them are the groups from Bell Telephone Laboratory (1, 10) and from the Novosibirsk Institute of Chemical Kinetics and Combustion (2, 3, 11-13), as well as other researchers, e.g. (14-18).

As a rule, in ESE experiments not all spins are excited by microwave pulses and thus contribute to the echo signal amplitude since the ESR spectrum width in magnetically diluted solids most often exceed the amplitude of the microwave field that arise in experiment and form the echo signals. The spins excited by

microwave pulses and contributing directly to the ESE signal are usually referred to as A spins, the other (unexcited) are called B spins. The d-d interaction between A spins manifest itself in ESE experiments in some other way compared to that between A and B spins. To illustrate this statement, let us consider a PC pair and discuss the partner d-d interaction contribution to the primary echo signal arising at a time moment 2τ subsequent to a Hahn-succession of two pulses $90^\circ - \tau - 180^\circ$. Assume also the spin relaxation flips to be too slow to occur within 2τ time interval. The Hamiltonian of this pair includes the Zeeman spin energies and the spin d-d interaction:

$$\hat{H} = \hbar\omega_1\hat{S}_{1z} + \hbar\omega_2\hat{S}_{2z} + \hbar D(r)\hat{S}_{1z}\hat{S}_{2z}, \quad (5)$$

where ω_1 and ω_2 are the Zeeman spin frequencies, $D(r)$ determines the d-d interaction and equals

$$D(r) = g_1g_2\beta^2\hbar^{-1}(1-3\cos^2\Theta)r_{12}^{-3}, \quad (6)$$

where g_1 and g_2 are spectroscopic splitting factors of the partners. If both pair spins are of A type, the 180° -pulse changes the sign of the Zeeman energy in eqn. 5, leaving the d-d interaction energy unchanged. Therefore, the d-d interaction energy must manifest itself in the echo signal at the time 2τ in the similar way as if there were no 180° -pulse, i.e. the echo signal amplitude will oscillate:

$$v(2\tau) \sim \cos[D(r)\tau]. \quad (7)$$

Thus, A spin d-d interactions are manifested in the primary echo signal decay in a similar way as in the free induction decay (2, 13, 19). The situation changes dramatically if one of the spins is of B type. In this case, the 180° -pulse turns only one spin of the pair and alters the d-d interaction sign. As a result, the d-d contribution to the spin precession within the time intervals $(0, \tau)$ and $(\tau, 2\tau)$ completely compensate one another. In this case,

$$v(2\tau) \sim 1, \quad (8)$$

i.e. the d-d interaction is not manifested in the ESE signal decay, with the processes induced by relaxation flips neglected. The case is different if within the time 2τ there occur relaxation flips of B spins. A time-dependent local dipolar field arises in the place of location of A spins. As a result, the A precession frequency varies randomly, spectral diffusion occurs. The A spin

frequency migration due to d-d interaction modulation by random spin flips results in irreversible spin dephasing. Random spin flips can be associated with either spin-lattice relaxation (T_1 type samples) or spin flip-flops induced by spin diffusion (T_2 type samples). Thus, the d-d interaction with B spins is manifested in the ESE signal decay due to random B spin flips by a spectral diffusion mechanism.

The A spin interaction shows itself in the ESE signal decay and in the absence of random spin flips (eqn. 7). In this case, instead of a random flip the spin is turned by the second microwave pulse forming the echo signal. By analogy with spectral diffusion, the d-d interaction between A spins is conventionally assumed to manifest itself in the echo signal decay by the so-called instantaneous diffusion mechanism. This mechanism of phase relaxation, typical of the echo signal, was first reported in (10) and then studied in detail in (19). A microwave pulse is meant to "instantaneously" change the local dipolar field.

In real experiments the manifestation of d-d interactions in the ESE signal decay is hampered by two factors. Microwave pulses, inducing the echo signal, turn the spins through different angles. As a result, one and the same spin can contribute to the echo signal simultaneously by an instantaneous diffusion mechanism, due to the rotation induced by the pulse, and by a spectral diffusion mechanism since the pulse does not turn the spin through 180° . As a result, the d-d contribution to the decay kinetics exhibits a strong dependence on the character of spin excitation by microwave pulses. The character of excitation is in turn dependent on the ESR spectrum shape of the PC under study, on the amplitude and duration of the microwave pulses.

Another complicating factor is a certain interference, or overlapping, of the instantaneous and spectral diffusion mechanisms that occurs when A spins reorient randomly during the time of observing the echo signals. Relaxation flips of A spins suppress their contribution to the instantaneous diffusion mechanism. Indeed, at the background of sufficiently frequent random flips, one or two more pulse-induced flips are of no importance. Thus, in the extreme case of very frequent random spin flips, the d-d contribution to the echo signal decay stops depending on the character of spin excitation by microwave pulses, and the spin dephasing results solely from the spectral diffusion mechanism. A detailed discussion of theory of echo signal decay in magnetically diluted solids can be found in a number of reviews (1-3, 11, 13). Results of theory obtained

for various possible types of spatial PC distributions in solids can be briefly summarized as follows.

B. Paramagnetic Particle Pairs

The echo signal decay for PC pairs was analyzed theoretically (2, 13). The d-d interaction of a spin with its partner makes the following contribution to the primary echo signal of the spin (13):

$$\begin{aligned} v(2\tau|r) &= [(ChR\tau + WShR\tau/R)^2 + \\ D^2(r)Sh^2R\tau/4R^2 - \langle \sin^2\Theta/2 \rangle g(\omega)] \times \\ D^2(r)Sh^2R\tau/2R^2] \exp(-2W\tau), \quad (9) \\ R^2 &\equiv W^2 - D^2(r)/4 \end{aligned}$$

providing the partner spin is $1/2$. Here W is the random flip frequency of the spin-partner, $W = 1/2T_1$ in T_1 samples. In T_2 samples W is the spin flip-flop rate, Θ is the angle through which the spin is turned around the Y-axis by the second pulse, $\sin^2\Theta/2$ is averaged over all possible angles of the spin-partner rotation, i.e. over all possible resonance frequencies of the partner. Relation 9 can be interpreted as follows. When the spin turns through Θ around the Y-axis, the spin projection onto the quantization axis does not vary with the probability $\cos^2\Theta/2$. Hence, all pairs can be divided into two subensembles. In one of them, with a statistical weight $\cos^2\Theta/2$, the interaction with the spin-partner contributes to the echo signal of the spin under study:

$$\begin{aligned} v_0 &= [(ChR\tau + WShR\tau/R)^2 + \\ D^2(r)Sh^2R\tau/4R^2] \exp(-2W\tau) \quad (10) \end{aligned}$$

This expression results from eqn. 9 with $\Theta = 0$. In the other ensemble, with the statistical weight $\sin^2\Theta/2$, the interaction with the partner contributes to the echo signal considered:

$$\begin{aligned} v_\pi &= [(ChR\tau + WShR\tau/R)^2 - \\ D^2(r)Sh^2R\tau/4R^2] \exp(-2W\tau) \quad (11) \end{aligned}$$

This expression is derived from eqn. 9 at $\Theta = \pi$. When averaged over both subensembles, the influence of the partner upon the echo signal under study is

$$v(2\tau|r) = \langle \cos^2\Theta/2 \rangle g(\omega) v_0 +$$

$$\langle \sin^2 \Theta / 2 \rangle g(\omega) v_\pi \quad (12)$$

which is identical to eqn. 9.

In extreme cases the above relations assume very simple forms. If there occur no random flips during the observation time, $W\tau \ll 1$, then

$$v(2\tau|r) = \langle \cos^2 \Theta / 2 \rangle g(\omega) + \langle \sin^2 \Theta / 2 \rangle g(\omega) \cos D(r)\tau \quad (13)$$

For the above reasoning, the d-d interaction in one subensemble ($\langle \cos^2 \Theta / 2 \rangle g(\omega)$ statistical weight) does not contribute to the echo signal decay (cf. eqn. 8), while that in the other one ($\langle \sin^2 \Theta / 2 \rangle g(\omega)$ statistical weight) modulates the echo signal (cf. eqn. 7). In the other extreme case of very frequent random spin flips, at $W\tau \gg 1$ and $W > |D(r)|$, eqn. 9 yields

$$v(2\tau|r) = \exp[-D^2(r)\tau/4W] \quad (14)$$

As it would be expected, at frequent random spin flips their contribution to the echo signal decay stops depending on the character of spin excitation by microwave pulses and is realized by the spectral diffusion mechanism.

In the case of a B partner, it contributes to the echo signal decay of the spin under study by the spectral diffusion mechanism at any W according to :

$$v_B(2\tau|r) = [1 + W \text{Sh} 2R\tau/R + 2W^2 \text{Sh}^2 R\tau/R^2] \exp(-2W\tau) \quad (15)$$

By now we have considered pairs with a fixed partner separation r_{12} . The echo signal observed experimentally is the result of averaging over the whole ensemble of pairs. Hence, eqn. 9 or 15 should be averaged by the pair distribution function:

$$\langle v(2\tau) \rangle = \int v(2\tau|r) n(r) dr \quad (16)$$

In an isotropic situation,

$$\langle v(2\tau) \rangle = 4\pi \int v(2\tau|r) n(r) r^2 dr \quad (17)$$

where $v(2\tau|r)$ is the echo signal decay in a pair subensemble with a set r and an arbitrary orientation of the radius vector r connecting the partners:

$$\langle v(2\tau|r) \rangle = \frac{1}{2} \int_0^\pi v(2\tau|r) \sin \Theta d\Theta \quad (18)$$

Of practical importance for pair distribution studies is the case of B spin-partners (20, 21). The dependence of ESE signal decay upon the partner separation was obtained by numerical integration of eqn. 18 (22). Figures 5-7 depict the

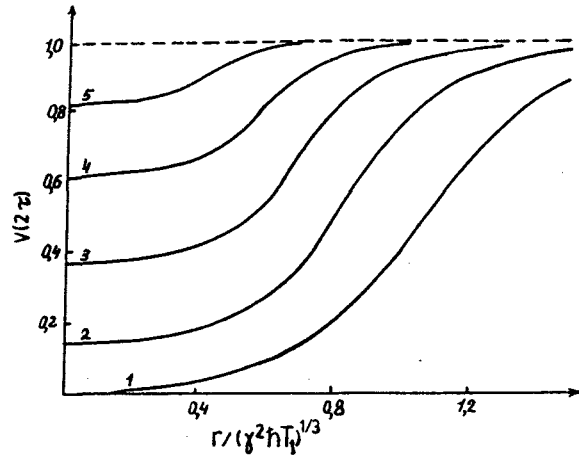


Figure 5. Plots of ESE signal intensity vs. the distance in a pair. The signal decays due to spectral diffusion. Different curves correspond to different values of the parameter τ/T_1 : (1) 5, (2) 2, (3) 1, (4) 0.5, (5) 0.2 (22).

results of numerical calculations.

Note some characteristic features of the function $v(2\tau|r)$.

At short partner separations (the region of strong interactions), when $g_A g_B \beta^2 \hbar^{-1} r^{-3} > W$, the B spin contribution to the A spin ESE decay becomes r -independent, Figure 5: the phase relaxation of the A spin results from dephasing of its precession due to random changes of the local field induced by the spin-partner and obeys the expression:

$$v(2\tau|r) = \exp(-2W\tau) = \exp(-\tau/T_{1B}) \quad (19)$$

At a sufficiently great partner separation, i.e. at $g_A g_B \beta^2 \hbar^{-1} r^{-3} < W$ (the region of weak interactions), random spin flips effectively average to zero the A spin frequency shift to d-d interactions; it is the phenomenon of exchange narrowing of dipolar broadening well-known in spectroscopy. In this case,

$$v(2\tau|r) \approx \exp[-D^2(r)\tau/4W] = \exp[-D^2(r)\tau T_{1B}/2]$$

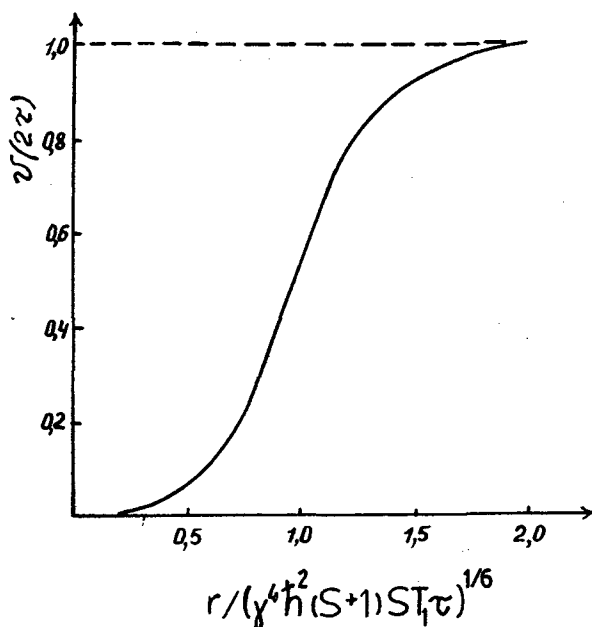


Figure 6. Plots of ESE signal intensity vs. the distance in a pair for short spin-lattice relaxation times of B spins, $T_1 \ll \tau$, $T_1 \Delta\omega > 1$ (22).

(20)

Here $D(r) \approx \gamma_1 \gamma_2 \hbar r_{12}^{-3}$.

Note also that the B spin contribution to the A spin phase relaxation depend substantially on the partner separation. At $r \rightarrow \infty$, $v(2\tau|r) \rightarrow 1$. Figure 7 demonstrates the ESE signal decay due to d-d interactions to follow the expression

$$\langle v(2\tau|r) \rangle = \exp[-f(r, T_1) \tau^{1/6}] \quad (21)$$

Comparing $\langle v(2\tau|r) \rangle$ calculated in the above way with experiment, one can determine the PC distribution parameters. In the general case, when the spin-partner is partially excited by a microwave pulse, one has to calculate $\langle \sin^2 \Theta/2 \rangle_{g(\omega)}$ for a particular shape of the partner ESR spectrum (see eqn. 9). Setting ω_0 , $\omega_1 = \gamma H_1$, t_p to be the frequency, amplitude and duration of the microwave pulse, one can find the angle Θ of rotation of a $S = 1/2$ spin with the resonance frequency ω :

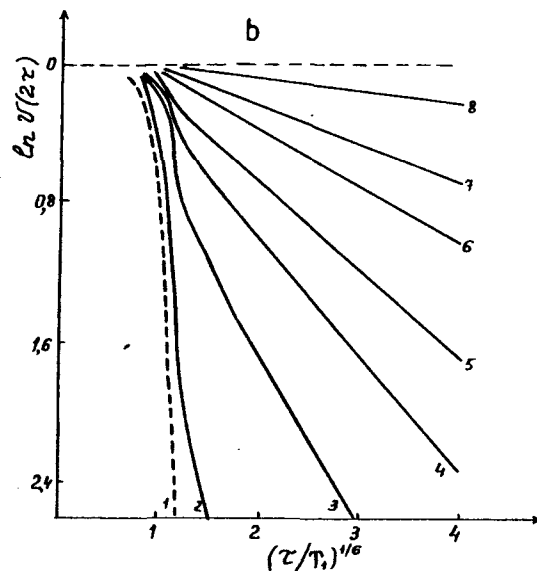
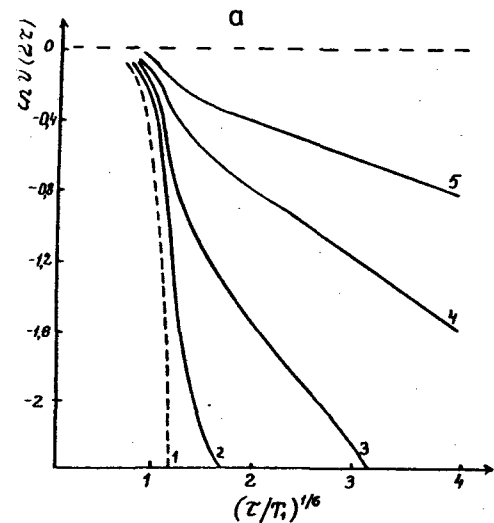


Figure 7. ESE signal decay due to spectral diffusion of B spins at various distance distribution functions $n(r)$ and parameters $a = r_0/(\gamma^2 \hbar T_1)^{1/3}$ (22). (a) $n(r) = (4\pi r^2 r_0)^{-1} \exp(-r/r_0)$, (1) 0, (2) 0.5, (3) 1, (4) 2, (5) 3; (b) $n(r) = (4\pi r_0^2 r)^{-1} \exp(-r/r_0)$, (1) 0, (2) 0.25, (3) 0.5, (4) 0.75, (5) 1, (6) 1.5, (7) 2, (8) 4.

$$\sin^2 \Theta(\omega)/2 = \omega_1^2 \sin^2(at_p/2)/a^2 \quad (22)$$

$a \equiv [\omega_1^2 + (\omega - \omega_0)^2]^{1/2}$ and the mean value of $\langle \sin^2 \Theta/2 \rangle_{g(\omega)}$ equals

$$\langle \sin^2 \Theta/2 \rangle_{g(\omega)} = \int_{-\infty}^{\infty} \sin^2 [\Theta(\omega)/2] g(\omega) d\omega \quad (23)$$

To give an idea of the scale of this quantity, its dependences on the ESR spectrum width and on the microwave pulse parameters, Figure 8 shows $\langle \sin^2 \Theta/2 \rangle_{g(\omega)}$ calculated for the Gaussian distribution of resonance frequencies $g(\omega)$ under the assumption that the microwave pulse frequency coincides with the center of the distribution $g(\omega)$ and the width of $g(\omega)$ is set by the mean quadratic deviation $\langle \Delta \omega^2 \rangle^{1/2} / \gamma H_1$. The mean value of $\langle \sin^2 \Theta/2 \rangle_{g(\omega)}$ depend on two dimensionless parameters: $\gamma H_1 t_p$ and $\langle \Delta \omega^2 \rangle^{1/2} / \gamma H_1$.

C. Uniform Volume PC Distribution

In magnetically diluted solids with uniform PC distributions the ESE signal decay due to the d-d interaction with all spin-partners can be written as

$$V(2\tau) = \langle \prod_k v_k(2\tau) \rangle \quad (24)$$

where $v_k(2\tau)$ is the signal decay due to the interaction with the k -th partner, $\langle \dots \rangle$ means averaging over all possible realizations of spatial PC distribution. The averaging yield the following results. The B spin contribution to the A spin dephasing is

$$V(2\tau) = \exp[-C_B \int d\tau (1 - v_0(2\tau | r, W_B))] \equiv \exp[-g_A g_B \beta^2 \hbar^{-1} C_B J_B(2W_B \tau)/2W_B] \quad (25)$$

where

$$J_B(2W\tau)/2W \equiv -g_A^{-1} g_B^{-1} \beta^{-2} \hbar \int d\tau (1 - v_0(2\tau | r, W)) \quad (26)$$

The A spin contribution to the ESE decay is

$$V(2\tau) = V'(2\tau) V''(2\tau) \quad (27)$$

where

$$V'(2\tau) = \exp[-C \int d\tau (1 - v_0(2\tau | r))] \\ V''(2\tau) = \exp[-C \langle \sin^2 \Theta/2 \rangle_{g(\omega)} \times \int d\tau [v_0(2\tau | r) - v_\pi(2\tau | r)]] \quad (28)$$

In eqns. 25 and 28 v_0 and v_π are set by formulae 10 and 11. The factor $V'(2\tau)$ gives the d-d contribution of the A spins to the ESE signal decay by a spectral diffusion mechanism as if the

A spins were B ones, i.e. not excited by microwave pulses:

$$V'(2\tau) = \exp[-g_A^2 \beta^2 \hbar^{-1} C_A J_B(2W_A \tau)/2W_A] \quad (29)$$

In the extreme cases of slow and fast spectral

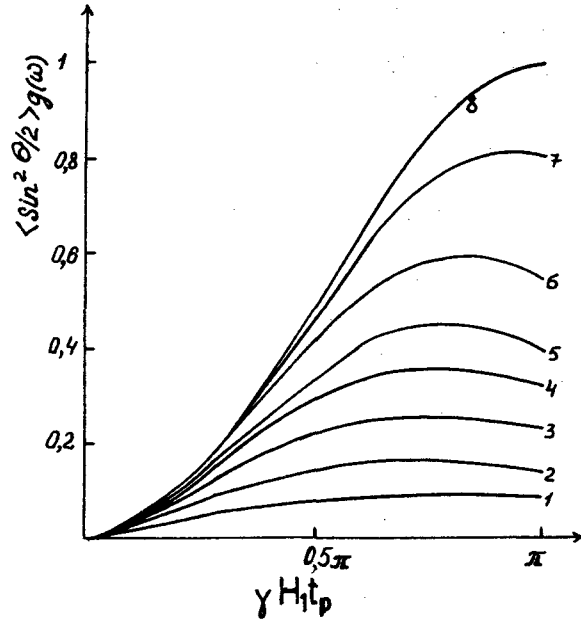


Figure 8. Values of $\langle \sin^2 \Theta/2 \rangle_{g(\omega)}$ for Gaussian line shape at varying $\Delta \omega_1 / \omega_1$: (1) 9, (2) 5, (3) 3, (4) 2, (5) 1.5, (6) 1, (7) 0.5, (8) 0.

diffusions we have

$$J_B(2W\tau)/2W \rightarrow 8\pi^2 W \tau^2 / 9\sqrt{3}; W\tau \ll 1 \\ J_B(2W\tau)/2W \rightarrow 8\pi \sqrt{\pi \sqrt{(\tau/W)}/9\sqrt{3}}; W\tau \gg 1 \quad (30)$$

The A spin d-d interaction contributes to the signal decay not only by a spectral diffusion mechanism; eqn. 27 contains the factor

$$V''(2\tau) = \exp[-g_A^2 \beta^2 \hbar^{-1} C_A \times \langle \sin^2 \Theta/2 \rangle_{g(\omega)} J_A(2W_A \tau)/2W_A] \quad (31)$$

where

$$J_A(2W\tau)/2W =$$

$$g_A^{-2} \beta^{-2} \hbar \int d\tau [v_0(2\tau|\tau)] - v_\pi(2\tau|\tau)]$$

At low frequencies of the random spin flips, i.e. at $W\tau \ll 1$,

$$V''(2\tau) \longrightarrow$$

$$\exp[-8\pi^2 g^2 \beta^2 \hbar^{-1} C\tau \langle \sin^2 \Theta/2 \rangle g(\omega)/9\sqrt{3}] \quad (32)$$

Relationship 32 describes the case of static dipolar interactions contributing to the ESE signal decay and was first derived in (19). In the other extreme case of $W\tau \gg 1$,

$$V''(2\tau) \longrightarrow \exp[-2\pi\sqrt{\pi} g^2 \beta^2 \hbar^{-1} / 9\sqrt{3} \times C\tau^{-1/2} W^{-3/2} \langle \sin^2 \Theta/2 \rangle g(\omega)] \quad (33)$$

The comparison of relationships 29 and 33 shows that in the case of frequent spin flips, $W\tau \gg 1$, the basic contribution from the A d-d interaction to the signal decay is made by a spectral diffusion mechanism; the spin flips induced by microwave pulses are negligible. Indeed, at $W\tau \gg 1$

$$J_B(2W\tau)/J_A(2W\tau) \sim W\tau$$

and eqns. 26 and 31 can be used to calculate $J_B(2W\tau)$ and $J_A(2W\tau)$ at any W (see Figure 9). At $W\tau > 1$ the function $J_A(2W\tau)/2W$ once again confirms the above statement that frequent random flips completely mask the effect produced by pulse-induced spin flips.

In real systems spins can also be described by distribution of the flip rates. For instance, in magnetically diluted solids the spin flip rates are (23):

$$\phi(W)dW =$$

$$\sqrt{3W_{\max}/2\pi} (W^{-3/2}) \exp[-3W_{\max}/2W] dW \quad (34)$$

where W_{\max} is the most plausible rate of random spin flips. In this case, the d-d contribution to the signal decay obeys an expression obtained from eqns. 29 and 31 by averaging $J_A(2W\tau)/2W$ and $J_B(2W\tau)/2W$ over the flip frequency distribution:

$$V(2\tau) = \exp\{2.5g^2 10^{-1} C[Q_B(\tau|W_{\max}) + \langle \sin^2 \Theta/2 \rangle g(\omega) Q_A(\tau|W_{\max})]\} \quad (35)$$

where

$$Q_B(\tau|W_{\max}) =$$

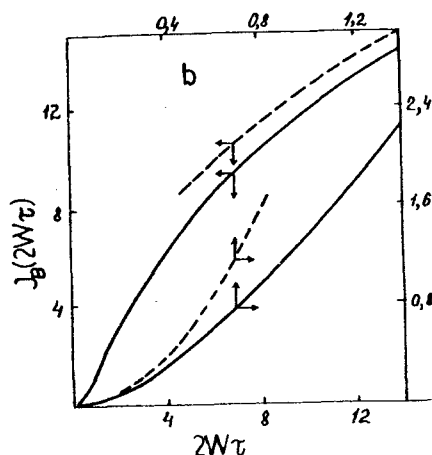
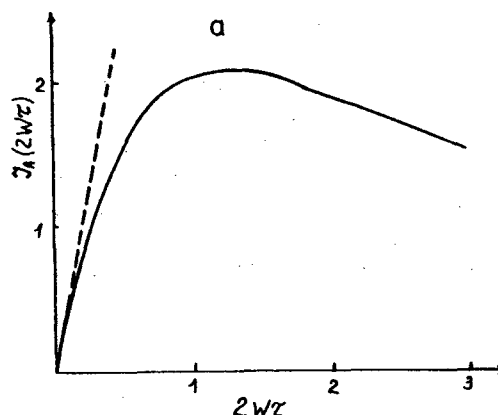


Figure 9. $J_A(2W\tau)$ (a) and $J_B(2W\tau)$ (b) for a homogeneous spin distribution (22). Dashed lines show asymptotic dependences

$$J_B(2W\tau) = \frac{16\pi\sqrt{\pi}\sqrt{W\tau}}{9\sqrt{3}} \text{ at } W\tau \gg 1$$

$$16\pi^2 W^2 \tau^2 / 9\sqrt{3} \text{ at } W\tau \ll 1$$

$$J_A(2W\tau) = \frac{16\pi^2 W\tau}{9\sqrt{3}} \text{ at } W\tau \ll 1$$

$$-4\beta^2 \hbar^{-1} 10^1 \int dW \phi(W) J_B(2W\tau)/2W$$

$$Q_A(\tau|W_{\max}) =$$

$$-4\beta^2 \hbar^{-1} 10^1 \int dW \phi(W) J_A(2W\tau)/2W$$

Figure 10 depicts calculated $Q_A(\tau|W_{\max})$ and

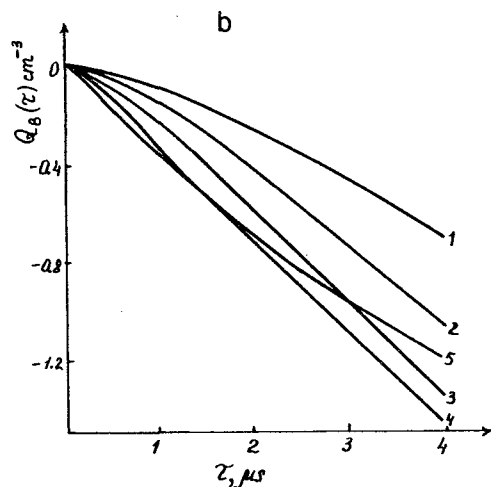
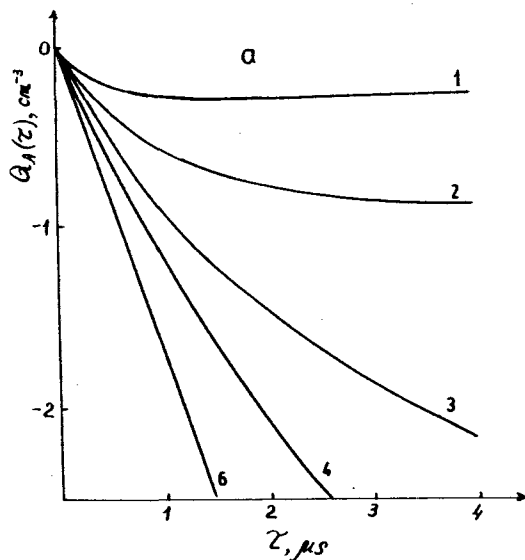


Figure 10. $Q_A(2W\tau)$ (a) and $Q_B(2W\tau)$ (b) for a homogeneous volume spin distribution at various values of the most probable flip-flop rate W_{\max} (22): (1) $3 \times 10^5 \text{ s}^{-1}$, (2) 10^5 s^{-1} , (3) $3 \times 10^4 \text{ s}^{-1}$, (4) 10^4 s^{-1} , (5) $3 \times 10^3 \text{ s}^{-1}$, (6) 0.

$Q_B(\tau|W_{\max})$.

D. Uniform Linear PC Distribution

The d-d interaction between PCs randomly distributed along a straight line contributes to the ESE signal decay by the law

$$V(2\tau) = \frac{1}{2} \int_0^{\pi} d\cos\Theta \exp[-\chi \int d\tau (1-v(2\tau|r))] \quad (36)$$

where $v(2\tau|r)$ is determined by eqn. 9, χ is the linear spin density, Θ is the angle between the spin distribution line and the external magnetic field direction H_0 . The inner integral in eqn. 36 can be written as

$$J = \int_{-\infty}^{\infty} d\tau (1-v)(2\tau|r) = [\alpha/W]^{1/3} \sqrt{\pi} \Gamma(5/6) \times \frac{2W\tau}{\int_0^{\infty} (I_{-1/3}(x)/x^{1/3}) e^{-x} dx} <\cos^2\Theta/2>_{g(\omega)} e^{-2W\tau \int_0^{\infty} (I_{-1/3}(x)/x^{1/3}) dx} \quad (37)$$

where $I_{-1/3}(x)$ are the modified Bessel functions of the order of $-1/3$ and $\alpha = \gamma^2 \hbar |1-3\cos^2\Theta|$. The averaging over $d\cos\Theta$ is carried out independently and, as shown by calculations (24), results in a negligible deviation of $V(2\tau)$ from the exponent. Calculations of u' ,

$$u' = \ln \left[\frac{1}{2} \int_0^1 dx \exp(-u|1-3x^2|^{1/3}) \right] \quad (38)$$

show that u'/u reduces from 1 to 0.85 at u ranging within 0 to 5. As in the volume case, let us use J in the form

$$J \approx [\gamma^2 \hbar/W]^{1/3} \chi [J_B(2W\tau) + <\sin^2\Theta/2>_{g(\omega)} J_A(2W\tau)] \quad (39)$$

In the extreme cases of low and high flip rates, we have for $J_A(2W\tau)$ and $J_B(2W\tau)$

$$J_A(2W\tau) = 2.35[W\tau]^{1/3} [1-2W\tau]$$

$$J_B(2W\tau) = 3.52[W\tau]^{4/3} \quad \text{at } W\tau \ll 1$$

$$J_A(2W\tau) = 0.14[W\tau]^{-5/6}$$

$$J_B(2W\tau) = 1.7[W\tau]^{1/6} \quad \text{at } W\tau \gg 1 \quad (40)$$

$J_A(2W\tau)$ and $J_B(2W\tau)$ at intermediate $W\tau$ values were calculated numerically by eqn. 37 (Figure 11). As in the volume case, the contribution to the signal decay by an instantaneous diffusion mechanism goes to zero with increasing frequency of spin flips, and $J_B(2W\tau)/J_A(2W\tau) \sim W\tau$.

One can readily demonstrate that in the case of uniform plane distribution

$$J_A(2W\tau) \sim [W\tau]^{2/3}$$

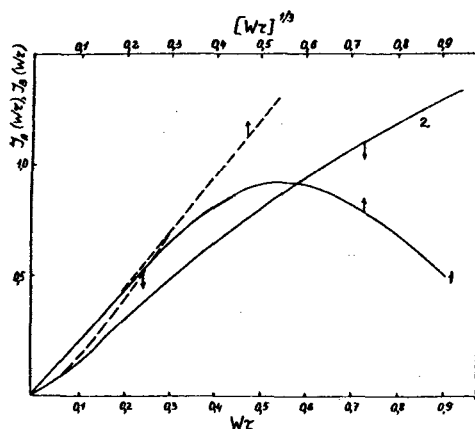


Figure 11. $J_A(2W\tau)$ (1) and $J_B(2W\tau)$ (2) for a homogeneous linear distribution (24). Dashed lines show dependences $J_A(W\tau) = 2.35[W\tau]^{1/3}$ and $J_B(W\tau) = 3.52[W\tau]^{1/3}$ corresponding to $W\tau \ll 1$.

$$J_B(2W\tau) \sim [W\tau]^{5/3} \quad \text{at } W\tau \ll 1 \quad (41)$$

$$J_A(2W\tau) \sim [W\tau]^{-2/3}$$

$$J_B(2W\tau) \sim [W\tau]^{1/3} \quad \text{at } W\tau \gg 1$$

The comparison of the results for uniform volume, plane and linear distributions shows that the signal decay is sensitive to the character of particle distribution. In the case of a linear distribution, the signal decays much slower than in the volume case since an increase of the distance between the spin under study and its partners does not change the number of the partners in the former case and increases it as r^2 in the latter case. A uniform spin distribution in a plane results in ESE signal decay kinetics which are intermediate between those at volume and linear distributions.

It is natural to expect that as the concentration of spins linearly distributed in a volume increases, the mean distance between PCs located at different lines becomes either comparable with or shorter than the mean distance between PCs along the lines, i.e. at $C^{1/3} \sim \chi$ the ESE signal decay approaches that obtained in the previous section (see eqn. 23). A similar

statement is valid for a uniform PC distribution in a plane. The kinetics come to correspond to volume distributions at $C^{2/3} \sim \delta$, where δ is the surface spin density.

E. Nonuniform PC Distribution

The d-d contribution to the signal decay at an arbitrary particle distribution in a solid matrix can be calculated by the expression

$$V(2\tau) = \langle \langle \Pi v(2\tau | \eta_{kn}) \rangle_n \rangle_k \quad (42)$$

where $v(2\tau | \eta_{kn})$ is the signal decay of the k -th particle due to its interaction with the n -th partner; it obeys eqn. 9.

In the general case, according to eqn. 42, the ESE signal decay is determined by the many-particle distribution function f_N . The function $f_N(r_1, r_2, \dots, r_N)$ is the density of the probability of finding particles in the vicinity of points with the radius vectors r_1, r_2, \dots, r_N

$$V(2\tau) = \int \dots \int \prod_{n=2}^N V(2\tau | r_{1n}) r_{1n} f_N dr_1 \dots dr_N \quad (43)$$

At a random uniform particle distribution $f_N = 1/V^N$ and the above formula yield the result of eqn. 27.

If PCs are stabilized in pairs, the pairs distributed uniformly throughout the sample, $V(2\tau)$ can be expressed through the pair distribution function. In this case, the ESE signal decay of the spin under study is

$$V(2\tau) = V_1(2\tau) V_2(2\tau) \quad (44)$$

where $V_1(2\tau)$ describes the signal decay due to d-d interaction of a given spin with its partner in a pair, $V_1(2\tau)$ is set by the relations 16 and 17. The term $V_2(2\tau)$ corresponds to the contribution from the spins of other pairs to the dephasing of the given spin:

$$V_2(2\tau) =$$

$$\exp\{-C_p \int dr_2 dr_3 n(r_{23}) [1 - v(2\tau | r_2) v(2\tau | r_3)]\} \quad (45)$$

where C_p is the mean pair concentration, $v(2\tau | r_2)$ and $v(2\tau | r_3)$ describe the contributions from spins located at the points r_2 and r_3 to the signal decay of the given spin located at the origin, $n(r_{23})$ is the pair function eqn. 1.

Similar generalizations are possible in the case of cluster PC distributions. Here $V(2\tau)$ can be expressed via the spin distribution function in a cluster.

Eqn. 42 can be employed to determine the

ESE signal decay for an arbitrary PC distribution. To exemplify this procedure, let us calculate the ESE signal decay for PCs stabilized in a fast electron track (24), Figure 4 showing this nonuniform distribution. Calculations of decay kinetics in ionizing particle tracks are divided into two independent procedures. First, determination of relative coordinates of ionization points; second, ESE signal decay calculations properly. Ionization point coordinates are calculated by the Monte Carlo technique on the basis of experimental data on the cross-sections of elastic and inelastic electron scatterings in the substance under study. It turned out that 8×10^3 ionization points sufficed for the calculations, the statistical error being no more than 2%.

With sets of tracks with a known relative distribution of ionization points one can calculate by eqn. 42 the signal decay induced by d-d interactions between PCs located at the ionization points:

$$V(2\tau) = \sum_k \Pi' v(2\tau | \tau_{kn}) \quad (46)$$

Figure 12 shows $V(2\tau)$ calculated at two spin flip rates W and some values of $\langle \sin^2 \Theta/2 \rangle$ and τ when ionization points are stabilized in a track of a 1 keV electron.

It is necessary to note that signal decay computations in a track by eqn. 42 are rather time consuming. Therefore, the ESE signal kinetics were analyzed (24) depending on the assumed approximation of the number of neighbors of the spin under study. It turns out that the approximation "ten neighbors to the left and to the right" of a given spin results in an error which does not exceed the statistical error at least up to a signal decay of some e^{-3} (as a rule, higher magnitudes of the signal decay cannot be observed experimentally).

The comparison of ESE signal decays due to PC d-d interactions in a track with those observed at uniform distributions shows a uniform linear distribution to be the best model of PC distributions in a track. As in the uniform linear case, the signal decay in a track can be divided into the components $V_A(2\tau)$ and $V_B(2\tau)$ associated with $J_A(2W\tau)$ and $J_B(2W\tau)$. Each component can then be compared with the analytic expressions given in Section III.D. This procedure is shown in Figure 12, the linear density χ serving as a fitting parameter.

As seen from Figure 12, analytic eqns. 34-38 fairly well describe the ESE signal decay in a track at various W . At $W\tau \ll 1$ the signal decay for a PC in a track is linearized in the coordinates $\ln V(2\tau) - \tau^{1/3}$ according to eqn. 40,

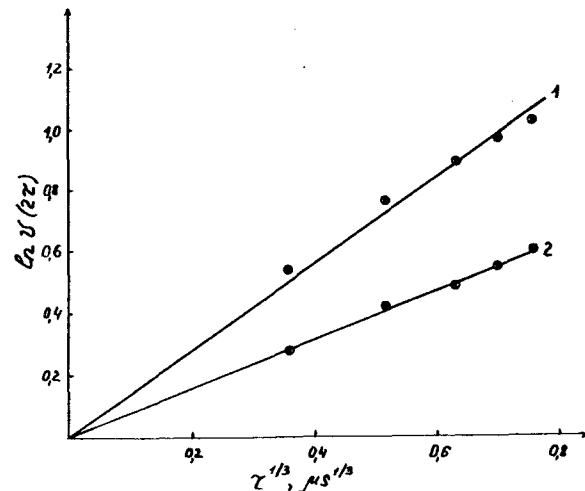
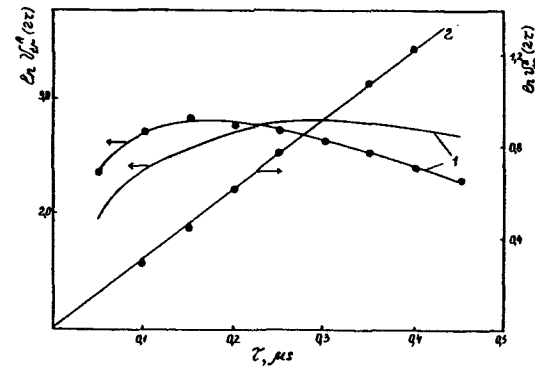


Figure 12. ESE signal decay in a track of an electron with the initial energy of 1 keV: (a) $W = 10^6 \text{ s}^{-1}$, (o) Monte-Carlo calculations with regard for all particles in the track, (x) the approximation of "ten neighbors to the left and to the right" (24). Solid lines show analytic calculations in the approximation of the track to a line with a homogeneous spin distribution at $\chi = 4.5 \times 10^6 \text{ cm}^{-1}$, (1) $v_{tr}^A(2\tau)$, (2) $v_{tr}^B(2\tau)$; (b) $W = 10^3 \text{ s}^{-1}$ and $\langle \sin^2 \Theta/2 \rangle_{g(\omega)}$ equal to (1) 0.2, (2) 0.01. Ordinates of curve 2 are 10-fold magnified. Analytic calculations (solid lines) correspond to $\chi = 5 \times 10^6 \text{ cm}^{-1}$.

the tangents of the slope of these dependences being proportional to $\langle \sin^2 \Theta/2 \rangle_{g(\omega)}$. The value of χ found from the tangents of the slope is $5 \times 10^6 \text{ cm}^{-1}$; this very value corresponds to a good

agreement between the analytic and calculated $V(2\tau)$ at other W values. The χ in a track of an electron with the initial energy of 1 keV is $7 \times 10^6 \text{ cm}^{-1}$ (24). Thus, the agreement between the analytic relationships for the signal decays in the uniform linear case and in the case of PC distribution in a track is not only qualitative but also quantitative. This fact substantially facilitates analysis of experimental data on ESE signal decays in tracks.

ESE signal decays for some types of nonuniform particle distributions were calculated in (25).

Unfortunately, model "island" distributions have not been so far calculated; however, as seen from the above data, the difficulties that are met are of calculation rather than fundamental character.

IV. METHODS OF SPATIAL PC DISTRIBUTION ANALYSIS IN ESE EXPERIMENTS

This section dwells upon the possibility of gaining information on spatial PC distributions from the decay kinetics resulting from PC d-d interactions.

A. The Inverse Problem of the ESE Method

The above results of the theory of d-d contribution to ESE signal decays demonstrate this contribution to substantially depend on spatial PC distributions in solid matrices. Therefore, ESE signal decay analysis can in principle supply one with a detailed information on spatial spin distributions.

ESE theory (see Section III) usually considers the direct problem of finding ESE signal decay kinetics induced by PC d-d interactions at a set of spatial PC distribution. In experiment one has to solve the inverse problem: to determine the type and parameters of the spatial spin distribution by echo signal decay data. Solution of this problem is hampered by a number of circumstances. In experiment ESE signal decay kinetics are measured within a limited time interval, $3 \times 10^{-7} < \tau < 5 \times 10^{-6} \text{ s}$ (26). Evidently, the shorter the time interval, the less reliable the spatial PC distribution obtained. When solving the inverse problem, one should remember that different PC distributions can pertain to the same signal decay, e.g. ESE signal decay asymptotics may coincide in some cases of pair and linear distributions (cf. eqns. 21 and 40). However, in real situations the inverse problem is often facilitated substantially since

some other data (not ESE data) provide information on possible or expected types of PC distributions in particular systems. For instance, under photochemical molecular decomposition in a solid there is often every reason to expect that geminate pairs of free radicals originate at early photolysis stages. A detailed character of the radical distribution in pairs can be found out by analyzing the ESE signal kinetics.

The d-d contribution to spin phase relaxation depend on the spin flip rate during the spin-lattice relaxation or spin diffusion. Therefore, to obtain information on spatial PC distributions from ESE data, it is desirable to find spin flip rates by independent experiments.

The PC d-d interaction is an important, however, not sole cause of spin phase relaxation. Electron-nuclear coupling (2), spin-lattice interactions, etc. are also of essential, sometimes paramount, importance in electron spin dephasing. Therefore, to obtain information of spatial PC distributions, it is first of all necessary to distinguish the d-d contribution to the echo signal decay. The procedure of finding W and distinguishing the d-d contribution in the total decay kinetics will be discussed in Section V.

Assume the ESE decay kinetics associated with d-d interactions to be distinguished in experiment. At present ESE decay have been fairly well analyzed for the following model PC distributions: uniform volume, surface, linear particle distributions and PC distributions by pairs. Analytical formulae and plots of ESE decay kinetics for these cases are adduced above. Thus, it is necessary to verify first of all whether experimental data correspond to theoretical results referred to one of the model cases. If there is no correspondence, one has to try other possible types of PC distributions, to use equations of the type 42 and 43 for numerical calculations. At a uniform PC distribution experiment yields only a mean concentration of PCs. In the case of pair spin distributions, there exists a well-developed procedure of calculating pair distribution functions based on partner separations.

B. Ways of Determining Pair Distribution Functions

According to theoretical data (see Section III), the spin phase relaxation due to d-d interactions between spin-partners depend on quite a number of parameters: random spin flip rate, degree of spin excitation by microwave pulses, partner separation. Since pairs of different PCs are most interesting from the viewpoint of practice, we are going to consider only pairs of A and

B spins with substantially differing resonance frequencies. In this case, microwave pulses inducing ESE signals excite only one of the pair spins. The B spin contribution to the A spin dephasing essentially depend on the B flip rate and hence the ways of determining the pair distribution functions by ESE data are different for B spins with low ($W\tau \ll 1$) and high ($W\tau \gg 1$) rates of random flips.

1. PC Pairs with $W\tau \gg 1$

In this case B spins induce A spin dephasing by a spectral diffusion mechanism. Figure 5 shows plots of ESE decay due to spin d-d interactions vs. partner separations. The dependence is of a specific S-shape. In approximate calculations it can be replaced by the step function

$$v(2\tau|r) = \begin{cases} \exp(-2\tau W) = \exp(-\tau/T_1) & r < r^* \\ 1 & r > r^* \end{cases} \quad (47)$$

where r^* is the point of the maximum slope of $v(2\tau|r)$. According to estimates (26), r^* is determined as

$$r^* = (1.1/\sqrt{2})(\gamma_A \gamma_B \hbar)^{1/3} (\tau T_{1B})^{1/6} \quad (48)$$

The ESE signal amplitude for the whole pair ensemble is obtained by substituting eqn. 47 into eqn. 17:

$$V_p(2\tau) = 4\pi [\exp(-\tau/T_{1B}) \int_0^{r^*} n(r)r^2 dr + \int_{r^*}^{\infty} n(r)r^2 dr] \quad (49)$$

Taking into account the normalization requirement $4\pi \int n(r)r^2 dr = 1$, it is possible to reduce eqn. 49 to the form

$$4\pi \int_{r^*}^{\infty} n(r)r^2 dr = [v_p(2\tau) - \exp(-\tau/T_{1B})] / [1 - \exp(-\tau/T_{1B})] \quad (50)$$

Relationship 50 assumes the simplest form when the B spins have very short spin-lattice relaxation times:

$$4\pi \int_{r^*}^{\infty} n(r)r^2 dr \approx v_p(2\tau), \quad (51)$$

i.e. at a moment 2τ the echo signal amplitude is in fact proportional to the PCs with the partner separation over r^* ; for this fraction the d-d interaction is sufficiently low and hence no spin dephasing can occur during the time interval 2τ . Measuring the ESE amplitude at various τ/T_{1B} , one can find the pair distribution function by eqn. 50 or 51. To this end let us introduce the volume

V^* restricted by a r^* -radius sphere,

$$V^* = (4/3)\pi r^{*3}, \quad (52)$$

and differentiate $V_p(2\tau)$ with respect to r^* , i.e

$$-dv_p/dV^* \approx n(r^*). \quad (53)$$

Note that $V^*(\tau T_{1B})$ is measured experimentally for a given type of B spins. For this purpose it is necessary to prepare a system with a uniform distribution of B spins. The B spin contribution to the A spin ESE decay obeys eqn. 26 in the case of a uniform volume distribution. Employing the approximation of eqn. 47, one can write eqn. 26 as

$$v_p(2\tau) = \exp\{-C_B[1 - \exp(-\tau/T_{1B})] \cdot 4\pi \int_0^{r^*} r^2 dr\} = \exp\{-C_B V^*[1 - \exp(-\tau/T_{1B})]\} \quad (54)$$

Thus, measuring the spin dephasing by a spectral diffusion mechanism for the case of a uniform volume distribution of B spins, one can determine the characteristic volume $V^*(\tau T_{1B})$ for any τT_{1B} and, subsequently, obtain the pair distribution function by eqn. 53.

The substitution of $v(2\tau|r)$ by the step function is naturally valid only if $n(r)$ varies with r slower than $v(2\tau|r)$.

To estimate the degree of reliability of the above equation for the pair distribution function $n(r)$, $v_p(2\tau)$ was calculated numerically for a number of model functions. A model analytic function was substituted into eqn. 17 to calculate ESE signal decays. Thereafter $n(r^*)$ was determined by eqns. 50-53 and compared with the initial $n(r)$. Figure 13 shows the results obtained. The procedure proposed is seen to fairly well describe the form of $n(r)$. As expected, noticeable errors arose only for functions that varied appreciably at short distances, e.g. δ - and step functions.

Expression 48 estimates the distance range wherein $n(r^*)$ can be determined by the above procedure. The inferior limit of measurable r^* is 10-15 Å at $\tau T_1 = 3 \times 10^{-11}$ s². The superior limit is reached at $\tau \sim T_1$ and is 100 Å for ions with a spin $S = 2$ (such ions are usually used in experiments).

2. PC Pairs with $W_B\tau \ll 1$

According to theoretical expressions given in Section III, in this case B spins do not practically contribute to A spin ESE signal decay. Hence, the ESE method seems to be inapplicable to

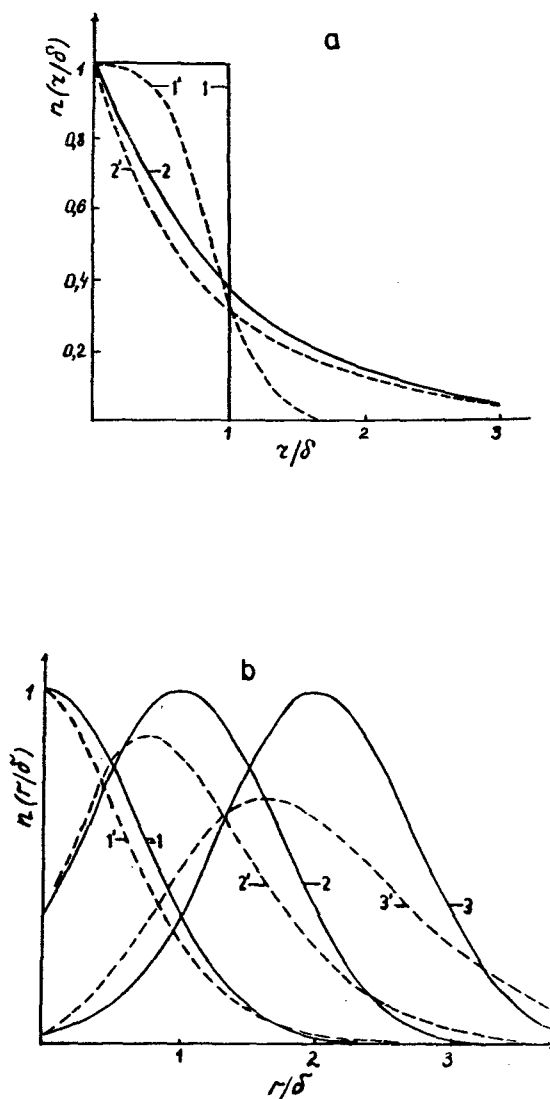


Figure 13. Approximate spatial distribution function $n(r)$ for radical-paramagnetic ion pairs, with one of the partners having short spin-lattice relaxation times. Solid line — the real model distribution density, dashed line — that calculated by eqn. 53 (22). (a) $-I-I'\Theta$ function; $2-2'\exp(-r/\delta)$ (b) $-I-I'\exp(-r^2/\delta^2)$; $2-2'\exp[-(r-\delta)^2/\delta^2]$, $3-3'\exp[-(r-2\delta)^2/2\delta^2]$.

determination of the pair distribution function. The problem can be solved, however, by the double resonance method (27). In this method, at a time moment t' after the first pulse of ω_A frequency inducing the ESE signal, a saturating

pulse is applied at the resonance frequency of B spins, ω_B . The role of the saturating pulse is to change the B spin orientation and thus to induce an "instantaneous" shift of the local dipolar field created by the B spins at the sites of location of the A spins. As a result, the B spins dephase the A ones by a mechanism analogous to that of instantaneous diffusion. The B spins contribute to the A spin ESE signal decay as (27):

$$V(T) = 1 - p[1 - 4\pi \int n(r)K(u)r^2 dr], \quad (55)$$

where $u = \gamma_A \gamma_B \hbar T r^{-3}$; $T = \tau - |\tau - t'|$; $p = \langle \sin^2 \Theta / 2 \rangle g(\omega)$;

$$K(u) = \int_0^\pi \cos[u(1 - 3\cos^2 \Theta')] d\cos \Theta'.$$

It has been proposed (27) that the distribution function $n(r)$ should be determined by the signal decay $V(T)$ measured. The oscillating kernel $K(u)$ of the integral eqn. 55 is substituted by the step function

$$K(u) = \begin{cases} 1 & 0 \leq u \leq 1,2 \\ 0 & u > 1,2 \end{cases} \quad (56)$$

In this case, eqn. 55 can be written in the form

$$V(T) = 1 - p[1 - \int_0^{r^*} n(r)r^2 dr] \quad (57)$$

with $r^* = (0.833\gamma_A \gamma_B \hbar T)^{1/3}$, and thus it is possible to determine the fraction of spins located within 0 to r^* . Using the relationship

$$f(r^*) = 4\pi n(r^*)r^{*2} = -dV'(T)/dr^*,$$

where $V'(T) = 1 - [1 - V(T)]/p$,

one can determine an approximate distribution function $n(r)$ with the help of an experimental ESE signal. Eqn. 57 estimates the distances at which the distribution function can be determined. At a real $T = 5 \times 10^{-6}$ s, $r^* \sim 100$ Å for spin-partners of 1/2. As in the previous case of $W\tau \gg 1$, approximate methods of determining the pair distribution function are applicable only if $n(r)$ is smoother than $K(u)$. Therefore, we are going to consider more reliable methods of $n(r)$ determination developed recently (23).

C. General Methods of Determining the Pair Distribution Function

The distance distribution function of spin-partners is the solution of an integral equation of the type:

$$\int_0^\infty v(2\tau|r)n(r)dr = V(2\tau) \quad (58)$$

where $V(2\tau)$ is known over the range $[\tau_A, \tau_B]$. The kernel $v(2\tau|r)$ can be represented as a series of eigenfunctions in the band $r = [0, \infty]$, $\tau = [\tau_A, \tau_B]$:

$$v(2\tau|r) = \sum_{i=0}^{\infty} \alpha_i \phi_i(r) \Psi_i(\tau) \quad (59)$$

The functions $\phi_i(r)$ and $\Psi_i(\tau)$ satisfy the following orthogonality relationships:

$$\begin{aligned} \int_0^{\infty} \phi_i(r) \phi_j(r) dr &= \delta_{ij}; \\ \int_{\tau_A}^{\tau_B} \Psi_i(\tau) \Psi_j(\tau) d\tau &= \delta_{ij} \end{aligned} \quad (60)$$

The expansion of eqn. 59 and the conditions of eqn. 60 readily yield

$$\begin{aligned} \Psi_i(\tau) &= (1/\alpha_i) \int_0^{\infty} \phi_i(r) v(2\tau|r) dr \\ \phi_i(r) &= (1/\alpha_i) \int_{\tau_A}^{\tau_B} \Psi_i(\tau) v(2\tau|r) d\tau \end{aligned} \quad (61)$$

which show that an operator inverse to $v(2\tau|r)$ is

$$v^{-1}(2\tau|r) = \sum_{i=0}^{\infty} (1/\alpha_i) \phi_i(r) \Psi_i(\tau) \quad (62)$$

Applying $v^{-1}(2\tau|r)$ to $V(2\tau)$, we find $n(r)$ as

$$n(r) = \sum_{i=0}^{\infty} (1/\alpha_i) \left(\int_{\tau_A}^{\tau_B} \Psi_i(\tau) V(2\tau) d\tau \right) \phi_i(r)$$

The eigenfunctions of $v^{-1}(2\tau|r)$ can be determined, e.g. as follows. The right side of eqn. 58 is measured at a certain set of points $\tau_0, \tau_2, \dots, \tau_{n-1}$. Hence, eqn. 60 is reduced to

$$\sum_{i=0}^{N-1} \Psi_i(\tau_l) \Psi_j(\tau_l) \omega_l = \delta_{ij} \quad (63)$$

where ω_l are some weight factors. All integrals in τ are calculated in a similar manner. Consider now the integral

$$S_{ij} = S_{ji} = \int_0^{\infty} v(2\tau_i|r) v(2\tau_j|r) dr \quad (64)$$

that can be written in the form

$$S_{ij} = \sum_{l=0}^{\infty} \alpha_l^2 \Psi_l(\tau_i) \Psi_l(\tau_j) \quad (65)$$

The coefficients α_l were shown (28) to go to zero with increasing l : $\alpha_{10} \leq 10^{-10}$, which fact makes it possible to use no more than 10 members of the summation. If $\Psi_l(\tau_j)$ is designated as b_{lj} , eqns. 63 and 65 yield for the matrices $B = \{b_{lj}\}$, $S = \{S_{ij}\}$, $\Lambda = \{\alpha_l^2 \delta_{ij}\}$, $\Omega = \{\omega_l \delta_{ij}\}$ the following equations:

$$B^T \Lambda B = S$$

$$B \Omega B^T = E \quad (66)$$

With the substitution $\bar{B} = B \Omega^{1/2}$ these equations take the form

$$\bar{B}^T \Lambda \bar{B} = \Omega^{1/2} S \Omega^{1/2} \quad (67)$$

$$\bar{B} \bar{B}^T = E$$

Thus, the problem is reduced to that of eigenvalues and eigenvectors \bar{B} of the matrix $\Omega^{1/2} S \Omega^{1/2}$.

With B and Λ known, one can determine $\Psi_i(\tau_j)$ and α_i and thus $\phi_i(r)$ (see eqn. 61):

$$\phi_i(r) = (1/\alpha_i) \sum_{l=1}^N \Psi_l(\tau_l) \omega_l v(2\tau_l|r) \quad (68)$$

and then the pair distribution $n(r)$:

$$\begin{aligned} n(r) &= \sum_{l=0}^K \beta_l \phi_l(r) / \alpha_l \\ \beta_l &= \sum_{i=0}^{N-1} \Psi_l(\tau_i) \omega_i V(2\tau_i) \end{aligned} \quad (69)$$

The above method of $n(r)$ determination has been used (28) with experimental data on ESE signal decay taken from (27). Figure 14 shows $n(r)$ calculated in this way and by approximate rela-

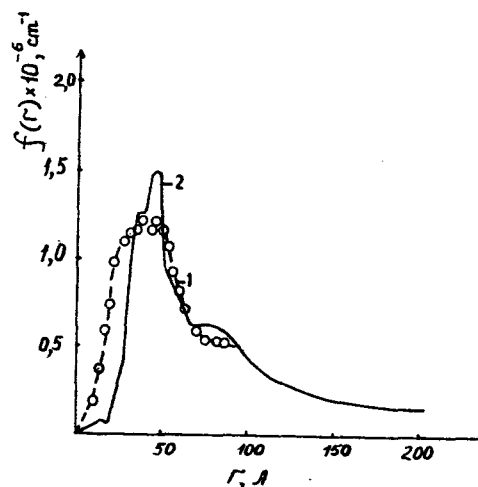


Figure 14. Distance distribution function of $H \cdots Q$ pairs (27, 28). Curves 1 and 2 are obtained by processing experimental data by different methods; curve 1 by the technique described in Section IV.B.2, curve 2 by that in Section IV.C.

tions (eqn. 47). The approximate method, with the step function substituted for the kernel $K(u)$, is seen to allow a reliable distribution function.

Thus, in Sections III and IV we have considered theoretical principles of phase relaxation due to d-d interactions in magnetically diluted solids. Let us discuss now methods of determining spatial PC distribution parameters based on experimental signal decays. The next section demonstrates experimental realization of the above program.

V. MEASUREMENTS OF ESE SIGNAL DECAYS DUE TO d-d INTERACTIONS OF PCs. EXPERIMENTAL DATA ON PHASE RELAXATION IN SYSTEMS WITH UNIFORM PC DISTRIBUTION

At the present moment there has been developed a definite sequence of experimental steps necessary for obtaining information on PC d-d interactions and spatial PC distribution.

An experimentalist has to start his work with solving two general problems: determination of the microwave field strength in the cavity of a spectrometer, and separation of the ESE signal decay contributed by the mechanisms of instantaneous and spectral diffusions.

A. Determination of Microwave H_1 Pulse Amplitude in a Spectrometer Cavity at the Location of a Sample

This parameter can be determined by analysis of the ESE signal shape. The ESE signal shape is known (29) to obey the expression

$$V(t) = \int_{-\infty}^{\infty} [\sin^3(a\sqrt{1+x^2})/(1+x^2)^2 \times \\ \sqrt{1+x^2} \cos(a\sqrt{1+x^2}) \cos(ax) + \\ x \sin(a\sqrt{1+x^2}) \sin(ax)/g(x) dx] \quad (70)$$

where

$$a = t, t_p/2 \quad c = t/2t_p \quad \omega_1 = \gamma H_1.$$

$g(x)$ is the line shape of a PC under study, τ_p is the pulse duration. Relation 70 is written for pulses of equal duration. Figure 15 depicts $V(t)$ calculated by eqn. 70 at various H_1 for Gaussian line shapes (19). Irrespective of the line shape, the ESE signal is seen to be of a double-peak shape at $\gamma H_1 t_p = \pi$ which solves the experimental problem of H_1 determination since t_p can be measured independently. All of the

subsequent H_1 values are set relatively to the obtained $H_1^* = \pi/\gamma t_p$ with the help of a calibrated attenuator mounted between the micro-

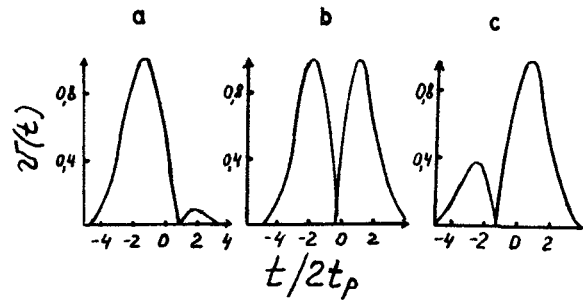


Figure 15. Primary ESE signal shape at the Gaussian excitation line shape, with the half-width between points of maximum slope equal to 2G and various values of the amplitude H_1 of a microwave pulse (19): (a) $\gamma H_1 t_p = 2.1$, (b) 3.14, (c) 3.6.

wave-pulse source and the spectrometer cavity.

B. Separation of Contributions from d-d Interactions, Spin-lattice Relaxation and Electron-Nuclear Interac- tions to the Total ESE Signal Decay Kinetics

Let us consider first the way of distinguishing contributions from various mechanisms to the ESE signal decay in systems with uniform volume distributions. In the general case, the ESE signal decay in such systems is

$$V(2\tau) = V'(2\tau)V^I(2\tau); \quad (71)$$

$$V' = V_N(2\tau)V_L(2\tau)$$

where $V_N(2\tau)$ is the decay associated with electron-nuclear interactions,

$$\ln V_N(2\tau) = -f_N(\tau) \quad (72)$$

$V_L(2\tau)$ is the decay due to spin-lattice interactions

$$\ln V_L(2\tau) = -\tau/T_{21} \quad (73)$$

$V^I(2\tau)$ is that contribution from d-d interactions,

$$\ln V^I(2\tau) = -\gamma^2 \hbar C [J_B(2W\tau)/2W + pJ_A(2W\tau)/2W] \quad (74)$$

$$p = \langle \sin^2 \Theta/2 \rangle_{g(\omega)}$$

The structure of eqns 71-74 prompts the following way of distinguishing each of the ESE decay contributions. The signal decay is measured at various spin concentrations and at a constant H_1 . The $\ln V(2\tau)$ values at each fixed τ are plotted as a function of PC concentration. The intercepts of the y-axis are $-\tau/T_2 - f_N(\tau)$ at each particular τ , the tangents of the slope being $\gamma^2 \hbar [J_B/2W + pJ_A/2W]$. Having plotted the intercepts as a function of τ , one obtains the signal decay resulting from electron-nuclear interactions and spin-lattice relaxation, $V^I(2\tau)$, eqn. 71. Next, by decreasing the temperature, one can obtain $V_L(2\tau) \sim 1$ within the τ range under study; $V_N(2\tau)$ is temperature-independent as has been confirmed experimentally (30). Hence, with these low temperature data one obtains $V_N(2\tau)$ and $V_L(2\tau)$ at various temperatures

$$V_L(2\tau) = V^I(2\tau)/V_N(2\tau) \quad (75)$$

Figures 16-20 illustrate the above procedure of

distinguishing various contributions to an ESE signal decay. The $\langle \sin^2 \Theta/2 \rangle_{g(\omega)}$ dependence of the signal decay is then analyzed at a fixed concentration of spins, and experimental results are plotted in the coordinates $\ln V(2\tau) - \langle \sin^2 \Theta/2 \rangle_{g(\omega)}$ at each fixed τ (Figure 18). The y-intercepts give $[\ln V^I(2\tau)]C\gamma^2 \hbar J_B/2W$, while the tangents of the slope afford $-C\gamma^2 \hbar J_A(2W\tau)/2W$. Since $V^I(2\tau)$ are determined by the above method, the procedure described allows one to find $J_A/2W$ and $J_B/2W$, i.e. to distinguish the contributions from instantaneous and spectral diffusions to $V^I(2\tau)$. Thus, carrying out experiments at various temperatures, concentrations and microwave strengths, one can distinguish all contributions to the signal decay.

In the case of nonuniform distributions, the procedure of distinguishing the d-d contribution is somewhat more elaborate. At a nonuniform PC distribution the total signal decay is

$$V(2\tau) = \underbrace{V_{in}(2\tau)V_r(2\tau)}_{V_d(2\tau)} \underbrace{V_N(2\tau)V_L(2\tau)}_{V^I(2\tau)} \quad (76)$$

where $V_{in}(2\tau)$ is the ESE signal decay due to d-d interactions of PCs in isolated regions of their

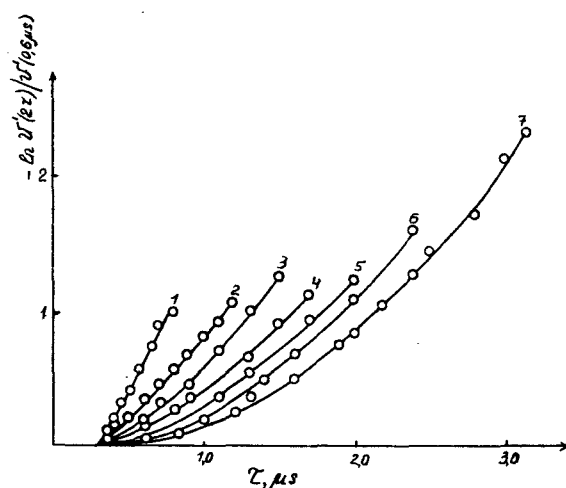


Figure 16. ESE signal decay of SO_4^- radical-ions at a concentration of $2 \times 10^{17} \text{ cm}^{-3}$ and various temperatures. At this spin concentration the ESE signal decays due to spin-lattice relaxation and the contribution from magnetic nuclei. (1) 77 K, (2) 64.5 K, (3) 50 K, (4) 40.6 K, (5) 24.8 K, (6) 17.9 K, (7) 4.2 K. At 4.2 K (curve 7) the signal decays due only to electron-nuclear interactions (13).

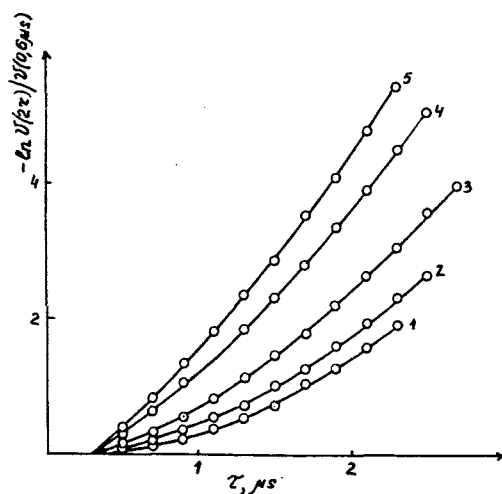


Figure 17. ESE signal decay of SO_4^- radical ions at $5 \times 10^{18} \text{ cm}^{-3}$, 11.6 K and various H_1 : (1) 0.44 Oe, (2) 0.89 Oe, (3) 1.41 Oe, (4) 2.22 Oe, (5) 2.8 Oe (13).

localization (pairs, tracks, etc.), $V_r(2\tau)$ is that due to PC d-d interactions between different regions of PC localization. The other terms are designated as in eqns. 72 and 73. The term $V'(2\tau)$ is determined in experiments with a uniform PC distribution and thus is considered to be known. Hence, $V_d(2\tau)$ can be obtained as

$$V_d(2\tau) = V(2\tau)/V'(2\tau) \quad (77)$$

The concentration dependence of $V_d(2\tau)$ is then analyzed since at each particular τ , $V_r(2\tau)$ is a linear function of a mean concentration within a certain concentration range, and at $C \rightarrow 0$, $V_r(2\tau) \rightarrow 1$, while $V_{in}(2\tau)$ does not depend on the mean concentration and is determined by the d-d interaction characteristic of a particular type of PC distribution. Therefore, if $\ln V_d(2\tau)$ is plotted vs. the mean spin concentration at a fixed τ , the intercept on the y-axis affords $V_{in}(2\tau)$. If it is necessary to distinguish the contributions from instantaneous and spectral diffusions to $V_{in}(2\tau)$, this procedure should be carried out at different

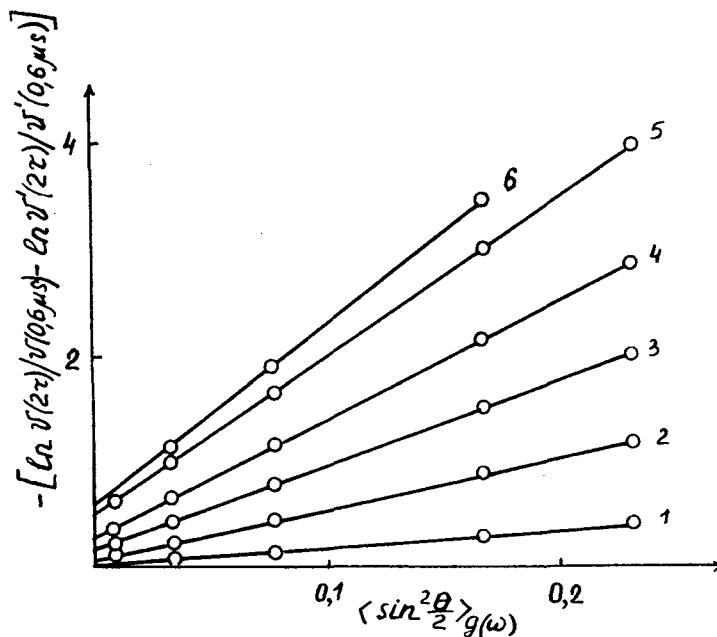


Figure 18. Plots of the ESE signal decay of SO_4^- radical-ions vs. $\langle \sin^2 \Theta / 2 \rangle_{g(\omega)}$ at fixed τ . Temperature of measurements is 11.6 K. Different curves correspond to different τ (in μs): (1) 0.5, (2) 0.8, (3) 1.3, (4) 1.7, (5) 2.3, (6) 2.5. SO_4^- concentration is $5 \times 10^{18} \text{ cm}^{-3}$ (13).

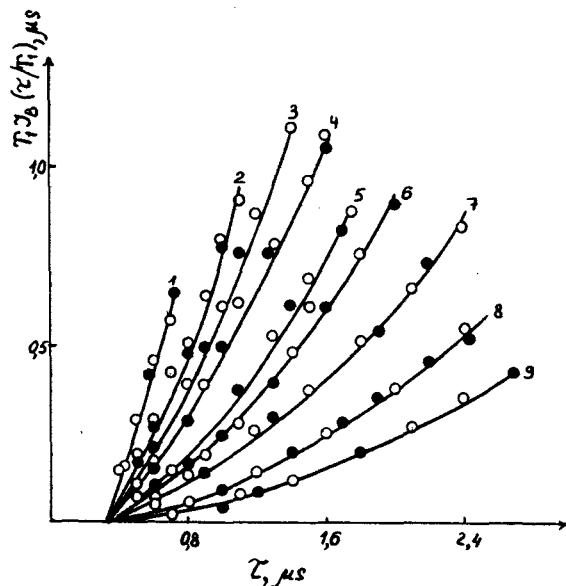


Figure 19. $T_1 J_B(\tau/T_1)$ at various temperatures for SO_4^- radical-ions. Results of two different experiments are shown: (o) the phase relaxation of SO_4^- was measured, (●) the influence of SO_4^- upon the phase relaxation of hydrogen atoms was investigated (13). $T - \text{K}$: (1) 77, (2) 64.5, (3) 50, (4) 40.6, (5) 30, (6) 24.8, (7) 17.9, (8) 14.9, (9) 11.6.

$\langle \sin^2 \theta / 2 \rangle_{g(\omega)}$ values.

Figures 21 to 23 exemplify the above processing of experimental data for the case of track distributions.

Experimentally the ESE signal decay kinetics can be investigated only starting with a certain time τ_0 , i.e. a "dead" time of a device which is 150-500 ns in modern ESE spectrometers (31, 32), the valuable information on the beginning of the decay, $V_{in}(2\tau)$, being lost. However, it is possible to determine the signal decay before the time moment τ_0 . To this end the ESE signal amplitude of a species with a uniform PC distribution is compared to that of the system under study. The mean PC concentration in both cases is chosen as a minimum so that $V_I(2\tau_0)$ and $V_{II}(2\tau_0) \approx 1$. Hence,

$$V_{in}(2\tau) = V_I(0)V(2\tau_0)/V_{II}(0)V'(2\tau_0) \quad (78)$$

where $V_I(0)$ and $V_{II}(0)$ are ESR signal

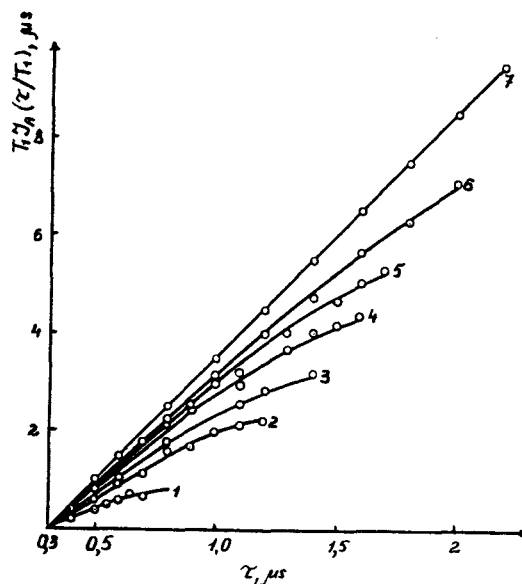


Figure 20. $T_1 J_A(\tau/T_1)$ for SO_4^- at various temperatures (13). Denotation of curves corresponds to that of Figure 19. The curves running via experimental points were calculated at the same T_1 as those shown in Figure 19.

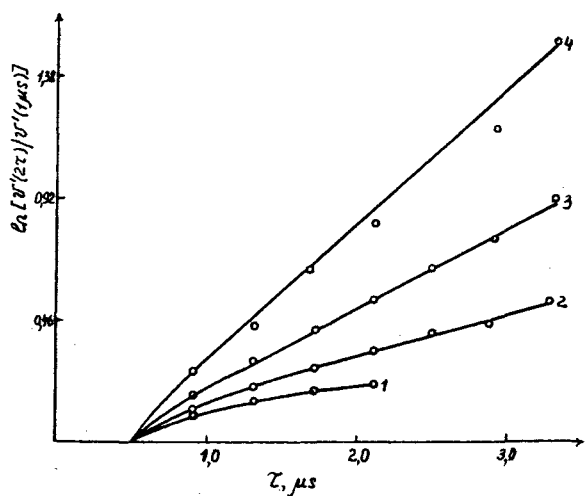


Figure 21. ESE signal decay $V_d(2\tau)/V_d(1 \mu s)$ in β -irradiated samples measured at 4.2 K and various $SO_4^{\cdot -}$ concentrations (cm^{-3}) (24): (1) 3.7×10^{16} , (2) 2.6×10^{17} , (3) 6.5×10^{17} , (4) 1.2×10^{18} , $\langle \sin^2 \Theta/2 \rangle_{g(\omega)} = 0.2$.

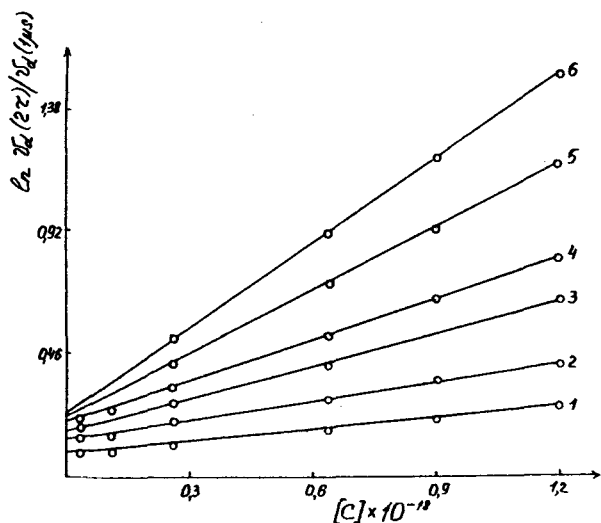


Figure 22. Spin concentration dependence of $V_d(2\tau)/V_d(1 \mu s)$ in β -irradiated samples at a fixed τ . At 4.2 K the τ values (μs) are (24): (1) 0.9, (2) 1.3, (3) 1.7, (4) 2.1, (5) 2.9, (6) 3.3.

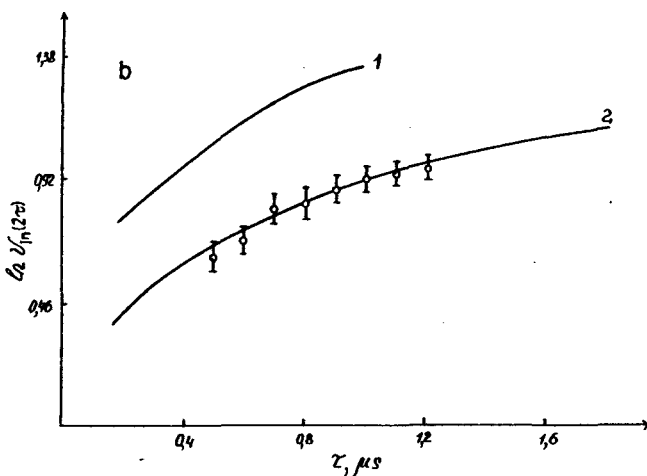
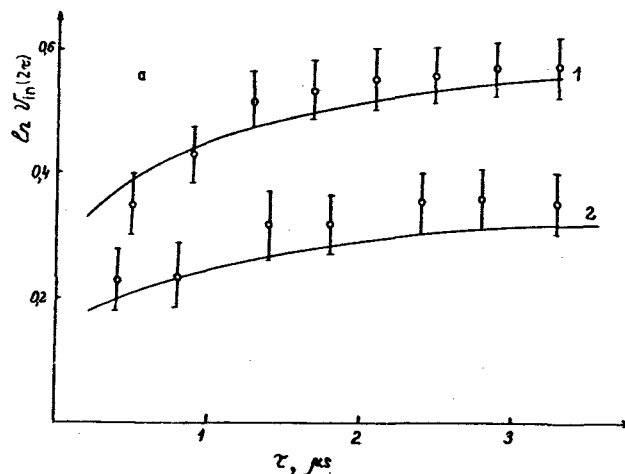


Figure 23. Time dependences of ESE signal decay for $SO_4^{\cdot -}$ radical-ions in the track of a T β -particle, $V_{in}(2\tau)$ determined at various temperatures. Solid curves — calculations, dots — experiment. Calculations were made at various radical recombination probability p in a track (24): (a) 4.2 K, $p = 0.5$, curves 1 and 2 correspond to different values of $\langle \sin^2 \Theta/2 \rangle_{g(\omega)}$: (1) 0.2, (2) 0.1; (b) 77 K, $p = 0$ (curve 1); $p = 0.5$ (curve 2).

amplitudes of the species under study and of that with a uniform PC distribution, respectively; $V(2\tau_0)$ and $V'(2\tau_0)$ are ESE signal amplitudes of these species at the time moment $2\tau_0$.

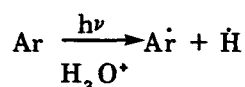
Thus, the method described makes it possible to determine the ESE signal decay due to d-d interactions in the interior of a sample with a

given nonuniform PC distribution.

C. Systems with a Uniform Volume PC Distribution

The present section furnishes examples of some systems when the PC distribution can be considered uniform to a high accuracy, e.g. frozen solutions of stable radicals and ions. A uniformity criterion is a well-resolved ESR spectrum of these glasses, that is the nonpresence of wide lines belonging to the microphase and the equality of mean concentrations determined by the ESR method and in a weighed sample of the PCs under study.

A uniform PC distribution can be obtained by photochemical generation of radicals. For instance, in acid matrices the photochemical reaction



results in radical pairs $\text{Ar}^\cdot \cdots \text{H}^\cdot$ generated from aromatic molecules. However, PCs are distributed uniformly in each subsystem — aromatic radicals and H atoms — because of a uniform light absorption in the sample. This is also the case with other photochemical systems considered below, namely the subsystems of the pairs $\text{Fe}^{3+} \cdots \text{H}^\cdot$ and $\text{Fe}^{2+} \cdots \text{R}^\cdot$, where R is an alcohol radical. These systems admit of a further randomization of the distribution. For example, H atoms in acid matrices are known (33) to migrate about the matrix even at 77 K. Therefore, a long-term annealing of the samples results in decomposition of the initial photochemical pairs and in a uniform distribution of PCs of both types in the matrix.

Systems involving alcohol radicals are subjected to a photodecomposition and subsequent thermoannealing. Let us consider this technique as applied to photogenerated pairs $\text{Fe}^{2+} \cdots \text{CH}_2\text{OH}^\cdot$. Under ultraviolet light $\text{CH}_2\text{OH}^\cdot$ radicals are transformed to CH_3^\cdot ones that react with the matrix in the dark forming $\text{CH}_2\text{OH}^\cdot$ once again. Each act of the dark reaction results in migration of the valency about the matrix and hence the PC distribution becomes uniform after repeated photo- and thermoannealing. A partial decay of the radicals due to random encounters during their migration is one more proof of randomizing the distribution.

In the case of radiation-chemical generation of radicals, the PC distribution in the sample can be made uniform by successive photo- and thermoannealings. In some radiation-chemical

systems, such as trapped electrons e_{tr}^- in alkaline matrices (34), a uniform PC distribution is achieved under a long-term irradiation since the mobile electrons formed by radiolysis randomly react with the trapped ones and thus eliminate the initial nonuniform distribution arising at early stages of radiolysis.

D. Experimental Results on Phase Relaxation at a Uniform PC Distribution

Our experiments on systems with a uniform PC distribution were aimed at verifying the theoretical relationships of Section III on the one hand; and at gaining information on the spin flip rate (a parameter necessary for the decay kinetic analysis in the case of a nonuniform PC distribution) on the other hand.

1. Phase Relaxation of $\text{SO}_4^{\cdot -}$ Radical-Ions in Glassy Solutions of Sulfuric Acid

The $\text{SO}_4^{\cdot -}$ phase relaxation has been investigated in detail over the temperature range from 4.2 to 77 K (13). Since in this system there also arise H atoms, the contribution from $\text{SO}_4^{\cdot -}$ radical-ions to the phase relaxation of H atoms was studied along with $\text{SO}_4^{\cdot -}$ phase relaxation. The d-d contribution to the total $\text{SO}_4^{\cdot -}$ signal decay was distinguished by the method described in Section V.B. Figures 19 and 20 show the basic results: dependences of $T_1 J_B(\tau/T_1)$ and $T_1 J_A(\tau/T_1)$ obtained at different temperatures. The $\text{SO}_4^{\cdot -}$ contribution to the phase relaxation of H atoms allowed us to independently measure $T_1 J_B(\tau/T_1)$. Figure 19 shows that $T_1 J_B(\tau/T_1)$ measured in both ways agrees fairly well. The curves drawn via experimental points were calculated by eqns. 25-29 by varying the spin flip frequency W . A good agreement was attained at one value T_1 for each temperature. Figure 24 presents the T_1 values obtained as a function of temperature, and T_{21} determined in the same experiments. The T_1 and T_{21} are seen to coincide within the experimental error which provides additional evidence for the correctness of the T_1 values used for the calculated curves.

As far as we know, the experiment described is the only one investigating $T_1 J_A(\tau/T_1)$ over a wide range of spin flip rates. However, the case of $W\tau \ll 1$, i.e. when the main contribution to the PC phase relaxation due to d-d interactions is made by instantaneous diffusion, has been studied in quite a number of systems. Experimental data obtained for these systems are discussed below.

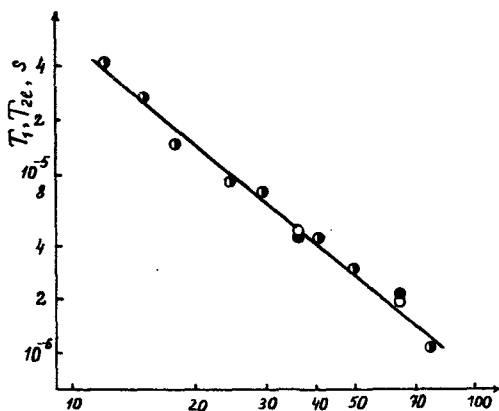


Figure 24. Temperature dependences of T_1 (○) and T_{21} (●) of SO_4^{2-} (13).

2. Phase Relaxation due to d-d Interactions at Low Rates of Spin Flips

The following systems were investigated at 77 or 4.2 K: trapped electrons e_{tr} in alkaline glasses, H atoms stabilized in glassy solutions of sulfuric, phosphoric and perchloric acids and in crystalline quartz, Cd^+ ions trapped in glassy methanol (19, 34, 35). The systems studied were characterized by various line shapes, $\langle \sin^2 \Theta/2 \rangle_{g(\omega)}$ ranging from 10^{-2} to 1. In all the experiments $T_1 J_A(\tau/T_1)$ was shown to coincide with the static limit within the experimental error and to equal 2.5τ according to eqn. 32.

3. Studies on the Spectral Diffusion Contribution to PC Phase Relaxation (36)

Alongside the example mentioned in Section V.D.1., the contribution from spectral diffusion to the ESE signal decay was investigated for a number of systems at spin flip rates of 10^{10} to 10^4 s^{-1} and thus at $W\tau$ varying from $W\tau \gg 1$ to $W\tau \ll 1$. The systems involved two types of spins. As A spins served hydrogen or deuterium atoms with $W\tau \ll 1$, B spins were Fe^{2+} or Cu^{2+} ions with the spin-lattice relaxation rate controlled by varying temperature within 77 - 8 K.

Figure 25 shows experimental data on the contribution from spectral diffusion of rapidly

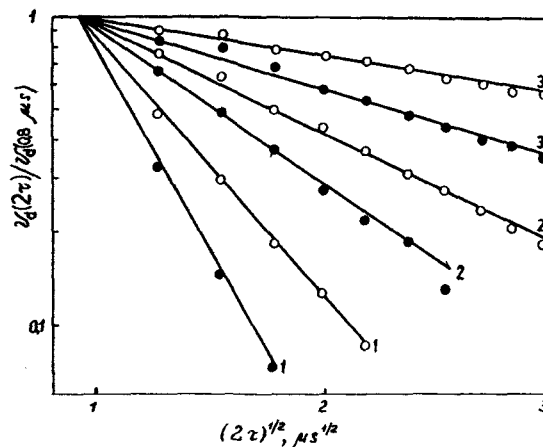


Figure 25. The phase relaxation of D atoms due to Fe^{2+} ions in frozen sulfate solutions at various concentrations and temperatures (36). $[\text{Fe}^{2+}]$ is $1.6 \times 10^{19} \text{ cm}^{-3}$ (○) and $2.3 \times 10^{19} \text{ cm}^{-3}$. (1) 11 K, (2) 19.6 K, (3) 77 K. According to theory for spins with short relaxation times ($W\tau \gg 1$), $\ln V(2\tau) \sim \tau^{-2}$.

relaxing Fe^{2+} ions to the D atom ESE signal decay. Preliminary ESR and ESE experiments on Fe^{2+} ions showed $W\tau \gg 1$ to hold for these ions. Indeed, all experimental decay kinetics are seen from Figure 25 to be fairly well linearized in the coordinates $\ln V(2\tau) - \sqrt{2\tau}$ which is in full agreement with eqn. 30. Experimental data were used to determine T_1 as a function of temperature (see Figure 26).

Figure 27 presents data on the phase relaxation of D atoms induced by the d-d interaction with Cu^{2+} ions at different temperatures. The curves passing through experimental points were calculated by eqn. 25 by varying T_1 . The temperature dependence of T_1 obtained is shown in Figure 28. Since Cu^{2+} ions can be observed in the ESE at 50 K and lower, it proved to be possible to find T_2 of these ions and to compare it with T_1 . Figure 28 shows T_1 and T_2 to have practically the same temperature dependence, their magnitude being twice as different. This fact can be readily explained in terms of the Aminov-Orbach spin-lattice relaxation mechanism.

Thus, the phase relaxation due to d-d interactions was studied experimentally for samples

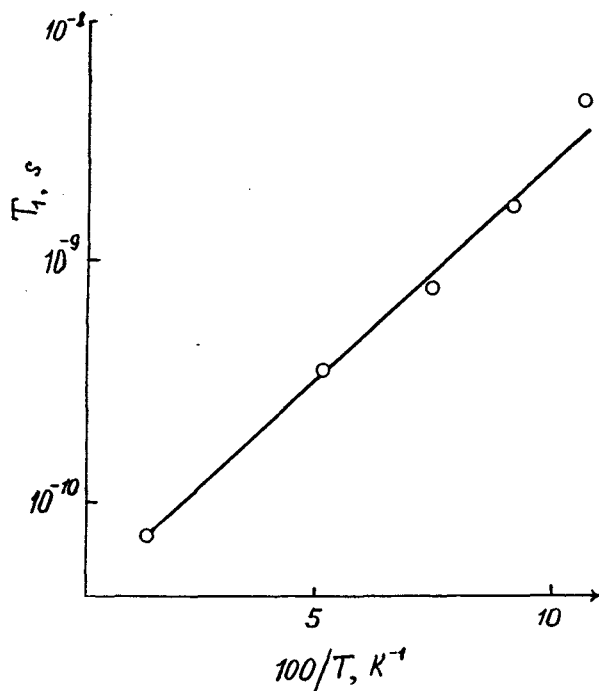


Figure 26. Temperature dependence of Fe^{2+} spin-lattice relaxation times in frozen sulfuric acid solutions.

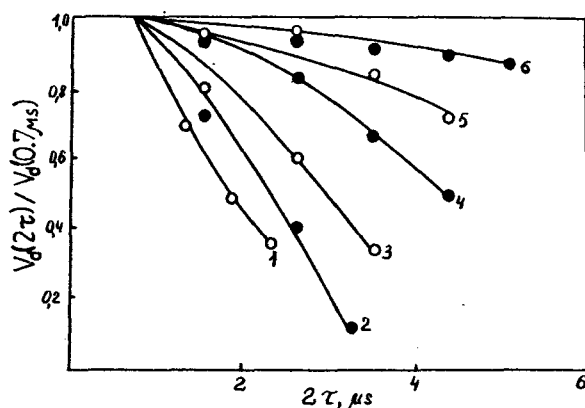


Figure 27. Phase relaxation of H atoms due to Cu^{2+} ions in frozen sulfuric acid solutions (36). $[\text{Cu}^{2+}] = 3.1 \times 10^{18} \text{ cm}^{-3}$. (1) 77 K, (2) 50 K, (3) 40 K, (4) 31 K, (5) 25 K, (6) 19.8 K.

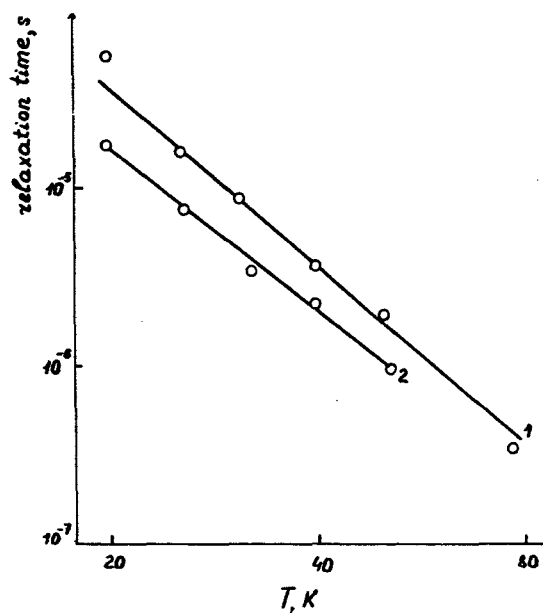


Figure 28. Temperature dependences of T_1 (1) and T_{21} (2) for Cu^{2+} ions (36).

with a uniform PC distribution at spin flip rates from 10^{10} s^{-1} to several s^{-1} . Experiment demonstrated an attractive fit to theory which made it possible to apply the theoretical tool discussed in Sections III and IV to problems of nonuniform PC distribution.

It should be noted that the experimental data adduced in Section V are referred to as samples of "type T_1 ." There is a number of studies on phase relaxation in samples of "type T_2 " (37, 38). For instance, as the spin concentration in a sample grows, the spin diffusion rate is shown (37) to increase hence inducing spectral diffusion in the spin system; the phase relaxation rate is demonstrated to obey the theoretical relation of eqn. 33 with good accuracy. PC phase relaxation was studied (38) as affected by spin flip-flops with forbidden electron-nuclear transitions. The spin flip rate was shown to follow the relation

$$W = I\gamma\hbar C \quad (79)$$

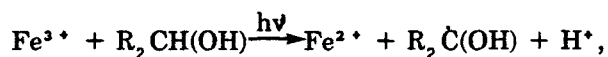
where I is the forbidden transition intensity. Varying the forbidden transition intensity made it possible to experimentally observe variations of the contributions from instantaneous and

spectral diffusions to the ESE signal decay. However, it should be mentioned that a number of problems associated with samples of "T₂ type" still remain to be solved in both theory and experiment.

VI. SYSTEMS WITH NONUNIFORM PC DISTRIBUTIONS

A. Distribution of Fe²⁺...R Pairs in Alcohol Matrices

This section is devoted to data on spatial distributions in radical-radical and radical-ion pairs and in ionizing particle tracks. Let us consider experimental results on the spatial distribution function of Fe²⁺...R pairs and its evolution during photo- and thermoannealing (20). Such pairs arise by the reaction of electron phototransfer in Fe³⁺ halogen complexes under $\lambda > 330$ nm ultraviolet light that does not destroy the pairs formed:



where R is H for methanol and CH₃ for isopropanol. A uniform PC distribution in this system can be readily obtained by photoannealing (see Section V.C.).

Experiments with systems with uniform PC distributions showed that $W\tau \gg 1$ for Fe²⁺ ions at a temperature of 8 to 20 K. Therefore, the distance distribution function for these pairs was obtained by eqn. 53; $V_p(2\tau) \equiv V_{in}(2\tau)$; $V_{in}(2\tau)$ was determined as described in Section V.A; V^* was measured in experiments with a uniform PC distribution. Figure 29 depicts $V_{in}(2\tau', T^0)$ vs. $V^*(T^0)$, where τ' is a fixed value of τ at the measured signal amplitude. Figure 30 shows the distance distribution function obtained by numerical differentiation of the V^* dependence of obtained demonstrates that the partners of the Fe²⁺...R radical pairs are close in space; in 80% of radical pairs the partners are no more than 17 Å away, i.e. once generated, the radicals travel only at a distance of several molecular diameters before their stabilization.

The distribution function $n(r^*)$ was studied (20) in the above systems under isothermal annealing, Figure 30 showing the results obtained. The function $n(r^*)$ is seen to increase with temperature at each particular r^* , which is attributed to radical diffusion from the ions to the matrix. This $n(r^*)$ behavior cannot be described in terms of conventional diffusion theory: at a given temperature it is impossible to entirely randomize the spins by increasing the

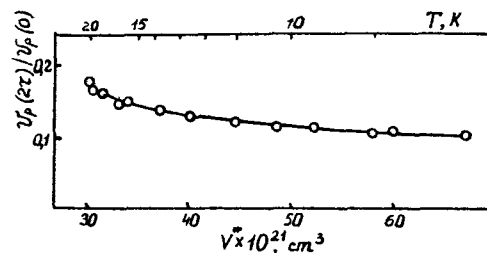


Figure 29. Plots of ESE signal intensity of CH₂OH radicals in samples with the pair spatial distribution vs. temperature and volume V^* at $\tau = 0.4 \mu\text{s}$. ($V^* = 4\pi r^{*3}/3$; paramagnetic ions contribute substantially to the radical phase relaxation only within the range of $r \leq r^*$).

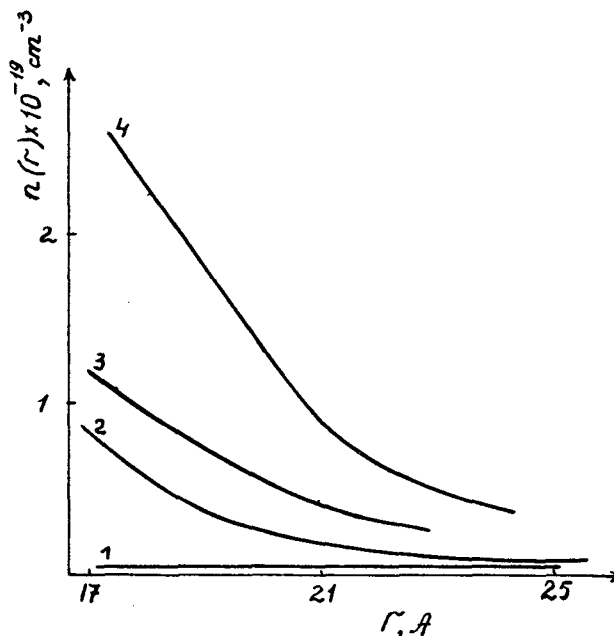


Figure 30. CH₂OH radical distribution function relatively Fe²⁺ ions at various annealing temperatures (20). Annealing times are 20 min. (1) $T = 112$ K, (2) Initial distribution function, (3) 96.5 K, (4) 100 K.

annealing times. The PC distribution can become uniform only with increasing temperature

(Figure 30).

Similar anomalous features were observed in radical diffusion in isopropanol (Figure 31). However, in this case the initial distribution function turns from a rapidly falling to increasing function due to the reaction of alcohol radicals with Fe^{2+} (Figure 31) and becomes minimum in the vicinity of an ion.

Thus investigations of the distribution function variations under isothermal annealing demonstrated the spatial scale of radical diffusion to be limited at each given temperature. This fact is believed (20) to result in the so-called step-by-step decay of radicals in solids.

The distribution function of isopropanol radicals with respect to Fe^{2+} was investigated (26) as affected by various photochemical transformations. Table 1 lists the diffusion ranges in photochemical and dark reactions.

Thus, we have demonstrated possible techniques of studying spatial distributions in pairs with one of the partners characterized by a short spin-lattice relaxation time, $W\tau \gg 1$, as applied to $\text{Fe}^{2+} \cdots R$ pairs.

If both partners have a long spin-lattice relaxation times, $W\tau \ll 1$, the spin-partner distribution function should be investigated by the method described in Section IV.B.2.

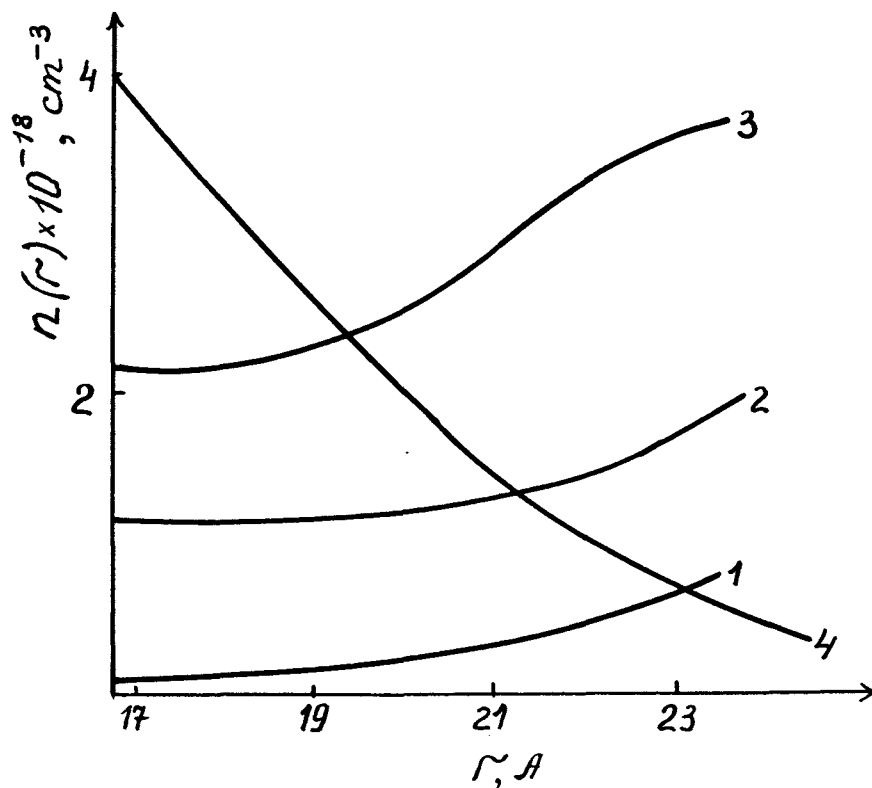


Figure 31. Distribution function of radical-paramagnetic ion pairs in isopropanol and its variations during isothermal annealing (20). (1) 124 K, (2) 121 K, (3) 118 K, (4) 77 K.

Table 1.

Migration of radicals due to photochemical
or thermal reaction in isopropanol

N	Reaction	Photolysis or annealing	The distance of migration
1	$R + M \rightarrow R'$	$\lambda > 330 \text{ nm}$	$\sim 8 \text{ \AA}^0$
2	$R' + M \rightarrow R$	106 K	$3-4 \text{ \AA}^0$
3	$R' \rightarrow R''$	$\lambda > 250 \text{ nm}$	$< 1 \text{ \AA}^0$
4	$R'' + M \rightarrow R$	106 K	$> 20 \text{ \AA}^0$

M - isopropanol,

$R' - \text{CH}_3\dot{\text{C}}\text{HCH}_3,$

$R - \text{CH}_3\text{C}(\text{OH})\text{CH}_3,$

$R'' - \text{CH}_3\text{CH}_2\dot{\text{C}}\text{H}_2$

B. Pairs with Long Relaxation Times

These pairs can be exemplified by those resulting from hydroquinone photolysis in acid matrices. In this case, pairs are constituted by hydroquinone radicals \dot{Q} and either \dot{H} or \dot{D} atoms depending on whether the process runs in a deuterated or protonated matrix. Both types of PCs have long relaxation times, $T_1 > 10^{-3}$ s, and well-resolved spectra which allows one to employ the double-resonance technique (27).

Figure 32 shows the experimental ESE signal decay kinetics resulting from d-d interaction

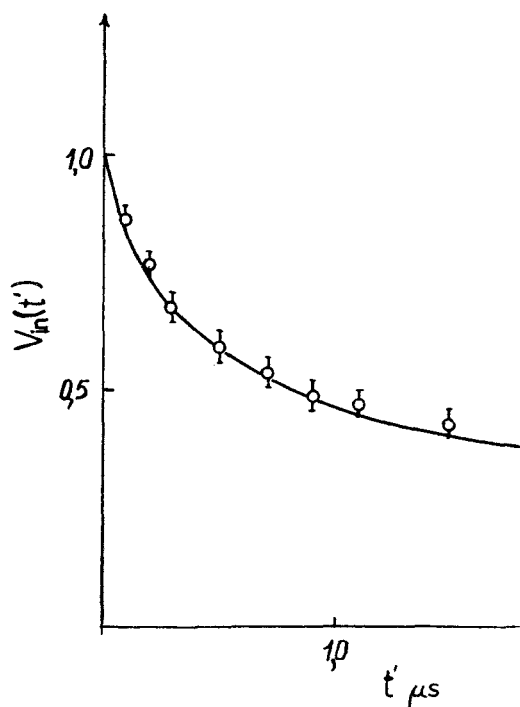


Figure 32. ESE signal decay kinetics $V_{in}(t')$ of \dot{H} atoms in $\dot{H} \cdots \dot{Q}$ pairs (27).

in these pairs. The signal decay is seen to be measurable within 0 to 2×10^{-6} s which guarantees determination of the distribution function up to some 80 Å. The pair distance distribution function $f(r)$ (Figure 14) was obtained by numerical differentiation of the decay kinetics (Figure 32). As seen, 63% of the pairs are within 0 to 85 Å, the rest 37% of them have distances exceeding 85 Å. To determine the spatial distribution at

distances longer than 85 Å, it is necessary to measure additionally the decay kinetics at long times. The distance distribution function obtained made it possible to determine the thermalization length of free electrons resulting from hydroquinone photoionization. This information cannot be obtained by any other method.

C. Some Examples of Investigating Pairs with $Wr \approx 1$

Though less detailed, the information on distribution functions for $\text{Fe}^{3+} \cdots \dot{D}$, $\text{Cr}^{3+} \cdots \dot{D}$, $\text{SO}_4 \cdots \dot{H}$ pairs obtained from ESE data proved to be extremely useful. The first two pairs were generated by photolysis of Fe^{2+} and Cr^{2+} in acid glasses (33), the third ones in γ -irradiated frozen solutions of sulfuric acid (39).

The spin-lattice relaxation times of Fe^{3+} and Cr^{3+} were measured in independent experiments with samples of uniform volume PC distributions. Analysis of the D atom ESE signal amplitude at a uniform D distribution throughout the sample, resulting from isothermal annealing, showed some fivefold change of the signal intensity at $\tau_0 = 0.4 \mu\text{s}$, the overall number of spins in the sample preserved. Since the signal intensity strongly depends on the partner separation in a pair (see Figure 6), the signal intensity observed, $V(2\tau_0) = 0.2$, correspond to the fraction of H atoms located at distances exceeding* $(2\alpha\tau T_1)^{1/2}$, i.e. 53 Å for Fe^{3+} and 44 Å for Cr^{3+} . Thus, the increase in the ESE signal amplitude in the sample with randomized spins is informative of the fact that some 80% of the spins in pairs are at distances shorter than 50 Å. Hence, photolysis results in pairs with rather close-distant radicals. Since D atom lines in an acid matrix are rather narrow ($\Delta\omega_{1/2} \sim 2\text{G}$), extra information on the pair distribution function was obtained by analyzing the dipolar broadening of D atom ESR lines (39). It was found out that about 30% of pairs have distances shorter than 17 Å. The comparison of ESE and ESR data allowed the distance distribution function shown in Figure 33. The shape of this function and the photochemical information (40) prompted the conclusion that the photolysis of the metal ions under study proceed without photoionization, H atoms are generated directly in the first coordination sphere of the complexes and then migrate until they are trapped. The distance distribution function of the process was calculated

* $\alpha = S(S+1)\gamma^2\hbar^2/3$

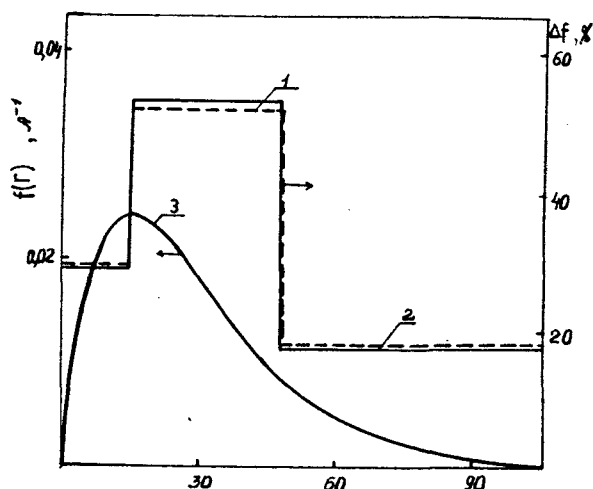


Figure 33. Experimental (1) and calculated (2) plots of distance distribution of $\text{Fe}^{3+} \cdots \text{D}$ pairs (33). The distribution function employed for calculations is $n(r) = (4\pi r_0^2 r)^{-1} \cdot \exp(-r/r_0)$, $r_0 = 16 \text{ \AA}$ (curve 3).

theoretically as

$$n(r) = (4\pi r_0^2 r)^{-1} \exp(-r/r_0) \quad (80)$$

where r_0 is a parameter depending on the free path of H atoms and on the trap concentration. Figure 36 depicts this function. A good agreement between calculated and experimental ESE and ESR data was achieved at $r_0 = 16 \text{ \AA}$ (Figure 34). In this way it has been determined that when generated, H atoms diffuse at a mean distance of some 30 Å before trapping, i.e. the problem of active particle diffusion in glassy matrices has been solved.

Pairs $\text{H} \cdots \text{SO}_4^-$ arise in irradiated glassy solutions of sulfuric acid. Studies on radiation-chemical processes running in this system show that ionized water molecules H_2O^+ are precursors of SO_4^- , while thermalized electrons are those of H atoms. As a result, the distribution of $\text{SO}_4^- \cdots \text{H}$ pairs is informative of a thermalization path of slow electrons relative to the parent ions. The radical-ion spin-lattice relaxation rate was measured in experiments reported in Section V.D.

Figure 35 shows the ESE signal decay due

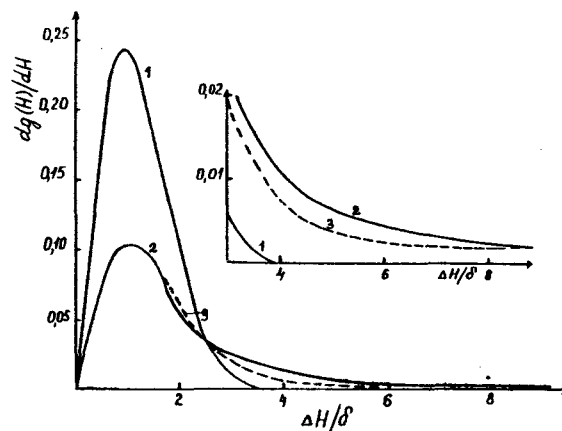


Figure 34. The first derivative of the high-field component of D ESR spectra after (1) and before (2) isothermal annealing (33). Curve 3 is the calculated distribution function for $\text{Fe}^{3+} \cdots \text{D}$ pairs $n(r) = (4\pi r_0^2 r)^{-1} \exp(-r/r_0)$.

to d-d interaction in $\text{H} \cdots \text{SO}_4^-$ pairs. The decay kinetics analyzed by eqn. 50 demonstrates a partner separation of 0 to 70 Å for 30% of all the pairs, the rest of them having longer radical-ion distances. With supplementary data on radiation-chemical and photoelectrochemical experiments, the distance distribution function can be presented as shown in Figure 35. This function adequately describes the ESE signal decay kinetics resulting from d-d interactions. Thus, analysis of the distance distribution function for $\text{H} \cdots \text{SO}_4^-$ pairs demonstrates that the thermalization path of slow electrons in glassy water solutions exceed hundred of Angstrom. This was quite a novel fact to radiation chemistry of water and water solutions since electrons were believed to be thermalized at distances not longer than 20-60 Å from the parent ions (41).

D. Spatial SO_4^- Radical-ion Distribution in Tracks of T β -particles

This section will be devoted to a nonuniform distribution of SO_4^- radical-ions generated in 8 M H_2SO_4 solutions irradiated with T β -particles. The technique described in Section V was used to determine the ESE decay induced by PC d-d interactions in a track. Measurements were

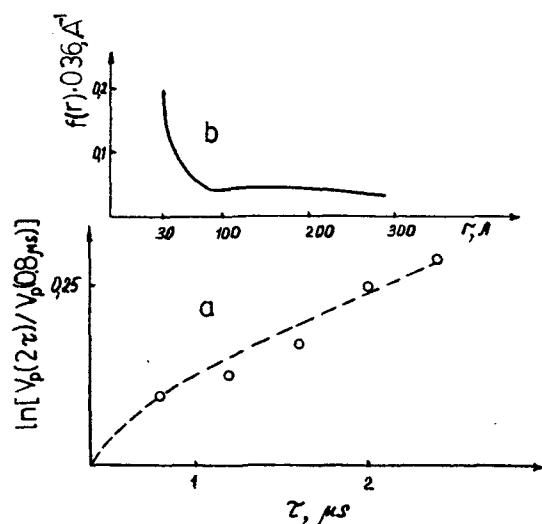


Figure 35. (a) ESE signal decay kinetics for H atoms in $\text{H} \cdots \text{SO}_4^-$ pairs. Dashed line: numerical calculations with the distribution function shown in (b) (39).

carried out at two temperatures: 77 and 4.2 K. In the latter case spectral diffusion did not contribute to the ESE signal decay. The results obtained are demonstrated in Figure 23. The signal decay logarithms are seen to nonlinearly depend on τ and to sharply increase at 0 to 0.5 μs with the subsequent much smoother trend.

Since SO_4^- precursors are ionized water molecules, experimental data were compared with those calculated by eqn. 42 with distances between primary ionization points used as r_{nk} (PC separation). All in all we recalculated 32 tracks created by electrons with the initial energy distributed in line with the well-known electron energy distribution observed under tritium decay. It was taken into account that a fraction of ions disappears in the process of initial recombination, the portion of those survived being $p = 0.5$.

As a result, the elementary decay kinetics of eqn. 42 were calculated as

$$v_{nk}'(2\tau|r_{nk}) = p + (1-p)v_{nk}(2\tau|r_{nk}) \quad (81)$$

Figure 23 depicts the ESE signal decay kinetics calculated. The calculated and experimental curves are seen to agree in the case of either

spectral (77 K) or instantaneous (4.2 K) diffusion making the basic contribution to the signal decay. This fact allows one to infer that a SO_4^- radical-ion track has a spatial structure similar to that of ionization points. Additional calculations demonstrate the theoretical kinetics to start varying when the track particles diffuse at some 20 Å from the points of their generation. Thus, SO_4^- radical-ions are localized relatively M^+ at distances no longer than 20 Å.

Summarizing, it can be pointed out that even in the case of so complex distributions as those of PCs in tracks, it proves to be possible to compare calculated and experimental decay kinetics and thus to obtain information on spatial particle distributions.

VII. CONCLUSION

The present paper is devoted to theoretical principles of phase relaxation in ESE experiments which are necessary for gaining information on spatial PC distribution.

We did not discuss ESE signal decay calculations for distributions mentioned in Section II.C (cluster and island distributions) since these are faced with difficulties of a calculation rather than fundamental character, and to our knowledge at present there is no experiment that demands such calculations.

In the above described investigations the experimentalists had some information on the spatial distribution prior to analysis of the decay kinetics. The problem is whether it is possible to obtain at least rough information on the type of distribution if the PC concentration cannot be varied experimentally and a uniform spin distribution cannot be attained. In the case of "T₁ type" samples, this question can be answered positively since one can always obtain the situation when $W\tau \ll 1$ and the signal decay is determined by an instantaneous diffusion mechanism. In this case, spin-lattice relaxation does not contribute to the ESE decay determined only by instantaneous diffusion and electron-nuclear interaction, the contribution from the latter being obtained at low H_1 values. Hence, there is the possibility of distinguishing the signal decay associated only with d-d interactions. In the case of a uniform distribution, the decay kinetics must be exponential, the relaxation rate and the mean PC concentration being related as

$$C = 1.25 \times 10^{12} b / \langle \sin^2 \Theta / 2 \rangle g(\omega) \quad (82)$$

where b is the decay rate. The nonexponential decay and the discrepancy between the mean

concentrations calculated by eqn. 82 and determined by stationary ESR spectroscopy unequivocally prove a nonuniform PC distribution. Thereafter one can try to determine the type of distribution by plotting the signal decay logarithm in the coordinates $\ln v_d(2\tau) - \tau^{1/3}$, $\tau^{2/3}$. Linear dependences obviously attest that the PC distribution is linear in the former case or plane in the latter (or close to them). However, one should remember that a pair distribution can imitate analogous time functions at some other $\langle \sin^2 \Theta / 2 \rangle_{g(\omega)}$ dependences. In the case of " T_2 samples", similar conclusions are possible only at a low concentration of magnetic nuclei. This situation is rather typical for inorganic crystals when one is faced with difficulties in varying spin concentrations. As a result, at sufficiently low temperatures a ESE signal decay results from spectral and instantaneous diffusions; each contribution can be determined by varying H_1 . The decay kinetics obtained are compared with calculated $Q_B(\tau)$ and $Q_A(\tau)$ using one of the experimental dependences for the determination of the most plausible spin flip rate. Thus, a uniform volume distribution can be distinguished from any other type of distributions in the case of " T_2 samples" too.

However, the problem of distribution and distribution function can be completely solved only by varying the concentration, temperature and H_1 and creating species with a uniform PC distribution in the matrix.

In conclusion one more important point should be mentioned. The present review summarizes particle spatial distribution studies based on principles of spin phase relaxation. However, d-d interactions of particles do not solely affect the spin dephasing but also result in cross-relaxation and spin excitation transfer processes. The spin excitation transfer influences the relaxation of the longitudinal magnetization component. As a result, some information on particle spatial distribution can be also gained from kinetic analysis of the longitudinal component restoration in ESE experiments. For instance, this method was used (42) to determine local concentrations of hydrogen atoms in tracks of β - and α -particles. It should be noted that some possibilities of studying nonuniform PC distributions with the help of cross-relaxation have been recently considered theoretically (43). However, a wide use of this approach demand further development of theory of cross-relaxation, spin diffusion, spin excitation transfer in disordered paramagnetic systems.

ACKNOWLEDGMENTS

The authors are thankful to Drs. V. V. Tregub, A. D. Milov, A. G. Maryasov, and Prof. Yu. D. Tsvetkov for extremely useful discussions of the problem of nonuniform PC distribution which took place while writing the present paper.

REFERENCES

- ¹W. B. Mims in *Electron Paramagnetic Resonance*, S. Geshwindt, Ed., Plenum Press, New York, 1972, p. 263.
- ²K. M. Salikhov, A. G. Semenov and Yu. D. Tsvetkov, *Electron Spin Echo and its Application*, Nauka, Novosibirsk, 1976.
- ³K.M. Salikhov and Yu. D. Tsvetkov, in *Time Domain Electron Spin Resonance*, L. Kevan and R. N. Schwartz, Eds., Wiley Interscience Publ., 1979, p. 231.
- ⁴J. S. Lebedev and V. I. Muromtzev, *EPR and Relaxation of Stabilized Radicals*, Chimia, Moscow, 1972.
- ⁵A. Mozumder and J. L. Magee, *Radiation Research* **28**, 203 (1966).
- ⁶V. A. Jiharev, A. R. Kessel, E. G. Harahashian, F. G. Cherkasov, and V. F. Yudanov, *Letters JETP (Russian)* **15**, 156 (1972).
- ⁷A. V. Kulikov and G. I. Lichtenstein, *Advances in Molecular Relaxation and Interaction Processes* **10**, 47 (1977).
- ⁸A. Abragam, *Nuclear Magnetism*, IL, Moscow, 1963, p. 254.
- ⁹E. L. Hahn, *Phys. Rev.* **80**, 580 (1950).
- ¹⁰J. R. Klauder and P. W. Anderson, *Phys. Rev.* **125**, 912 (1962).
- ¹¹A. D. Milov, K. M. Salikhov and Yu. D. Tsvetkov, *J. Exp. Teoret. Phys. (Russian)* **63**, 2329 (1972).
- ¹²A. D. Milov, K. M. Salikhov and Yu. D. Tsvetkov, *Fizika Tverdogo Tela* **15**, 1187 (1973).
- ¹³K. M. Salikhov, S. A. Dzuba and A. M. Raitsimring, *J. Magn. Reson.* **42**, 255 (1981).
- ¹⁴S. R. Hartmann and P. Hu, *J. Magn. Reson.* **15**, 226 (1974).
- ¹⁵E. R. Gilasitdinov, *Visokomolekularnye Soedineniya* **16**, 49 (1974).
- ¹⁶L. Kevan and R. N. Schwartz, Eds., *Time Domain Electron Spin Resonance*, Wiley Interscience Publ., 1979.
- ¹⁷G. Volkel, W. Brunner, W. Windsh and D. Stendel, *Phys. Status Solidi* **95**, 99 (1979).
- ¹⁸S. A. Altshuler, I. N. Kurkin and V. I. Shlenkin, *JETP* **79**, 1591 (1980).
- ¹⁹A. M. Raitsimring, K. M. Salikhov, Yu. D. Tsetkov and B. A. Umanskii, *Fizika Tverdogo Tela* **16**, 756 (1974).
- ²⁰S. A. Dzuba, A. M. Raitsimring and Yu. D. Tsvetkov, *Chem. Phys.* **44**, 357 (1979).

- ²¹S. A. Dzuba, A. M. Raitsimring and Yu. D. Tsvetkov, *Teoreticheskay i Experimentalnay Khimiya* **14**, 193 (1978).
- ²²S. A. Dzuba, K. M. Salikhov, A. M. Raitsimring and Yu. D. Tsvetkov, Preprint N 5, Institute of Chemical Kinetics and Combustion, Novosibirsk, 1980.
- ²³A. D. Milov, K. M. Salikhov and Yu. D. Tsvetkov, *Fizika Tverdogo Tela* **14**, 2259 (1972).
- ²⁴A. M. Raitsimring and V. V. Tregub, *Chem. Phys.* **77**, 123 (1983).
- ²⁵S. A. Dzuba, A. M. Raitsimring and Yu. D. Tsvetkov, *J. Phys. Chem. (Russian)* **53**, 2842 (1979).
- ²⁶S. A. Dzuba, A. M. Raitsimring and Yu. D. Tsvetkov, *Teoreticheskay i Experimentalnay Khimiya* **15**, 541 (1979).
- ²⁷A. D. Milov, K. M. Salikhov and M. D. Shirov, *Fizika Tverdogo Tela* **23**, 975 (1981).
- ²⁸A. Yu. Pusep and Shokhirev, *Optica i Spectroscopia* **57**, 792 (1984).
- ²⁹W. B. Mims, *Rev. Scient. Instruments* **10**, 78 (1965).
- ³⁰A. M. Raitsimring, S. F. Bychkov, K. M. Salikhov and Yu. D. Tsvetkov, *Fizika Tverdogo Tela* **17**, 484 (1975).
- ³¹A. G. Semenov, M. D. Shirov, V. D. Zhidkov, V. E. Chmelinskii and E. V. Dvornikov, Preprint N 5, Institute of Chemical Kinetics and Combustion, Novosibirsk, 1980.
- ³²A. E. Stillman and R. N. Schwartz, *J. Phys. Chem.* **85**, 3031 (1981).
- ³³V. V. Konovalov, S. A. Dzuba, A. M. Raitsimring, K. M. Salikhov, and Yu. D. Tsvetkov, *High Energy Chemistry (Russian)* **14**, 525 (1980).
- ³⁴A. M. Raitsimring, R. I. Samoylova and Yu. D. Tsvetkov in *Proceedings of 4 Tinany Symposium on Radiation Chemistry, Budapest, Academia Keado, Hungary, 1978*, p. 691.
- ³⁵A. M. Raitsimring, R. I. Samoylova and Yu. D. Tsvetkov, *Int. J. Radiat. Phys. Chem.* **10**, 171 (1977).
- ³⁶S. A. Dzuba, A. M. Raitsimring and Yu. D. Tsvetkov, *J. Magn. Reson.* **40**, 83 (1980).
- ³⁷A. M. Raitsimring, K. M. Salikhov, Yu. D. Tsvetkov and S. A. Dikanov, *Fizika Tverdogo Tela* **17**, 3174 (1975).
- ³⁸A. M. Raitsimring, V. I. Popov, K. M. Salikhov and Yu. D. Tsvetkov, *Fizika Tverdogo Tela* **20**, 1703 (1978).
- ³⁹S. A. Dzuba, A. M. Raitsimring and Yu. D. Tsvetkov, *High Energy Chemistry (Russian)* **15**, 37 (1981).
- ⁴⁰J. Moan, O. Kaalhaus and B. Hvik, *Chem. Phys. Lett.* **55**, 3026 (1979).
- ⁴¹J. R. Freeman, *J. Chem. Phys.* **46**, 2822 (1967).
- ⁴²A. M. Raitsimring and Yu. D. Tsvetkov, *High Energy Chemistry (Russian)* **12**, 122 (1980).
- ⁴³M. K. Bowman and J. R. Norris, *J. Phys. Chem.* **86**, 3385 (1982).

INSTRUCTIONS FOR AUTHORS

Because of the ever increasing difficulty of keeping up with the literature there is a growing need for critical, balanced reviews covering well-defined areas of magnetic resonance. To be useful these must be written at a level that can be comprehended by workers in related fields, although it is not the intention thereby to restrict the depth of the review. In order to reduce the amount of time authors must spend in writing we will encourage short, concise reviews, the main object of which is to inform nonexperts about recent developments in interesting aspects of magnetic resonance.

The editor and members of the editorial board invite reviews from authorities on subjects of current interest. Unsolicited reviews may also be accepted, but prospective authors are requested to contact the editor prior to writing in order to avoid duplication of effort. Reviews will be subject to critical scrutiny by experts in the field and must be submitted in English. Manuscripts should be sent to the editor, Dr. David G. Gorenstein, Chemistry Department, University of Illinois at Chicago, Box 4348, Chicago, Illinois, 60680, USA.

MANUSCRIPTS must be submitted in triplicate (one copy should be the original), on approximately 22 x 28 cm paper, typewritten on one side of the paper, and double spaced throughout. If the manuscript cannot be submitted on computer tapes, floppy disks, or electronically (see below), please type with a carbon ribbon using either courier 10 or 12, gothic 12, or prestige elite type face with 10 or 12 pitch. All pages are to be numbered consecutively, including references, tables, and captions to figures, which are to be placed at the end of the review.

ARRANGEMENT: Considerable thought should be given to a logical ordering of the subject matter and the review should be divided into appropriate major sections, sections, and subsections, using Roman numerals, capital letters, and Arabic numerals respectively. A table of contents should be included.

TABLES: These are to be numbered consecutively in the text with Arabic numerals. Their place of insertion should be mentioned in the

text, but they are to be placed in order at the end of the paper, each typed on a separate sheet. Each table should be supplied with a title. Footnotes to tables should be placed consecutively, using lower case letters as superscripts.

FIGURES are also to be numbered consecutively using Arabic numerals and the place of insertion mentioned in the manuscript. The figures are to be grouped in order at the end of the text and should be clearly marked along the edge or on the back with figure number and authors' names. Each figure should bear a caption, and these should be arranged in order and placed at the end of the text. Figures should be carefully prepared in black ink to draftsman's standards with proper care to lettering (typewritten or freehand lettering is not acceptable). Graphs should include numerical scales and units on both axes, and all figures and lettering should be large enough to be legible after reduction by 50-60%. Figures should be generally placed on sheets of the same size as the typescript and larger originals may be handled by supplying high-contrast photographic reductions. One set of original figures must be supplied; reproduction cannot be made from photocopies. Two additional copies of each figure are required. Complex molecular formula should be supplied as ink drawings.

REFERENCES to the literature should be cited in order of appearance in the text by numbers on the line, in parentheses. The reference list is to be placed on separate sheets in numerical order at the end of the paper. References to journals should follow the order: author's (or authors') initials, name, name of journal, volume number, page, and year of publication. The abbreviation of the journal follows that used in the Chemical Abstracts Service Source Index. Reference to books should include in order: author's (or authors') initials, name, title of book, volume, edition if other than the first, publisher, address, date of publication, and pages.

FOOTNOTES should be used sparingly and only in those cases in which the insertion of the information in the text would break the train of thought. Their position in the text should be marked with a superscript Arabic numeral and the footnote should be typed at the bottom of the

relevant page in the text, separated from the latter by a line.

SYMBOLS AND ABBREVIATIONS: Mathematical symbols should be typewritten wherever possible. Greek letters should be identified in pencil in the margin. In reviews containing a number of mathematical equations and symbols, the author is urged to supply a list of these on a separate sheet for the assistance of the printer; this will not appear in print. Standard abbreviations will follow the American Chemical Society's **HANDBOOK FOR AUTHORS** names and symbols for units.

PERMISSIONS: It is the responsibility of the author to obtain all permissions concerned with the reproduction of figures, tables, etc, from copyrighted publications. Written permission must be obtained from the publisher (not the author or editor) of the journal or book. The publication from which the figure or table is taken must be referred to in the reference list and due acknowl-

edgement made, e.g., reprinted by permission from ref. (00).

REPRINTS: Thirty reprints of a review will be supplied free to its senior author and additional reprints may be purchased in lots of 100

INSTRUCTIONS FOR SUBMITTING MANUSCRIPTS ON COMPUTER TAPES, FLOPPY DISKS OR ELECTRONICALLY: If you have used a word processor to type your manuscript, please forward your manuscript after review and revision, in a computer readable form. Tape should be unlabeled, in a standard IBM format, 1600 BPI, 80x80 blocks and ASCII image. Floppy disks readable on IBM, PDP 11, or MacIntosh personal computers are also acceptable. For direct submission over the phone lines use either 300 or 1200 baud ASCII transmission. Additional details will be provided for the appropriate hand-shake requirements. Please supply us with the code for interpreting superscripts, greeks, etc. on your word processor.